ASSESSING CLIMATE CHANGE ADAPTATION STRATEGIES FOR MAJOR CROPS IN TEXAS: A CASE STUDY IN TWO REGIONS

A Dissertation

by

KRITIKA KOTHARI

Submitted to the Office of Graduate and Professional Studies of
Texas A&M University
in partial fulfillment of the requirements for the degree of

DOCTOR OF PHILOSOPHY

Chair of Committee,	Srinivasulu Ale
Co-Chair of Committee,	Vijay Singh
Committee Members,	Clyde Munster
	Bruce McCarl
	David Briske
Head of Department,	Stephen Searcy

May 2019

Major Subject: Biological and Agricultural Engineering

Copyright 2019 Kritika Kothari

ABSTRACT

Agriculture is arguably the most vulnerable sector to climate change (CC). Producers in Texas not only face challenges from CC, but also from dwindling irrigation water supplies. This study was aimed at assessing the CC impacts on crop production and evaluating adaptation strategies in two agricultural regions in Texas: Texas High Plains (THP) and Edwards Aquifer (EA) region. Crop yield and irrigation water use for sorghum, cotton, winter wheat, and corn (for EA region only) were assessed under multiple CC scenarios using the CMIP5 climate data projected by nine Global Climate Models. Special emphasis was placed on grain sorghum in the THP because it was not studied well before despite its lower water requirement. Scenario-based analyses were conducted using the Decision Support System for Agrotechnology Transfer (DSSAT) model at Bushland, Halfway and Lamesa in the THP, and with the Soil and Water Assessment Tool (SWAT) model in the Lower Medina Watershed in the EA region.

Optimum thresholds to start and stop irrigation for grain sorghum in the THP were found to be 50% and 85% of plant available water content, respectively. Deficit irrigation during early reproductive stages optimized irrigation water use efficiency. Simulated sorghum yield and irrigation water use in the mid-century (2036–2065) decreased within 2–14% and 3–9 %, respectively in the THP compared to the baseline (1976–2005). Cotton and winter wheat yield increased (2–21%) at Bushland and Halfway and decreased (2–7%) at Lamesa. Cotton irrigation water use increased (5–8%) and wheat irrigation decreased (0.4–5.5%) at all sites. The differences across sites were attributed to the differences in soils and climate. Among the genetic traits tested, high yield potential was found to be beneficial for most crops and sites, and long maturity cultivar increased irrigation water use significantly. Changing root physical and hydraulic properties had mixed effect across sites and crops. For the EA region, increase in yield (5–47%) and reduction in irrigation water use (23–42%) was simulated for the four crops considered, mainly due to CO_2 fertilization. Out of the heat tolerance and deep rooting adaptations evaluated, increasing root depth by 20% percentage showed substantial benefits.

DEDICATION

Dedicated to my parents, Mrs. Meena and Mr. Tika Ram Kothari.

ACKNOWLEDGEMENTS

I would like to thank my committee co-chairs, Dr. Srinivasulu Ale and Dr. Vijay Singh, and my committee members, Dr. Clyde Munster, Dr. Bruce McCarl, and Dr. David Briske, for their guidance and support throughout the course of this research. My deepest gratitude goes to my co-advisor, Dr. Srinivasulu Ale, for his consistent encouragement and thorough feedback on my writing and research ideas. I whole-heartedly thank Dr. Ale for providing necessary training and resources to carry out this research. Thank you for always finding the time to listen to me and help me with any issues big and small. I would also like to thank Dr. Ale for introducing me to Mr. James Bordovsky, Dr. Dana Porter, Dr. Kelly Thorp, Dr. Gerrit Hoogenboom, Dr. Gary Marek, Dr. Steve Mauget, and Dr. Nithya Rajan. It has been a pleasure and privilege to have worked with my advisors, committee members, and collaborators. I will be forever grateful to everyone for their time and confidence in me.

Special thanks to Dr. Munster for providing me with multiple opportunities to teach, as a Teaching Assistant (TA) and a Course Instructor. His continued supervision despite his relocation and help with financial assistance is greatly appreciated. I would also like to acknowledge the support from Graduate Teaching Fellows Program and Dr. Vikram Kinra. I would like to take this opportunity to thank Dr. Robert Hardin for the opportunity to work as a TA with him.

I would like to acknowledge the professors whom I have had the pleasure of taking classes with: Dr. Gretchen Miller, Dr. Manuel Piña, Jr., Dr. Marian Eriksson, and Dr.

Patricia Smith. The skills learned in these classes have been beneficial in my dissertation research. Thanks also go to Dr. Patricia Goodson for sharing effective writing skills, through the POWER writing studios. I also wish to acknowledge the BAEN department and AgriLife staff, especially Cheryl Yeager, David Riggs, Stormy Kretzschmar, Susan Corgiat, and Rebecca Williamson, for helping me with the administrative work.

A big vote of thanks to my friends and colleagues and the department faculty for making my time at Texas A&M University a great experience. I wish to acknowledge my friends at the department for creating a pleasant work environment, especially Fernando, Victoria, Sayantan, and Duncan. I would also like to thank Abhishek Singh for helping me during my initial days in College Station.

Finally, thanks to my parents and siblings, Anjna, Archana, and Vikas, for their unconditional love and support. This dissertation, or anything I have accomplished so far, would not have been possible without their support.

CONTRIBUTORS AND FUNDING SOURCES

Contributors

This work was supervised by a dissertation committee consisting of Professors Srinivasulu Ale (advisor), Vijay Singh (co-advisor), and Clyde Munster of the Department of Biological and Agricultural Engineering, Professor Bruce McCarl of the Department of Agricultural Economics, and Professor David Briske of the Department of Ecosystem Science and Management.

The field data, which formed the basis for Chapters II–V was provided by Mr. James Bordovsky, Research Scientist at Texas A&M AgriLife Research, Halfway, TX. The manuscript associated with Chapter II was reviewed by Dr. Dana Porter of Texas A&M AgriLife Extension Service, Lubbock, TX, and Dr. Kelly Thorp of USDA-ARS, Arid-Land Agricultural Research Center, Maricopa, AZ. Dr. Thorp provided initial guidance on model calibration. Dr. Gerrit Hoogenboom of University of Florida, Gainesville, FL, provided suggestions for climate change impact and adaptation scenarios presented in Chapters IV–V. Data used for Chapter VI was provided by Dr. Qingwu Xue, Associate Professor at Texas A&M AgriLife Research, Amarillo and Drs. Nithya Rajan (Associate Professor) and Ahmed Attia (former Postdoctoral Fellow) of the Department of Soil and Crop Sciences. All work for this dissertation was completed by the student independently, under the guidance of aforementioned advisors and committee members.

Funding Sources

Dissertation research was supported by the College of Agriculture and Life Sciences (COALS) at the Texas A&M University. This work was also made possible in part by support from the Ogallala Aquifer Program, a consortium between the United States Department of Agriculture-Agricultural Research Service (USDA-ARS), Kansas State University, Texas A&M AgriLife Research, Texas A&M AgriLife Extension Service, Texas Tech University, and West Texas A&M University. Contents of this dissertation are solely the responsibility of the author(s) and do not necessarily represent the official views of the Texas A&M University and the U.S. Department of Agriculture.

NOMENCLATURE

CC	Climate Change
CERES	Crop Environment Resource Synthesis
CO_2	Carbon di-oxide
DSSAT	Decision Support System for Agrotechnology Transfer
EA	Edwards Aquifer
ET_c	Crop Evapotranspiration
FACE	Free-Air CO_2 Enrichment
NASS	National Agricultural Statistics Service
SWAT	Soil and Water Assessment Tool
THP	Texas High Plains
USDA	United States Department of Agriculture
USGS	United States of Geological Survey

TABLE OF CONTENTS

Page

LIST OF FIGURES

Page

LIST OF TABLES

Page

1. INTRODUCTION

1.1. Motivation

Texas ranks first in the total farm and ranch land in the United States (US). Agriculture is crucial to the Texas economy with agricultural production estimated at $24 billion in 2015 (Gleaton and Robinson, 2016). Increasing incidences of weather extremes and uncertainty in irrigation water supply are some of the key challenges faced by the producers in Texas. For example, the infamous drought of 2011 resulted in about $7.6 billion agricultural losses (Long et al., 2013). Additionally, climate change (CC) studies project warmer growing conditions and decline in rainfall in the future (Modala et al., 2017; Nielsen-Gammon, 2011; Venkataraman et al., 2016). Venkataraman et al. (2016) also reported that the impact of decreasing rainfall would be significant on groundwater, which would exacerbate water availability for agricultural production. Historically, prolific groundwater resources, e.g., Ogallala Aquifer, allowed production of water intensive and higher value crops in the Texas High Plains (THP), however this has led to water extraction at higher rates than the natural recharge of the aquifer (Hornbeck and Keskin, 2014). Extrapolation of the water depletion rates suggest that 35% of the southern Ogallala Aquifer, major irrigation source for the THP, will not be able to support irrigation within the next 30 years (Scanlon et al., 2012). On the other hand, agricultural water users in the Edwards Aquifer (EA) region of Texas face challenges from competition from other stakeholders. The aquifer provides water to the seventh largest city in the US (San Antonio) and feeds springs that support endangered species (Adams et al., 2015). The

Edwards Aquifer is an annually recharged karst aquifer, and water availability in this aquifer could potentially decrease under CC (Chen et al., 2001). Considering the projections of water shortage and shift in growing season climatic conditions, it becomes necessary to adjust crop management and irrigation practices to enhance climate resilience of Texas agriculture, especially in the THP and EA regions.

1.2. Research Questions

In this dissertation, attempts were made to address the following research questions:

- What irrigation management strategies for grain sorghum would optimize water use efficiency while maintaining crop yield at profitable levels?
- How CC would affect yield and water use of major crops (grain sorghum, corn, cotton and winter wheat) in Texas?
- What crop-genotype adaptations would be better suited for Texas under CC?
- What genetic traits would result in water savings without causing reductions in crop yield?

1.3. Study Area and Crops

Two important agricultural regions in the state of Texas were selected in this study: the THP and the EA regions. For CC impact and adaptation assessment, four major crops in the study regions were selected—grain sorghum, cotton, winter wheat, and corn (Colaizzi et al., 2009; Piccinni et al., 2009). More emphasis was placed on grain sorghum in the THP, in view of its lesser water demand than other crops (e.g., corn) in the region

(Amosson et al. (2005) and several irrigation management schemes were tested for this crop. More information about the study areas is given in the following sub-sections.

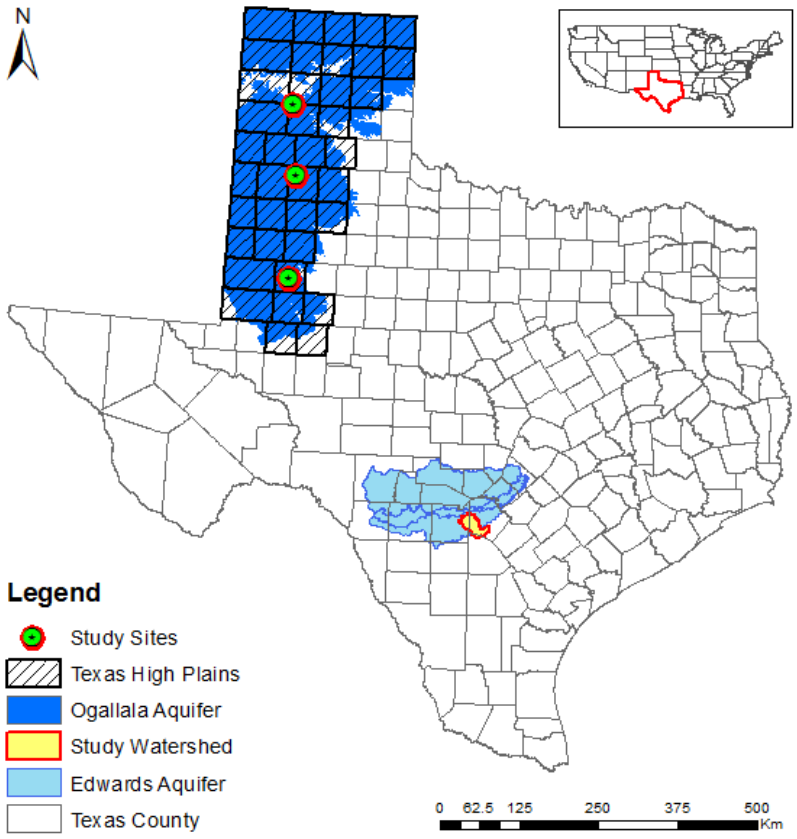

Figure 1.1 Study areas in the Texas High Plains and the Edwards Aquifer regions.

1.3.1. The Texas High Plains (THP)

The THP region comprises of 39 counties located in the northwest Texas. All counties in the THP are either partly or fully underlain by the Ogallala Aquifer. About 85% of the water extracted from the aquifer is used for irrigation purposes in the THP (TWDB, 2012). The THP region has a cropland area of about 5.5 million ha, of which 1.8 million ha are irrigated (Weinheimer et al., 2013). The average annual rainfall and

temperature in the THP for the 1981–2010 period were 492 mm and 15°C, respectively (NOAA, 2018). Three sites located within the THP region were selected for this study—Bushland, Halfway, and Lamesa (Figure 1.1) to represent agroclimatic conditions in the northern, central and southern parts of the THP, respectively. These sites were also chosen due to the availability of data from the Texas A&M AgriLife and the USDA-ARS research farms at these locations for the evaluation of the crop growth model used in this study. Three major crops in the THP including grain sorghum, cotton and winter wheat were considered in this study.

1.3.2. The Edwards Aquifer (EA) Region

The EA region is located in central Texas (Figure 1.1). Water from the Edwards Aquifer is used for multiple purposes, viz. agricultural, industrial, military, municipal, and recreational purposes (Chen et al., 2001). Majority of the groundwater withdrawal for agriculture takes place in Uvalde, Medina, and Bexar counties (Schaible et al., 1999). This study focused on a watershed located partly in Medina and Bexar Counties. This watershed was selected due to—the presence of representative crop mix within the EA region, and its location in the artesian zone of the aquifer, which minimizes modeling complications arising from karstic formations present in the recharge zone of the aquifer. Four major crops in the EA region including grain sorghum, cotton, corn and winter wheat were considered in this study.

1.4. Literature Review

Several published studies/reports in the literature were reviewed in order to identify and simulate potential water-use-efficient and climate-change-adaptive strategies for Texas. Key highlights of the literature review are presented in the following sub-sections.

1.4.1. Irrigation Management Strategies for Grain Sorghum Production

Several methods for deciding the timing and amount of irrigation application based on soil water status, crop development stage, and crop evapotranspiration (ET_c) demand are available in the literature. Previous studies conducted in the THP region, demonstrated effects of different irrigation schemes on sorghum production (Eck and Musick, 1979; Hao et al., 2014; Musick and Dusek, 1971; O`Shaughnessy et al., 2014; Tolk and Howell, 2003; Unger and Baumhardt, 1999). However, most of these studies were field studies that were conducted over six or fewer growing seasons. Assessing sorghum yield and water use efficiency under several other irrigation schemes, over multiple growing seasons, and under projected future climate, would enable development and evaluation of efficient irrigation strategies for grain sorghum production under the current and future climatic conditions.

1.4.2. Climate Change Impacts on Agriculture

The impacts of CC on agriculture are complex due to the dynamic interaction between multiple climate variables and crop growth processes involved. The response of agricultural production to changes in temperature, atmospheric carbon dioxide (CO_2), and

rainfall, as expected under CC (IPCC, 2014), tends to vary with the type of crop and geographic location (Hatfield et al., 2011). The increase in CO_2 concentration facilitates crop growth and yield by increasing photosynthesis and reducing transpiration per unit leaf area (Adams et al., 1998), also known as the CO_2 fertilization or CO_2 enrichment effect. However, the beneficial effects of CO_2 are reduced or completely negated when the air temperatures exceed the optimum range for crop production (Prasad et al., 2008). Different crops respond to the changes in atmospheric CO_2 in different ways. Generally, crops with C3 type of photosynthetic pathway such as cotton and wheat benefit from CO_2 enrichment by a greater extent than those with the C4 pathway such as corn and sorghum (Bloom et al., 2012; Leakey et al., 2006). However, large uncertainty exists in the crop yield projections for any given crop. For example, researchers have simulated both increasing (14% to 29%; (Adhikari et al., 2016)) and decreasing (−12% to −30%; (Rahman et al., 2018)) trends in cotton yields by mid-century under CC in Texas and Punjab, Pakistan, respectively, in spite of similar agroclimatic conditions at both places. Therefore, conducting a more detailed CC impact assessment of major crops specific to Texas growing conditions would be useful for Texas producers and farm managers.

1.4.3. Climate Change Adaptation Approaches

Adaptation strategies based on management practices alone may not be sufficient under extreme CC, and modifications in genotypes would be required to sustain crop yields. Most crop simulation models include a wide range of crop genotype parameters, which can be used to develop crop genotypes with different traits. Singh et al. (2014c)

tested heat tolerance, drought tolerance, yield potential and crop maturity traits for CC resilience of grain sorghum in India and Mali. This methodology has been adopted for other crops with slight modifications—chickpea (Singh et al., 2014a), groundnut (Singh et al., 2014b), grain sorghum (Singh et al., 2014c) and corn (Tesfaye et al., 2018). Other researchers (Loison et al., 2017; Semenov and Stratonovitch, 2015) have evaluated climate-change-adaptive genetic traits, using simulation models, by iteratively changing genotype parameters within a certain range and analyzing its effect on crop yields. All these studies demonstrated that process-based crop growth and hydrologic simulation models allow the development and testing of a wide range of crop genetic traits under varying climatic conditions. Studies evaluating CC adaptation strategies for major crops in the THP and EA regions are lacking.

1.4.4. Process-Based Crop and Hydrologic Simulation Models

Crop growth models and hydrologic models with good crop algorithms, when thoroughly calibrated against field data, can reliably simulate crop growth under different management and climate scenarios. In addition, these models enable simulation of numerous hypothetical experiments and conduct of scenario analyses, which save time and costs associated with field/laboratory experiments. The Decision Support System for Agrotechnology Transfer (DSSAT) cropping system model (CSM) is a process-based model, which has been extensively used across the globe for CC assessment and it has the capability to simulate crops with varying genetic characteristics (Guo et al., 2010; Malla, 2008; Marin et al., 2013; Rahman et al., 2018). For example, the DSSAT CSM

CROPGRO-Cotton model was successfully used in the THP (Adhikari et al., 2016) to simulate the impact of CC on cotton production. The Soil and Water Assessment Tool (SWAT) hydrologic model (Arnold et al., 2012) is a physically based model that can reliably simulated water budget and crop yield (Srinivasan et al., 2010). SWAT model has been used for many CC impact studies (Ashraf Vaghefi et al., 2014; Palazzoli et al., 2015; Sun and Ren, 2014). In this study, the DSSAT model was used for the THP region due to the availability of extensive field experiment data required for model parameterization. For the EA region, the SWAT model was used. SWAT model provides an additional advantage of simulating hydrologic processes and streamflow.

1.5. Objectives

The overarching goal of this study was to provide recommendations on water-use-efficient and climate-change-adaptive strategies to sustain agricultural productivity in the THP and EA regions under CC, with a special focus on grain sorghum in the THP. The research carried out in this study is aimed at helping producers in Texas in making informed decision about crop production in the future, and to contribute to the research efforts focused on achieving global food and water security. The specific objectives of this study were to:

1. Evaluate efficient irrigation management strategies for grain sorghum production in the THP region under current and future climate scenarios by:
    a. Determining optimum thresholds of soil water at planting, and thresholds to trigger and stop irrigation under long-term historic weather conditions.

b. Developing irrigation strategies for grain sorghum under projected future climate based on critical crop growth stages and/or soil water depletion.

2. Assess the impacts of CC on crop yield and irrigation water use of grain sorghum, cotton, corn and winter wheat in the THP and EA regions.
3. Identify potential climate-change-adaptive genetic traits of the selected crops for the THP and EA regions based on crop yield and irrigation water use.

The above objectives were achieved using the DSSAT CSM crop modules CERES-Sorghum, CERES-Wheat, CROPGRO-Cotton model for the THP region and the SWAT model for the EA region.

1.6. Organization of Dissertation

This Dissertation consists of eight chapters. Chapter I describes general background, rationale behind the study, and outlines the study objectives. Chapters II and III address objective 1a and 1b of the study, respectively with a focus on Halfway site in the THP. While Chapter II presents evaluation of the CERES-Sorghum and CROPGRO-Cotton modules for Halfway in the THP along with the evaluation of efficient irrigation schemes for grain sorghum under historic climate, Chapter III investigates the impacts of CC on grain sorghum production at Halfway and evaluates efficient full and deficit irrigation strategies for grain sorghum under future climatic conditions. The remaining chapters address objectives 2 and 3 of this study. Chapter IV assesses CC impacts on grain sorghum production at three sites in the THP and evaluates CC-adaptation strategies. Similarly, Chapters V and VI assesses CC impacts and evaluates CC-adaptation strategies

for cotton and winter wheat, respectively, at three sites in the THP. Chapter VII focuses on the EA region, in which SWAT model was used to assess the CC impacts and test two types of genetic adaptations. Chapter VIII summarizes the key findings from the study and provides recommendations for future work.

2. SIMULATION OF EFFICIENT IRRIGATION MANAGEMENT STRATEGIES FOR GRAIN SORGHUM PRODUCTION OVER DIFFERENT CLIMATE VARIABILITY CLASSES[*]

2.1. Synopsis

The Texas High Plains (THP) is a productive agricultural region, and it relies heavily on the exhaustible Ogallala Aquifer for irrigation water for crop production. Efficient use of irrigation water is critical for the sustainability of agriculture in the THP. Grain sorghum is one of the major crops grown in the region, and it is known for its drought tolerance and lower water requirement compared to other cereal crops such as corn. In this study, the CERES-Sorghum and CROPGRO-Cotton modules of the Decision Support System for Agrotechnology Transfer (DSSAT) were evaluated using data from cotton-sorghum rotation experiments at Halfway, Texas over a period of nine years (2006–2014). The evaluated CERES-Sorghum model was then used to identify the optimum (i) initial soil moisture at planting (ISM); (ii) threshold to start irrigation (ITH); (iii) threshold to terminate irrigation; and iv) deficit/excess (DFI) irrigation strategy for grain sorghum production based on simulated sorghum yield, irrigation water use efficiency (IWUE), and grain water use efficiency (WUE). In addition, the effect of weather conditions on simulated strategies was elucidated by dividing the long-term (1977–2016) weather data into cold, warm, wet, dry, and normal climate variability classes.

[*]Reprinted with permission from "Simulation of efficient irrigation management strategies for grain sorghum production over different climate variability classes" by Kothari K., S. Ale, J.P. Bordovsky, K.R. Thorp, D.O. Porter, and C.L. Munster, 2019. *Agricultural Systems*, 170, 49–62, doi: 10.1016/j.agsy.2018.12.011, Copyright 2019 Elsevier Ltd.

The DSSAT model adequately simulated the grain sorghum and seed cotton yields during calibration (average Percent Error (PE) of 1.3% (sorghum) and 3.4% (cotton)) and evaluation (average PE of –2.2% (sorghum) and –10.5% (cotton)). The results from long-term simulations indicated that weather conditions played a key role in selecting appropriate irrigation management strategies. Under normal/cold/wet weather, ISM of 75% available water holding capacity (AWC), ITH of 50%, and DFI 85% were found to be adequate for irrigated grain sorghum production. However, in warm/dry weather, ISM of 75%, ITH 60%, and DFI at 100% reduced sorghum yield loss.

2.2. Introduction

The semi-arid Texas High Plains (THP) is an important agricultural region in the United States with 1.8 million ha of irrigated land (Weinheimer et al., 2013). The primary source of irrigation in the THP region is the Ogallala Aquifer. Water has been withdrawn from this aquifer at a much higher rate than it has been replenished. This has resulted in a rapid decline in the groundwater levels, especially in the southern portion of the aquifer (Chaudhuri and Ale, 2014; Scanlon et al., 2012). In view of the declining groundwater resources, the Groundwater Conservation Districts in the THP have started imposing restrictions on groundwater pumping (HPWD, 2015). These restrictions are designed to achieve certain percent volumetric storage (varies within the Groundwater Management Area) available in 50 years, also known as Desired Future Conditions (Mace et al., 2008). Recent studies (Modala et al., 2017; Nielsen-Gammon, 2011) project warm and dry future climate in the region, which necessitate larger groundwater withdrawals to meet higher

crop evapotranspiration requirements, and hence raise further concerns about future groundwater availability for irrigation. Therefore, it becomes imperative to adopt efficient water management practices to sustain agricultural production in this region.

Colaizzi et al. (2009) studied irrigation trends in the THP and suggested that replacing high-water demand crops with low-water demand crops could reduce groundwater withdrawals by nearly 20%. Grain sorghum is one of the important low-water use crops grown in the THP. Major crops grown in the THP region are cotton, wheat, corn and sorghum with planted acres equal to 52%, 25%, 12% and 8%, respectively of the total field crop acreage in the THP in 2017 (USDA-NASS, 2018). Annual planted area of grain sorghum during 1977–2016 was on average 0.5 million ha (USDA-NASS, 2018). Although the popularity of grain sorghum in the region declined after the late 1970s, there is a renewed interest in this crop in recent times due to its lower water requirement and dependable performance under varied weather patterns and ethanol production (Rooney et al., 2007). Development and evaluation of efficient irrigation strategies for sorghum production could not only assist producers in efficiently utilizing valuable groundwater resources from the Ogallala Aquifer, but also provide useful information for sorghum growers and researchers working in similar agro-climatic regions.

Previous studies in the THP, mostly field experiments, focused on studying the effects of soil water and irrigation management practices on grain sorghum yields (Hao et al., 2014; Musick and Dusek, 1971; O`Shaughnessy et al., 2014; Tolk and Howell, 2003; Unger and Baumhardt, 1999). Unger and Baumhardt (1999) performed a regression analysis between annual and growing-season rainfall, soil water content at planting, soil

water use, and crop evapotranspiration (ET_c) to identify the reasons for the steady increase in dryland sorghum yields from 1939 to 1997 at Bushland in the THP. They found that an increase in soil moisture at planting, mainly due to adoption of conservation-tillage that improved crop residue retention, was the dominant factor for yield increase apart from the use of improved hybrids. In another study at Bushland, Tolk and Howell (2003) evaluated four irrigation treatments (100%, 50%, 25%, and 0% ET_c replacement) in two growing seasons (1998–1999) and concluded that irrigation water use efficiency (IWUE) decreased with increasing irrigation, and IWUE was higher in milder (lower temperature, high rainfall) climatic conditions. They have also reported that the sorghum grain yields were more susceptible to changes in environmental conditions in a Pullman clay loam soil than in Ulysses and Amarillo soils. In a more recent deficit irrigation evaluation study conducted at Bushland from 2009–2011, O`Shaughnessy et al. (2014) reported higher grain sorghum yields with higher irrigation amounts (80% of full replenishment of soil water depletion to field capacity in the top 1.5 m soil profile) than those reported in lower irrigation (55%, 30%, and 0% of full replenishment) treatments. However, IWUE was higher with a 55% of full replenishment irrigation when compared to 80% of full replenishment, except for the drought year of 2011. Hao et al. (2014) also noted a difference in IWUE response to irrigation under different climatic conditions at Bushland, with a general trend of higher IWUE for biomass yields in photoperiod-sensitive sorghum (bioenergy crop) in limited irrigation when compared to full and no irrigation conditions. Nearly all these field studies were conducted at the USDA-ARS Conservation and

Production Research Laboratory at Bushland and they spanned over three or fewer growing seasons only.

Bordovsky et al. (2011) conducted a long-term deficit irrigation study on cotton-grain sorghum rotation at the Texas A&M AgriLife Research Station at Halfway in the THP. The treatments included both rainfed and irrigated with those having maximum irrigation capacities of 1.7 mm d^{-1} and 3.4 mm d^{-1} irrigation. Grain sorghum yields and IWUE in this experiment were generally higher for the 3.4 mm d^{-1} treatment compared to the other two treatments. Although, the study provided useful comparison of sorghum IWUE and grain yields over six growing seasons (2003–2008), it did not consider the crop yield responses to soil moisture at planting. Moreover, irrigation was supplied to fulfill cotton ET requirements first and the remainder of available water was applied to grain sorghum, resulting in non-uniform irrigation application for grain sorghum in different years of the experiment. A critical understanding of the interactive effects of climate variables and irrigation management decisions (e.g. soil water at planting, soil water threshold for initiating irrigation, deficit irrigation levels, etc.) on crop growth and yield over a longer period is of utmost importance for developing efficient irrigation strategies for grain sorghum production.

After a thorough calibration using field data sets, crop models can be useful complements to field experiments for quickly and inexpensively evaluating different irrigation strategies with reasonable confidence, based on generally available long-term weather data. They simulate crop growth and development under numerous crop management and agro-climatic scenarios. The Decision Support System for

Agrotechnology Transfer Cropping System Model (DSSAT-CSM) (Jones et al., 2003) has been successfully applied in the THP and nearby Texas Rolling Plains for simulating deficit irrigation for cotton (Modala et al., 2015) , winter wheat (Attia et al., 2016), and corn (Marek et al., 2017). Although the CERES-Sorghum (Alagarswamy and Ritchie, 1991) module of DSSAT-CSM has been used by a few researchers (Carbone et al., 2003; Fu et al., 2016) to simulate the effect of different management practices and environmental conditions on sorghum production at different locations in the US, it has not been evaluated for the THP region.

The specific objectives of this study were to (i) evaluate the DSSAT CSM CERES-Sorghum module for the THP region using measured data from long-term cotton-grain sorghum rotation experiments at the Helms Farm, Halfway, TX, and (ii) use the evaluated CSM CERES-Sorghum model to determine the optimum soil moisture content at planting, identify the optimum soil moisture threshold for initiating irrigation, and suggest appropriate deficit irrigation strategies for sorghum in the THP region. Since measured data used for evaluating the CERES-Sorghum module came from a cotton-grain sorghum rotation experiment (instead of a grain sorghum monoculture experiment), a DSSAT sequential project was created and the CROPGRO-Cotton module was also evaluated simultaneously in this study. This additional step was necessary to ensure that the water and nutrient balances during the years when cotton was grown (in between two grain sorghum crops) and during the fallow periods between grain sorghum/cotton growing seasons were simulated accurately.

2.3. Material and Methods

2.3.1. Study area/ experiment site

In this study, field data from cotton-sorghum rotation experiments (TALR, 2016) conducted at Halfway, TX (34° 9′ N, 101° 57′ W, 1071 m above mean sea level, Figure 2.1), from 2006 to 2014, were used for the evaluation of CERES-Sorghum and CROPGRO-Cotton (Boote et al., 1998) modules. Sorghum was grown after two years of cotton in two adjacent sections of a Low Energy Precision Application (LEPA) center pivot irrigation system, namely plots 5b and 5f (Figure 2.1). Irrigation was applied at three levels, i.e., base, high, and low levels. These three variable irrigation rates were replicated in four spans of the center pivot. The base water level approximately matched 80% of the crop evapotranspiration rate (ET_c) from 2006 to 2009, and 60% of the ET_c from 2010 to 2014. The high and low irrigation levels were kept at ±20% of the base level in the year 2006, and ±50% of the base level from 2007–2014.

The sequence of crops and the irrigation amounts applied for the three treatments in this study are summarized in Table 2.1. The climate at the study site is semi-arid and the soil is deep well-developed Pullman Clay Loam (Fine, mixed, superactive, thermic Torrertic Paleustolls). Additional information about climate, soil, and cropping system at the study area is provided in the model input section.

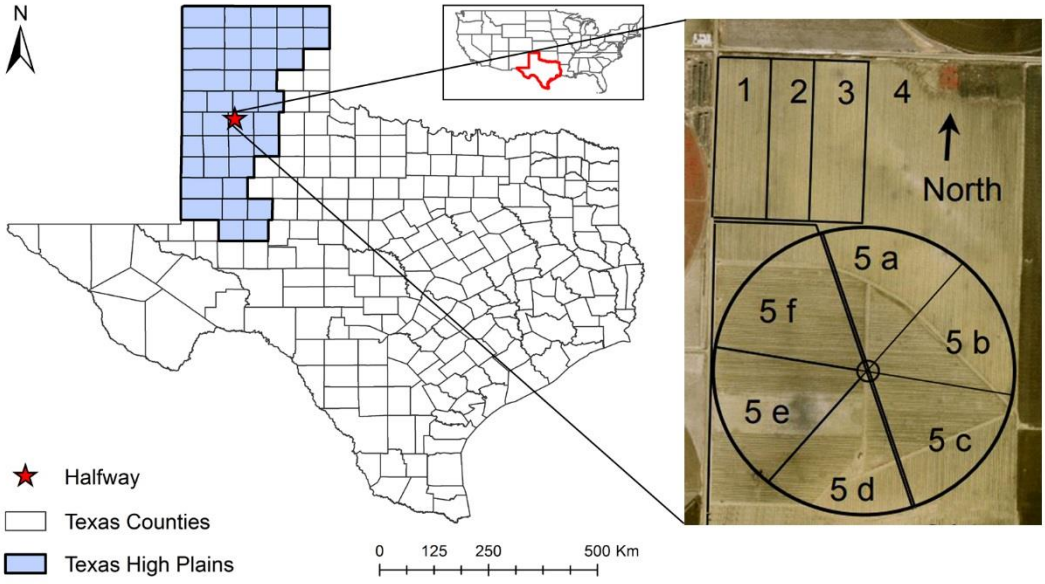

Figure 2.1 Location of Helms Farm near Halfway in the Texas High Plains (left). Layout of the center pivot system at the farm (right) (TALR, 2016).

Table 2.1 Summary of growing season irrigation amounts applied, and rainfall received during cotton-sorghum rotation experiments at Halfway.

Plot	Year	Crop	Irrigation during growing season (mm)			Seasonal rain (mm)
			High	Base / Medium	Low	
5b	2006	Cotton	429	389	332	278
	2007	Sorghum	330	218	112	335
	2008	Cotton	449	307	171	232
	2009	Cotton	276	187	104	316
	2010	Sorghum	229	162	104	292
	2011	Cotton	492	342	191	68
	2012	Cotton	395	275	151	236
	2013	Sorghum	299	200	86	263
5f	2011	Cotton	451	300	150	68
	2012	Sorghum	367	255	138	236
	2013	Cotton	319	226	130	263
	2014	Cotton	92	63	36	483

2.3.2. DSSAT-CSM Description

The DSSAT-CSM (Jones et al., 2003) simulates crop growth and yield as well as soil water, carbon, and nitrogen processes over time based on weather, soils, crop management, and crop cultivar data. The latest DSSAT 4.6.1 version (Hoogenboom et al., 2015) contains over 42 different crop growth simulation models including models for cereals, legumes, fruit, fiber, oil, sugar, vegetables, and forage crops.

The DSSAT-CSM provides five methods for simulating irrigation, out of which two methods are available for automatic irrigation: (i) automatic when required and (ii) fixed amount automatic. Amount of irrigation water applied through automatic irrigation (auto-irrigation) is estimated based on the soil available water content (AWC), which is equal to the difference between the field capacity (SDUL) and wilting point (SLLL) soil water contents. Auto-irrigation is triggered when the soil moisture drops to the irrigation lower limit and ends once the water is replenished up to upper limit of auto-irrigation. The "Automatic when required" method allows setting the lower limit as percent of maximum AWC while keeping the upper limit as constant at 100%, whereas in the "fixed amount automatic" method, in addition to lower limit, the amount of irrigation to be applied (in mm) to refill soil profile can be specified. In this study, the "automatic when required" option was used for determining optimum soil moisture at planting and threshold to start irrigation, and the "fixed amount automatic" option was used for creating deficit irrigation scenarios.

A sequence analysis was initially carried out in this study during the model evaluation to mimic cotton-sorghum rotation field experiments at Halfway, and then

seasonal analysis was conducted to run long-term (1977–2016) sorghum monoculture scenarios.

2.3.3. Model Input Data

2.3.3.1. Weather Data

The weather data for this study was obtained from the Texas High Plains Evapotranspiration Network (TXHPET) (Porter et al., 2005) weather station at Halfway, TX for the period from 1977 to 2016. The climate variables included minimum and maximum air temperature (^{o}C), precipitation (mm), solar radiation (MJ m^{-2}), wind speed (m s^{-1}), and relative humidity (%). Missing values were filled with the data obtained from the National Oceanic and Atmospheric Administration (NOAA, 2017), Agricultural Modern-Era Retrospective Analysis for Research and Applications (AgMERRA) (Ruane et al., 2015a) and NASA's Prediction of Worldwide Energy Resource (Stackhouse, 2006). The average annual precipitation at Halfway over the period from 1977 to 2016 was about 463 mm, and the daily mean temperature varied from −15 °C to 32 °C. A summary of annual rainfall and sorghum growing period (May–October) rainfall and average temperature is presented in Figure 2.2.

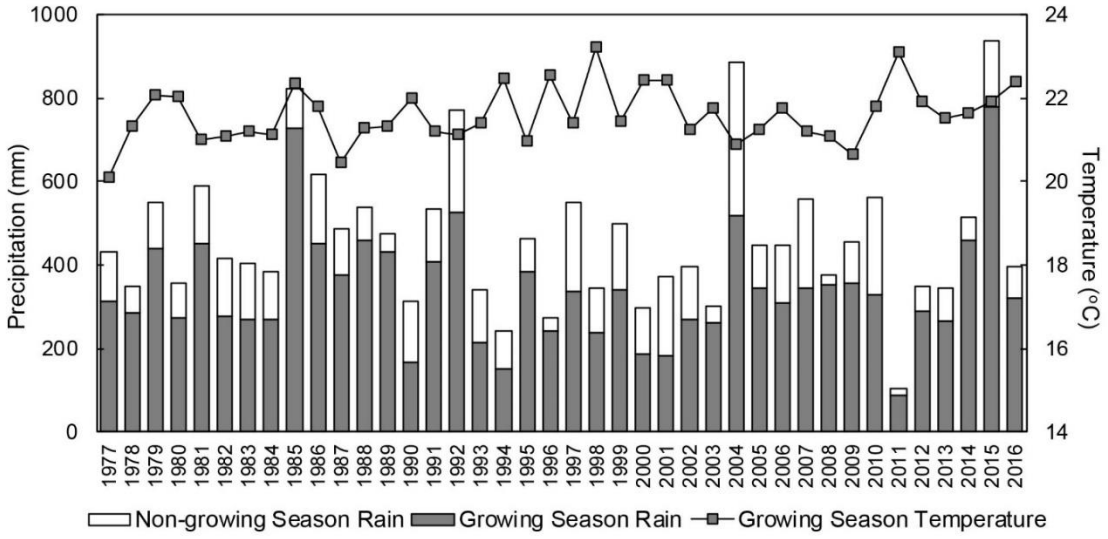

Figure 2.2 Annual and growing season (May–October) precipitation and growing season average air temperature at Halfway, TX from 1977–2016.

2.3.3.2. Weather Data Classification

Long-term weather data at Halfway was classified into nine different climate variability classes based on growing season air temperature and precipitation (Figure 2.2). The years with growing season precipitation below the 33rd percentile (272 mm) were considered "dry" years, and those with precipitation above the 66th percentile (356 mm) were considered "wet" years. Similarly, the years with average growing season temperature below 33rd percentile (21.2 °C) and above 66th percentile (21.8 °C) were classified as "cold" and "warm" years, respectively (Figure 2.3). The years that did not fall under any of the above four categories were considered "normal" years. The thresholds chosen in this study were intermediate to the 25th and 75th percentiles used by Chmielewski and Potts (1995) and the 40th and 60th percentiles used by Auer and Böhm (1994). Based on these five categories of years, nine climate variability classes were defined, and the years falling within each climate variability class are listed in Table 2.2.

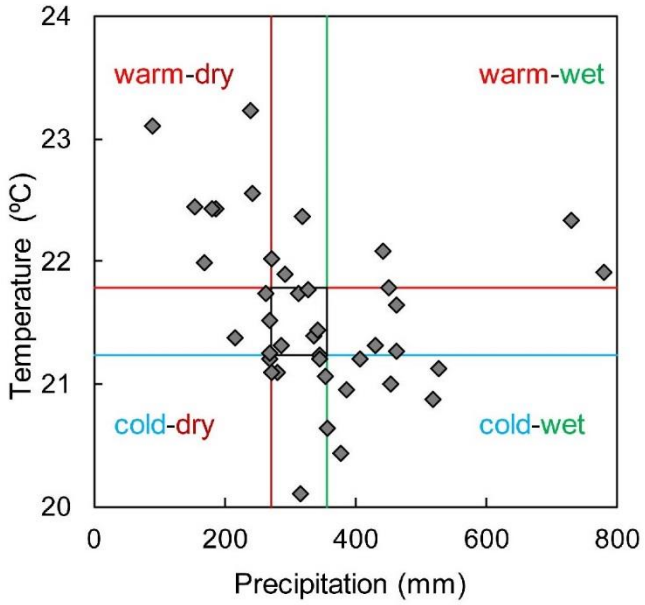

Figure 2.3 Classification of long-term weather data at Halfway, TX based on 33rd and 66th percentiles of air temperature and precipitation.

Table 2.2 Climate variability classes defined for climate variability impact assessment.

Climate variability class	Code	Number of Years	Years
Warm-Wet	WW	4	1979, 1985, 1986, 2015
Warm-Dry	WD	8	1980, 1990, 1994, 1996, 1998, 2000, 2001, 2011
Cold-Wet	CW	7	1981, 1987, 1991, 1992, 1995, 2004, 2009
Cold-Dry	CD	2	1983, 1984
Warm-Normal	WN	2	2012, 2016
Cold-Normal	CN	5	1977, 1982, 2005, 2007, 2008
Normal-Normal	NN	5	1978, 1997, 1999, 2006, 2010
Normal-Dry	ND	4	1993, 2002, 2003, 2013
Normal-Wet	NW	3	1988, 1989, 2014

2.3.3.3. Crop Management Data

The crop management data for cotton-sorghum rotation experiments at Halfway were obtained from Helms Farm Annual Reports, which are available on the Texas A&M AgriLife Research website (TALR, 2016). Data from a total of 36 treatments from 8 cotton and 4 sorghum growing seasons in combination with three irrigation levels were used in this study. Seeds were planted at a 3.8 cm depth in circular rows 1.02 m apart using a John Deere MaxEmerge™ Planter. One or more crop varieties were planted within each irrigation treatment in a year, and the varieties changed over time depending on availability. The DSSAT evaluation was performed based on field data collected for the early-maturity cotton cultivars (Sharma et al., 2015; Snowden et al., 2014; Speed et al., 2008) including DP 104B2RF, FM 9180 B2F and FM 2011 GT, and medium-maturity grain sorghum cultivars (Schnell et al., 2015), DKS 44-20 and DKS 49-45. The aim of the calibration effort in this study was to develop a generic set of cultivar parameters for a medium-maturity grain sorghum and an early-maturity cotton, which would reasonably simulate phenology and crop yield over the 9-year period, and eventually use those calibrated parameters for suggesting efficient irrigation strategies for grain sorghum over a variety of climate classes. The hypothesis behind this methodology was that the parameters developed from a wide range of seasonal conditions would be more robust than those developed from a single season (He et al., 2017; Timsina and Humphreys, 2006).

Table 2.3 Crop management related inputs used in the DSSAT CSM.

	Halfway, TX sorghum production year†				Sorghum long-term simulations*
	2007	2010	2012	2013	1977–2016
Cultivar:	DKS 37-07	DKS 44-20	DKS 44-20	DKS 49-45	
Planting data:					
Planting date	May 19	May 26	May 31	June 4	June 1
Seeding density, seeds/m^2	$24^{(H)}$, $19^{(B)}$, $14^{(L)}$	$17^{(H)(B)(L)}$	$24^{(H)}$, $19^{(B)}$, $14^{(L)}$	$19^{(H)(B)(L)}$	$18^{(irrigated)}$, $6^{(dryland)}$
Fertilizer data:					
Total nitrogen applied, N kg/ha	$272^{(H)}$, $222^{(B)}$, $173^{(L)}$	$156^{(H)(B)(L)}$	$187^{(H)}$, $111^{(B)}$, $60^{(L)}$	$175^{(H)}$, $128^{(B)}$, $90^{(L)}$	$150^{(irrigated)}$, $60^{(dryland)}$
Timing, month/day	7/3, 7/19, 7/25, 7/28, 8/1	4/1, 6/17	3/5, 6/22	3/20, 7/3	6/20, 7/10

	Halfway, TX cotton production year†						
	2006	2008	2009	2011	2012	2013	2014
Cultivar:	FM960 B2R	DP104 B2RF	DP104 B2RF	FM9180 B2F	FM9180 B2F	FM2011 GT	FM2011 GT
Planting data:							
Planting date	May 10	May 14	May 13	May 11	May 8	May 14	June 4
Seeding density, seeds/m^2	13	13	13	13.3	13	13	12.8
Fertilizer data:							
Total nitrogen applied, N kg/ha	$175^{(H)}$, $170^{(B)}$, $150^{(L)}$	$168^{(H)(B)(L)}$	$180^{(H)}$, $142^{(B)}$, $105^{(L)}$	$125^{(H)}$, $78^{(B)(L)}$	$187^{(H)}$, $111^{(B)}$, $60^{(L)}$	$175^{(H)}$, $128^{(B)}$, $90^{(L)}$	$217^{(H)}$, $179^{(B)}$, $135^{(L)}$
Timing, month/day	4/7–10, 5/23, 6/28–29, 7/12–27	3/19, 7/7, 8/1	3/2, 7/21–23, 8/3–6	3/14, 3/21, 6/16	3/5, 6/25	4/3, 6/26, 6/28	2/7, 3/27–28, 4/1, 7/22

†Helms Research Farm, Halfway actual planting and fertilizer methods used for DSSAT evaluation.
$^{(H), (B), (L)}$ correspond to the irrigation levels, high, base, and low, respectively as described in Table 2.1.
*Common practices in the THP used to create long-term (1977–2016) sorghum dryland and irrigated scenarios (McClure et al., 2010).

The details of planting and fertilizer application are presented in Table 2.3. For the long-term (1977–2016) irrigated and dryland sorghum simulations, crop management-related model inputs were specified based on the actual practices adopted in the Halfway

experiments and common cultural practices followed for sorghum production in the THP region as outlined in the High Plains Production Handbook (McClure et al., 2010) (Table 2.3). For the auto-irrigation used in the long-term simulations, a management depth of 0.3 m of topsoil (default) and an irrigation efficiency of 90% were considered to represent the Low Energy Precision Application (LEPA) center-pivot irrigation system used at the location (Bordovsky and Lyle, 1996; Colaizzi et al., 2009).

2.3.3.4. Soil Data

Some of the soil input parameters were directly obtained from soil sample analysis results from the study site (Adhikari et al., 2016), and the remaining parameters were generated using the SBuild tool distributed with the DSSAT model (Uryasev et al., 2004). The parameters taken from soil sample tests include percentages of clay, silt, organic carbon and total nitrogen, pH and cation exchange capacity (cmol kg^{-1}). The parameters generated using these values in the SBuild were saturated hydraulic conductivity (cm h^{-1}), soil water lower limit (cm cm^{-1}), drained upper limit (cm cm^{-1}), soil water at saturation (cm cm^{-1}), soil bulk density (g cm^{-3}), and soil root growth factor (Table 2.4). The simulated plant available water content of 21.3 cm in the top 200 cm profile was close to the values reported for Halfway in a previous study, which varied between 17.5 cm and 21.0 cm (Clouse, 2006). The lower and upper soil water limits and saturated hydraulic conductivity used in this study were also within the range of values estimated using pedotransfer functions by Nelson et al. (2013) for this study site.

Table 2.4 Soil hydraulic and physical properties used in the DSSAT simulations.

Depth (cm)	SLLL ($cm^3\ cm^{-3}$)	SDUL ($cm^3\ cm^{-3}$)	SSAT ($cm^3\ cm^{-3}$)	SBDM ($g\ cm^{-3}$)	SSKS ($m\ s^{-1}$)	SRGF
0–5	0.13	0.23	0.41	1.48	7.2×10^{-6}	1.0
5–15	0.13	0.23	0.41	1.48	7.2×10^{-6}	1.0
15–30	0.17	0.29	0.43	1.44	1.2×10^{-6}	0.6
30–45	0.20	0.31	0.43	1.44	6.4×10^{-7}	0.5
45–60	0.22	0.34	0.43	1.44	6.4×10^{-7}	0.4
60–90	0.21	0.32	0.43	1.45	6.4×10^{-7}	0.2
90–120	0.20	0.31	0.42	1.48	6.4×10^{-7}	0.1
120–150	0.20	0.30	0.41	1.51	6.4×10^{-7}	0.1
150–180	0.20	0.30	0.41	1.51	6.4×10^{-7}	0.0
180–210	0.20	0.30	0.41	1.51	6.4×10^{-7}	0.0

SLLL = soil water lower limit, SDUL = drainable upper limit, SSAT = saturation, SBDM = bulk density, SSKS = saturated hydraulic conductivity, SRGF = soil root growth factor

2.3.4. Model Calibration and Evaluation

The CERES-Sorghum and CROPGRO-cotton modules of the DSSAT-CSM were calibrated against the measured data from the "High" irrigation treatments, because it is recommended to calibrate the DSSAT CSM under no-stress conditions (Boote, 1999). Measured data from the "Base" and "Low" irrigation treatments were then used for model evaluation. New sorghum and cotton cultivars, "DK Halfway" and "FiberMax Halfway TX", respectively were added to the DSSAT cultivar database to represent the medium maturity sorghum and early maturity cotton varieties used in the field experiments. A step-wise manual calibration was carried out in three phases by changing one cultivar or ecotype parameter at a time.

Initially, sorghum cultivar parameters were adjusted to get a reasonable match between simulated and generally observed dates of onset of crop growth stages, followed

by adjusting several other parameters to match simulated yields with measured sorghum yields. After obtaining a satisfactory calibration for sorghum, cotton parameters were adjusted first according to the dates of onset of crop growth stages and then seed cotton yields. Lastly, both cotton and sorghum cultivar parameters and initial field moisture and nitrogen concentration were fine-tuned simultaneously to get an overall good match of crop yields with the measured data. Measured data on initial soil conditions (soil water and nitrogen contents at the beginning of first growing season in the cropping sequence) were not available and therefore they were decided during the model calibration. Simulation start date was set at about 50 days before the planting date and this spin-up period allowed stabilization of soil water and nutrient contents as a result of rainfall received and irrigation water applied before planting, and thereby reduced the effect of bias resulting from defining initial soil conditions (Müller and Robertson, 2013). The measured seed cotton and grain sorghum yields were reported at 8% and 13% seed and grain moisture content, respectively. Therefore, measured seed cotton and grain sorghum yields were reduced by 8% and 13%, respectively, since DSSAT simulates dry weight (Araya et al., 2017).

For grain sorghum, additional evaluation for seasonal irrigation water use efficiency (IWUE, Equation 2.1) was performed. For calculating IWUE, dryland grain sorghum yields were simulated by mimicking dryland experiments conducted at Halfway. The planting density was equal to that of the "low" irrigation treatment. Fertilizer amounts were average of those applied at Halfway during the 2001–2008 period (Bordovsky et al., 2011).

$$\text{IWUE} = \left[\frac{Irrigated\ Yield - Dryland\ Yield}{Seasonal\ Irrigation}\right] \quad (2.1)$$

2.3.5. Performance Statistics

Model performance during the calibration and evaluation was evaluated using four quantitative statistical performance indicators (Adhikari et al., 2016) and graphical techniques. The statistical indicators used are percent error (*PE*), percent root mean square error (*%RMSE*), coefficient of determination (R^2), and index of agreement (*d*) as given in Equations 2−5:

$$\text{PE} = \left(\frac{\hat{\text{Y}} - \bar{\text{Y}}}{\bar{\text{Y}}}\right) \times 100 \quad (2.2)$$

$$\%\text{RMSE} = \sqrt{\frac{\sum_{i=1}^{N}\left(\hat{Y}_i - Y_i\right)^2}{N}} \times \frac{100}{\bar{Y}} \quad (2.3)$$

$$R^2 = \frac{\left\{\sum_{i=1}^{N}\left[(Y_i - \bar{Y}) \times (\hat{Y}_i - \hat{Y})\right]\right\}^2}{\left[\sum_{i=1}^{N}(Y_i - \bar{Y})^2\right] \times \left[\sum_{i=1}^{N}(\hat{Y}_i - \hat{Y})^2\right]} \quad (2.4)$$

$$d = 1 - \frac{\sum_{i=1}^{N}\left(\hat{Y}_i - Y_i\right)^2}{\sum_{i=1}^{N}\left(\left|\hat{Y}_i - \bar{Y}\right| + \left|Y_i - \bar{Y}\right|\right)^2} \quad (2.5)$$

where $\hat{Y}_i$ and Y_i are the i^{th} simulated and measured values, respectively, with i varying from 1 to N. N is number of observations, and $\hat{Y}$ and $\bar{Y}$ are the averages of simulated and measured crop yields, respectively.

PE varies between −100 to ∞. *%RMSE* ranges from 0 to ∞, and it indicates the average magnitude of the difference between measured and simulated values. A value of *PE* and *%RMSE* closer to zero indicates a better fit. Model performance in this study was considered as excellent, if %RMSE < 10; good, if 10 < %RMSE < 20; fair, if 20 < %RMSE < 30; and poor, if %RMSE > 30 (Bannayan and Hoogenboom, 2009; Jamieson et al.,

1991). We have aimed to achieve good model performance during both calibration and evaluation periods. R^2 varies from 0 to 1 with a value of 1 representing a perfect fit between two series. The *d* ranges between 0 to 1 with 1 representing a perfect agreement between the two series. Model calibration was carried out until *PE* and *%RMSE* between measured and simulated yield were < 15%, and *d* was > 0.5.

2.3.6. Irrigation Management Scenarios

A seasonal project was created with the evaluated DSSAT-CSM CERES-Sorghum model to study the effects of variability in historical climate and deficit irrigation strategies on grain sorghum yield and water use, and to determine optimum soil moisture at planting and optimum soil moisture threshold for initiating irrigation. A total of four volumetric soil water contents at planting, 25%, 50%, 75%, and 100% of AWC in the top 2.1 m soil profile were considered in the simulations. Irrigated yield, dryland yield, total irrigation water applied, irrigation water use efficiency (IWUE, Equation 2.1), and grain water use efficiency (WUE, Equation 2.6) were computed for each scenario. These initial soil moisture (ISM) scenarios were referred to as ISM 25, ISM 50, ISM 75, and ISM 100 with the numeric value representing percent of AWC.

$$\mathrm{WUE} = \left[\frac{Irrigated\ Yield}{Seasonal\ Evapotranspiration}\right] \tag{2.6}$$

After deciding an optimum ISM based on yields, irrigation water use, IWUE, and WUE, the effects of soil moisture threshold for initiating auto-irrigation (ITH) were analyzed by keeping the ISM at the selected optimum value. In these simulations, the ITH was varied by varying the soil water lower limit and keeping the soil water upper limit

constant at 100% of AWC. The ITHs tested include 30%, 40%, 50%, 60%, 70%, and 80% of AWC, similar to the approach followed by Kisekka et al. (2016) for corn. For example, the ITH 30 scenario indicates that auto-irrigation was triggered when water in the soil profile was depleted to 30% AWC and refilled to 100% AWC. Finally, various deficit/excess irrigation strategies to replenish soil water up to 55%, 70%, 85%, 100%, 115%, and 130% of AWC were simulated by keeping the ITH and ISM at the optimum values determined in preceding steps. These scenarios were designated as DFI followed by a numeral that represents the targeted final percent of AWC (DFI 55 to DFI 130). These scenarios were created by first determining the "average daily" irrigation water (~ 21 mm) required to fill the soil profile from the optimum ITH to 100% AWC (DFI 100) using the "automatic when required" auto-irrigation option. The estimated DFI 100 average daily irrigation depth was then increased/decreased proportionately for other DFI scenarios, and applied using the "fixed amount automatic" auto-irrigation option.

2.4. Results and Discussion

2.4.1. Model Calibration and Evaluation

2.4.1.1. Phenological Stages

Parameters adjusted during the calibration of CERES-Sorghum and CROPGRO-Cotton modules are shown in Tables 2.5 and 2.6, respectively. The simulated dates of onset of cotton and sorghum growth stages during the calibration and evaluation were close to the observed dates for cotton (Adhikari et al., 2016; Kerns et al., 2009) and sorghum (Gerik et al., 2003; McClure et al., 2010) in the THP region (Table 2.7). In 2014,

cotton did not reach physiological maturity, as it was planted late (i.e., it was replanted after the first cotton stand was damaged during heavy rains), and freezing temperatures (<0 °C) were encountered during the reproductive growth stage (data not shown). Nonetheless, the freezing date was close to the actual harvest date at Halfway, TX.

Table 2.5 Parameters adjusted during CSM-CERES-Sorghum model calibration.

Parameter	Description	Testing range	Calibrated value
P1	Thermal time from seedling emergence to the end of the juvenile phase (expressed in degree days above TBASE, i.e., 8 °C)	317–495	334
P2	Thermal time from the end of the juvenile stage to tassel initiation under short days (degree days above TBASE)	80–102	102
P2O	Critical photoperiod or the longest day length (in hours) at which development occurs at a maximum rate	14.5–15.5	15.2
P2R	Extent to which phasic development leading to panicle initiation (expressed in degree days) is delayed for each hour increase in photoperiod above P2O	1–40	40
PANTH	Thermal time from the end of tassel initiation to anthesis (degree days above TBASE)	585–875	617.5
P3	Thermal time from to end of flag leaf expansion to anthesis (degree days above TBASE)	152.5–200	152.5
P4	Thermal time from anthesis to beginning grain filling (degree days above TBASE)	81.5–190	81.5
P5	Thermal time from beginning of grain filling to physiological maturity (degree days above TBASE)	350–670	575
PHINT	Phylochron interval; the interval in thermal time between successive leaf tip appearances (degree days)	49–65	49
G1	Scaler for relative leaf size	0–22	3.5
G2	Scaler for partitioning of assimilates to the panicle (head)	6–8	7

Table 2.6 Parameters adjusted during CSM-CROPGRO-Cotton model calibration.

Parameter	Description	Testing range	Calibrated value
Cultivar parameters			
EM-FL	Time between plant emergence and flower appearance (photothermal days)	34–44	38
FL-SH	Time between first flower and first pod (photothermal days)	3–8	5
FL-SD	Time between first flower and first seed (photothermal days)	6–13	12
SD-PM	Time between first seed and physiological maturity (photothermal days)	38–50	40
FL-LF	Time between first flower and end of leaf expansion (photothermal days)	55–75	65
LFMAX	Maximum leaf photosynthesis rate at 30 C, 350 vpm CO_2, and high light (mg CO_2 m^{-2} s^{-1})	1.1–1.7	1.3
SLAVR	Specific leaf area of cultivar under standard growth conditions (cm^2 g^{-1})	160–175	170
SIZLF	Maximum size of full leaf (three leaflets) (cm^2)	250–320	250
XFRT	Maximum fraction of daily growth that is partitioned to seed + shell	0.7–0.9	0.8
SFDUR	Seed filling duration for pod cohort at standard growth conditions (photothermal days)	24–35	29
PODUR	Time required for cultivar to reach final pod load under optimal conditions (photothermal days)	8–12	8
THRSH	Threshing percentage. The maximum ratio of (seed/(seed+shell)) at maturity	65–70	70
Ecotype parameters			
RWDTH	Relative width of this ecotype in comparison to the standard width per node	0.8–1	0.9
RHGHT	Relative height of this ecotype in comparison to the standard height per node	0.85–0.95	0.9
FL-VS	Time from first flower to last leaf on main stem (photothermal days)	40–65	65
LNGSH	Time required for growth of individual shells (photothermal days)	6–12	9
TRIFL	Rate of appearance of leaves on the mainstem (leaves per thermal day)	0.20–0.25	0.25

Table 2.7 Comparison of simulated and generally observed sorghum and cotton phenological stages during calibration and evaluation.

Phenological stage	Observed (days after planting)	Simulated (days after planting)			
		Calibration (High water treatment)		Evaluation (Base and low water treatments)	
SORGHUM		Range	Average	Range	Average
Emergence[a]	5–10	5–7	6	5–7	6
Panicle Initiation[a]	35–40	29–35	31	29–35	31
End Leaf Growth[b]	59	57–65	60	57–65	60
Anthesis[a]	64–70	65–74	69	65–74	69
Physiological Maturity[a]	101–115	107–117	111	107–117	111
COTTON					
Emergence[c]	4–9	6–12	8	6–12	8
First Leaf[d]	11–25	12–18	14	12–18	15
Anthesis[c]	60–70	58–64	61	58–65	61
Physiological Maturity[c]	130–160	133–167	148	129–160	144
Harvest[e]	151–188	143–177	158	139–170	154

[a](Gerik et al., 2003); [b](McClure et al., 2010); [c](Adhikari et al., 2016); [d](Kerns et al., 2009) ; [e](TALR, 2016)

2.4.1.2. Crop Yields

There was an acceptable agreement between simulated and measured crop yields at Halfway (Figure 2.4) as indicated by average *PE* of 1.3% and 3.4% for sorghum and cotton, respectively, during calibration (Table 2.8). The maximum *PE* for grain sorghum yield was 15% in the year 2007, which substantially lowered R^2 value during the calibration period. Higher *PE* was obtained in 2007 because a medium-early maturity variety, DKS 37-07 (Schnell et al., 2015) was planted in that year as opposed to the medium maturity varieties that were planted in other years and targeted during calibration. Differences in sorghum yields between these two varieties have also been reported in

sorghum variety trials in Texas (TALR, 2014), Virginia (Balota et al., 2013), and New Mexico (Marsalis et al., 2015). The over-prediction of seed cotton yield in 2008 could be due to the carry-over effect from the previous year. Over-prediction of sorghum residue in the previous year most likely resulted in overestimation of soil organic carbon (SOC) (Soler et al., 2011) and soil nitrogen (N) (Havlin et al., 1990). Higher SOC is generally associated with higher seed cotton yields (Mitchell and Entry, 1998). On the other hand, sorghum is reported to uptake high N and thereby reduce soil nitrate-N levels (Booker et al., 2007), which is consistent with this study. The depleted nitrate-N during the growing seasons was stabilized by fertilization, and no nitrogen stress was simulated in any cotton years (data not shown). The underestimation of seed cotton yield in 2014 could be explained due to the freeze damage. The average measured and simulated dry grain sorghum yields during the calibration were 8513 kg ha^{-1} and 8623 kg ha^{-1}, respectively. The average measured and simulated seed cotton yields during the calibration were 3546 kg ha^{-1} and 3666 kg ha^{-1}, respectively.

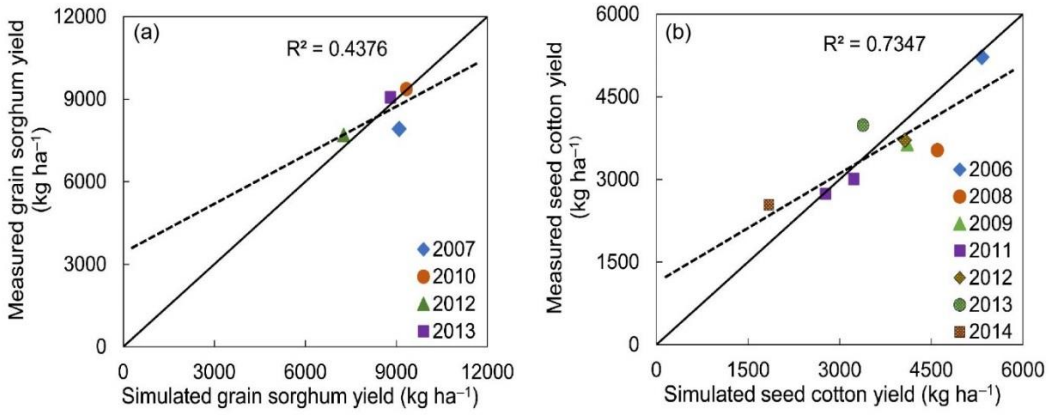

Figure 2.4 Comparison of measured and simulated (a) grain sorghum and (b) seed cotton yields at Halfway during model calibration for the "High" water treatment. The solid line is 1:1 line and the dashed line is ordinary least-squares linear regression line.

Table 2.8 Model performance statistics during the DSSAT CSM Evaluation for crop yield simulation.

Criteria	Calibration (High water)	Evaluation (Base and Low water)
Sorghum		
Number of observations	4	8
Average PE	1.3	–2.2
%RMSE	7.6	16.3
d	0.82	0.96
Cotton		
Number of observations	8	16
Average PE	3.4	–10.5
%RMSE	15.5	25.9
d	0.90	0.94

PE = percent error, RMSE = root mean square error, d = index of agreement

Although the model performance during the calibration (high water treatment) was good, results were not as good for cotton under water-limiting conditions during evaluation and resulted in an average *PE* of –10.5% (Figure 2.5 and Table 2.8). This is similar to previous studies (Modala et al., 2015; Nouna et al., 2000; Thorp et al., 2014), which reported unsatisfactory model performance under dry conditions. Nouna et al. (2000) have also reported an underestimation in maize yields under water-stress conditions largely due to inadequate simulation of soil water deficits and leaf area, using the CERES-Maize model. More recently, (DeJonge et al., 2012; Thorp et al., 2014) have also reported unsatisfactory performance of the ET routines currently available in the DSSAT-CSM under water stress conditions. ET was calculated using the FAO-56 method (Allen et al., 1998) option available in DSSAT. Leaf area, soil moisture, biomass and ET were not measured during the field experiments, hence their simulation accuracy could

not be evaluated. The simulated maximum leaf area index (LAI) for grain sorghum (5.56 m^2 m^{-2}) and cotton (3.33 m^2 m^{-2}) were within the range of reported values in the THP region (Adhikari et al., 2017; Howell et al., 2008). The CERES-Sorghum model performance was markedly poor in the year 2012 for low irrigation treatment during evaluation, which was preceded by a severe drought year in 2011. In general, there is a potential for error propagation in the "sequence" analysis due to continuous long-term simulation of soil processes (Bowen et al., 1998). Relatively poor model performance during the model evaluation suggests that error propagation was more prominent under resource-limiting conditions. Additional performance statistics that indicate the robustness of the model evaluation (Willmott, 1981) are reported in Table 2.8.

As absolute values of sorghum yields were much higher as compared to seed cotton yields, *PE* is not an appropriate measure for comparing performances of CERES-Sorghum and CROPGRO-Cotton modules of DSSAT. In addition, *PE* is sensitive to the large error values, therefore, normalized RMSE (*%RMSE*) values were also calculated to assess model performance. Further, the *d*-statistic was estimated between measured and simulated yields to assess overall model performance, as it is widely used to report crop model performance (Palosuo et al., 2011; Sau et al., 2004; Timsina et al., 2008).

The *%RMSE* in simulation of crop yield was the lowest (7.6%) during sorghum calibration and the highest (25.9%) during cotton evaluation (Table 2.8). In contrast, *d*-statistic during sorghum calibration was found to be lowest (0.82) amongst both cotton and sorghum evaluations. This was due to the limited number of observations and higher magnitude of error in sorghum yield simulation in the year 2007 during calibration.

Overall, based on model performance statistics, it can be concluded that the DSSAT cotton and sorghum modules simulated crop yields with reasonable accuracy in well-watered conditions.

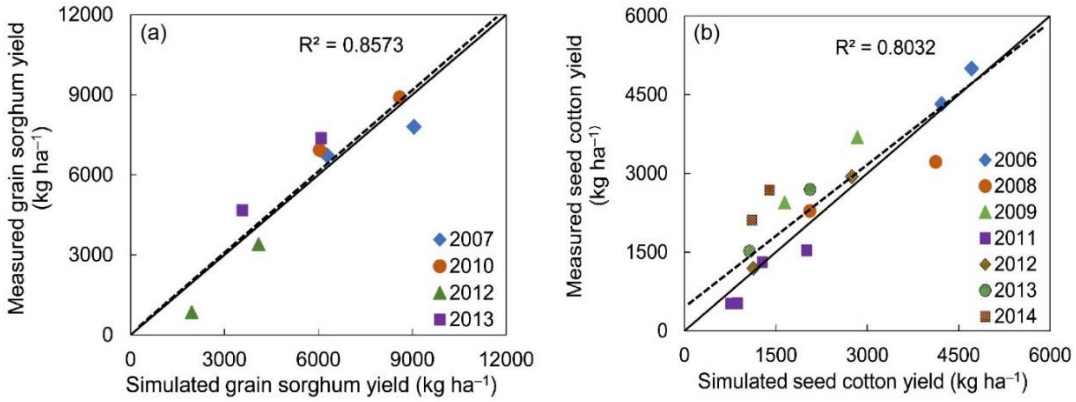

Figure 2.5 Comparison of measured and simulated (a) sorghum and (b) seed cotton yields at the Helms Farm during the model evaluation for the "Base" and "Low" water treatments.

2.4.1.3. Irrigation Water Use Efficiency (IWUE)

The simulated IWUEs for grain sorghum were close to the measured values (except for the year 2007) with an average *PE* of 7.4% (Figure 2.6). A difference larger difference in maturity and yield traits of the variety used in 2007 compared to the remaining three years was most likely the reason due to the poor model performance in 2007. This limits the extrapolation of current results to other grain sorghum varieties that are different from the medium maturity varieties (DKS 44-20 and DKS 49-45) simulated in this study. The underestimation of IWUE in the year 2010, especially under base and low irrigation treatments, is likely due to over-prediction of dryland grain sorghum yield in 2010 (data not shown).

Although the DSSAT model was successfully evaluated against phenology, crop yield, and IWUE data available from three irrigation treatments over four sorghum and eight cotton growing seasons, non-availability of in-season data such as LAI, soil moisture, biomass and ET for model evaluation is one of the major limitations of this study. As suggested by He et al. (2017), evaluation of crop growth models against in-season data on crop growth and soil processes in addition to the end-of-the-season data such as crop yield is desirable to enhance confidence in model application, and hence future calibration efforts should focus on overcoming this limitation.

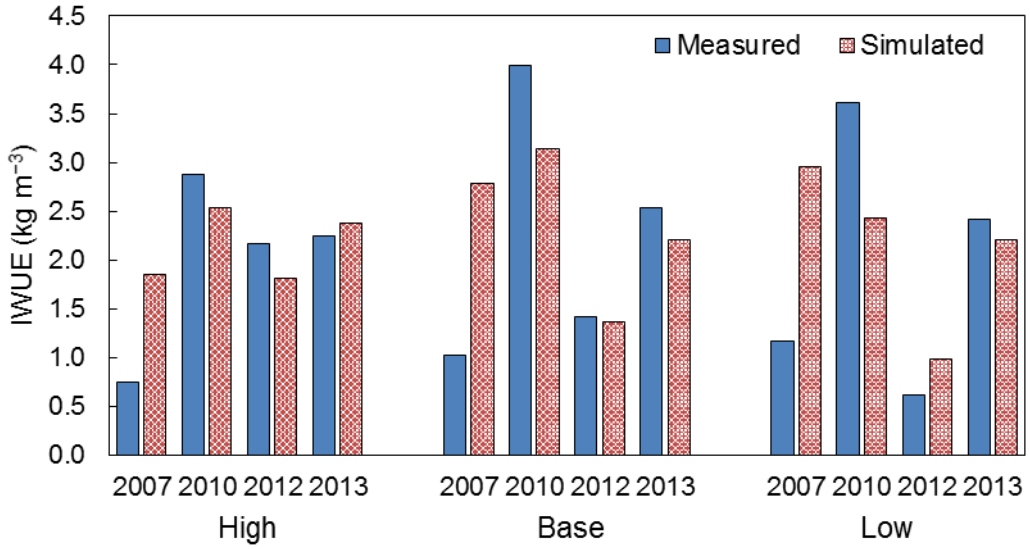

Figure 2.6 Comparison of measured and simulated grain sorghum irrigation water use efficiency (IWUE) under different irrigation treatments; High, Base, and Low, over four years.

2.4.2. Model Application

2.4.2.1. Crop *response to soil moisture at planting*

Irrigated grain sorghum yields under different ISM scenarios were comparable except for the ISM 25 scenario (Figure 2.8a). This suggests that irrigated sorghum yields

were not substantially affected by soil moisture at planting of ≥ 50% AWC. However, initial soil water content of ≤ 25% AWC (or 75% or more soil water depletion) could be detrimental to sorghum yields, especially during dry years. Under the ISM 25 scenario, 14% more irrigation water was applied and the grain sorghum yields were 6% and 2% lower when compared to the ISM 100 in dry and wet years, respectively. Simulated grain sorghum yields were the lowest under ISM 25 scenario, but the highest ISM did not result in the highest irrigated sorghum yields among all climate variability classes. Simulated sorghum yields were high under ISM 75 scenario in wet years (CW, NW, and WW) and under ISM 100 scenario in the remaining climate variability classes.

The probable reasons for differences in irrigated grain sorghum yields across climate variability classes were rainfall distribution pattern over the growing season and differences in length of the growing season (data not shown). The rainfall distribution over time affected irrigated grain sorghum yields by influencing nitrogen (N) leaching and N uptake by the plant. In the years 1982, 1992, and 2003, heavy rainfall events shortly after fertilizer application led to N leaching, which reduced simulated N uptake and hence simulated grain sorghum yields (Figure 2.7). This is consistent with the findings of Gérardeaux et al. (2013), who found that N uptake was the main driver of cotton yields simulated using the CROPGRO-Cotton model, and the negative correlation between excessive rainfall and cotton yields was attributed to N leaching. Although, there were no measurements at the field to confirm this relation, similar pattern has been reported in a field study (Errebhi et al., 1998) at Becker, MN, where heavy rainfall and subsequent N leaching events reduced N recovery and the marketable potato yield. In warm-dry years

(1980, 1998, 2001, and 2011), the crop matured about 12 days earlier than the average growing season. The shortening of growing season is known to reduce grain sorghum yields (Singh et al., 2014c).

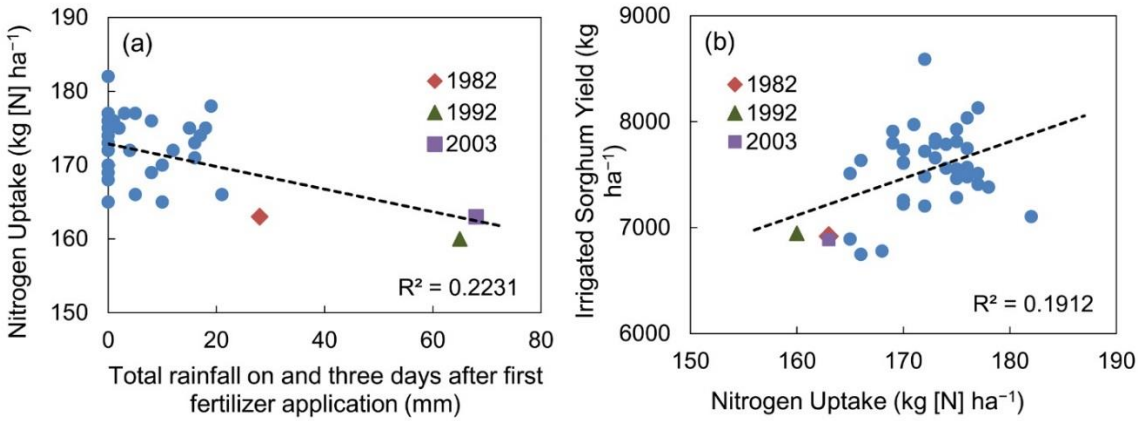

Figure 2.7 Relation between seasonal nitrogen uptake and (a) rainfall occurring on and three days after the first fertilizer application, and (b) irrigated grain sorghum yield, for the ISM 100 treatment. The dots represent years from 1977–2016.

Simulated dryland grain sorghum yields were about 10% (in WD) to 39% (in CW) of the irrigated sorghum yields (Figure 2.8b). As expected, the dryland sorghum yields decreased as the soil water at planting decreased. Dryland grain sorghum yields under ISM 25 scenario were about 55% lower than those under ISM 100 scenario. Dryland grain sorghum yields were 48% lower in normal years and 50% lower in dry years when compared to wet years. Cold weather was found to be more favorable for dryland sorghum than normal and warm temperatures. Dryland grain sorghum yields in warm years were 36% and 50% of that in cold years during dry and normal rainfall years, respectively. In wet growing seasons, simulated dryland grain sorghum yields were relatively stable among all temperature classes.

In general, sorghum IWUE was the highest under ISM 75 scenario (or 75% AWC) followed by ISM 50 (Figure 2.8c). IWUE was the lowest under ISM 100 in wet years (CW, NW, and WW), due to smaller difference between the irrigated and dryland sorghum yields in those years (resulting in smaller numerator in Equation 2.5). In the remaining climate variability classes, IWUE was the lowest under ISM 25 mainly due to higher irrigation applied compared to other ISM scenarios. Among climate variability classes, IWUE varied between 1.11 kg m^{-3} (CW) and 1.58 kg m^{-3} (CD). The comparatively higher than average IWUE in CD class is attributed to the low irrigation water applied (11% less than the average climate variability class). Although the irrigation applied is about the same (365 mm) in the CW class, it has a lower IWUE due to high dryland grain sorghum yields resulting in a smaller difference between irrigated and dryland sorghum yields. This is also true for other wet climate variability classes (NW and WW).

Grain sorghum WUE was the lowest under ISM 25 in all climate variability classes (Figure 2.8d). The WUE was the highest under ISM 100 in ND, CN, and WW climate variability classes, and under ISM 75 in the remaining climate variability classes. Like IWUE, sorghum grain WUE was also high in cold-dry (CD) years compared to other climate variability classes, this was due to substantially low ET (15% lower than average climate) compared to other climate variability classes. In a typical year in a climate variability class, ET did not change substantially (< 14 mm) under different ISM scenarios; therefore, the changes in WUE within ISM scenarios were due to the differences in irrigated grain sorghum yield. On the other hand, among the climate scenarios considered,

ET varied from −91 mm (−15%) to +42 mm (+7%) from the average. Therefore, changes in WUE were due to the combined effect of differences in ET and grain sorghum yield.

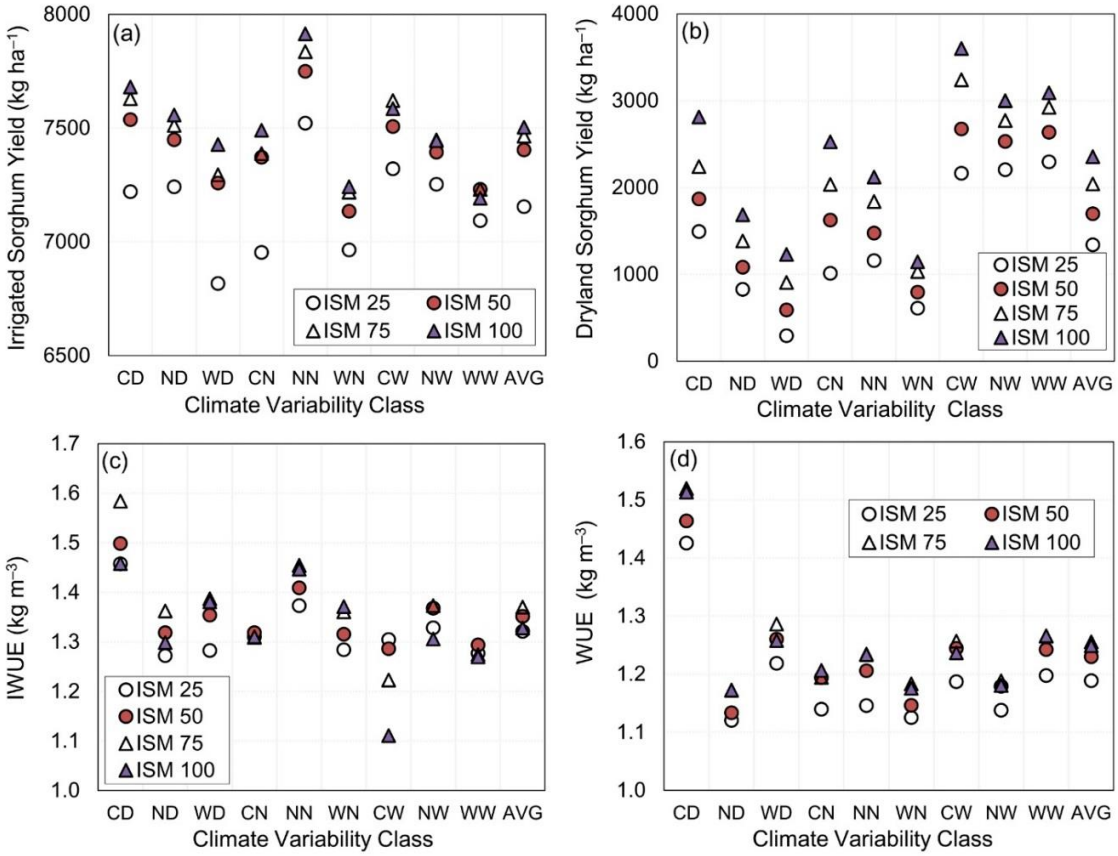

Figure 2.8 Grain sorghum (a) irrigated yields, (b) dryland yields, (c) irrigation water use efficiency, and (d) water use efficiency under different initial soil moisture (ISM) and weather conditions.

Overall, maintaining ISM at 75% AWC optimized irrigation water use without lowering grain sorghum yields substantially. In wet years, however, ISM at 50% is also an acceptable option. Soil water depletion below 25% AWC can negatively impact sorghum yields, especially in drought years. For dryland sorghum production, yield loss should be expected if ISM is < 75% AWC. Different conservation practices such as

conservation tillage and residue management that enhance soil water retention can help maintain adequate soil moisture at planting (Baumhardt and Jones, 2002). Conservation tillage has been estimated to increase available soil water around planting by 25 mm in the THP (Colaizzi et al., 2009). Unger (1978) reported over 20 cm increases in plant available soil moisture within the upper 1.8 m of soil profile by using straw mulch residue in Bushland, TX.

2.4.2.2. Crop response to the threshold to start irrigation

Among the six irrigation trigger thresholds studied, irrigated grain sorghum yields were low under the lowest ITH scenarios (ITH 30 and ITH 40) except in CD climate (Figure 2.9a). Although the simulated grain sorghum yields under ITH ≥50 scenarios were about the same (average difference 144 kg ha^{-1}) in a climate variability class, the ITH 70 scenario was found to be slightly better on average. The difference in simulated irrigated grain sorghum yield between the best and the least ITH scenarios was smaller in cold years (103 kg ha^{-1} in CN) compared to warm years (812 kg ha^{-1} in WD), suggesting that ITH decisions are critical in warmer years. Between ITH 50 and 60, the average difference in irrigated grain sorghum yields and applied irrigation was 80 kg ha^{-1} and 16 mm, respectively. In WD years, the irrigated sorghum yield difference between ITH 50 and 60 increased up to 466 kg ha^{-1} and additional 51 mm irrigation was required. In general, the effect of ITH on grain sorghum yield was much less when compared to that of soil moisture at planting (ISM) and hence ISM should be a key factor in the identification of optimum irrigation strategies.

Simulated irrigation amount required to maintain soil water at a minimum of 80%, 70%, 60%, 50%, 40%, and 30% of AWC in the top 30 cm soil profile was found to be 462, 436, 416, 402, 377 and 347 mm, respectively. Considering the annual groundwater pumping limit of 460 mm specified by the High Plains Water District (HPWD, 2015), ITH 80 does not seem practical for the THP region. The IWUE decreased as the amount of irrigation increased (Figure 2.9b), and this result is in accordance with the previous studies (Colaizzi et al., 2009; Hao et al., 2014; Tolk and Howell, 2003). In a climate variability class between ITH scenarios, the IWUE was consistently lower under ITH 70 (average 1.27 kg m^{-3}) and ITH 80 (average 1.19 kg m^{-3}) scenarios, suggesting that maintaining soil profile at ≥ 70% AWC is not efficient in terms of irrigation water use. The IWUE was highest under ITH 30 (average 1.52 kg m^{-3}) in all climate variability classes except WD, this was due to low irrigated sorghum yields under ITH 30 in WD climate. When grain sorghum IWUE were compared between climate variability classes, the highest and the lowest IWUE were simulated under CD (average 1.55 kg m^{-3}) and CW (average 1.20 kg m^{-3}) classes, respectively.

Similar to IWUE, the simulated grain sorghum WUE decreased as the amount of irrigation increased (Figure 2.9c). Irrigated grain sorghum yields and seasonal ET varied within 11% and 23% of the average between irrigation scenarios, respectively. This suggests that variation in WUE could be explained due to changes in ET. This result is consistent with Tolk and Howell (2003), who had also attributed increases in WUE in milder climates to the reduction in ET rather than the increase in sorghum yield. Simulated

ET was the lowest in the cold-dry (CD) weather and hence the WUE for this climate variability class was the highest (Figure 2.9c–d).

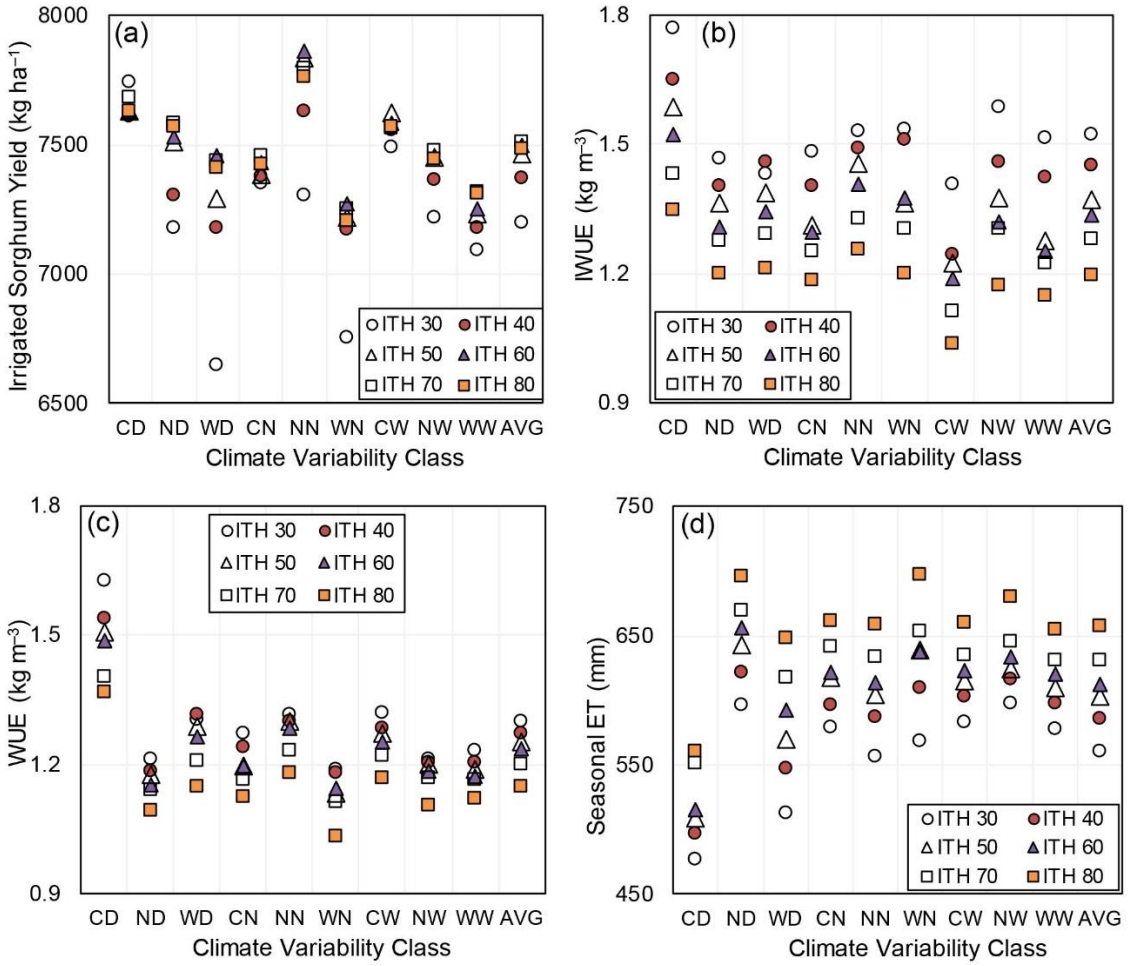

Figure 2.9 Grain sorghum (a) irrigated yields, (b) IWUE, (c) WUE, and (d) seasonal ET under different thresholds to start irrigation (ITH) and climate variability classes.

Overall, based on the simulated sorghum yield, IWUE and WUE, ITH 50 and ITH 60 were found to be appropriate thresholds for triggering irrigation in normal/cold/wet weather conditions (CD, ND, CN, NN, WN, CW, NW, and WW) and warm-dry years (WD), respectively. Although the IWUE and WUE for ITH 30 and ITH 40 were higher

under most weather conditions, those two thresholds were not recommended due to poor/low irrigated sorghum yields. In the subsequent deficit irrigation simulations, a better threshold of ITH 50 was used.

2.4.2.3. Crop response to deficit/excess irrigation

The DFI 115 and 130 scenarios resulted in the highest grain sorghum yield in the majority of climate variability classes, suggesting that replenishing the soil profile up to 15 to 30% more than field capacity would result in slightly higher grain sorghum yields when compared to deficit irrigation (< DFI 100) strategies (Figure 2.10a). Direct comparison of the simulated results with results from field studies was a challenge because the highest amount of irrigation water applied in most of the field experiments in the THP (Kiniry and Bockholt, 1998; Porter et al., 1960; Schneider and Howell, 2000; O`Shaughnessy et al., 2014; W. Marek et al., 2016) was to replenish water to field capacity. An exception to this practice, to our knowledge, was a field study at Halfway in which researchers (Bordovsky and Lyle, 1996) tested deficit to excess irrigation strategies including 40%, 70%, 100%, and 130% of grain sorghum ET_c replacement over three years period, and they found that grain yields for irrigation treatments ≥70% ET_c were not significantly different. The simulated irrigated grain sorghum yields varied within a range of 39 to 240 kg ha^{-1} (1 to 3% of the DFI average) among the different DFI scenarios within a climate variability class. One of the reasons behind simulating smaller differences in sorghum yields across different DFI scenarios within a climate variability class could be the assumption of higher threshold of 50% to trigger irrigation (i.e. soil water content was

maintained at 50% AWC or higher at all times, which avoided any severe water stress). However, the maximum difference in simulated irrigated sorghum yield across all climate variability classes was found to be 585 kg ha^{-1} (8% of the average sorghum yield) between NN (highest) and WW (lowest) climate variability classes. The differences in simulated sorghum yield across DFI scenarios were primarily due to water stress especially during the reproductive growth stage of sorghum.

In general, IWUE decreased as irrigation water use increased, and this trend was consistent with previous studies (O`Shaughnessy et al., 2014; Hao et al., 2014; Tolk and Howell, 2003). Simulated IWUE was the least and second least under DFI 130 and DFI 115 under all weather conditions, respectively (Figure 2.10b). The simulated IWUE was higher for DFI≤85 than those in DFI >85 strategies by 6% (0.07 kg m^{-3}), 3% (0.05 kg m^{-3}), and 2% (0.03 kg m^{-3}) in wet, normal, and dry climate variability classes, respectively. However, the decreasing IWUE trend with increasing irrigation was not true for all the years simulated, especially the extreme dry years. This is likely due to reduced irrigated sorghum yields in DFI <85 scenarios, consistent with O'Shaughnessy et al. (2014), who have also reported higher IWUE when soil water was replenished to 55% of field capacity than when it was replenished to 80% of field capacity (the highest irrigation level tested), except in the drought year of 2011. The low IWUE under DFI ≥115 scenarios was due to excess irrigation water use, which did not always result in proportionate sorghum yield gains (Figure 2.10a). Among the nine climate variability classes, the simulated IWUE was the highest and the lowest in CD and CW climate variability classes, respectively. The average IWUE of dry and wet years was 1.41 kg m^{-3} and 1.29 kg m^{-3},

respectively. This supports the results of Musick and Dusek (1971), who reported higher IWUE when irrigation was applied in dry years.

Simulated WUE generally increased as irrigation amount increased (Figure 2.10c). The WUE was the least for DFI 55 in most climate variability classes. There was no systematic increasing or decreasing trend in IWUE from DFI 85 to DFI 130 in any climate variability class. The WUE was highest for different irrigation strategies under different climate variability classes: DFI 130 in case of CD and NN years; DFI 115 in CN, CW, and NW years; DFI 100 in WD and WW years; and DFI 85 in ND, and WN years. This could be attributed to the smaller difference in simulated irrigated grain sorghum yields and ET. Irrigated sorghum yields varied within 7% (498 kg ha^{-1}) and ET varied within 6% (36 mm) between the DFI strategies (Figure 2.10d). Simulated WUE among climate variability classes ranged between 1.18 kg m^{-3} (in ND) and 1.50 kg m^{-3} (in CD). A substantially higher WUE in CD years was due to low seasonal ET, which was 95 mm (16%) lower than the average ET.

Simulated average grain sorghum yields, IWUE, and WUE were the highest under DFI 130 and DFI 55, and DFI 85 strategies, respectively. During WD years, IWUE of DFI 100 was highest. Nonetheless, the DFI 85 strategy saved up to 22% irrigation water with a maximum of 6% yield loss compared to the DFI 130 strategy. In general, a DFI 85 scenario or replenishment of soil profile up to 85% AWC utilized irrigation water efficiently without substantially reducing grain sorghum yields. The DFI 85 strategy was therefore found to be an appropriate irrigation strategy during normal and wet years, and the DFI 100 during warm-dry years.

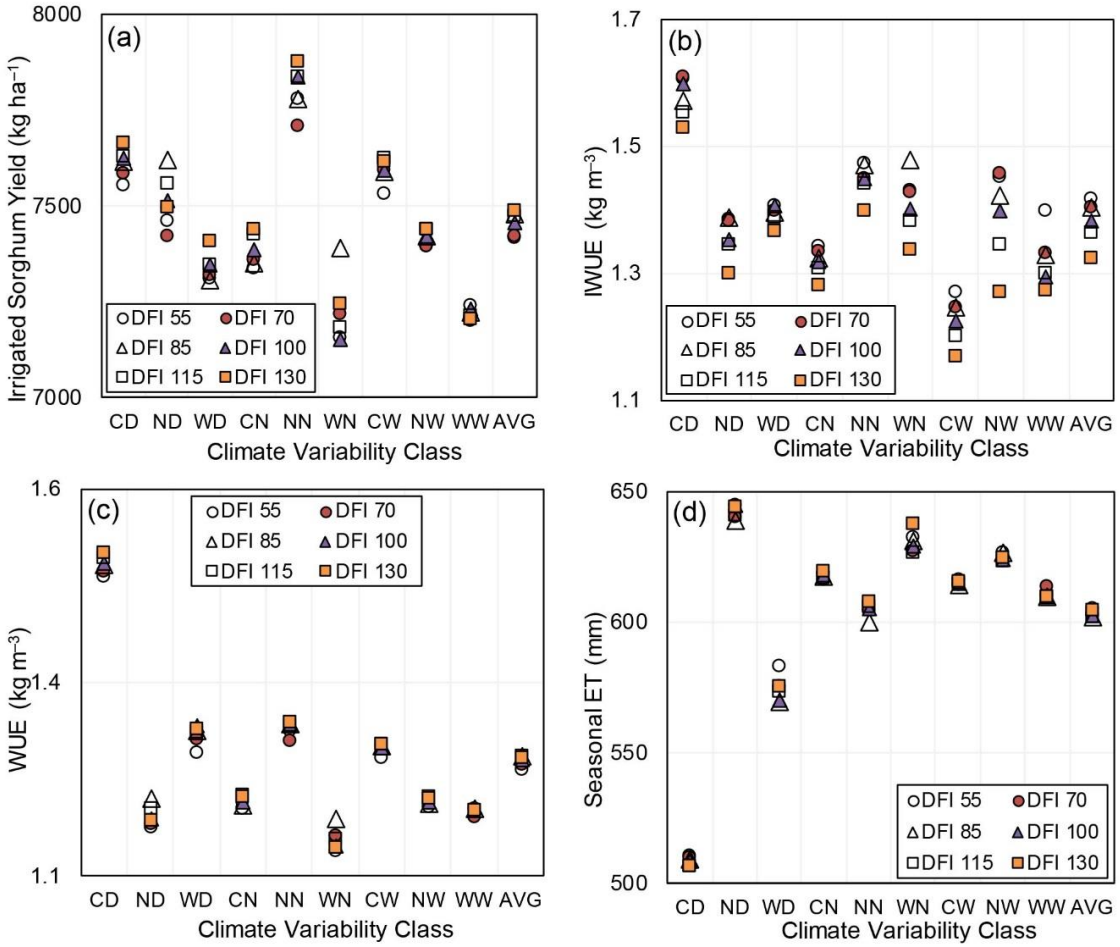

Figure 2.10 Grain sorghum (a) irrigated yields, (b) IWUE, (c) WUE, and (d) seasonal ET under different thresholds to terminate auto-irrigation (DFI) and weather conditions.

2.5. Conclusions

The CERES-Sorghum and CROPGRO-Cotton modules distributed with the DSSAT model were successfully evaluated using experimental data from a cotton-sorghum rotation at Halfway in the THP. Several irrigation management scenarios were then simulated to suggest optimum irrigation management decisions for grain sorghum production in the THP region. The differences in grain sorghum yield, IWUE, and WUE

were greater across climate variability classes than between irrigation scenarios, suggesting that grain sorghum production is highly susceptible to changes in climatic conditions. Simulated IWUE and WUE were consistently higher in cold-dry (CD) years, indicating that the most efficient use of applied irrigation water was achieved under CD conditions that are associated with less ET and smaller amount of excess water.

An initial soil water content (ISM) of 75% AWC was found to be optimum for irrigated sorghum production in the THP. For dryland sorghum production, ISM of less than 100% AWC (in normal to dry years) or 75% (in wet years) is expected to result in yield reduction. A threshold of 60% AWC to trigger irrigation is advisable in warmer and drier years, while a 50% AWC threshold is adequate in normal, cold and wet years. Applying irrigation water to refill the soil profile up to 85% AWC was found to be sufficient in normal and wet years, however, it would be desirable to replenish soil profile to field capacity or 100% AWC in warm and dry years. The recommendations on irrigation management made in this study were based on the magnitude and distribution of seasonal rainfall and temperature during the simulation period, and the effects of days with extreme hot/cold temperatures were not investigated. In addition, irrigation water was applied regularly to maintain soil water content at appropriate levels throughout the season, and hence the effect of water stress during critical growth stages (e.g. panicle initiation and boot stage) was not investigated. Our future efforts will focus on addressing these important issues. The methodology developed in this study is not site-specific, and it can be applied to other crops and geographical regions to design water-use-efficient irrigation schemes with some modifications.

3. ASSESSING THE CLIMATE CHANGE IMPACTS ON GRAIN SORGHUM YIELD AND IRRIGATION WATER USE UNDER FULL AND DEFICIT IRRIGATION STRATEGIES

3.1. Synopsis

Groundwater overdraft from the Ogallala Aquifer for irrigation use and anticipated climate change impacts pose a major threat to the sustainability of agriculture in the Texas High Plains (THP) region. In this study, DSSAT-CSM-CERES-Sorghum model was used for simulating grain sorghum production under different climate change, and full and deficit irrigation strategies. The simulated irrigation strategies were designed based on, i) grain sorghum growth stages, and ii) soil water depletion and replenishment.

For the first strategy, seven deficit irrigation and one full irrigation scenarios were simulated: three scenarios with a single 100 mm irrigation scheduled between panicle initiation to boot (T1), boot through early grain filling (T2), and between early and late grain filling (T3) growth stages; three 200 mm irrigation treatments, T4, T5, and T6, with combinations of T1 and T2, T1 and T3, and T2 and T3, respectively; One 300 mm irrigation scenario (T7) that was a combination of T1, T2, and T3; and a full irrigation scenario (T8) in which irrigation was applied throughout the grain sorghum growing season to maintain at least 50% of plant available water in the top 30 cm soil profile.

For the second strategy, the irrigation schedule obtained from auto-irrigation (T8) was mimicked to create a full irrigation scenario I100 and 6 deficit irrigation scenarios. In deficit irrigation scenarios, water was applied on the same dates as I100, however, the

irrigation amounts of I100 scenario were reduced by 10%, 20%, 30%, 40%, 50%, and 60% to create I90, I80, I70, I60, I50, and I40 deficit irrigation scenarios, respectively.

Projected climate forcings were drawn from 9 global climate models (GCMs) and two representative concentration pathways (RCPs 4.5 and 8.5), and they were statistically downscaled using the Multivariate Adaptive Constructed Analogs method. Climate change analysis indicated that the simulated grain sorghum yields under T8 treatment (full irrigation) are expected to reduce by 5% and 15%, by mid-century (2036–2065) and late-century (2066–2095), respectively under RCP 8.5 scenario with respect to the baseline period (1976–2005). Grain sorghum yields declined sharply beyond a growing season average temperature of 26°C, which is equivalent to 2°C temperature rise than the current conditions at Halfway. Simulated irrigation water demand of grain sorghum reduced due to improved dry matter- and yield-transpiration productivity, likely due to CO_2 fertilization.

Based on simulated grain sorghum yields and irrigation water use efficiency, the most efficient 100 mm and 200 mm deficit irrigation treatments were found to be T1 and T4, respectively, suggesting that the best use of limited irrigation could be achieved by applying irrigation during early reproductive stages of grain sorghum (panicle initiation through early grain filling). A 20% irrigation deficit (I80) could be optimal for current and future conditions. However, similar irrigation deficits could result in higher yield losses compared to full irrigation in the future than under current conditions.

3.2. Introduction

With a total cropland area of 5.4 million ha (Weinheimer et al., 2013), the Texas High Plains (THP) region contributed over $6.6 billion annually to the Texas economy, between 2008 and 2012 (Guerrero and Amosson, 2013). Irrigated agriculture in the THP is heavily dependent on the Ogallala Aquifer, which has been depleting at a much faster rate than its replenishment (Chaudhuri and Ale, 2014). Groundwater levels in the Ogallala Aquifer in Texas have declined on average by 11 m from 1950s to 2000s, with localized depletion exceeding 50 m (Scanlon et al., 2012). In order to extend the usable life time of the aquifer, the High Plains Underground Water Conservation District has set up a limit on the withdrawal of water from the aquifer for irrigation beginning January 2015 at 1.5 acre-feet per Contiguous Acre per year (45.7 cm) (HPWD, 2015). In view of the declining groundwater resources, the Agricultural Demands and Projections Committee formed under Texas Senate Bill 1 identified and evaluated seven water management strategies for the THP region, of which converting irrigated corn acreage to irrigated sorghum, cotton and soybean resulted in the maximum water savings (Amosson et al., 2005). Grain sorghum [*Sorghum bicolor* (L.) Moench] is gaining popularity in the region due to its high water-use efficiency, drought tolerance, and potential for ethanol production (Rooney et al., 2007). Only few studies (Bordovsky and Lyle, 1996; Eck and Musick, 1979; O`Shaughnessy et al., 2014; Tolk and Howell, 2003) have tested efficient irrigation strategies for grain sorghum production in the THP, and the impacts of climate change on grain sorghum production have not been studied doe the THP.

In a field study conducted at Halfway in the THP (Bordovsky and Lyle, 1996), grain sorghum response to different deficit/excess irrigation levels (preplant only irrigation to 130% crop evapotranspiration (ET_c) replacement) was evaluated over three growing seasons from 1992–1994. In these experiments, planting was done when soil water was near field capacity, and the grain sorghum yields varied between 3.54 Mg ha^{-1} (at preplant only irrigation) and 8.65 Mg ha^{-1} (at 247 mm seasonal irrigation). Similarly, in a field study in Bushland from 2009–2011 (O`Shaughnessy et al., 2014), several other deficit irrigation strategies were tested, which were designed based on moisture content in the top 1.5 m soil profile. The grain sorghum yields for the least (preplant only irrigation) and the highest irrigation amount (412 mm) strategies were measured to be 1.9 Mg ha^{-1} and 7.8 Mg ha^{-1} dry grain, respectively. These studies elucidated the effects of different irrigation schemes on grain sorghum yields, however, in these studies, the irrigation was applied at regular time intervals throughout the growing season. There is a scope for further improvement of irrigation water use efficiency for grain sorghum production by scheduling irrigation based on critical growth stages of grain sorghum instead of regularly applying throughout the growing season. Furthermore, predicting grain sorghum yield and irrigation under projected future climate change scenarios could assist sorghum growers in the THP and similar agroclimatic regions in the world in optimizing irrigation water use for sorghum production in the future.

Grain sorghum development can be divided into three distinct growth stages — GS I, GS II and GS III (Gerik et al., 2003). The GS I growth stage is characterized by the development of vegetative growth structures such as leaves and tillers. The GS II stage

spans from panicle initiation to anthesis/flowering (or boot stage). The stage when the final leaf (flag leaf) has fully expanded, is known as the "boot" stage. Water stress during boot stage impedes panicle exertion and reduces the number of florets and hence the number of grains. The GS III stage begins with flowering and continues until physiological maturity. After flowering, grain filling starts and the kernels undergo transformation from milk stage to soft dough to hard dough. Lewis et al. (1974) evaluated the effect of water deficit at different growth stages on grain sorghum yields at College Station, TX. They reported that water deficit during late vegetative to boot stage, boot through bloom, and milk through soft dough stage (early grain filling) resulted in a grain yield reduction of 17%, 34%, and 10%, respectively, compared to no water deficit treatment. In another field study at Bushland in the THP (Eck and Musick, 1979), a 14-day stress lowered grain sorghum yields by less than 7%, while a 28-day stress from boot through heading, heading through late grain filling, and early grain filling through maturity reduced grain yields substantially by 29%, 26%, and 12%, respectively.

Sweeten and Jordan (1987) reviewed multiple studies conducted in the THP region and suggested that if irrigation were restricted to only one 100 mm application during a sorghum growing season, the best use of irrigation water could be achieved by applying irrigation at either mid to late boot or heading to flowering stage. There has been no further research into irrigation scheduling for grain sorghum based on growth stages in recent years. Researchers in other regions (Craufurd and Peacock, 2008; Yadav et al., 2005) have also reported that the period from boot through early grain filling is critical for grain sorghum water use. These studies indicated that irrigation timing is crucial for maximizing

grain sorghum yields for the water applied. Quantification of the effects of applying different amounts of irrigation at critical growth stages on grain sorghum yields could thus assist in the development of efficient deficit irrigation strategies under current and projected future climatic conditions.

In the face of changing climate (IPCC, 2014), changes in crop growing conditions will impact crop yields and water requirement (Hatfield et al., 2011; Kimball et al., 2002). Climate model projections show that the rise in greenhouse gas emissions at accelerated rates (in the absence of mitigative and adaptive efforts) would increase global mean surface temperatures between 2.6 °C and 4.8 °C by the end of the 21st century relative to 1986–2005 (IPCC, 2014). Photosynthetic rates of C_4 plants including grain sorghum are saturated at current atmospheric carbon dioxide (CO_2) levels, and further increase in CO_2 should not theoretically stimulate crop yields (Leakey et al., 2006). However, the Free Air CO_2 Enrichment (FACE) experiments at Maricopa, AZ (Ottman et al., 2001) and open top field chamber studies at Auburn, AL (Prior et al., 2003) have shown mixed changes in grain sorghum yields with increasing CO_2. Grain sorghum yields under irrigated conditions either increased (+15%, Prior et al., 2003), remained about the same (+1%, Ottman et al., 2001), or decreased (–11%, Ottman et al., 2001), by doubling CO_2 concentration in these field experiments. In contrast, under low-water treatments, grain sorghum yields consistently increased by a greater extent than those under ample water conditions (+25%, Ottman et al., 2001). This was due to the improved water use efficiency of grain sorghum due to partial closure of stomata under higher CO_2 levels (Wall et al., 2001).

While FACE studies are useful in elucidating CO_2 effects on crop growth, the number of combinations considered are limited and the effect of temperature changes on crop growth is often not studied. Prasad et al. (2006) studied the interactive effect of elevated CO_2 and temperature on grain sorghum growth using outdoor soil-plant-atmospheric-research chambers with controlled air temperature and CO_2 in Gainesville, FL. They reported that under lower maximum/minimum temperature (32/22 °C) regimes, elevated CO_2 resulted in a 26% increase in seed yield, whereas under higher temperature (36/26 °C), elevated CO_2 reduced seed yields by 10%. They concluded that positive effects of elevated CO_2 on sorghum production diminished as temperatures increased. In addition to rising temperatures, climate models predict a decline in the rainfall in the THP region in the future (Modala et al., 2017), which further necessitate larger groundwater withdrawals to meet the higher crop water requirement, and hence raise further concerns about future groundwater availability for irrigation.

Recommendations on efficient irrigation strategies for grain sorghum that better adapt the crop to climate change while complying with groundwater pumping restrictions (HPWD, 2015) are therefore needed for the producers in the THP region in order to sustain grain sorghum production in the future. The Decision Support System for Agrotechnology Transfer (DSSAT), a process-based cropping system model (CSM) (Jones et al., 2003) is very useful for this purpose. DSSAT CSM has been widely used for developing and evaluating efficient irrigation strategies for cotton (Adhikari et al., 2016; Modala et al., 2015) in the THP and adjacent Texas Rolling Plains regions, and for studying the impact of climate change on various crops including grain sorghum (Fu et al., 2016; Singh et al.,

2014c). The specific objectives of this study were to: (i) assess the impacts of climate change on grain sorghum yield and irrigation water use under different future climate change scenarios, and (ii) suggest ideal deficit irrigation strategies under projected future climatic conditions.

3.3. Material and Methods

3.3.1. DSSAT-CSM-CERES-Sorghum Model

The CSM-CERES-Sorghum (Alagarswamy and Ritchie, 1991; White et al., 2015) module within the DSSAT (Jones et al., 2003) can reliably simulate sorghum growth and development over a wide range of environmental conditions and management practices. The subroutines of CSM-CERES-Sorghum are described in detail in White et al. (2015). Daily CO_2 assimilation is based on radiation use efficiency and photosynthetically active radiation. Stress factors related to soil water, nitrogen deficit, and temperature are included in the daily biomass calculation. Sorghum development stages are simulated based on daily thermal time (similar to growing degree days), assuming base and optimum temperatures of 8°C and 34°C, respectively. DSSAT allows four types of crop modeling analysis; experimental, seasonal, sequence, and spatial analysis, which are suitable for single crop studies, replications of "single growing season" with different input, continuous simulation of "multiple cropping seasons", and simulation over space, respectively (Thornton and Hoogenboom, 1994; Thornton et al., 1995). The DSSAT version 4.6 (Hoogenboom et al., 2015) was used in this study. The model inputs include

weather, soil, crop management and sorghum cultivar data. Seasonal analysis was used in this study to simulate long-term irrigation and climate change scenarios.

3.3.2. Study Area and Model Input

The THP region comprising 39 counties located in the Northwest Texas, is a semi-arid region with average (1981–2010) annual rainfall of 490 mm and temperature of 15°C (NOAA, 2018). In this study, DSSAT CSM was set up for one location close to the center of the THP: Halfway (34° 11' N, 101° 56' W, 1071 m aMSL) in Hale county. The soil at the study site is Pullman Clay Loam (Fine, mixed, superactive, thermic Torrertic Paleustolls). In this study, the DSSAT CSM CERES-Sorghum model that was evaluated as a part of Chapter II, was used. A detailed description of model inputs is included in that chapter. Crop management data for long-term grain sorghum simulations in this study were based on common practices adopted in the THP region (McClure et al., 2010), and they are similar to Kothari et al. (2019). Grain sorghum was planted on June 1, at 3.8 cm depth and 1.02 m row spacing. Planting seed rate of irrigated and dryland grain sorghum were 18 and 6 seeds m^{-2}, respectively. Amount of fertilizer applied for irrigated and dryland grain sorghum was 150 and 60 kg N ha^{-1}, respectively, applied in two splits on 20 and 40 days after planting. The seasonal analysis in DSSAT considers same user-specified initial conditions for soil water and nitrogen balance at the beginning of each growing season. In this study, initial nitrogen content was decided based on literature (Hao et al., 2014; Unger, 1991) as 100 kg N ha^{-1} and 45 kg N ha^{-1} for irrigated and dryland conditions, respectively. However, initial water content at different soil depths was

estimated by first running a sequence analysis with the same crop management practices, based on the methodology used by Tsvetsinskaya et al. (2003). In the sequence analysis, soil water and nutrient balances are carried over to the next season, and hence the resultant soil water balance from the sequence analysis provided a more realistic estimate of soil water at the simulation start date (about 80% of plant available water content), which was then used in the long-term (1950–2099) seasonal analysis.

3.3.3. Model Calibration and Evaluation

The DSSAT-CSM-CERES-Sorghum model was evaluated against cotton-grain sorghum field experimental data from irrigation experiments conducted at Halfway between 2006 and 2014 (TALR, 2016). More details about the model evaluation procedure is reported in Chapter 2 (Kothari et al., 2019). The dataset used for model evaluation included the dates of onset of growth stages, grain yield, and irrigation water use efficiency (IWUE) over four sorghum growing seasons. In the field experiment, irrigation water was applied at three levels: base (60–80% of crop evapotranspiration), high (20–50% higher than base), and low (20–50% lower than base) levels. For model calibration, crop yield data from "high" irrigation levels was used. For model evaluation, data from "base" and "low" levels was used. The simulated dates of onset of sorghum growth stages were within the range of typically observed onset of growth stages for a generic medium maturity grain sorghum in the THP. The simulated and measured grain yield matched closely during model calibration (average error 1.3%; root mean square error, RMSE, 7.6%) and evaluation (average error −2.2%; RMSE 16.3%). An average error of 7.4% was obtained

during the evaluation of IWUE. In summary, the model adequately simulated crop phenology, grain yield and IWUE during model evaluation under three irrigation levels and four growing seasons, indicating that the evaluated model could be used as a tool for assessing irrigation vs. environment interaction.

3.3.4. Climate Change Scenarios

Daily weather data projected from nine global climate models (GCMs), which were bias corrected and statistically downscaled using the Multivariate Adaptive constructed Analogs (MACA) technique (Abatzoglou and Brown, 2012) with training dataset of Abatzoglou (2013), were used in this study. This dataset has been used in multiple climate change studies in the United States (Cammarano and Tian, 2018; Elias et al., 2018; Karimi et al., 2018; Zhang et al., 2017). The climate variables in this dataset include minimum and maximum temperature (°C), precipitation (mm), solar radiation (MJ m^{-2}), wind speed (m s^{-1}), and relative humidity (%). The future climatic projections assumed two possible representation concentration pathways (RCPs) of greenhouse gas emissions, RCP 4.5 and RCP 8.5 (Van Vuuren et al., 2011). The annual atmospheric CO_2 levels were varied gradually from 380 ppm in 2005 to 544 ppm and 912 ppm in 2099 under RCPs 4.5 and 8.5, respectively, according to IPCC (2014). Historic atmospheric CO_2 concentrations were downloaded from the NOAA/ESRL portal (Keeling et al., 1976; Thoning et al., 1989).

3.3.5. Deficit Irrigation Scenarios

3.3.5.1. Deficit irrigation strategies based on critical growth stages

Deficit irrigation scenarios were developed based on grain sorghum water use in critical growth stages, i.e. reproductive growth stages (Assefa et al., 2010). Based on the recommendations of Sweeten and Jordan (1987), 100 mm irrigation was applied once, twice, or three times during the entire sorghum growing season. However, instead of applying 100 mm irrigation in a single application (Sweeten and Jordan, 1987), irrigation amount was split into four applications of 25 mm each and applied on four consecutive days during the growth stage considered, to avoid runoff and nutrient leaching. The DSSAT v 4.6 does not allow scheduling irrigation based on crop growth stages, and irrigation can either be applied on specified dates or automatically throughout the growing season using the auto-irrigation tool. In this study, irrigation was applied on specific dates assuming a growing season length of 100 days, which was decided based on long-term (2000–2099) DSSAT simulations using auto-irrigation with GCM projected climate data. Deficit irrigation scenarios considered in this study included applying irrigation during early reproductive stage (between panicle initiation and early boot, T1), boot to anthesis (T2), and during grain filling (T3) alone and combinations of the above three treatments (Table 3.1). In order to compare sorghum production under deficit and well-watered conditions, an additional well-watered irrigation scenario (T8) was simulated. In this scenario, when soil water in the top 30 cm soil profile dropped to 50% plant available water content, it was replenished to field capacity using the auto-irrigation feature in the DSSAT model.

Table 3.1 Irrigation scheduling under different deficit irrigation treatments (T), based on growth stages of grain sorghum.

Treatment	Total irrigation (mm)	Panicle initiation to boot (46–49 DAP[a])	Boot to early grain filling (61–64 DAP)	Early to late grain filling (82–85 DAP)
T1	100	x[b]		
T2	100		x	
T3	100			x
T4	200	x	x	
T5	200	x		x
T6	200		x	x
T7	300	x	x	x
T8	Varied	Soil profile maintained at 50% plant available water content at all times.		

[a] DAP refers to days after planting.
[b] 'x' indicates that irrigation was applied at a rate of 25 mm per day for four consecutive days.

3.3.5.2. Deficit irrigation strategies based on soil water depletion

The auto-irrigation tool used in the well-watered treatment (T8) generated an irrigation schedule i.e., dates of application and amount of irrigation for different years in the simulation period. This irrigation schedule was mimicked to create a full irrigation scenario I100, in which irrigation was applied on reported dates, using the same schedule. Deficit irrigation scenarios I90, I80, I70, I60, I50, and I40, were then created by using the same dates of irrigation application as I100, but reducing the irrigation amounts of I100 scenario by 10%, 20%, 30%, 40%, 50%, and 60%, respectively (Figure 3.1).

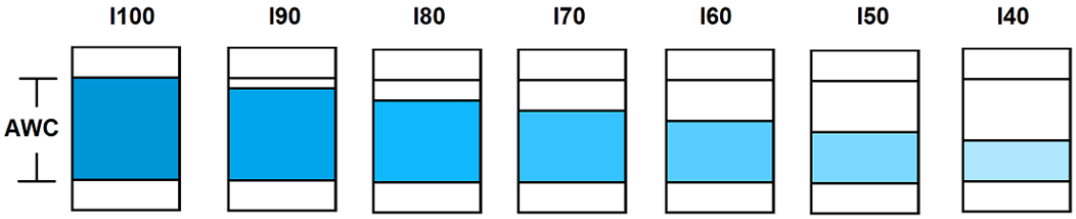

Figure 3.1 Schematic of different full and deficit irrigation scenarios (I). Columns represent soil profile, which was filled up to 100% plant available water content (AWC) in I100.

Various irrigation strategies simulated in this study were evaluated based on grain sorghum yield, irrigation amount applied, and irrigation water use efficiency (IWUE, Equation 3.1).

$$\text{IWUE} = \left[\frac{Irrigated\ Yield - Dryland\ Yield}{Seasonal\ Irrigation}\right] \quad (3.1)$$

3.4. Results and Discussion

3.4.1. Climate Change Impact on Grain Sorghum Production

The projected changes in grain sorghum growing season (Planting–Harvest) precipitation and average temperature in the mid-century (2036–2065) and late-century (2066–2095) periods as compared to the baseline period (1976–2005) are summarized in Table 3.2. The percent changes in simulated grain sorghum yield and irrigation water use for the well-watered irrigation treatment (T8) are presented in Figure 3.2. The differences between simulated grain sorghum yield in mid-century and baseline period varied between –8% and 3%, among the nine GCMs. These differences increased substantially (–31% to 0.4%) when grain sorghum yields for the late-century and baseline periods were compared. Under the RCP 4.5 scenario, the maximum reduction in grain sorghum yield

for the mid-century period was –6% under IPSL-CM5A-LR GCM, which had the second highest decline in seasonal rainfall (–70 mm) and the highest increase in average seasonal temperature (+3.6°C) compared to the baseline period among all GCMs (Table 3.2). Interestingly, simulated grain sorghum yield increased only under one GCM and one RCP scenario (GFDL-ESM2M, RCP 4.5 mid-century), for which changes in seasonal rainfall and temperature compared to the baseline were +15 mm and +1.4°C, respectively. Under the RCP 8.5 scenario for the late-century period, the maximum reduction in grain sorghum yield in the future was –31% under IPSL-CM5A-LR GCM, for which changes in seasonal rainfall and temperature were –125 mm and +7.1°C, respectively.

Overall, average (ensemble of GCMs) reduction in irrigated grain sorghum yield under RCP 4.5 was 3% and 5% in mid- and late-century periods, respectively. Under RCP 8.5, average yield loss was 5% and 15% in mid- and late-century periods, respectively. In general, grain sorghum yields decreased by a greater extent under RCP 8.5 compared to RCP 4.5, and in the late-century period than in mid-century, compared to baseline yields. Among the nine GCMs considered, GFDL-ESM2M was the most optimistic and IPSL-CM5A-LR was the worst-case GCM. Changes in irrigated grain sorghum yields (Figure 3.2) followed the pattern of changes in growing season average temperature (Table 3.2), as indicated by a high correlation (R^2=0.84) between the two (Figure 3.3a). This is consistent with a previous study (Fu et al., 2016), in which researchers concluded that grain sorghum yields were more sensitive to temperature than precipitation or CO_2. Rise in growing season temperature by 3°C resulted in irrigated grain sorghum yield loss up to

9%; whereas the temperature rise beyond 5°C resulted in more than 15% loss in irrigated grain sorghum yield, compared to the baseline yield.

Table 3.2 Comparison of total precipitation (P) and average temperature (T) during the sorghum growing season (planting–harvest) as projected by nine GCMs under two RCPs.

GCM	Mid-century (2036–2065)				Late-century (2066–2095)			
	RCP 4.5		RCP 8.5		RCP 4.5		RCP 8.5	
	ΔP (mm)	ΔT (°C)	ΔP (mm)	ΔT (°C)	ΔP (mm)	ΔT (°C)	ΔP (mm)	ΔT (°C)
BCC-CSM1.1	–66	3.1	–59	3.5	–64	3.1	–95	5.5
CCSM4	–77	2.9	–92	4.1	–70	3.7	–96	5.2
CNRM-CM5.1	–26	2.0	6	2.4	–18	2.7	–52	4.5
CSIRO-MK3.6	–16	3.1	–22	3.8	–9	4.0	–54	6.3
GFDL-ESM2M	15	1.4	36	1.7	17	1.9	–20	4.1
IPSL-CM5A-LR	–70	3.6	–63	4.0	–93	4.2	–125	7.1
MIROC5	–3	2.5	–22	2.8	–23	3.4	–17	5.1
MRI-CGCM3	1	1.7	–2	2.6	18	2.0	–19	4.5
NorESM1-M	–36	2.8	–61	3.9	–69	3.4	–73	5.0

ΔP and ΔT are changes in sorghum growing season precipitation (mm) and average temperature (°C) from the baseline, respectively.

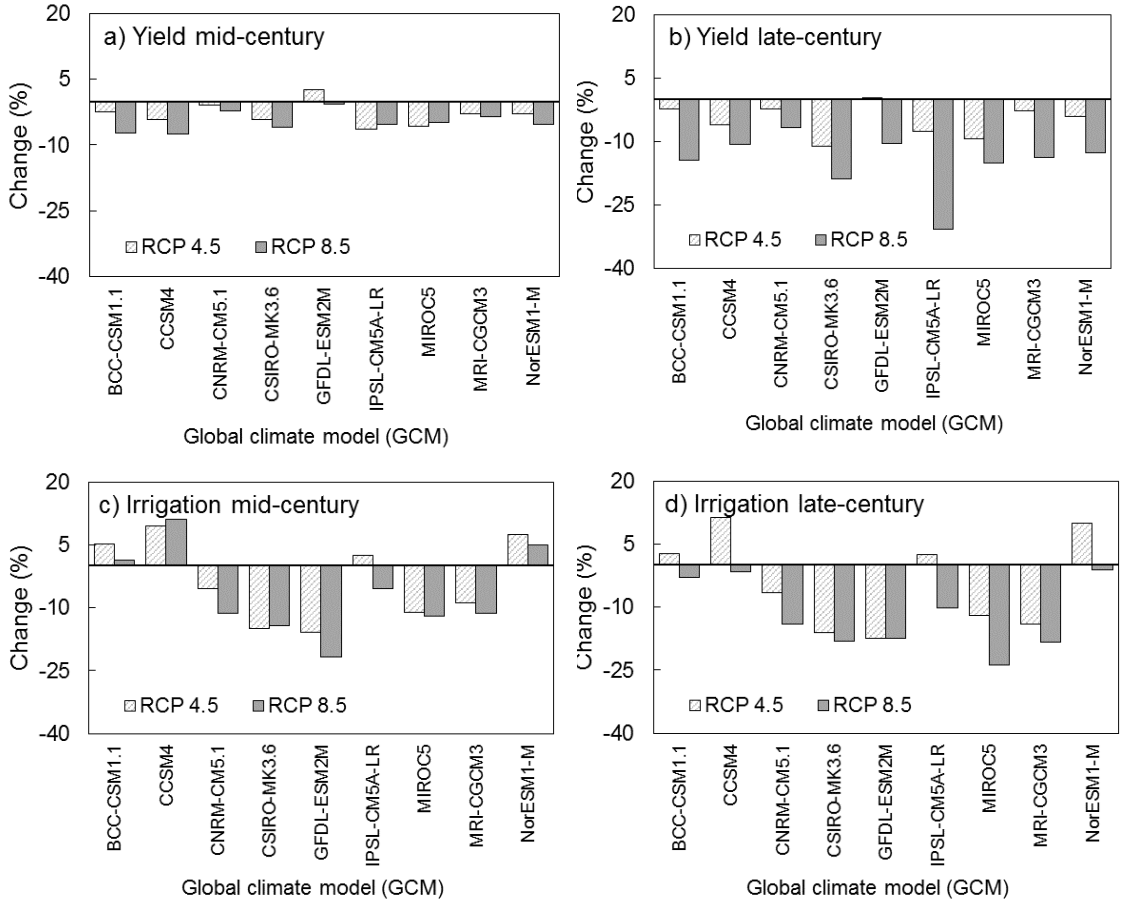

Figure 3.2 Simulated changes in grain sorghum yield (a. mid-century, and b. late-century) and irrigation water use (c. mid-century, and d. late-century) compared to the baseline period (1976–2005) with the future climate data projected by nine GCMs in case of T8.

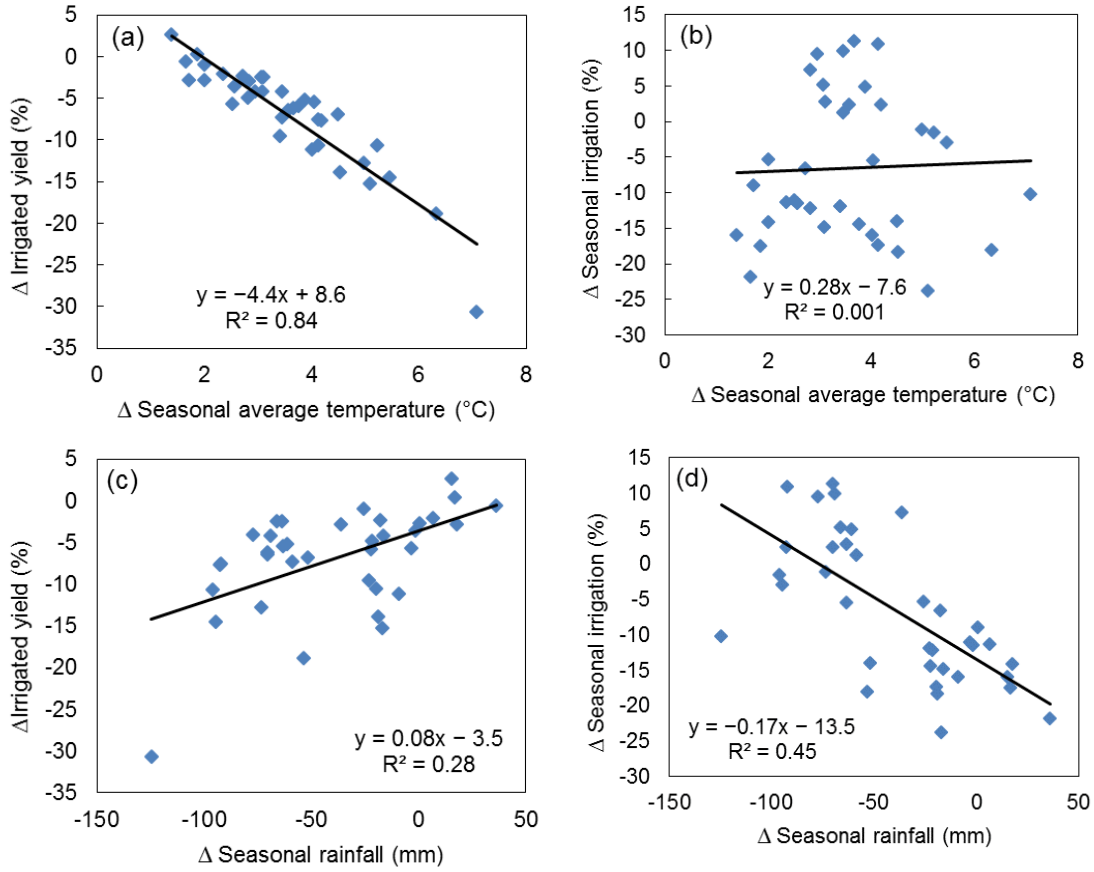

Figure 3.3 Relation between changes in—grain sorghum yield and irrigation water use in response to changes in growing season (Planting–Harvest) average temperature and rainfall—in the future (mid- and late-century) versus the baseline period, 2 RCPs×9 GCMs.

Most GCMs projected a decline in total growing season irrigation water use as simulated by the auto-irrigation tool (Figure 3.2c–d). The difference between simulated seasonal irrigation in the future and baseline periods varied between –22% and +11% among the climate projections made by different GCMs. Overall, ensemble average of change in irrigation water use in the future when compared to the baseline under RCP 4.5 was –4% in both mid- and late-century periods. Under RCP 8.5, average difference in irrigation water use was –7% and –12% in mid- and late-century periods, respectively

compared to the baseline. Unlike grain sorghum yield changes, which were highly correlated with growing season temperature changes; changes in irrigation water use could not be explained by changes in growing season air temperature (Figure 3.3b). Although seasonal rainfall changes were more correlated with irrigation water use changes than temperature changes were with irrigation; only 45% of the variation in irrigation demand fluctuations could be described by seasonal rainfall variations (Figure 3.3d).

Other researchers (Elliott et al., 2014; Konzmann et al., 2013) who have reported reduction in crop irrigation water use under climate change—attributed it to precipitation increase, shortening of growing season, and beneficial effects of CO_2 on crop water use efficiency. Water stress, temperature stress or higher than optimal temperatures, and reduced evapotranspiration have also been identified as potential reasons behind reduction in irrigation water demand under climate change for soybean and corn (Woznicki et al., 2015). In this study, grain sorghum growing season (Planting–Harvest) precipitation was higher in the future than in the baseline under three GCMs: CNRM-CM5.1 (under RCP8.5 scenario), GFDL-ESM2M (under both RCP4.5 and 8.5), and MRI-CGCM3 (under RCP4.5) (Table 3.2). However, reduction in irrigation water use despite rainfall reductions in the majority of the GCMs suggests that rainfall changes alone do not explain changes in irrigation water use.

In order to identify major drivers of irrigation water use, other DSSAT parameters/outputs including evapotranspiration, growing season length, number of days with temperature > 34°C, atmospheric CO_2 level, maximum leaf area index, nitrogen uptake, canopy weight at maturity, irrigation water productivity, and water stress factor,

were analyzed (Table 3.3). These time series included annual data from nine GCMs, two RCPs, and all of the simulated years (1950–2099) (data not shown).

Table 3.3 Correlation coefficient (r) and coefficient of determination (R2) between seasonal irrigation water use and several DSSAT outputs.

	Correlation coefficient (r)	Coefficient of determination (R^2)
Yield-irrigation productivity	−0.80	**0.50**
Dry Matter-transpiration productivity	−0.72	**0.53**
Dry Matter-irrigation productivity	−0.71	**0.50**
Seasonal (planting–harvest) rainfall	−0.69	**0.48**
Yield-transpiration productivity	−0.58	0.36
Yield-evapotranspiration productivity	−0.38	0.15
Grain yield	−0.13	0.02
Seasonal soil evaporation	−0.11	0.01
Seasonal nitrogen uptake	0.00	0.00
Seasonal average temperature	0.21	0.05
Days with maximum temperature > 34°C	0.31	0.10
Seasonal evapotranspiration	0.36	0.12
Seasonal transpiration	0.51	0.25
Water stress effect on photosynthesis	0.64	0.41
Water stress effect on growth	0.74	**0.54**

Based on coefficient of determination, R^2 (Legates and McCabe, 1999), at least 48% of variation in irrigation water use could be explained by—seasonal precipitation, yield-irrigation productivity (kg[yield] ha^{-1} mm[irrigation]$^{-1}$), dry matter-irrigation productivity, dry matter-transpiration productivity, and water stress factor. The Pearson's correlation coefficient (r) indicated a positive correlation ($r > 0.5$) between irrigation water use and—seasonal plant transpiration and water stress factor. Irrigation water use was negatively correlated ($r < -0.5$) to—seasonal precipitation, yield-irrigation productivity,

yield-transpiration productivity, dry matter-irrigation and dry matter-transpiration productivity. The relation between irrigation, rainfall, transpiration, and irrigation water productivity is direct, therefore, a strong correlation is expected between them. Other possible reasons for the reduction in irrigation water use under climate change ($0.2< |r| <0.5$) were—shorter growing season length, reduced maximum leaf area index, decreased canopy weight at maturity, and decline in seasonal evapotranspiration.

As discussed earlier, anticipated temperature rise in the future was the primary reason behind reduction in irrigated grain sorghum yield under climate change. A graphical analysis revealed that beyond a certain threshold of growing season average temperature, irrigated grain sorghum yields declined sharply (Figure 3.4a). This threshold was close to 26°C, which is 2°C more than the current growing season average temperature at Halfway, THP. A rapid decline in irrigated grain sorghum yield was simulated when the number of days with maximum temperature greater than 34°C exceeded 70 days (Figure 3.4b). The effect of growing season temperature threshold (~26°C) was also noticeable in grain sorghum irrigation water use (Figure 3.4c). Irrigation water use increased with temperature rise up to the threshold and declined on further temperature rise beyond the threshold. The temperature stress beyond the optimal/threshold temperature, which reduced sorghum grain yield, biomass, leaf area, and transpiration; combined with increased dry matter-transpiration and yield-transpiration productivity, most likely due to CO_2 fertilization, were identified as the possible reasons for grain sorghum irrigation demand reduction under climate change (Figure 3.4).

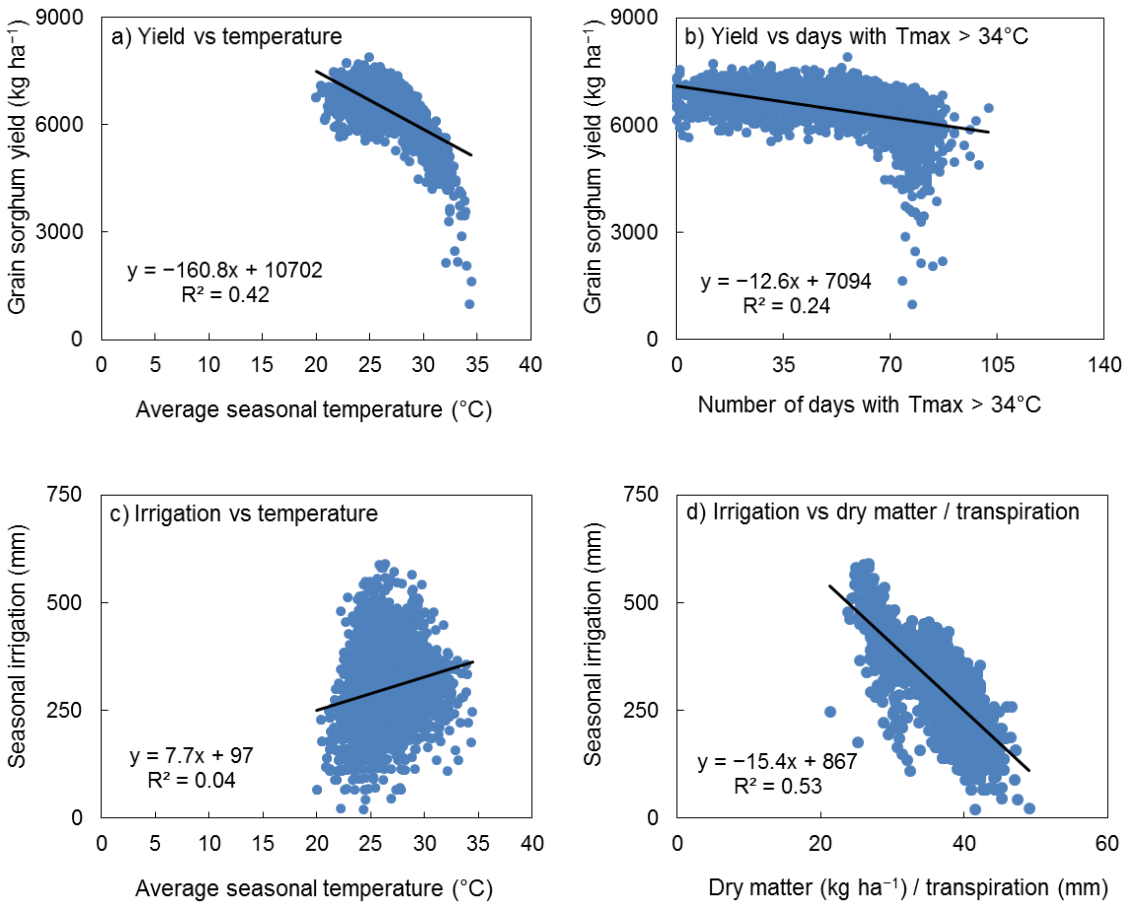

Figure 3.4 Some of the drivers of irrigated grain sorghum yield and irrigation water use change under the changing climate. Simulated under T8 irrigation scenario for 2 RCPs, 9 GCMs and 150 years (1950–2099).

3.4.2. Grain sorghum Response to Deficit Irrigation

3.4.2.1. Deficit irrigation strategies based on critical growth stages

The percent differences in grain sorghum yield between different deficit irrigation treatments, which were designed based on grain sorghum growth stages (Table 3.1), and the well-watered irrigation treatment (T8) for the baseline, mid-century, and late-century periods are summarized in Table 3.4. Grain sorghum yields were the highest under well-

watered irrigation treatment (T8) followed by three 100 mm irrigation applications (T7), and two 100 mm irrigation applications during early reproductive stages (T4).

Among the single 100 mm irrigation treatments (T1, T2 and T3), simulated grain sorghum yield and IWUE were the lowest in the T3 treatment (Table 3.4; Figure 3.5), suggesting that applying limited irrigation water during mid grain filling stage alone is inefficient and the resultant reduction in grain sorghum yields compared to those under full irrigation (T8) would fall between 55–69%. Among the other 100 mm irrigation treatments (T1 and T2), grain sorghum yields were slightly better under T2 in the baseline period and under T1 in the future periods (mid- and late-century and both RCPs) (Table 3.4). The difference in grain sorghum yield between T1 and T2 treatments was particularly prominent in late-century under RCP 8.5, which is likely due to the higher air temperatures and substantially shorter growing season compared to the baseline period. The simulated median IWUE under T1 was higher compared to T2 (Figure 3.5), therefore, in case of single 100 mm irrigation applications, applying irrigation between panicle initiation through boot (T1) is recommended. In addition, the inter-annual coefficient of variability (CV) in grain sorghum yields was lower under T1, further confirming that T1 treatment is more likely to be reliable than T2.

Table 3.4 Percent difference in grain sorghum yield (ΔY) under different deficit irrigation treatments (Ti; where i = 1–7) compared to the well-watered irrigation treatment (T8), and inter-annual coefficient of variation (CV).

	Baseline (1976–2005)		Mid-century (2036–2065)				Late-century (2066–2095)			
			RCP 4.5		RCP 8.5		RCP 4.5		RCP 8.5	
Irrigation treatment	ΔY[a] (%)	CV[b] (%)	ΔY (%)	CV (%)	ΔY (%)	CV (%)	ΔY (%)	CV (%)	ΔY (%)	CV (%)
T1	–41	12	–44	13	–37	12	–43	15	–37	14
T2	–36	13	–46	16	–42	18	–48	21	–50	21
T3	–55	22	–68	25	–65	26	–68	30	–69	29
T4	–16	6	–22	9	–17	8	–23	11	–21	13
T5	–31	12	–41	13	–34	11	–40	15	–36	15
T6	–27	14	–43	17	–39	18	–45	20	–49	22
T7	–8	6	–19	9	–15	8	–21	10	–21	13

[a] $\Delta Y = (Y_{Ti} - Y_{T8}) \div Y_{T8} \times 100$

[b] CV = (standard deviation ÷ average) ×100

Among the 200 mm irrigation treatments, grain sorghum yield and IWUE were consistently higher and CV was lower for the T4 treatment in comparison with T5 and T6, under the baseline and all future periods (Table 3.4 and Figure 3.5). The reduction in grain sorghum yield under T4 compared to well-watered treatment varied between –16% and –23% (Table 3.4). This indicated that the best use of two 100 mm irrigations could be achieved by scheduling irrigation applications between panicle initiation through early grain filling stage.

The 300 mm irrigation water treatment resulted in an 8% reduction in grain sorghum yield under baseline period and 21% reduction in yield under RCP 8.5 in late-century (Table 3.4). The greater difference between deficit and well-watered treatments in the future periods when compared to the baseline could be attributed to the sharp decline in grain sorghum yields beyond the optimal growing season temperature as discussed

earlier, and shortening of growing season length, consistent with Singh et al. (2014c). The variation in the length of growing season under a wide range of climatic conditions simulated in this study limited direct comparison between irrigation treatments across different time periods. Although, the scheduled irrigation dates fell within the intended sorghum development stages in majority of the simulations, in some years, under higher growing season temperatures (RCP 8.5 late-century), grain sorghum attained close to maturity stage (~84 DAP) during the third irrigation application.

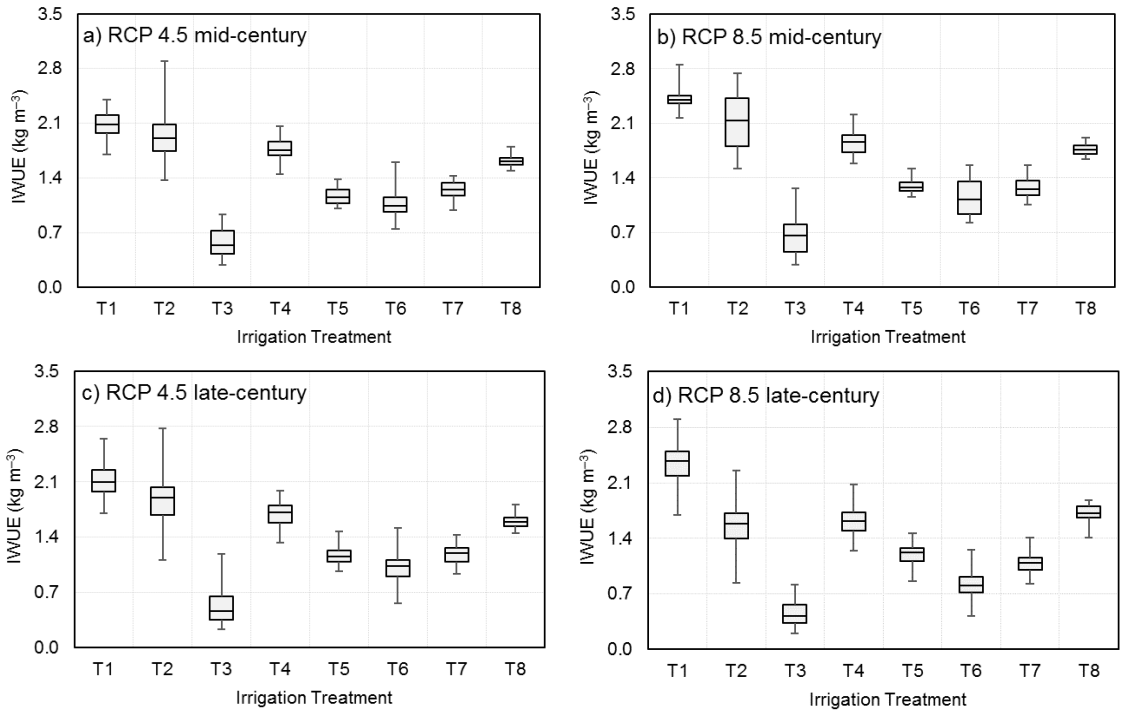

Figure 3.5 Comparison of irrigation water use efficiency, under different irrigation treatments (T) designed based on critical growth stages. The error bars and peripheral box represent minimum, first quartile, median, third quartile and maximum values.

In general, based on the simulated grain sorghum yields and IWUE, it can be concluded that one 100 mm irrigation water application is most efficiently utilized when applied between panicle initiation to boot stage (T1) or boot through early grain filling stage (T2). Consequently, two 100 mm irrigation applications maximized yields when timed between panicle initiation and early grain filling stage (T4). Starting irrigation after the beginning of grain filling stage did not recover sorghum grain yield loss, and this loss was greater when irrigation was further delayed during the grain filling phase.

3.4.2.2. Deficit irrigation strategies based on soil water depletion

The percent difference between various deficit irrigation treatments, which were designed based on different soil water replenishment levels (Figure 3.1), and the full soil water replenishment treatment (I100) for the baseline, mid-century, and late-century periods are summarized in Table 3.5. Grain sorghum yield reduced consistently as irrigation amount reduced for all the time periods and RCPs. Consequently, maximum yield losses were simulated under the highest irrigation deficit treatment (I40) when compared to other irrigation treatments. For a 60% irrigation deficit (I40), grain sorghum yields reduced by 37% and 44% compared to full irrigation in the baseline and late-century periods (under RCP 8.5), respectively. Further, considering individual years in the mid-century period under both RCPs; for 10%, 20%, 30%, 40%, 50%, and 60% irrigation deficits, percent reduction in grain sorghum yields compared to I100 treatment varied within 2–6, 5–15, 10–24, 15–32, 21–44, and 27–56, respectively. The range of yield loss due to irrigation deficit between different years was larger for low irrigation amounts than

for high irrigation amounts. In other words, as the amount of irrigation water reduced, inter-annual CV in grain sorghum yields increased. The inter-annual CV in grain sorghum yield under RCP 8.5 in late-century was almost double of that under baseline period. The higher CV associated with low irrigation amounts and climate change scenarios suggests that, the risk of yield loss under the same irrigation deficit will likely be higher in the future than in the baseline period. This higher CV under future climate change than in the baseline period is likely due to a shift of growing conditions, especially temperature shift from optimal to marginal conditions.

Table 3.5 Percent difference in grain sorghum yield (ΔY) under different deficit irrigation treatments (Ii; where i = 40–90) compared to the well-watered irrigation treatment (I100), and inter-annual coefficient of variation (CV).

Irrigation treatment	Baseline (1976–2005)		Mid-century (2036–2065)				Late-century (2066–2095)			
			RCP 4.5		RCP 8.5		RCP 4.5		RCP 8.5	
	ΔY[a] (%)	CV[b] (%)	ΔY (%)	CV (%)	ΔY (%)	CV (%)	ΔY (%)	CV (%)	ΔY (%)	CV (%)
I40	–37	10	–43	12	–41	13	–44	14	–44	18
I50	–28	7	–33	9	–32	10	–34	11	–34	15
I60	–20	5	–24	7	–24	8	–25	9	–26	13
I70	–14	4	–18	6	–17	7	–18	7	–19	12
I80	–8	3	–10	4	–10	6	–11	6	–11	11
I90	–3	2	–4	3	–4	5	–5	5	–4	10

[a] $\Delta Y = (Y_{Ii} - Y_{I100}) \div Y_{I100} \times 100$

[b] CV = (standard deviation ÷ average) ×100

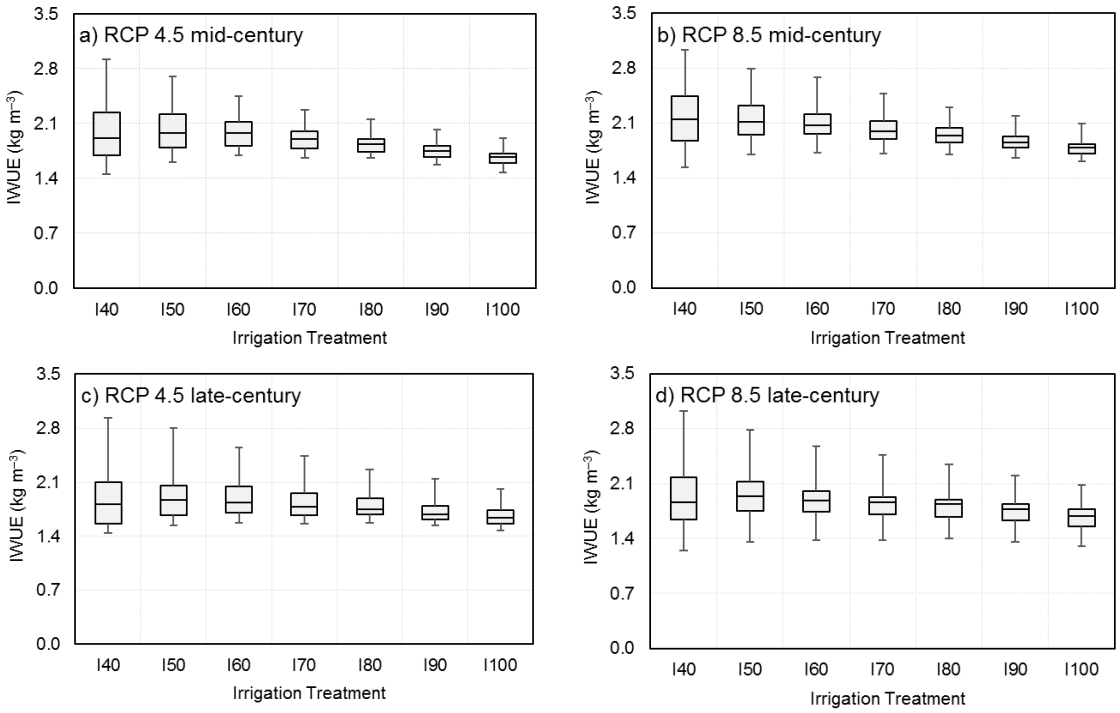

Figure 3.6 Comparison of irrigation water use efficiency, IWUE under different irrigation treatments (I) designed based on soil water depletion. The error bars and peripheral box represent minimum, first quartile, median, third quartile and maximum values.

The median and the range of IWUE increased as the irrigation amount decreased (Figure 3.6). However, the median IWUE was the highest under the second lowest irrigation treatment (I50). Under I50 treatment, simulated grain sorghum yields were 28% and 34% lower than under I100 treatment under the baseline and late-century periods, respectively (Table 3.5). Therefore, while I50 optimized irrigation water use, it is not recommended due to substantial yield losses. Under baseline scenario, grain sorghum yields reduced by up to 20% under I70 compared to I100. Yield reduction with I80 and I90 were <5% and <10%, respectively, therefore, I80 could be a suitable strategy for current and future growing conditions.

3.5. Conclusions

The DSSAT-CSM-CERES-Sorghum model that was evaluated in the preceding chapter, was used in this study. The evaluated model was used to simulate grain sorghum yield and irrigation water use under several climate change, deficit and full irrigation scenarios. The primary objectives were to elucidate climate change impacts on grain sorghum production and to identify efficient deficit irrigation strategies under climate change for the THP region. Simulation results indicated that irrigated grain sorghum yields would reduce in the future under climate change, primarily due to temperature rise. When the growing season average temperature increased beyond a certain threshold (~26°C), which corresponds to a 2°C temperature rise in the current conditions at Halfway, THP, grain sorghum yields plummeted. Irrigation water demand of grain sorghum also reduced under climate change due to the combined effect of temperature stress beyond the optimal temperature threshold and improved crop water use productivity due to CO_2 fertilization. Temperature stress reduced the growing season length, maximum leaf area index, canopy weight at maturity, which reduced crop transpiration and the duration for which irrigation was required.

Irrigation/transpiration productivity or the amount of yield and dry matter produced per unit of crop transpiration/irrigation was higher under climate change, most likely due to CO_2 fertilization effect. Under the current and future climate conditions, limited irrigation application can be more efficient if irrigation water is applied during early reproductive stages beginning from the panicle initiation. Scheduling irrigation after grain filling has begun, would not be enough to recover grain sorghum growth from water

stress. Growing grain sorghum under deficit irrigation resulted in grain sorghum yield loss, however, irrigation water use efficiency increased with reduced irrigation. The percent yield loss under deficit irrigation versus full irrigation was higher in the future under climate change than under baseline conditions. An irrigation deficit of 30% resulted in a yield loss of up to 20%, 25%, and 27%, under the baseline, mid-century, and late-century periods, respectively. A 20% or lower irrigation deficit is recommended. It should be noted that the deficit irrigation scenarios were not scheduled during the vegetative stages and they were designed based on fixed irrigation application dates. Future efforts should focus on utilizing latest DSSAT irrigation routine to schedule irrigation based on growth stages and for a wide range of growth stages. In this study, simulation efforts were based on one location. Similar efforts on other soil types and agroclimatic regions would further enhance the knowledge base which would benefit grain sorghum growers and irrigation water managers in different parts of the world.

4. POTENTIAL BENEFITS OF GENOTYPE-BASED ADAPTATION STRATEGIES FOR GRAIN SORGHUM PRODUCTION IN THE TEXAS HIGH PLAINS UNDER CLIMATE CHANGE

4.1. Synopsis

Adaptation measures are required to enhance climate change (CC) resilience of agricultural systems and reduce risks associated with CC at both regional and global scales. The Texas High Plains (THP) is a semi-arid region that faces a major challenge of sustaining irrigated agriculture under a dwindling groundwater supply from the exhaustible Ogallala Aquifer, in addition to CC risks. The overall goal of this study was to assess the impacts of CC on yield and water use of grain sorghum and evaluate CC adaptation strategies for three locations in the THP (Bushland, Halfway, and Lamesa). Future climate data projected with nine Global Circulation Models (GCMs) under two Representative Concentration Pathways (RCPs) of greenhouse gas emissions (RCPs 4.5 and 8.5) were used as input for the CSM-CERES-Sorghum model of DSSAT. The CC adaptation strategies were designed by modifying crop genotype and soil characteristics to incorporate drought tolerance, heat tolerance, high yield potential, and long maturity traits. Irrigated and dryland grain sorghum yield and irrigation water use were projected to decrease at varying percentages at the study sites in the future. For example, simulated irrigated grain sorghum yield decreased significantly by 7% for the mid-century (2036–2065) and 20% for the late-century (2066–2095), compared to the historic period (1976–2005) under RCP 8.5 at Halfway. Simulated irrigation water use reduced by 7% for the

mid-century and 14% for the late-century under RCP 8.5 at Halfway. Dryland grain sorghum yield reduced significantly under RCP 8.5 at Lamesa by 11% for the mid-century and 19% for the late-century when compared to the historic period. Among the adaptation strategies that were evaluated, a virtual cultivar with high yield potential trait resulted in maximum grain sorghum yield gains in the future under both irrigated (6.9%–19.3%) and dryland (7.5%–17.1%) conditions, when compared to the baseline cultivar. Enhancing drought tolerance by increasing root density at different soil depths and adopting longer maturity cultivar also resulted in a significantly higher irrigated grain sorghum yield than the baseline cultivar. However, irrigation water use of long maturity cultivar was significantly higher than the baseline cultivar. The results from this study suggest that increasing yield potential traits and root density were the optimum CC adaptation strategies for irrigated and dryland grain sorghum production in the THP. A longer maturity cultivar will likely increase irrigation water use and, therefore, is not recommended for water limited conditions.

4.2. Introduction

Climate change (CC) is a major threat to global food security (Challinor et al., 2014; Rosenzweig and Parry, 1994). Rise in anthropogenic greenhouse gas emissions, especially carbon dioxide (CO_2), since the industrial revolution is most likely the primary driver of CC and has led to an overall increase in energy uptake of the climate system. The global mean surface temperature increased by about 0.6°C over the 20th century, and is projected to increase between 1°C to 3.7°C by the end of 21st century relative to 1986–

2005 (IPCC, 2014). It is likely that the frequency and intensity of temperature and precipitation extremes will increase in the future as a result of CC (IPCC, 2014). Atmospheric greenhouse gas emissions continue to rise and stringent mitigation efforts are required to ameliorate CC risks (IPCC, 2014). The interactive effect of different climate variables (e.g., temperature, precipitation, and atmospheric CO_2) on agricultural systems and their response to adaptation strategies varies with the type of crop and the agroclimatic region (Lobell and Burke, 2008). It is therefore important to develop crop-specific adaptation strategies at both regional and global scales to sustain crop production and maintain profitable crop yield under CC (Howden et al., 2007). This study focused on the Texas High Plains (THP), which is one of the most intensive agricultural regions in the United States of America (USA) and on grain sorghum due to its economic importance to the THP region. Sorghum has a high drought and heat tolerance (Rooney et al., 2007) and its production requires less irrigation water than other major crops in the THP region such as corn (Amosson et al., 2005).

Grain sorghum [*Sorghum bicolor* L. Moench] is the fifth major cereal crop in the world, the majority of which is grown in the USA, Nigeria, Mexico, India, Argentina, Sudan, and Ethiopia (Dicko et al., 2006). The USA is the largest producer and exporter of grain sorghum (Awika and Rooney, 2004), which is primarily used for livestock feed (Schober et al., 2005). In recent years, there has been a growing interest in this crop due to current and emerging domestic and international markets such as a gluten-free whole grain diet substitute (Schober et al., 2005) and ethanol production (Rooney et al., 2007). About 9% (0.2 million ha) of the total and 32% of the irrigated grain sorghum crop area

in the USA are in the THP region (NASS, 2012). The semi-arid THP region faces many challenges for sustaining irrigated agriculture such as rapidly declining groundwater resources in the Ogallala Aquifer and projected warmer and drier future climatic conditions (Chaudhuri and Ale, 2014; Modala et al., 2017; Scanlon et al., 2012). Agricultural industry in the THP plays a vital role in Texas economy contributing over $6.6 billion annually (Guerrero and Amosson, 2013) and CC could thus severely affect farm income in Texas. Expansion of area under grain sorghum could be one of the strategies to maintain economic yields under limited irrigation water availability in the THP under CC.

Grain sorghum is a C_4 plant, implying that its photosynthesis rate is saturated at current atmospheric CO_2 levels and a further increase in CO_2 concentration should not theoretically stimulate crop yield (Leakey et al., 2006). However, free air CO_2 enrichment (FACE) (Ottman et al., 2001; Wall et al., 2001) experiments at Maricopa, AZ and open top field chamber (Prior et al., 2003) experiments at Auburn, AL, have shown mixed trends in grain sorghum yields at twice the ambient CO_2 levels. The effects of CO_2 enrichment on grain sorghum yields were positive under water-limited conditions, whereas the effects were both positive and negative under ample water conditions. Prasad et al. (2006) used outdoor soil-plant-atmospheric-research chambers to study grain sorghum growth at different combinations of CO_2 and day/night temperature regimes. They reported that doubling of CO_2 concentration increased grain sorghum yields by 26% under lower daytime maximum/nighttime minimum temperature regimes (32/22°C), while under higher temperatures (36/26°C) grain sorghum yield decreased by 10%.

Process-based crop simulation models have been used extensively to elucidate the impacts of different climate variables on crop production under CC. A simulation study at different locations in India using the InfoCrop-SORGHUM model estimated a 6–37% decline in dryland grain sorghum yields with a 5°C increase in air temperature without considering CO_2 fertilization effect (Srivastava et al., 2010). However, when atmospheric CO_2 level was increased from 369 ppm to 550 ppm, grain sorghum yield increased by about 8%. Another study using the SARRA-H model predicted up to 41% reduction in grain sorghum yield for 6°C temperature rise and 20% rainfall reduction in Sub-Saharan West Africa (Sultan et al., 2013). Both studies suggested that any amount of rainfall increment would not be enough to recover grain sorghum yield loss beyond +2°C temperature increase. Several other simulation studies (Carbone et al., 2003; Chipanshi et al., 2003; Tubiello et al., 2000) have also shown similar negative impacts of CC on grain sorghum yield. In contrast, fewer simulation studies have also reported a positive effect of CC on grain sorghum. For example, grain sorghum yields simulated by DSSAT and APSIM models increased between 5% and 23% in Tanzania (Msongaleli et al., 2014). Overall, these studies indicate that the changes in grain sorghum yield under CC were different for different geographic location, and they suggest that positive effects of CO_2 fertilization on grain sorghum production are far less when compared to the negative impacts of rising temperatures and resultant grain sorghum yield will most likely decrease under CC without adaptation.

The CC adaptation measures tested in the previous studies include genetic alterations (Singh et al., 2014c) and changes in crop management decisions such as

planting date (Srivastava et al., 2010). Singh et al. (2014c) used the CSM-CERES-Sorghum model to quantify the potential benefits of altering crop genetic characteristics that would enable better adaptation to CC at two sites each in India and Mali, West Africa. They found that a longer duration grain sorghum cultivar with 10% increase in maturity period resulted in a 7−33% increase in grain yield. Under future climate, grain yield increased by 0-8%, 0-12% and 4-17%, respectively when drought tolerance, heat tolerance, and both drought and heat tolerance traits were incorporated. Singh et al. (2014c) considered only dryland grain sorghum production and the future projections were for the mid-century period (2040–2069). In another study in India (Srivastava et al., 2010), there was a 1−11% yield gain for dryland grain sorghum by shifting the planting date in 2050s.

Most of the previous studies analyzed either irrigated or dryland grain sorghum yield, and the effect of CC and CC adaptation on irrigation water use was not well documented. In addition, previous studies used a single atmospheric CO_2 concentration value for the entire baseline period and a single higher value for the future period. Simulation studies in which CO_2 concentration is varied gradually over time, are more realistic (Harrison and Butterfield, 1996), but such gradual increase in CO_2 concentration was rarely incorporated into CC studies. The impact of CC on grain sorghum production and the response to genetic-based adaptation have not been studied for the THP region. Therefore, the specific goals of this study were to: (a) assess the impacts of CC on grain sorghum production (i.e., irrigated and dryland yields and irrigation water use) at three locations, Halfway, Bushland and Lamesa in the THP region using the DSSAT CSM-

CERES-Sorghum model, and (b) evaluate the impacts of potential CC adaptation strategies on sorghum yield and water use. In this study, we have used the CERES-Sorghum module that we have recently evaluated for Halfway site using measured data from a cotton-sorghum rotation experiment over a nine year period in a separate study (Kothari et al., 2019).

4.3. Material and Methods

4.3.1. Study Area/Sites

The Texas High Plains (THP) region, located in the northwest Texas, comprises of 39 counties and borders the states of New Mexico and Oklahoma (Figure 4.1). This study focused on three locations in the THP region; namely, Bushland (35° 11’ N, 102° 6’ W, 1170 m aMSL), Halfway (34° 11’ N, 101° 56’ W, 1071 m aMSL), and Lamesa (32° 46’ N, 101° 56’ W, 915 m aMSL). These sites were selected due to the availability of data required for parameterization of the DSSAT model and the differences in soil types and climate among the sites. The average annual precipitation for the 1980–2010 period at Bushland, Halfway, and Lamesa were 494 mm, 515 mm, and 478 mm, respectively (NOAA, 2017). The average annual temperatures at these sites during the same period, were 14.2°C (Bushland), 15.1°C (Halfway), and 16.1°C (Lamesa).

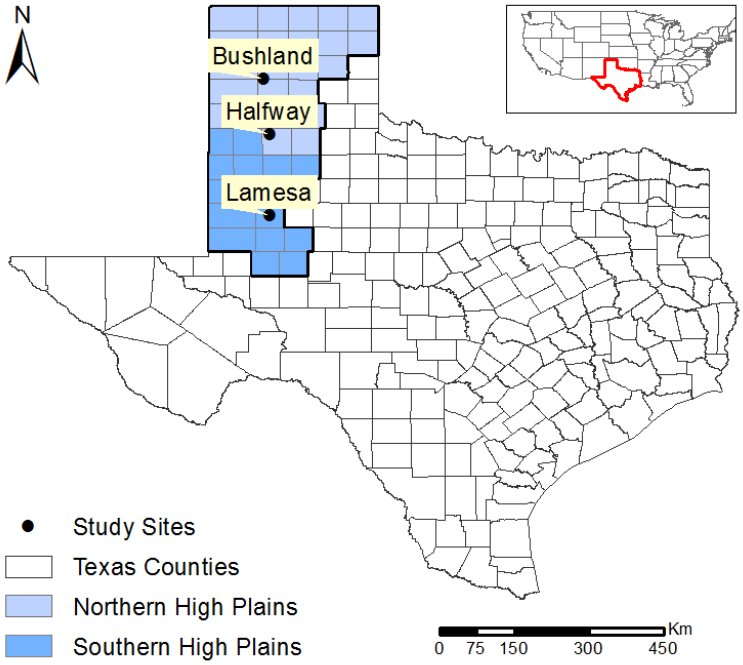

Figure 4.1 Location of the study sites in the northern and southern High Plains Agricultural Statistical Districts, collectively known as the Texas High Plains.

4.3.2. The DSSAT Model

The Decision Support System for Agrotechnology Transfer (Jones et al., 2003) Cropping System Model (DSSAT-CSM) version 4.6 (Hoogenboom et al., 2015) was used in this study. The CSM-CERES-Sorghum module (Alagarswamy and Ritchie, 1991; White et al., 2015) within the DSSAT was used to simulate grain sorghum growth and development. In the CSM-CERES-Sorghum module, duration of different growth stages is simulated based on daily thermal time accumulation which is calculated from minimum and maximum temperatures with a base temperature of 8°C (Alagarswamy and Ritchie, 1991). Daily potential biomass production is a function of radiation use efficiency and photosynthetically active radiation, with adjustment factors for atmospheric CO_2, plant

population, and leaf area index (White et al., 2015). Calculation for actual biomass incorporates stress factors related to temperature, soil water and nitrogen deficits. Changes in atmospheric CO_2 are reflected in daily biomass accumulation and transpiration rates (Singh et al., 2014c). Further details of sorghum growth, phenology and root dynamics as simulated with the CSM-CERES-Sorghum model in DSSAT can be found in Alagarswamy and Ritchie (1991), White et al. (2015), (Ritchie et al., 1998) and (Adam et al., 2018).

The typical inputs required to simulate crop growth and development in DSSAT include: crop management, daily weather data, soil characteristics, and crop specific genotype (cultivar, ecotype and species) parameters (Hoogenboom et al., 2012; Hunt et al., 2001). Out of the four types of analysis available in DSSAT (Thornton and Hoogenboom, 1994; Thornton et al., 1995), "seasonal" analysis was used in this study, in which soil water and nutrient balance were not carried over to the next season and these conditions were re-initialized at the beginning of each year. The same initial conditions and crop management practices were repeated each year from 1950 to 2099 with different weather inputs.

4.3.3. Model Input Data

4.3.3.1. Crop Management Inputs

Crop management related inputs for sorghum production such as planting date and fertilizer amount and application date, commonly adopted in the THP region were obtained from the High Plains Production Handbook (McClure et al., 2010) and used in

this study. Crop management inputs were kept the same for all three sites. Sorghum was planted on June 1st at a rate of 18 seeds m^{-2} for irrigated and 6 seeds m^{-2} for dryland conditions. For irrigated and dryland sorghum production, 150 kg N ha^{-1} and 60 kg N ha^{-1} nitrogen fertilizer was applied, respectively. Half of the fertilizer dose was applied at 20 days after planting (DAP) and the other half at 40 days (DAP). Tillage operation was done one month prior to planting, with a V-ripper at 13 cm depth (Bean et al., 2003).

Seeds were planted at 3.8 cm depth at a row spacing of 1.02 m. Irrigation was simulated using "auto-irrigation" feature of DSSAT. Irrigation was applied to replenish plant available water content in the top 30 cm profile to 100% whenever it dropped to 50%. The initial soil water for irrigated conditions was assumed to be 100% of plant available water content. For dryland conditions, initial soil water was set at 75% of plant available water content, which is close to the average soil water at planting measured at Bushland (Unger, 1978; Unger and Baumhardt, 1999). Initial soil nitrogen content in the top 210 cm soil profile for irrigated and dryland sorghum were set at 100 kg N ha^{-1} and 45 kg N ha^{-1}, respectively. These values were within the range of measured/adopted values for sorghum in the THP under irrigated (Hao et al., 2014) and dryland (Eck and Jones, 1992) conditions. These initial conditions were reinitialized each year on the simulation start date, i.e., January 1.

4.3.3.2. Soil Data Input

Soil parameters for selected sites were either directly obtained from field measurements as documented in Adhikari et al. (2016), or generated using the SBuild tool

within DSSAT (Uryasev et al., 2004) (Table 4.1). The parameters taken from field measurements were percentages of clay, silt, total nitrogen, organic carbon, pH, and cation exchange capacity (cmol kg^{-1}). The parameters estimated from the SBuild were hydraulic conductivity (cm h^{-1}), soil bulk density (g cm^{-3}), soil water at saturation (cm cm^{-1}), drained upper limit (cm cm^{-1}), soil water lower limit (cm cm^{-1}), and soil root growth factor. The soil type at the Bushland and Halfway experimental sites is a Pullman clay loam (Fine, mixed, superactive, thermic Torrertic Paleustolls), whereas the soil at the Lamesa site is Amarillo fine sandy loam (Fine-loamy, mixed, superactive, thermic Aridic Paleustalfs).

Table 4.1 Physical and hydraulic properties of soils at the selected locations in the Texas High Plains.

Site	Depth (cm)	Clay (%)	Sand (%)	Lower limit (cm^3 cm^{-3})	Drained upper limit (cm^3 cm^{-3})	Saturated hydraulic conductivity (m s^{-1})	Bulk density (g cm^{-3})
Bushland	0–15	33	21	0.12	0.34	1.7×10^{-6}	1.26
	15–30	39	21	0.13	0.33	1.1×10^{-6}	1.48
	30–45	35	19	0.12	0.33	1.0×10^{-6}	1.56
	45–60	37	21	0.13	0.33	1.1×10^{-6}	1.62
	60–90	37	23	0.13	0.33	1.0×10^{-6}	1.62
Halfway	0–15	17	64	0.13	0.23	7.2×10^{-6}	1.48
	15–30	25	48	0.17	0.29	1.2×10^{-6}	1.44
	30–45	31	42	0.20	0.31	6.4×10^{-7}	1.44
	45–60	36	40	0.22	0.34	6.4×10^{-7}	1.44
	60–90	34	42	0.21	0.32	6.4×10^{-7}	1.45
Lamesa	0–15	7	75	0.06	0.14	7.2×10^{-6}	1.53
	15–30	9	77	0.07	0.14	7.2×10^{-6}	1.58
	30–45	11	75	0.09	0.15	7.2×10^{-6}	1.59
	45–60	11	75	0.09	0.16	7.2×10^{-6}	1.58
	60–90	11	75	0.08	0.15	7.2×10^{-6}	1.59

4.3.3.3. Climate Data

Weather data inputs for the model include daily solar radiation, maximum and minimum temperature, rainfall, wind speed, and relative humidity. Daily climate data projections used in this study were obtained from the Coupled Model Intercomparison Project Phase 5 (CMIP5) of the Climate Research Program, which were bias corrected and statistically downscaled at either 4 km or 6 km resolution using the Multivariate Adaptive Constructed Analogs (MACA) technique (Abatzoglou and Brown, 2012). The observed training dataset (Abatzoglou, 2013) used for downscaling came from two sources: North American Land Data Assimilation System Phase 2 (NLDAS-2) and the Parameter-elevation Regressions on Independent Slopes Model (PRISM). The MACAv2-METADATA dataset contains maximum and minimum temperature, precipitation, relative humidity, solar radiation, and wind speed for historic (1950–2005) and future (2006–2099) periods, as specified in the data source. The MACA dataset was used for both historic and future periods due to non-availability of good long-term historic weather data at the selected locations. Although the length of available rainfall and temperature data at these sites was fairly reasonable, daily values of other climate variables (solar radiation, wind speed, and relative humidity) were not available for the entire duration and for all locations. In addition, a comparison between observed weather data at the study sites and the bias corrected and statistically downscaled GCM projected MACA dataset (Abatzoglou, 2013) showed a close match between the two datasets (Figures A1 to A3). MACA dataset was also directly used in several other published CC impact studies on crop production in the Southwestern US (Elias et al., 2018), Southeast US (Cammarano

and Tian, 2018), and US Pacific Northwest (Antle et al., 2018; Karimi et al., 2018; Kerr et al., 2018; Stöckle et al., 2018; Zhang et al., 2017).

In view of high variability in the future climate projections, a total of 18 CC scenarios, generated from 9 GCMs (Table 4.2) and two representative concentration pathways (RCPs), i.e., 4.5 and 8.5, were used. When compared to other RCPs, the RCP 8.5 scenario assumes higher greenhouse gas emissions resulting from high population growth, increased energy consumption, land use changes, and slow income and technology growth (Riahi et al., 2011). In contrast, RCP 4.5 is an intermediate scenario with an assumption of practicing adaptive policies such as low emission technologies and afforestation, which stabilize radiative forcing at 4.5 W m^{-2} in the year 2100 (Thomson et al., 2011). Atmospheric CO_2 concentration is projected to reach 544 ppm and 912 ppm in 2099 under RCPs 4.5 and 8.5, respectively (IPCC, 2014). In this study, CO_2 was varied annually using the "environmental modification" setting in DSSAT. Future projections of atmospheric CO_2 were taken from IPCC (2014); and historic CO_2 levels were obtained from the NOAA/ESRL portal (Keeling et al., 1976; Thoning et al., 1989).

Table 4.2 Summary of the 9 CMIP5 GCMs used to project daily weather data under climate change.

GCM Name	Institution	Main reference	Atmosphere Resolution (Lon×Lat)
BCC-CSM1-1	Beijing Climate Center, China Meteorological Administration	(Wu, 2012)	2.8°×2.8°
CCSM4	National Center for Atmospheric Research, USA	(Gent et al., 2011)	1.25°×0.94°
CSIRO-Mk3-6-0	Commonwealth Scientific and Industrial Research Organization and Queensland Climate Change Centre of Excellence, Australia	(Rotstayn et al., 2012)	1.8°×1.8°
GGFDL-ESM2M	NOAA Geophysical Fluid Dynamic Laboratory, USA	(Dunne et al., 2012)	2.5°×2.0°
CNRM-CM5.1	National Centre of Meteorological Research, France	(Voldoire et al., 2013)	1.4°×1.4°
IPSL-CM5A-LR	Institute Pierre Simon Laplace, France	(Dufresne et al., 2013)	3.75°×1.8°
MIROC5	University of Tokyo, Japanese National Institute for Environmental Studies, and Japan Agency for Marine-Earth Science and Technology	(Watanabe et al., 2010)	1.4°×1.4°
MRI-CGCM3	Meteorological Research Institute, Japan	(Yukimoto et al., 2012)	1.1°×1.1°
NorESM1-M	Norwegian Climate Centre, Norway	(Kirkevag et al., 2008)	2.5°×1.9°

Climate forcings from the Multivariate Adaptive Constructed Analogs dataset (Abatzoglou, 2013), retreived from https://climate.northwestknowledge.net/MACA/index.php

4.3.3.4. Genotype Parameters

The cultivar, ecotype, and species parameters are collectively known as genotype parameters in DSSAT. Cultivar parameters are specific to a crop variety, ecotype parameters apply to a group of cultivars, and species traits are common to all cultivars in a particular crop species (Pathak et al., 2007). In this study, grain sorghum cultivar and ecotype parameters estimated in a recent study (Kothari et al., 2019), based on field experiments at Halfway, TX (TALR, 2016), were used. The field experiments comprised of three irrigation treatments in two adjacent wedges of a center pivot irrigation system, in which sorghum was rotated after two years of cotton from 2006–2014. The genotype parameters were calibrated and evaluated for the onset of phenological stages and crop yield for both cotton and sorghum. The genotype parameters evaluated for Halfway in our previous study (Kothari et al., 2019), were used for all three sites further calibration. These genotype parameters are referred to as baseline parameters and the evaluated grain sorghum cultivar is referred to as the baseline cultivar in this study.

4.3.4. Adaptation Strategies/ Virtual Cultivars

A total of eight CC adaptation strategies that are aimed at maintaining crop yield and achieving sustainable use of irrigation water were evaluated in this study. These adaptation strategies were developed by creating virtual cultivars by modifying genotype parameters and root characteristics in the soil file from the baseline cultivar. This methodology was based on and extends the work done by Singh et al. (2014c). The following CC adaptation strategies were evaluated in this study.

4.3.4.1. Drought Tolerance cultivars I to IV

Root variation is an important factor in drought tolerant hybrid selection (Assefa et al., 2010), but it has not received sufficient attention in the screening of drought resistance in grain sorghum (Krupa et al., 2017). In this study, the first drought tolerant grain sorghum cultivar was created by increasing the root density in different soil layers to improve the capability of crops to extract water from the soil. This was achieved by increasing root density in the soil (*.SOL) input file by modifying the formula used for soil root growth factor (SRGF) estimation from $e^{-0.02\times Z}$ to $(1–Z/500)^6$; where Z is the soil depth in cm. This strategy was similar to Singh et al. (2014c), however, in this study only SRGF was changed and the soil lower limit (LL) was kept the same for drought tolerant and non-drought-tolerant cultivars.

The second drought tolerant cultivar was created by altering other root parameter in the species file. The species parameter RLWR (root length to weight ratio, cm/g) was increased by 20% from 0.98 (default) to 1.18. RLWR was increased in accordance with a field study (Tsuji et al., 2005), in which drought tolerant hybrid had a higher root length to weight ratio under dry conditions than drought susceptible hybrid; indicating an increase in fine roots in drought tolerant hybrid under water stress. This is corroborated by another field study (Magalhães et al., 2016), in which an increase in fine root length was associated with drought tolerance in sorghum. In previous CSM-CERES-Sorghum studies, researchers have used the default value of RLWR parameter, and, therefore, a range of values for this parameter was not available in the literature.

While root physical characteristics have been a focus of many breeding programs for drought tolerance, a few researchers (Vadez, 2014) have also highlighted the importance of root hydraulics. Variation in potential water extraction from soil profile has been found among different sorghum genotypes (Tardieu et al., 2017; Vadez et al., 2011), and it could be used to test for drought tolerance. Extracting more water from soil under water stress can lead to drought tolerance (Hao et al., 2015). However, faster depletion of soil water in case of limited water supplies can be detrimental to plant growth in later stages (Lilley and Kirkegaard, 2016). Therefore, both higher and lower potential water uptake per unit length than the default value were considered for drought tolerance. The third virtual drought tolerant cultivar tested for drought tolerance was created by increasing maximum water uptake per unit length (RWMX cm^3 water cm^{-1} root) from 0.03 (default) to 0.04, which is close to the maximum value (0.0375) used by Lopez et al. (2017).

The fourth virtual drought tolerant cultivar tested for drought tolerance was created by decreasing maximum water uptake per unit length (RWMX cm^3 water cm^{-1} root) from 0.03 (default) to 0.02 which is close to the minimum value (0.0225) used by Lopez et al. (2017).

4.3.4.2. Heat Tolerance cultivars I and II

The first heat tolerance cultivar was created by increasing upper optimum (TOP2) and failure (TMAX) temperatures in the species (*.SPE) file by 2°C. The TOP2 was

changed from 27°C to 29°C and TMAX was changed from 35°C to 37°C for the relative grain filling rate process, similar to Singh et al. (2014c).

The default values of TOP2 (27°C) and TMAX (35°C) in DSSAT v4.6 were decided based on response of a sorghum genotype to different temperature regimes grown in growth chambers (Prasad et al., 2006). In a recent study (Singh et al., 2015), researchers reported that threshold temperature for seed set and tolerance varied within the twenty genotypes grown in a controlled environment. Some genotypes had significantly lower seed-set at a maximum temperature regime of 38°C compared to that at 36°C, while for a few genotypes seed-set at the two temperature regimes were only marginally different. These differences in temperature threshold and tolerance level among genotypes could be explored to screen grain sorghum genotypes for heat tolerance. Therefore, the second heat tolerant cultivar was created by increasing TOP2 and TMAX by 3°C each from their default values. The TOP2 was changed from 27°C to 30°C and TMAX was changed from 35°C to 38°C for the relative grain filling rate process.

4.3.4.3. High Yield Potential cultivar

A high yielding crop variety was developed by increasing leaf size, partitioning factor, and/or radiation use efficiency in the cultivar (*.CUL) and ecotype (*.ECO) files. For grain sorghum, original values of scaler for relative leaf size (G1 = 3.4), scaler for partitioning of assimilates to the panicle (G2 = 7), and radiation use efficiency in g dry matter/MJ PAR (RUE = 3.2), were increased by 10%, similar to Singh et al. (2014c).

4.3.4.4. Long Maturity cultivar

A long maturity virtual cultivar was created by increasing total length of the growing season by 10% (Singh et al., 2014c).The thermal time from seed emergence to the end of juvenile phase (P1, degree days above 8 °C) was changed from 334 to 390; P2O (critical photoperiod at which development occurs at the maximum rate, hours) was changed from 15.2 to 14.2; and P5 (thermal time from beginning of grain filling to physiological maturity, degree days above 8 °C) parameter was changed from 575 to 640.

4.3.5. DSSAT CSM CERES-Sorghum Model Evaluation

As mentioned earlier, evaluation of the CERES-Sorghum model for one of the selected sites, Halfway, was carried out as a part of our previous study (Kothari et al., 2019). The experimental data for model evaluation were obtained from cotton-sorghum experiments conducted at the AgriLife Research Farm at Halfway, TX, over nine years (2006–2014), which included four sorghum growing seasons (2007, 2010, 2012 and 2013). The model was calibrated and evaluated against the onset of growth stages, sorghum grain yields, and irrigation water use efficiency (IWUE). After a systematic evaluation, CERES-Sorghum model adequately simulated grain sorghum yield during the calibration (average percent error (PE) of 1.3% and root mean square error (RMSE) of 7.6%) and evaluation (average PE of −2.2% and RMSE of 16.3%) periods. An average PE of 7.4% was obtained during the evaluation of model for IWUE prediction. A satisfactory simulation of sorghum grain yield and IWUE over four growing seasons and

twelve irrigation treatments suggested that the model could be used for evaluating CC adaptation strategies for Halfway and the other two THP sites with reasonable confidence.

4.3.6. Evaluation of Climate Change Adaptation Strategies

Climate data projected by nine GCMs considered in this study were initially grouped into three time periods including historic or baseline (1976–2005), 2050s or mid-century (2036–2065), and 2080s or late-century (2066–2095) periods for three selected sites. The ensemble of nine GCM projections under RCP 4.5 and 8.5 were then averaged over the above mentioned three time periods and projected future changes in rainfall and average temperature in the mid- and late-century were assessed. DSSAT simulations were then run for both irrigated and dryland conditions using the climate data projected by each GCM under RCP 4.5 and 8.5 scenarios. The simulated average irrigated/dryland grain sorghum yield and irrigation water use were estimated for the historic, mid-century and late-century periods for each GCM and RCP scenario, and the variability in simulated grain sorghum yield and irrigation water use under different RCPs and time periods was studied.

Additionally, average grain sorghum yield and irrigation water use for nine GCMs under each RCP scenario were estimated for each year, and 30-year average grain sorghum yield and irrigation water use under each RCP scenario over the historic, mid-century and late-century periods were finally estimated and used for assessing the impacts of CC on grain sorghum production and evaluation of CC adaptation strategies. The percent differences between the 30-year average historic and future yields/irrigation water use,

and the coefficient of variability (CV, standard deviation divided by the 30-year average) were estimated and used for CC impact assessment. The statistical significance of the difference in the 30-year average historic and future yield/irrigation was tested using the two-sample t-test for unpaired data (Welch, 1938) at 95% confidence interval. For the evaluation of adaptation strategies, simulated grain sorghum yield and irrigation water use under a "specific adaptation" and "no adaptation" scenario were compared. Apart from irrigated and dryland crop yields and irrigation water use, other model outputs such as the length of growing season, maximum leaf area, growing season rainfall, temperature, nitrogen uptake, canopy weight at maturity were also analyzed to elucidate the effects of CC on different crop growth processes.

4.4. Results and Discussion

4.4.1. Future Climate Projections

Projected future changes in average temperature and rainfall in the mid-century (2036–2065) and the late-century (2066–2095) compared to the historic period (1976–2005), under two RCPs are presented in Figure 4.2a–c. Mean monthly temperatures are expected to rise under all future scenarios compared to the historic period. The increase in mean monthly temperature compared to the historic period was greater under RCP 8.5 scenario than under RCP 4.5, and greater for the late-century than for the mid-century period. The increase in mean monthly temperature varied from 1.5°C (November, RCP 4.5 at Lamesa) to 2.9°C (June, RCP 8.5 at Bushland) for the mid-century; and from 1.9°C (December, RCP 4.5 at Halfway) to 5.0°C (June, RCP 8.5 at Bushland) for the late-

century. Average temperature in summer months increased by a greater magnitude than winter months under CC when compared to historic period. This is consistent with the temperature projections for Texas reported in a previous study (Jiang and Yang, 2012). The month of June (when sorghum was planted in this study) had the highest temperature rise among all the months. The differences in temperature rise in different months indicate that shifting planting dates to avoid hottest months could be a strategy to adapt to CC. However, in a recent simulation study with the APSIM model (Singh et al., 2017), researchers found that changing planting date did not reduce the risk of heat stress during anthesis, whereas genetic manipulations could mitigate sorghum yield losses. In this study, adaptation strategies were, therefore, restricted to altering crop genetics rather than changing management decisions. The pattern of temperature increase under different RCPs and different months was similar across the three sites studied.

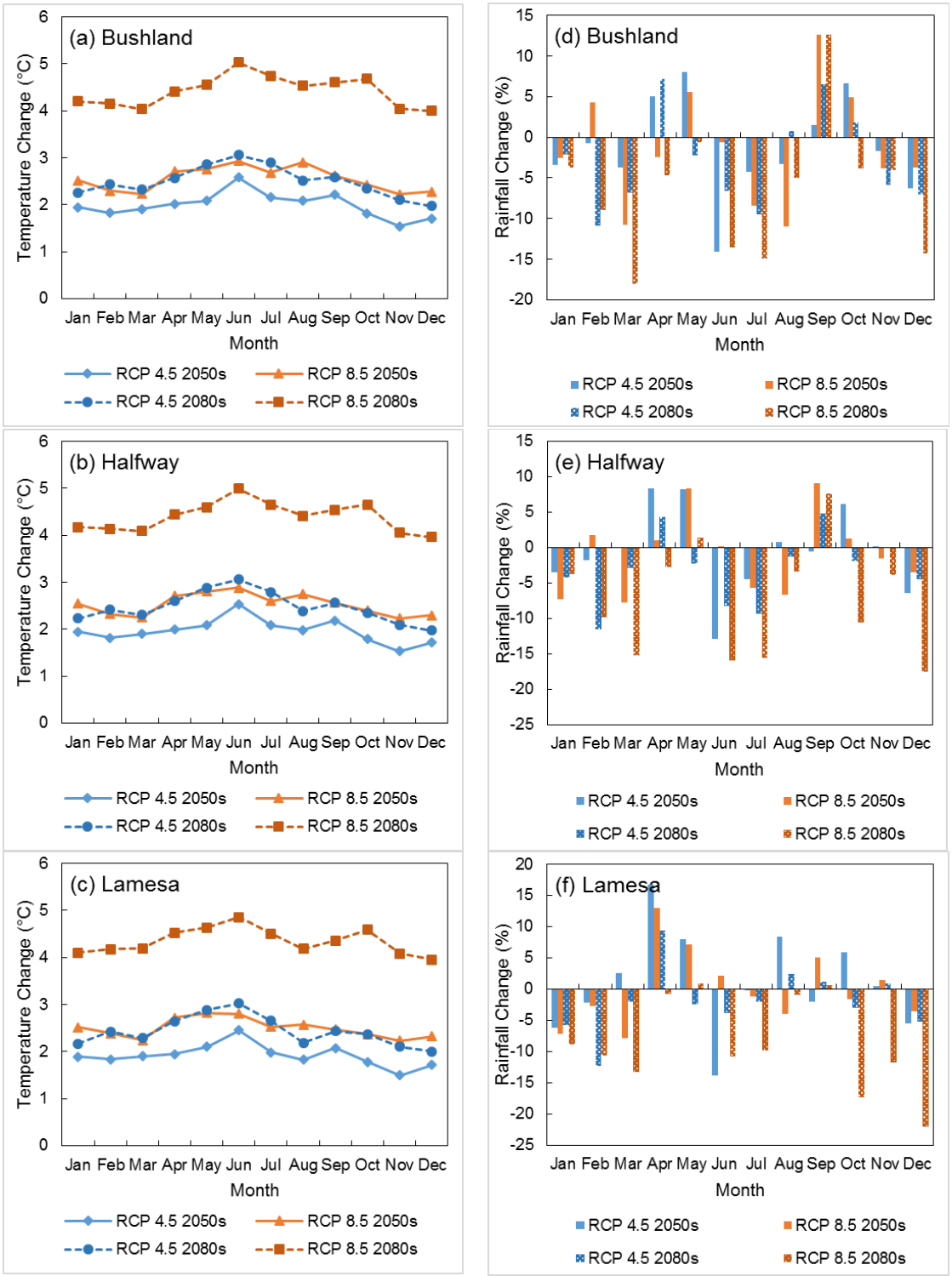

Figure 4.2 Projected changes in monthly average (ensemble average of nine GCMs) temperature (a–c) and rainfall (d–f) in 2050s (2036–2065) and 2080s (2066–2095), compared to the historic period (1976–2005), under RCPs 4.5 and 8.5.

The differences between the projected future and historic monthly rainfall showed a mixed, but predominantly decreasing trend (Figures 4.2d–f). The projected monthly rainfall during the growing season increased up to 6 mm (about 12% increase, September 2050s Bushland, RCP 8.5) and decreased up to 13 mm (about 15% reduction, June 2080s Halfway, RCP 8.5), compared to the historic period. Monthly rainfall for the late-century period (2080s) was lower than that in the historic period for all the months, except September under RCP 8.5, and September and April under RCP 4.5. Likewise, for the mid-century (2050s), April, May, and September months were wetter in the future compared to the historic period. The first two months from grain sorghum planting (June and July) were drier in the future compared to the historic period, and hence could potentially affect sorghum yields negatively. The pattern of future rainfall deviation from the historic period for different months and RCPs was not consistent among the three sites.

4.4.2. Climate Change Impact on Grain Sorghum Production

The impact of CC on irrigated and dryland grain sorghum production and irrigation water use are presented in the following sections.

4.4.2.1. Irrigated Grain Sorghum Yield

The simulated irrigated grain sorghum yield decreased significantly in the future when compared to the historic yield under all RCPs at all the three sites (Table 4.3). Irrigated grain sorghum yield declined according to climate change projections by most GCMs, with a few exceptions (Figure 4.3). The difference between future and historic

irrigated grain sorghum yield varied between –51% (RCP 8.5 2080s at Lamesa under IPSL-CM5A-LR GCM) and 2% (RCP 4.5 2050s at Halfway under GFDL-ESM2M GCM) among CC projections by nine GCMs. As expected, the yield decline was larger under RCP 8.5 than under RCP 4.5, and larger in the late-century than in the mid-century. For example, the decrease in yield at Halfway under RCP 4.5 in the mid-century was much smaller (4%) than that under RCP 8.5 in the late-century (20%). Interestingly, irrigated grain sorghum yield reduction under RCP 4.5 in the late-century (7% at Halfway) was comparable to that under RCP 8.5 in the mid-century (7% at Halfway). The extents of differences in irrigated grain sorghum yield reduction among different RCPs and future time periods could be attributed to the differences in temperature rise under these scenarios (Figure 4.2). The rise in growing season temperature significantly shortened the growing season length (data not shown), which has been associated with grain sorghum yield loss (Singh et al., 2014c; Srivastava et al., 2010). Warming leads to hasty crop development and less time for grain filling, thus reducing grain yield crops (Amthor, 2001). For example, the simulated length of growing season at Bushland was shorter by 15 days and 22 days under RCP 8.5 in mid-century and late-century, respectively when compared to the historic period.

Interannual variability in the simulated irrigated grain sorghum yield, as indicated by CV, increased under CC for all the three sites (Table 4.3). For example, CV in simulated irrigated grain sorghum yield increased from 4% (historic period) to 11% (under RCP 8.5 in the late-century) at Lamesa. The increase in CV suggests that climate in the

THP will shift from optimal to marginal growing conditions under CC (Doherty et al., 2003).

Among the three locations studied, irrigated grain sorghum yield was the lowest at Lamesa (Table 4.3). The CV in irrigated grain sorghum yield was also slightly higher at Lamesa than that at Halfway or Bushland. The soil at Lamesa has a much greater sand percentage and lower water holding capacity than Halfway and Bushland soils (Table 4.1), which led to drought stress in spite of replenishing the soil profile to 100% plant available water content. Differences in grain sorghum yield between sandy loam and clay loam soils have also been reported in field experiments at Bushland, TX (Tolk and Howell, 2003; Tolk et al., 1997). The percent reduction in irrigated grain sorghum yield in the future compared to historic yield was higher at Lamesa than at the other two sites (Table 4.3). Under RCP 4.5 in the late-century, irrigated grain sorghum yield was 4%, 7%, and 13% lower than historic yield at Bushland, Halfway, and Lamesa, respectively. The difference in grain sorghum response to CC at the three sites could be attributed to the differences in the current and future climatic conditions and soil type. The historic June–Sept average temperature at Bushland, Halfway, and Lamesa was 23.5°C, 24.0°C and 25.5°C, respectively. The projected increase in temperature likely resulted in a larger departure of growing season temperature from the optimum temperature for sorghum growth at Lamesa, resulting in a larger yield loss compared to the other two sites. While the mean June–Sept temperature (ensemble average of nine GCMs) in the late-century under RCP 8.5 was 28.3°C, 28.6°C, and 30.0°C at Bushland, Halfway and Lamesa, respectively. The optimum mean temperature for vegetative growth in grain sorghum ranges between 26°C

to 34°C, and that for reproductive stages ranges between 25°C to 28°C (Maiti, 1996; Prasad et al., 2006).

4.4.2.2. Dryland Grain Sorghum Yield

The simulated dryland grain sorghum yield also decreased in the future when compared to the historic period (Table 4.3), owing to the decline in June–Aug rainfall and increase in temperature (Figure 4.2). The changes in future dryland grain sorghum yield compared to the historic yield, varied between –53% (RCP 8.5 2080s at Halfway under IPSL-CM5A-LR GCM) and 28% (RCP 8.5 2050s at Bushland under GFDL-ESM2M GCM) among CC projections by nine GCMs (Figure 4.3). The greatest reduction in dryland grain sorghum yield of 53% under RCP 8.5 at Halfway in late-century was the result of 53% lower growing season (planting–harvest) rainfall, 7.2°C warmer growing season, and 28 days shorter crop cycle than the historic period under projected climate by the IPSL-CM5A-LR GCM. On the other hand, the maximum increase in dryland grain sorghum yield (28%) was simulated under RCP 8.5 at Bushland in the mid-century due to 16% higher growing season rainfall, 1.8°C warmer growing season, and 10 days shorter crop cycle than the historic period as projected by the GFDL-ESM2M GCM. It is interesting to note that the effects of elevated atmospheric CO_2 levels are simulated in DSSAT in terms of increased radiation use efficiency and reduced transpiration (Singh et al., 2014b; White et al., 2015). In DSSAT v4.6, upon doubling CO_2, sorghum grain yield increased by 4%, which was decided based on the FACE study at Maricopa, AZ (Ottman et al., 2001) and growth chamber study at Gainesville, FL (Prasad et al., 2006). Upon

doubling CO_2, the evapotranspiration of non-water-stressed sorghum was reduced by 13% in the FACE study conducted at Maricopa, AZ (Triggs et al., 2004). In our study, dryland grain sorghum benefitted from an increase in rainfall and CO_2 fertilization when the temperature increase was moderate (<3ºC). However, out of 108 total scenarios (9 GCMs × 3 sites × 2 RCPs × 2 future periods), dryland grain sorghum yield decreased in 87 scenarios when compared to the historic period. Similar to irrigated yield trends, the percent decline in dryland grain sorghum yield under RCP 4.5 in the late-century was comparable to that under RCP 8.5 in the mid-century (e.g., 5% reduction at Bushland). The highest reduction in grain sorghum yield was found for RCP 8.5 in the late-century at all three sites.

Interannual variability in dryland grain sorghum yield generally increased in the future compared to the historic period (Table 4.3). The CV in dryland grain sorghum yield under historic conditions was lowest at Bushland among the three sites and it increased marginally in the future, which could be due to higher water holding capacity and milder current temperatures at Bushland as discussed previously. The CV in dryland grain sorghum at Halfway and Lamesa was comparable under historic and mid-century time periods, and slightly higher at Halfway for the late-century (Table 4.3).

Among the three locations, the historic dryland grain sorghum yield was lowest at Lamesa (Table 4.3). Overall, average dryland grain sorghum yield (ensemble average based on nine GCM projections) reduced in the future compared to the historic period. This reduction was the highest at Halfway and the lowest at Bushland. This reduction in grain sorghum yield in the future was statistically significant—at Bushland under RCP 8.5

in the late-century; at Halfway for all RCPs and future periods; at Lamesa for all RCPs and time periods, except RCP 4.5 in the mid-century (Table 4.3). The reasons behind higher and more significant reduction in dryland grain sorghum yield at Halfway than at Lamesa was most likely due to the greater reduction in June–August rainfall at Halfway than at Lamesa (Figure 4.2). The lowest reduction in dryland grain sorghum yield at Bushland when compared to other two sites could be attributed to its higher water holding capacity and lower current temperatures as discussed in the previous section.

4.4.2.3. Grain Sorghum Irrigation Water Use

The simulated average irrigation water use decreased in the future when compared to the historic values under all RCP scenarios and at all three sites (Table 4.3). This reduction in irrigation water use was significant under all cases, except under RCP 4.5 at Bushland. The difference between future and historic irrigation water use of grain sorghum, as simulated under individual GCM projections (Figure 4.3g–i), varied between –30% (RCP 8.5 2080s at Bushland under MIROC5 GCM) and 13% (RCP 8.5 2050s at Bushland under NorESM1-M GCM). The greatest reduction in irrigation water use of 30% at Bushland in the late-century was the result of 2% higher June–August rainfall, 5.2°C warmer growing season, and 22 days shorter crop cycle than the historic period. On the other hand, the maximum increase in irrigation water use (13%) was simulated at Bushland in the mid-century, mainly due to 23% lower rainfall received during June–August when compared to the historic period. Out of 108 total scenarios (9 GCMs × 3 sites × 2 RCPs × 2 future periods), simulated irrigation water use of grain sorghum

decreased in 79 scenarios, when compared to the historic period. Other possible reasons behind reductions in irrigation water use in the future compared to the historic period could be the reduced transpiration per unit leaf area under elevated atmospheric CO_2 levels (Conley et al., 2001; Singh et al., 2014c), shorter growing season, reduction in maximum leaf area and canopy weight at maturity, and increased growing season rainfall. In contrast, irrigation water use increased under 29 out of total 108 scenarios when growing season rainfall reduced substantially.

The CV in grain sorghum irrigation water use was comparable between the historic and future periods, although the CV in irrigated grain sorghum yield was higher in the future than in the historic period (Table 4.3). The CV in irrigation water use was the lowest for Lamesa and the highest for Bushland among all scenarios. Simulated irrigation water use under different GCM projections showed mixed trends in the future at Bushland and Halfway, and predominately decreasing trend at Lamesa (Figure 4.3g–i). The primary reason behind these differences between the three sites could be the difference in current growing season temperature regimes. The beneficial effects of CO_2 fertilization tend to lessen at higher temperatures. Using controlled environment in growth chambers, Prasad et al. (2006) showed that at elevated CO_2 levels the percent reduction in transpiration was larger for the higher temperature regimes. Historic growing season temperatures at Lamesa were higher than those at Bushland and Halfway, and a further increase in temperature in the future decreased irrigated grain sorghum yield as well as irrigation water use rapidly at Lamesa.

Table 4.3 Projected irrigated and dryland grain sorghum yield, and irrigation water used and temporal/inter-annual coefficient of variation (CV).

	Historic (1976–2005)		2050s (2036–2065)				2080s (2066–2095)			
			RCP 4.5		RCP 8.5		RCP 4.5		RCP 8.5	
	Y (kg ha^{-1}) or I (mm)	CV[a] (%)	ΔY[b] (%)	CV (%)	ΔY (%)	CV (%)	ΔY (%)	CV (%)	ΔY (%)	CV (%)
Irrigated grain sorghum yield (Y)										
Bushland	6511	1.4	–2.1†	2.1	–4.8†	4.0	–3.7†	3.1	–15.8†	8.3
Halfway	6990	1.9	–3.9†	3.0	–6.7†	4.4	–6.5†	3.6	–19.8†	9.6
Lamesa	4927	3.7	–9.6†	4.3	–13.8†	7.0	–12.9†	4.6	–27.5†	11.1
Dryland grain sorghum yield (Y)										
Bushland	2638	10.1	–2.5	10.5	–5.0	13.2	–4.7	13.1	–11.2†	13.5
Halfway	2262	17.5	–12.6†	21.7	–13.6†	23.4	–15.8†	23.5	–27.2†	25.5
Lamesa	1289	16.8	–8.3	20.8	–11.4†	24.6	–9.5†	21.1	–19.3†	22.2
Sorghum irrigation water use (I)										
Bushland	273	11.6	–2.5	11.9	–7.5†	9.6	–4.4	12.2	–13.7†	9.7
Halfway	334	8.6	–4.9†	8.4	–6.9†	8.9	–5.6†	8.8	–13.6†	8.2
Lamesa	326	6.4	–6.2†	6.2	–9.0†	8.1	–8.4†	7.6	–17†	7

[a] CV is coefficient of variation: CV = (standard deviation) ÷ (30-year average yield).

[b] ΔY is the percent change in yield/irrigation from the baseline: $\Delta Y = (Y_i - Y_{Historic}) \div Y_{Historic} \times 100$.

† indicates that the change is significant at 0.05 significance level

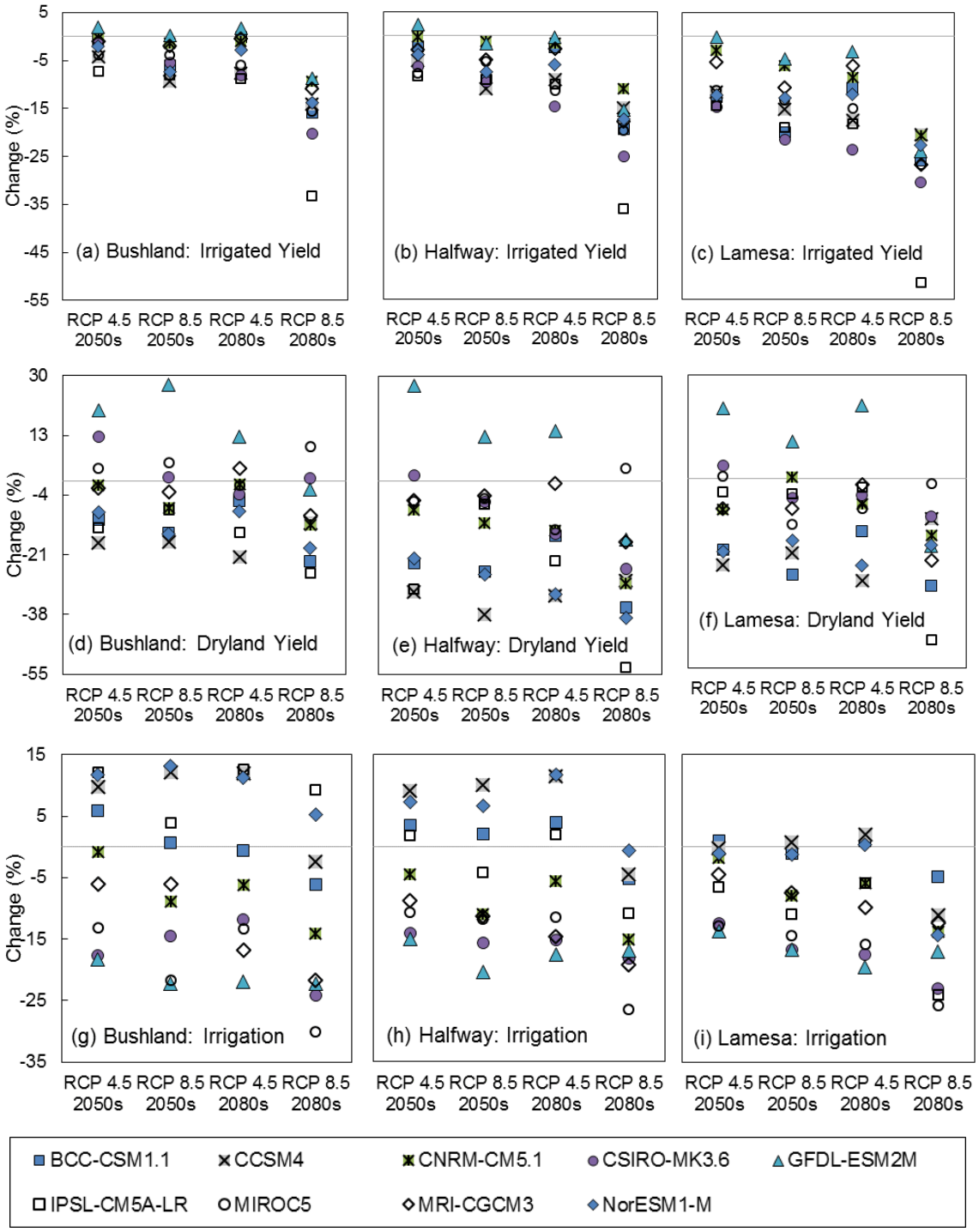

Figure 4.3 Percent change in irrigated and dryland grain sorghum yield and irrigation in 2050s and 2080s compared to historic period under nine GCMs.

4.4.3. Climate Change Adaptation Strategies

4.4.3.1. Bushland

All adaptation strategies, except drought tolerant II and IV resulted in a yield gain for irrigated grain sorghum at Bushland (Table 4.4). Yield gain refers to the percent increase in grain sorghum yield under a virtual cultivar compared to the baseline cultivar for the corresponding time period and RCP. These yield gains were significant for drought tolerant I, heat tolerant I and II, high yield potential, and long maturity virtual cultivars. Among the drought tolerant strategies, increasing root density at different soil depths (drought tolerance I) increased irrigated grain sorghum yield by an order of 7% for the mid-century and 5–6% for the late-century. Reducing root length to weight ratio or making roots finer (drought tolerance II) and reducing maximum water uptake per unit root length (drought tolerance IV) had a slightly negative effect on irrigated grain sorghum yield (<0.4% yield loss). Irrigated grain sorghum yield gains under heat tolerance II strategy were slightly higher than those under heat tolerance I strategy, especially under RCP 8.5 in the late-century. This is expected since the projected temperature rise under RCP 8.5 was higher than that under RCP 4.5. The virtual cultivar with higher yield potential resulted in the highest irrigated grain sorghum yield gains among all of the eight virtual cultivars tested under both RCPs and time periods. The yield gain by incorporating high yield potential was 6.9% and 8.2% under RCP 4.5 and RCP 8.5 in the mid-century, respectively; and of the order of 7.7% and 12.4% under RCP 4.5 and RCP 8.5 in the late-century, respectively. The long maturity virtual cultivar resulted in the third highest irrigated grain sorghum yield gain among the adaptation strategies tested under both RCPs

in mid-century and under RCP 4.5 in the late-century. The ranking of yield gains under different adaptation strategies was slightly different under RCP 8.5 in the late-century; where the first, second and third highest yield gains were simulated under high yield potential, long maturity, and heat tolerant II virtual cultivars, respectively.

Irrigation water use of grain sorghum, which was simulated using the auto-irrigation tool in DSSAT, was lower under drought tolerant I cultivar than the baseline cultivar (Table 4.4). This difference was significant under RCP 8.5 for both mid-century (−6.1%) and late-century (−6.4%) periods. This is primarily due to improved capability of roots to extract water from deeper soil layers. Irrigation water use slightly decreased (up to −2.0%) under drought tolerant II and IV, and high yield virtual cultivars compared to the baseline cultivar. Irrigation water use marginally increased (up to 3.8%) under drought tolerant III and heat tolerant I and II virtual cultivars compared to the baseline cultivar. The irrigation water use was significantly higher under long maturity virtual cultivar than the baseline cultivar for both RCPs and future time periods. The increase in irrigation water use in case of longer maturity cultivar compared to the baseline cultivar was 12.6% and 11.8% under RCP 4.5 and RCP 8.5 for the mid-century, respectively, and of the order 10.4% and 8.7% under RCP 4.5 and RCP 8.5 for the late-century, respectively.

Table 4.4 Simulated changes (%) in irrigated and dryland grain sorghum yield (ΔY), and irrigation water use (ΔI) under different adaptation scenarios with respect to the no adaptation scenario for Bushland, TX.

	Change in Irrigated Grain Sorghum Yield (ΔY)[+]				Change in Dryland Grain Sorghum Yield (ΔY)				Change in Irrigation Water Use (ΔI)[‡]			
	2050s (2036–2065)		2080s (2066–2095)		2050s (2036–2065)		2080s (2066–2095)		2050s (2036–2065)		2080s (2066–2095)	
RCP / Adaptation	4.5	8.5	4.5	8.5	4.5	8.5	4.5	8.5	4.5	8.5	4.5	8.5
Drought tolerant I	6.8†	6.5†	6.4†	5.0†	9.5†	11.7†	10.6†	14.2†	−6.1	−6.1†	−5.6	−6.4†
Drought tolerant II	−0.3	−0.2	−0.2	−0.1	−0.2	0.1	−0.2	0.6	−1.0	−1.1	−1.4	−1.2
Drought tolerant III	0.3	0.3	0.3	0.2	−0.8	−0.5	−0.7	−0.3	1.0	1.1	0.5	0.6
Drought tolerant IV	−0.4	−0.4	−0.4	−0.3	1.4	0.8	1.5	1.0	−0.9	−1.1	−1.2	−1.2
Heat tolerant I	1.2†	2.5†	1.8†	5.4†	1.2	1.7	1.7	3.7	0.6	1.3	0.8	2.3
Heat tolerant II	1.4†	2.9†	2.1†	7.2†	1.3	2.0	2.1	4.6	0.6	1.6	1.0	3.8
High yielding	6.9†	8.2†	7.7†	12.4†	7.5†	8.1†	7.6†	10.3†	−1.2	−0.9	−2.0	−1.8
Long maturity	2.3†	3.7†	3.1†	8.1†	−2.9	−3.2	−1.7	0.3	12.6†	11.8†	10.4†	8.7†

† indicates that the change is significant at 0.05 significance level

[+] $\Delta Y = [(\text{Yield (Adaptation, i)} - \text{Yield (No Adaptation)}) \div \text{Yield (No Adaptation)}] \times 100$

‡ $\Delta I = [(\text{Irrigation (Adaptation, i)} - \text{Irrigation (No Adaptation)}) \div \text{Irrigation (No Adaptation)}] \times 100$

A simultaneous examination of irrigated grain sorghum yield and irrigation water use across different adaptation strategies was performed to identify ideal strategies for irrigated grain sorghum production at Bushland under CC. While drought tolerant I trait minimized irrigation water use, high yield potential trait maximized irrigated grain sorghum yield under all RCPs and time periods (Table 4.4). The yield gains were comparable under both the virtual cultivars expect under RCP 8.5 in the late-century. When heat stress was dominant, greater yield gains were simulated with heat tolerant, high yield potential, and longer maturity traits than drought tolerant I trait. This shows that, increasing root density at different soil depths (drought tolerant I cultivar) could result in irrigation water savings while enhancing irrigated grain sorghum yield, given the temperature remains close to the optimum level for grain sorghum production. However, under extreme heat stress conditions, enhancing yield potential traits (RUE, G1, and G2) and heat tolerance during grain filling could be a potential adaptation strategy. Although the longer maturity trait resulted in irrigated grain sorghum yield gains, the associated increase in irrigation water use makes this adaptation less favorable in places such as THP where irrigation water conservation is of prime importance.

With regards to the dryland grain sorghum production, drought tolerant I cultivar resulted in the maximum yield gains followed by high yield potential cultivar under both RCPs and future time periods (Table 4.4). Yield gains were also simulated under drought tolerant IV, heat tolerant I and II virtual cultivars in the order of 1%, 3.7%, and 4.6%, respectively under RCP 8.5 in the late-century. Surprisingly, incorporating the longer maturity trait resulted in dryland grain sorghum yield loss at Bushland. This outcome is

contrary to that of Singh et al. (2014c), who simulated yield gains for longer maturity grain sorghum cultivar under dryland conditions for both historic and future periods at all four sites in India and Mali. A possible reason for this might be the temporal distribution of rainfall at Bushland; lengthening growing season has likely led to reduced availability of rainfall during critical stages of grain sorghum production. The average length of growing season in the mid-century for the baseline and long maturity cultivars was 99 and 110 days, respectively. The months of June (when sorghum was planted) and August were typically wetter than July and September at Bushland. The longer maturity cultivar was designed by increasing the duration of both vegetative (time between emergence to end of juvenile phase) and reproductive phases (time between beginning of grain filling to maturity). Increased vegetative growth due to the cultivar design as well as CO_2 enrichment could be another reason for reduced availability of water during reproductive growth stage (grain filling). Further work is required to elucidate the relationship between rainfall distribution and performance of longer maturity sorghum cultivar under rainfed conditions at Bushland. These results suggest that increasing soil root density and enhancing yield potential traits could significantly increase dryland grain sorghum yields under CC. Performance of longer maturity cultivars under dryland conditions will likely depend upon the rainfall distribution over the growing season. Adopting a longer maturity grain sorghum cultivar as an adaptation strategy under dryland conditions will require additional caution due to the higher uncertainty associated with rainfall projections than the temperature projections under CC.

4.4.3.2. Halfway

At Halfway, all adaptation strategies except drought tolerant IV resulted in an increase in yield for irrigated grain sorghum (Table 4.5). These yield gains were significant for drought tolerant I, heat tolerant II, high yield potential, and long maturity virtual cultivars under both RCPs and future time periods. Similar to the trends at Bushland, the largest increase in yield was simulated for the cultivar with high yield potential traits among all the virtual cultivars that were evaluated. The increase in yield by incorporating high yield potential were 7.4% and 8.4% under RCP 4.5 and RCP 8.5 in the mid-century, respectively; and of the order 8.3% and 13.6% under RCP 4.5 and RCP 8.5 in the late-century, respectively. The second largest increase in yield gains was simulated under drought tolerant I cultivar for the mid-century, and for the long maturity cultivar for the late-century period. The increase in yield by incorporating drought tolerance I was comparable across RCPs and future time periods, whereas, the increase in yield progressively increased with heat tolerance, long maturity, and high yield potential traits as the temperature rise increased from RCP 4.5 to RCP 8.5 and from mid- to late-century.

Table 4.5 Simulated changes (%) in irrigated and dryland grain sorghum yield (ΔY), and irrigation water use (ΔI) under different adaptation scenarios compared to no adaptation scenario for Halfway, TX.

	Irrigated Yield (ΔY)[+]				Dryland Yield (ΔY)				Irrigation Water Use (ΔI)[‡]			
	2050s (2036–2065)		2080s (2066–2095)		2050s (2036–2065)		2080s (2066–2095)		2050s (2036–2065)		2080s (2066–2095)	
RCP / Adaptation	4.5	8.5	4.5	8.5	4.5	8.5	4.5	8.5	4.5	8.5	4.5	8.5
Drought tolerant I	4.6†	4.8†	4.5†	3.8†	7.0	7.9	6.9	7.7	−1.8	−2.0	−2.1	−2.5
Drought tolerant II	−0.05	0.2	0.1	0.3	2.3	2.1	2.3	3.2	−0.2	−0.4	−0.4	−0.4
Drought tolerant III	0.04	0.3	0.01	0.2	0.2	−0.1	−0.2	0.05	0.7	0.7	0.5	1.1
Drought tolerant IV	−0.5	−0.3	−0.5	−0.4	0.3	−0.04	0.3	0.1	−1.1	−1.2	−1.7	−1.4
Heat tolerant I	1.4	2.4†	1.9†	5.9†	1.2	2.5	1.5	4.5	0.3	0.5	0.3	1.3
Heat tolerant II	1.6†	2.7†	2.2†	7.8†	1.4	3.0	1.9	5.7	0.3	0.8	0.3	1.7
High yielding	7.4†	8.4†	8.3†	13.6†	14.3†	13.8†	14.4†	17.1†	−0.7	−1.2	−0.4	0.0
Long maturity	3.1†	4.7†	4.9†	10.9†	7.2	5.8	6.7	9.1	10.7†	9.6†	9.7†	11.4†

† indicates that the change is significant at 0.05 significance level

[+] $\Delta Y = [(\text{Yield (Adaptation, i)} - \text{Yield (No Adaptation)}) \div \text{Yield (No Adaptation)}] \times 100$

‡ $\Delta I = [(\text{Irrigation (Adaptation, i)} - \text{Irrigation (No Adaptation)}) \div \text{Irrigation (No Adaptation)}] \times 100$

The drought tolerant I virtual cultivar consumed less irrigation water than the baseline cultivar (e.g. 2.5% lower irrigation water use under RCP 8.5 in the late-century; Table 4.5). Irrigation water use for the longer maturity cultivar was significantly higher than the baseline cultivar under both RCPs and time periods. The difference between the irrigation water use of longer maturity cultivar and baseline cultivar was 10.7% and 9.6% under RCP 4.5 and RCP 8.5 for the mid-century, respectively; and of the order of 9.7% and 11.4% under RCP 4.5 and RCP 8.5 for the late-century, respectively. Irrigation water use of other virtual cultivars was comparable with that of the baseline cultivar. Unlike at Bushland, the differences in irrigation water use under drought tolerant I and high yield potential cultivars were comparable at Halfway. These results suggest that improving yield potential traits could be an optimal CC adaptation strategy for irrigated grain sorghum production at Halfway.

For dryland grain sorghum production, the highest increase in yield gains was simulated for the high yield potential virtual cultivar (up to 17.1%) followed by the long maturity (up to 9.1%) and drought tolerant I (up to 7.9%) cultivars (Table 4.5). The heat tolerant II (up to 5.7%) cultivar produced a relatively higher yield than the heat tolerant I (up to 4.5%) cultivar. These results corroborate with the findings of Singh et al. (2014c). Interestingly, unlike at Bushland, the drought tolerant II cultivar (20% higher root length-to-weight ratio than the baseline cultivar) resulted in an increase in yield of 2.1% and 3.2% for the mid- and late-century under RCP 8.5, mainly because of an increase in the nitrogen (N) uptake rate. While the simulated N uptake of drought tolerant II cultivar at Halfway was on an average about 3% greater than that of the baseline cultivar under dryland

conditions, the N uptake rate at Bushland was about the same for both cultivars under dryland conditions (data not shown). Based on field and greenhouse studies of common bean, Polania et al. (2017) also reported a higher N uptake from a soil with a fine root system under drought stress. Fine roots can facilitate greater water and nutrient acquisition under low soil water conditions, due to their greater surface area per unit mass (Huang and Fry, 1998). Similar effect of increase in peanut pod yield with increasing root length-to-weight ratio was simulated in a previous DSSAT study (Naab et al., 2015), due to increased rooting volume for phosphorus (P) extraction. The effect was more prominent under low P fertility conditions. Overall, the increase in yield by increasing root length-to-weight ratio were not statistically significant and they were lower than those simulated with a higher root density (drought tolerant I cultivar). In summary, the results indicate that dryland grain sorghum production at Halfway in the future could benefit from improving yield potential traits, increasing soil root density, and using longer maturity cultivar.

4.4.3.3. Lamesa

All adaptation strategies resulted in an increase in grain sorghum yield for yield for irrigated grain sorghum at Lamesa (Table 4.6). These increases were significant for all strategies, except drought tolerant III and IV cultivars under RCP 4.5, and for all strategies except drought tolerant II, II and IV under RCP 8.5, for both the future periods. The largest and second largest increase in yield was simulated with high yield potential and long maturity traits, respectively for all RCPs and future periods. The third largest increase in

yield was simulated with drought tolerant I trait under both RCPs in the mid-century, and RCP 4.5 in late-century. Under RCP 8.5 for the late-century, the third largest increase in yield was simulated with the heat tolerant II trait. The increase in yield by incorporating high yield potential was 14.1% and 15.7% under RCP 4.5 and RCP 8.5 in the mid-century, respectively; and about 15.7% and 19.3% under RCP 4.5 and RCP 8.5 for the late-century, respectively. The increase in yield under high yield potential was the largest compared to other CC adaptation strategies for all three sites. However, the magnitude of the increase in yield at Lamesa was almost double compared to the yield increase for both Bushland and Halfway. One of the possible reasons for this trend is the differences in the crop cycle among the three sites. According to Singh et al. (2014c), who compared sorghum yield with different genetic traits, increasing yield potential traits resulted in larger increase in yield for the shorter cycle cultivar than for longer cycle cultivars. For the historic period, the average growing season duration for grain sorghum at Bushland, Halfway, and Lamesa were 114, 110, and 100 days, respectively.

The simulated irrigation water use of the adaptive cultivars was comparable with that for the baseline cultivar, except for the long maturity cultivar (Table 4.6). For the long maturity cultivar, irrigation water use was significantly higher than for the baseline cultivar. The difference between irrigation water use for the long maturity cultivar and baseline cultivar was 11.8% and 12.5% under RCP 4.5 and RCP 8.5 for the mid-century, respectively, and about 12.8% and 14.3% under RCP 4.5 and RCP 8.5 for the late-century, respectively. These results further support the use of high yield potential as an optimum CC adaptation strategy for irrigated grain sorghum production in the THP in the future,

and indicate that the long maturity cultivars would increase irrigation water use significantly.

The first, second and third largest increase in dryland grain sorghum yield were simulated with the high yield potential, drought tolerant I, and long maturity cultivars, respectively, for all RCPs and future time periods (Table 4.6). However, the increase in yield was significant for only the high yield potential cultivar. Marginal yield loss was simulated with drought tolerant III cultivar. The recommendations for optimum virtual cultivars for Lamesa are similar to those for Halfway with high yield potential being the most effective strategy among the CC adaptation strategies tested. However, the magnitude of the yield increase was different for different locations, suggesting that same adaptation strategy may not be equally effective at all sites in the THP.

Table 4.6 . Simulated changes (%) in irrigated and dryland grain sorghum yield (ΔY), and irrigation water use (ΔI) under different adaptation scenarios with respect to the no adaptation scenario for Lamesa, TX.

	Irrigated Yield (ΔY)[+]				Dryland Yield (ΔY)				Irrigation Water Use (ΔI)[‡]			
	2050s (2036–2065)		2080s (2066–2095)		2050s (2036–2065)		2080s (2066–2095)		2050s (2036–2065)		2080s (2066–2095)	
RCP / Adaptation	4.5	8.5	4.5	8.5	4.5	8.5	4.5	8.5	4.5	8.5	4.5	8.5
Drought tolerant I	8.9†	9.3†	9.0†	7.7†	9.5	11.3	9.7	10.7	−1.9	−1.7	−1.7	−2.1
Drought tolerant II	2.6†	3.1	3.0†	3.3	2.2	2.6	2.4	2.8	0.7	0.9	0.7	1.0
Drought tolerant III	1.7	2.3	2.1	2.2	−0.3	−0.2	−0.2	−0.2	−0.4	−0.4	−0.2	−0.4
Drought tolerant IV	0.7	0.9	1.0	0.9	0.4	0.3	0.5	0.5	−1.4	−1.6	−1.3	−1.5
Heat tolerant I	5.5†	7.4†	6.3†	9.0†	3.2	3.8	3.3	5.4	−0.7	−0.5	−0.4	−0.5
Heat tolerant II	6.5†	9.1†	7.4†	11.7†	3.7	5.0	4.1	7.5	−0.7	−0.5	−0.5	−0.5
High yielding	14.1†	15.7†	15.7†	19.3†	14.6†	15.7†	15.2†	16.7†	0.6	0.5	1.0	1.6
Long maturity	11.0†	12.1†	13.0†	16.7†	8.6	7.2	8.3	8.2	11.8†	12.5†	12.8†	14.3†

† indicates that the change is significant at 0.05 significance level

[+] $\Delta Y = [(\text{Yield (Adaptation, i)} - \text{Yield (No Adaptation)}) \div \text{Yield (No Adaptation)}] \times 100$

‡ $\Delta I = [(\text{Irrigation (Adaptation, i)} - \text{Irrigation (No Adaptation)}) \div \text{Irrigation (No Adaptation)}] \times 100$

4.5. Conclusions

The CC impacts on grain sorghum production at three locations in the Texas High Plains (Bushland, Halfway, and Lamesa) were studied under 18 CC scenarios (projections from 9 GCMs × 2 RCPs) in order to assess the combined impact of future temperature, rainfall, and atmospheric CO_2 levels on grain sorghum yield for irrigated and dryland production systems and associated water requirements for irrigation. For irrigated conditions, sorghum yield, on average (of nine GCMs), was reduced between 2% and 14% for the mid-century and between 4% and 28% for the late-century compared to the historic period, primarily due to heat stress and resultant shortening of growing season length. For dryland conditions, sorghum yield based on different GCM climate projections showed a larger variation than for irrigated conditions. A severe increase in growing season temperature (>°3C) when coupled with large rainfall reductions (>20%), resulted in a decrease in dryland grain sorghum yield up to 53% and on average 23%. Due to the beneficial effects of CO_2 fertilization, yield for dryland conditions was comparable or even increased in the future compared to the historic period when the increase in growing season temperature was moderate and the rainfall amount was about the same or higher. The interannual variability in irrigated and dryland grain sorghum yield increased under CC in the future compared to baseline, indicating that climate will shift from optimal to marginal growing conditions. Irrigation water use for grain sorghum decreased under CC, which could be attributed to a reduction of the growing season length, maximum leaf area, canopy weight at maturity, transpiration per unit leaf area, and increase in growing season

rainfall in case of some GCM projections. Grain sorghum yield and water use predictions for the three sites varied due to the differences in soil properties and climatic conditions.

Among the virtual cultivars tested, a maximum and significant increase in yield for both irrigated and dryland conditions was simulated with the high yield potential trait under both RCPs and future periods compared to the standard cultivar. The drought tolerant I strategy also significantly increased irrigated grain sorghum yields at all the three locations, and dryland grain sorghum yields at Bushland. Other drought tolerant strategies (II, III and IV) had negligible effect on both irrigated and dryland grain sorghum yields and irrigation water use at all the three sites. Heat tolerant trait resulted in yield gain, however, the percent yield gain was not in the top three among all the virtual cultivars tested. The efficacy of different adaptation strategies was not consistent at the three locations, suggesting that a single adaptation method for sustaining grain sorghum production may not be applicable for all the locations in the THP. Enhancing yield potential traits was found to be the optimum strategy as it maximized grain sorghum yield without substantially altering irrigation water demand. The longer maturity cultivar had a significantly higher irrigation water demand and thus was not suitable for the THP.

5. POTENTIAL BENEFITS OF GENOTYPE-BASED ADAPTATION STRATEGIES FOR COTTON PRODUCTION IN THE TEXAS HIGH PLAINS UNDER CLIMATE CHANGE

5.1. Synopsis

Cotton is a major cash crop in the Texas High Plains (THP), which contributes to about 25% of the total and 37% of irrigated cotton acreage in the United States. This region depends on the exhaustible Ogallala Aquifer for irrigation water. Research efforts are needed to develop cotton cultivars that would help in sustaining cotton production under limited water conditions and climate change (CC). In this study, the DSSAT-CSM-CROPGRO-Cotton model evaluated in Chapter II was used to develop and assess cotton cultivars for CC adaptation. Potential climate-change-adaptive genetic traits were tested for drought tolerance, heat tolerance, high yield potential, and longer maturity. These simulations were repeated at three sites in the THP, Bushland, Halfway, and Lamesa. The trend and direction of change in seed cotton yield in the future were different for the three sites. Sites with finer soil and currently lower temperature (Bushland and Halfway) are expected to benefit from carbon dioxide (CO_2) enrichment. Irrigated seed cotton yield at Bushland and Halfway is expected to increase by 21% and 13%, respectively, by mid-century (2036–2065) compared to the historic period (1976–2005). In contrast, irrigated seed cotton yield at Lamesa (with hotter weather and coarser soil) is expected to reduce by 2% by mid-century compared to the historic period, primarily due to higher than optimal temperature during cotton growing season. Irrigation water use is expected to

increase at all three sites by an average of 8% in the mid-century compared to the historic period. Among the adaptation scenarios tested, maximum gains in seed cotton yield were obtained with the long maturity trait (8%) followed by high yield potential trait (7%) and drought tolerance (7%) compared to no adaptation. However, irrigation water use of cotton with long maturity trait was significantly higher (9% more) than the no adaptation scenario. These results show that cotton production may benefit from CO_2 enrichment if the mean temperature during the cotton growing season remains below the optimal limit (~25°C). Shifting to a longer maturity cultivar under CC could minimize yield loss, if any, due to temperature rise; however, associated increase in irrigation water requirement makes it a less desirable trait for irrigated cotton production in the THP. Increasing area of full leaf, enhancing partitioning of assimilates to reproductive growth (high yield potential), and increasing root length per unit root weight (drought tolerance) were identified as desirable climate-change-adaptive traits for irrigated cotton production in the THP region.

5.2. Introduction

Crop growth is highly dependent on climatic conditions and hence agricultural sector is susceptible to climate change (CC) (Rosenzweig et al., 2001). Increase in rainfall variability and frequency of extreme weather events, as expected under a warming climate (Coumou and Rahmstorf, 2012; IPCC, 2014), would likely affect agriculture on global and regional scales. The Texas High Plains (THP) region in the United States (US) has extensive agricultural acreage. The sustainability of agriculture in this region is further

affected by its dependence on the exhaustible Ogallala Aquifer (Chaudhuri and Ale, 2014). Research efforts are needed to identify potential strategies that are aimed at efficiently utilizing irrigation water in the region while maintaining profitable crop yield under CC. Cotton is a major cash crop in the THP. About 35% of the total upland cotton acreage in the United States is in the THP region, of which 43% is irrigated, according to 2010–2018 annual average (USDA-NASS, 2018). Farmers and planners in the region could benefit from enhanced understanding of potential CC impacts on cotton production in the region. Response of cotton to CC is widely documented in controlled-environment and simulation modeling studies (Adhikari et al., 2016; Gérardeaux et al., 2018; Kimball et al., 2002).

Air temperature, rainfall, and atmospheric carbon dioxide (CO_2) concentration are primary drivers of crop response to CC (Parry et al., 2004). Cotton [*Gossypium hirsutum* L.] is a C_3 plant, which shows substantial increase in photosynthesis rates at elevated CO_2 levels (Kimball et al., 2002). Researchers at Maricopa, AZ reported a 43% increase in harvestable cotton yield in a Free Air CO_2 Enrichment (FACE) experiment at ambient temperature with 550 ppm CO_2 (Mauney et al., 1994). In a recent study in Richmond, Australia (Broughton et al., 2017), cotton was grown in a greenhouse under two CO_2 (400 ppm and 640 ppm), and two day/night temperature regimes (28/17°C and 32/21°C). It was reported that elevated CO_2 increased vegetative biomass at lower temperature treatments, but not at higher temperature treatments. Water use of cotton increased by 7% under elevated CO_2 treatments for both temperature treatments. Researchers at Mississippi State, MS, have previously used naturally lit growth chambers with controlled environments (Reddy et al., 1995). They reported that—CO_2 enrichment

increased the number of bolls by 28%, but not the boll weight at optimum temperatures. At higher temperature, (>35.5°C) no bolls were produced at any CO_2 treatment (Reddy et al., 1995). Boll retention was found to be the most temperature-sensitive stage and 32°C temperature was identified as the maximum temperature for cotton boll survival (Reddy et al., 1999). It is evident from these studies that the positive effects of CO_2 fertilization on cotton yields vary with the air temperature. Therefore, studying interactive effect of these two parameters, atmospheric CO_2 concentration and temperature, under a wide range of regimes, which is difficult to obtain in a controlled environment setting, would be beneficial in developing CC adaptation strategies for cotton growth.

The Decision Support System for Agrotechnology Transfer (DSSAT) CROPGRO-Cotton model, a process-based cropping system model, has been widely used to simulate cotton growth under CC. Adhikari et al. (2016) assessed the impacts of CO_2 fertilization on cotton yield in the THP region and reported a 14–29% increase in seed cotton yield in 2041–2070 when compared to 1971–2000 under non-water limiting conditions. Anapalli et al. (2016) also reported an increase in irrigated seed cotton yield under CC in the Mississippi Delta region under moderate temperature rise; but yields decreased beyond 2050 under extreme temperature rise (2.6–4.6°C). However, in a recent study in Punjab, Pakistan (Rahman et al., 2018), the simulated seed cotton yields were 12% and 30% lower than baseline seed cotton yields in near term (+1.8°C temperature rise) and mid-century (+3.5°C temperature rise), respectively.

Few researchers have used simulation models for evaluating potential cotton ideotypes in Cameroon, Africa Loison et al. (2017), evaluated several crop parameters for

CC adaptation using the DSAT-CROPGRO-Cotton model. They found that ideotypes with early flowering and longer reproductive periods were best suited under CC. Similarly, Gérardeaux et al. (2018) found that longer maturity and thicker leaves are potential traits for cotton production in Sub-Saharan Africa. Majority of the researchers have tested cotton genotypes for dryland conditions and there is little published data on potential adaptation strategies for irrigated conditions and on irrigation water use. In addition, the interaction between soil, climate, and genetic traits could affect the performance and selection of potential adaptation strategies. Producers and water managers in the THP region, a major cotton producing area in the US, could benefit from similar recommendations for adaptive cotton genotypes. The objectives of this study are to: (a) assess climate change impacts on cotton yield and irrigation water use in the THP region; and (b) evaluate multiple genetic traits for CC adaptation, using the DSSAT-CSM-CROPGRO-Cotton model.

5.3. Material and Methods

5.3.1. The DSSAT Model

The CROPGRO crop template model, initially developed for grain legumes (Boote et al., 1998), computes crop growth processes for a crop using its species traits and cultivar parameters (Jones et al., 2003). Cotton was later integrated into the CROPGRO model using the data for parametrization from literature (Messina et al., 2004; Pathak et al., 2007). In the CROPGRO model, crop development stages are predicted based on temperature, photoperiod, and water deficit (Boote et al., 1998). If all the three conditions

are optimal on any given day, it is counted as one physiological day; and once the accumulated physiological days reach the required number, the crop development phase is completed. Photosynthesis is computed using the hedgerow light interception model and leaf related parameters, with adjustments for atmospheric CO_2, row spacing, and cultivar specific photosynthesis rate (Boote and Pickering, 1994). The daily carbon assimilation rate has an asymptotic response to CO_2. An overview of CROPGRO model and photosynthesis response to CO_2 can be found in (Boote et al., 1998) and (Alagarswamy et al., 2006), respectively. The inputs required for crop growth simulation include soil properties, weather data, crop management data, and initial conditions (Jones et al., 2003).

5.3.2. Study Sites and Model Inputs

Three sites within the THP region were chosen due to the availability of input data for model parameterization. The three sites, Bushland, Halfway, and Lamesa, are located in the northern, middle, and southern parts of the region, respectively. There is a temperature gradient from north to south (warmer) and average annual rainfall is comparable at the three sites. Soils at Bushland and Halfway site are fine textured, whereas that at Lamesa site is coarser. Soil data was either obtained from field measurements, as given in (Adhikari et al., 2016), or estimated using the SBuild tool in DSSAT. Measured soil inputs include percentages of sand and clay, pH, nitrogen and organic carbon, and cation exchange capacity.

The CROPGRO-Cotton model parameters, calibrated previously (Kothari et al., 2019) against field data from the Halfway site, were used for scenarios analysis at all three sites. Measured data used for calibration was obtained from field experiments conducted at Halfway over eight growing seasons and three irrigation experiments. Systematic adjustment of genotype parameters related to phenology, development, and yield resulted in a close match between simulated and observed onset of growth stages and yield. Mean difference between observed and simulated seed cotton yield during model calibration and evaluation was 3.4% and −10.5%, respectively. More details about model calibration are given in Kothari et al. (2019).

Weather data projected by nine global climate models (GCMs), which was bias corrected and statistically downscaled using the Multivariate Adaptive Constructed Analogs (MACA) method (Abatzoglou, 2013), were used. More details about the future climate data are available in Chapters III–IV. Crop management inputs were obtained from reported values for the THP region (Adhikari et al., 2016; Bordovsky et al., 2015; Bronson et al., 2009; Segarra et al., 1991).

Cotton was planted on May 11th at 13 seeds m^{-2} (Bordovsky et al., 2015). Seeds were planted at a 3.8 cm depth with a row spacing of 1.02 m. Fertilizer was applied at the rate of 120 kg N ha^{-1} and 52 kg N ha^{-1} for irrigated and dryland cotton, respectively, based on average values from field experiments at Halfway (Bordovsky et al., 2011). For dryland cotton, fertilizer amount was halved and applied at 35 and 60 DAP, whereas for irrigated cotton, fertilizer amount was split into three equal doses and applied at 35, 60, and 70 DAP. The fertilizer scheduling in case of cotton roughly corresponded to the first square,

first bloom and mid bloom growth stages, respectively as suggested by Bronson and Bowman (2009). Tillage practices simulated include the use of field cultivator (on 25-Jan), bed roller (on 1-Mar) and rotary hoe (31-Mar), similar to Bordovsky et al. (2015). Irrigation was simulated using "auto-irrigation" feature of DSSAT, assuming 90% irrigation efficiency. Irrigation was applied to replenish plant available water content in the top 30 cm profile (default) to 100% whenever it dropped to 50%. The initial soil water for irrigated and dryland conditions was assumed as 100% and 75% of plant available water content, respectively. Initial soil nitrogen in the top 210 cm profile for irrigated conditions was set at 120 kg N ha^{-1}, which was close to the measured value in Lubbock, TX (Bronson et al., 2001), and within the range of values reported at eight cotton fields across the southern THP (Bronson et al., 2009). For dryland cotton, initial soil nitrogen was assumed to be 52 kg N ha^{-1}. The initial conditions in this seasonal analysis were updated at the beginning of each year on January 1.

5.3.3. Adaptation Scenarios/ Virtual Cultivars

Genotype parameters obtained after model calibration were used as it is for climate change impact assessment. For testing adaptation scenarios, however, the genotype parameters were changed to create virtual cultivars. The methodology used in this study was built upon the methodology used by Singh et al. (2014c) for sorghum and Loison et al. (2017) for designing cotton ideotypes. A total of six virtual cultivars were tested in this study.

5.3.3.1. Drought Tolerance I and II

Some of the characteristics of drought tolerant cotton are—efficient and vigorous root system, smaller and thicker leaves, lower transpiration and higher photosynthetic rates than non-drought-tolerant varieties (Iqbal et al., 2013; Levi et al., 2009; Ullah et al., 2017). These characteristics were incorporated by changing relevant model parameters. Drought tolerant I virtual cultivar was created by increasing parameters *RFAC1* (root length per unit root weight, cm/g), *RWUMX* (Maximum water uptake per unit root length, constrained by soil water (cm^3[water] / cm[root]) and *LFMAX (*Maximum leaf photosynthesis rate) and decreasing *RWUEP1* (soil water supply to potential transpiration ratio). The ***RFAC1*** parameter was increased from 12000 (default) to 17000 (value used in a cotton root-knot nematode modeling study in Tifton, Georgia (Ortiz et al., 2009)). This is in accordance with a field study in Pakistan (Riaz et al., 2013), where researchers reported that the most drought tolerant cotton line/variety had the highest root length to root weight ratio, among the six lines studied. The ***RWUMX*** parameter was increased from 0.04 (default) to 0.08 (calibrated for Northern Cameroon under current climate conditions (Loison et al., 2017)). The ***LFMAX*** parameter was increased from 1.3 (calibrated) to 1.4. The ***RWUEP1*** parameter was reduced from 1.5 (default) to 1.2 (Loison et al., 2017). Drought tolerant II cultivar was designed in the same way as drought tolerant I, except that RWMUX was decreased from 0.04 to 0.02.

5.3.3.2. Heat Tolerance I and II

Heat stress can negatively affect seed cotton yields by affecting boll retention and reducing boll size (Lokhande and Reddy, 2014; Singh et al., 2007). Heat tolerant cotton

cultivar is expected to have better boll retention at higher temperature (Liu et al., 2006). In order to incorporate heat tolerance, the upper optimum and failure temperature thresholds of boll addition rate (***FNPDT***), and partitioning to boll (***YXFTEM***) were increased (Figure 5.1). These thresholds were increased by 2 ºC and 3 ºC in Heat Tolerant I and Heat Tolerant II cultivars, respectively. This methodology is a modified version of the approach used by Singh et al. (2014a) for chickpea.

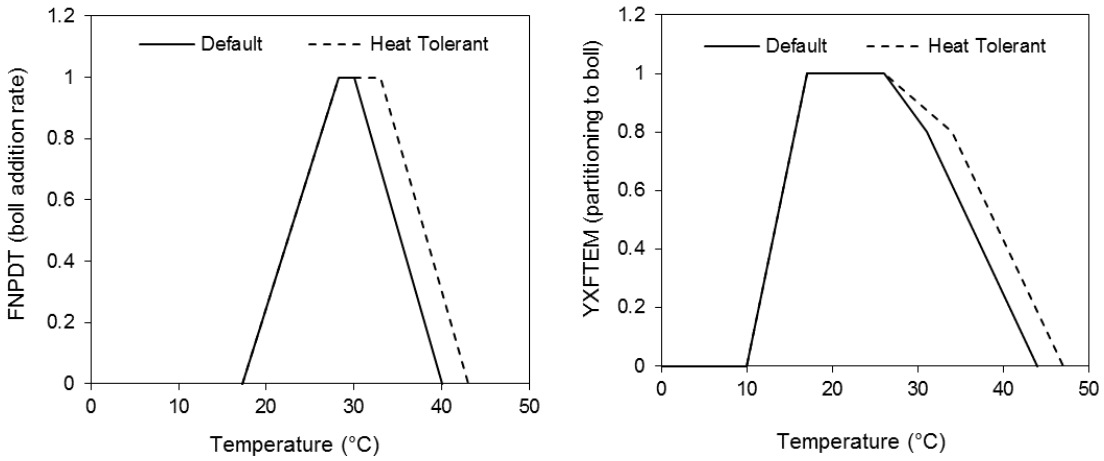

Figure 5.1 Default and modified (for heat tolerance) temperature response functions for cotton boll addition rate (left) and partition to boll (right), adapted with permission from Singh et al. (2014a).

5.3.3.3. High Yield Potential

A high yielding cultivar was designed by targeting yield related parameters. Maximum size of full leaf in cm^2 (***SIZLF***) was changed from 250 to 275; maximum fraction of daily growth that is partitioned to seed + shell (***XFRT***) was changed from 0.8 to 0.88; and the maximum ratio of (seed/(seed+shell)) at maturity (***THRSH***) was changed from 70 to 72.

5.3.3.4. Long Maturity

As suggested by Loison et al. (2017), early flowering and longer reproductive phase could optimize crop yields under climate change. A long maturity cultivar was created by lengthening crop cycle by 10% (as implemented by Singh et al. (2014c)), and inducing earlier flowering. Parameter ***EM-FL*** (time between plant emergence to flower appearance, photothermal days) was changed from 38 to 34; and ***SD-PM*** (time between first seed and physiological maturity, photothermal days) was changed from 40 to 51.

5.4. Results and Discussion

5.4.1. Climate Change Impact Assessment

Irrigated yield showed a mixed trend in the future across different sites (Figure 5.2 and Table 5.1). The percent change in irrigated yield in the future compared to the baseline period varied between –20% (RCP 8.5 2080s at Lamesa) and +26% (RCP 4.5 2080s at Bushland) (Figure 5.2). The primary reason for the increment in irrigated seed cotton yield was "CO_2 fertilization" effect, which resulted in increased maximum leaf area index (data not shown). On the other hand, increase in atmospheric temperatures adversely affected seed cotton yields, mainly by reducing the length of growing season. The interannual variability (CV) in the baseline period and future period were comparable, except slight increase in CV at Lamesa (Table 5.1). This suggests that interannual variability in irrigated yield may not change substantially under CC.

The percent change in dryland yield was more variable than the changes in irrigated yield. The percent change in dryland yield varied between –50% (RCP 8.5 2080s

at Lamesa) and 60% (RCP 8.5 2080s at Halfway) (Figure 5.2). Similar to irrigated cotton scenario, the length of growing season decreased significantly, and the maximum LAI increased. The GCM, GFDL-ESM2M, which projected increase in rainfall and a milder temperature rise, resulted in maximum increase in dryland yield across all scenarios. The cotton crop cycle at Halfway under RCP 8.5, reduced by 17 days in 2050s and 22 days in 2080s, when compared to the baseline. The CV in the dryland yield for baseline and future periods were also comparable with minor increases/decreases (Table 5.1).

Finally, the simulated ensemble average irrigation water use of cotton increased significantly under all future climate scenarios (Table 5.1). The percent change in irrigation water use varied between –11% (RCP 8.5 2050s at Bushland) and 41% (RCP 8.5 2080s at Bushland) (Figure 5.2). Given that the length of growing season decreased significantly, the potential reason for increased irrigation water use could be the increased leaf area as a result of increased photosynthesis rate at elevated CO_2 levels for all three locations and reduced rainfall. The average increase in irrigation water use, across three sites in the THP was 8% and 15% in mid- and late-century, respectively. This suggests that irrigation water use would stay within the current HPWD pumping limit of 460 mm (HPWD, 2015); however, it may exceed the pumping limit in the late-century.

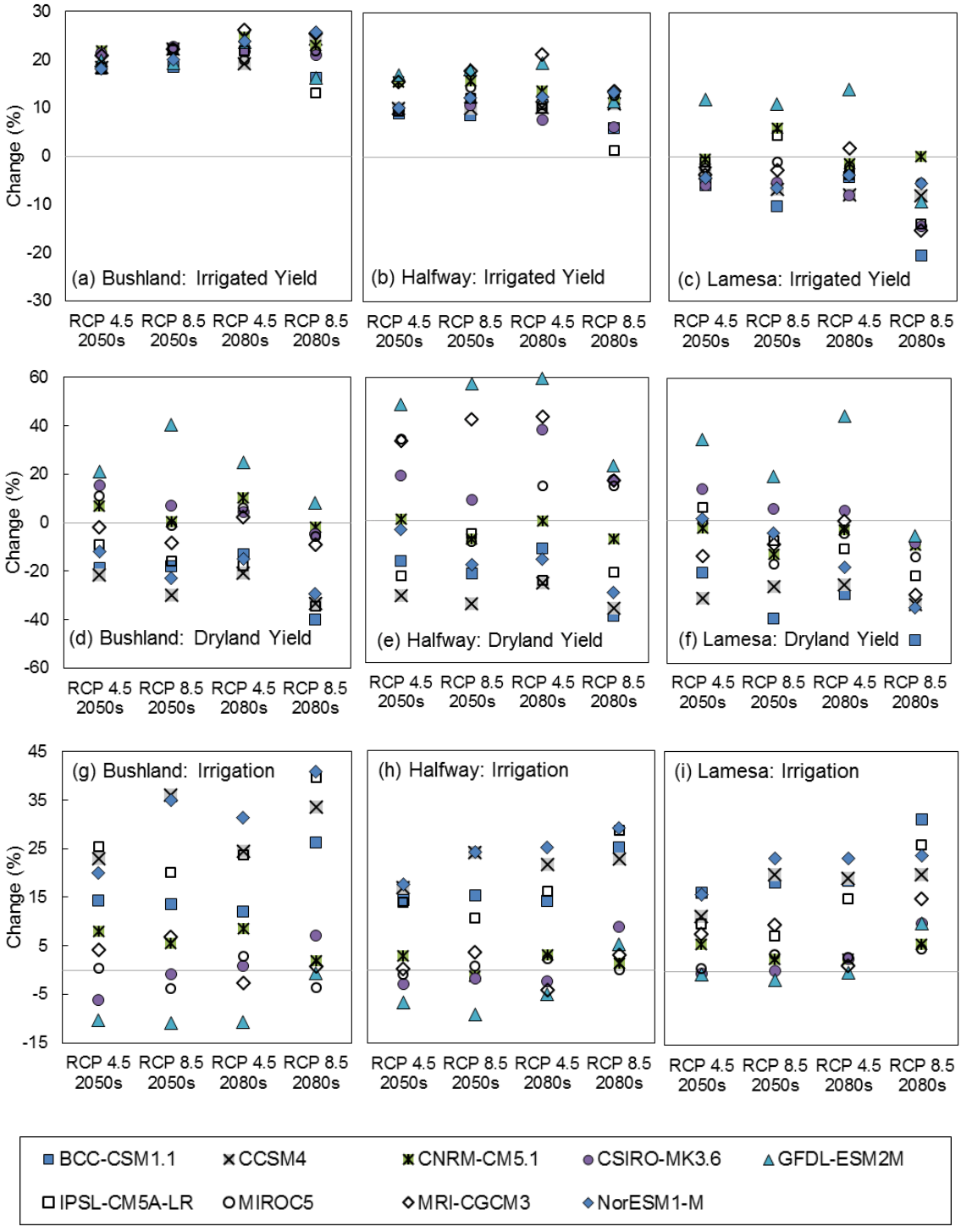

Figure 5.2 Percent change in irrigated and dryland seed cotton yield and irrigation in 2050s and 2080s compared to historic period under nine GCMs.

Table 5.1 Projected (ensemble average) irrigated and dryland seed cotton yields, and irrigation water used and temporal/inter-annual coefficient of variation (CV)

	Baseline (1976–2005)		2050s (2036–2065)				2080s (2066–2095)			
			RCP 4.5		RCP 8.5		RCP 4.5		RCP 8.5	
	Y (kg ha^{-1}) or I (mm)	CV[a] (%)	ΔY[b] (%)	CV (%)	ΔY (%)	CV (%)	ΔY (%)	CV (%)	ΔY (%)	CV (%)
Irrigated yield (Y)										
Bushland	4467	6	19	2	21	3	22	2	21	3
Halfway	4492	4	12	3	13	3	13	3	10	3
Lamesa	3354	4	–2	4	–2	5	–2	4	–10†	8
Dryland yield (Y)										
Bushland	1328	15	–1	15	–8	19	–3	22	–18†	17
Halfway	999	24	1	23	–3	28	2	29	–10	21
Lamesa	691	21	–3	19	–13†	25	–8	24	–26†	22
Irrigation water use (I)										
Bushland	372	10	8	9	8	9	9	11	14	9
Halfway	423	7	5	8	7	8	7	8	13	8
Lamesa	399	6	7	6	8	8	9	7	16	7

[a] CV is coefficient of variation: CV = (standard deviation) ÷ (30-year average yield)
[b] ΔY is the percent change in yield/irrigation from the baseline: $\Delta Y = (Y_i - Y_{Baseline}) \div Y_{Baseline} \times 100$
† indicates that the change is significant at 0.05 significance level

5.4.2. Climate Change Adaptation

The differences in yield and irrigation water use of a virtual cultivar compared to the baseline cultivar are summarized in Table 5.2. Nearly all virtual cultivars resulted in a significant increase in irrigated yield compared to baseline cultivar. The highest increase in irrigated yield was simulated with longer maturity trait followed by high yielding trait. Drought tolerant II and heat tolerant I were the least efficient cultivars. Increase in yield due to adaptation was slightly higher under RCP 8.5 than under RCP 4.5. The magnitude of yield increase was maximum at Lamesa in the late-century under RCP 8.5. These results suggest that the benefits of adaptation would be more prominent under severe CC.

Table 5.2 Simulated changes (%) in seed cotton yield (Y), and irrigation water use (I) under different adaptation scenarios with respect to no adaptation.

	2050s (2036–2065)						2080s (2066–2095)					
	Bushland		Halfway		Lamesa		Bushland		Halfway		Lamesa	
RCP / Adaptation	4.5	8.5	4.5	8.5	4.5	8.5	4.5	8.5	4.5	8.5	4.5	8.5
Irrigated Seed Cotton Yield (ΔY)												
Drought tolerant I	5.6†	5.9†	6.7†	6.0†	6.4†	6.9†	5.8†	6.1†	6.6†	5.5†	7.1†	6.5†
Drought tolerant II	3.9†	3.8†	3.1†	2.0†	3.0†	3.2†	3.8†	3.7†	2.7†	2.1†	3.1†	2.4
Heat tolerant I	3.2†	4.3†	3.2†	4.1†	4.2†	5.2†	4.5†	6.6†	4.5†	5.5†	5.1†	12.2†
Heat tolerant II	4.2†	5.5†	4.2†	5.4†	5.4†	6.9†	5.5†	8.6†	5.8†	7.7†	6.5†	16.4†
High yielding	8.1†	7.3†	6.7†	6.4†	7.1†	6.4†	7.2†	7.7†	6.2†	8.1†	6.4†	5.2†
Long maturity	7.6†	7.7†	7.9†	8.2†	6.8†	5.6†	8.1†	8.2†	8.5†	7.0†	4.9†	10.5†
Dryland Seed Cotton Yield (ΔY)												
Drought tolerant I	–5.0	–4.7	5.0	4.8	–2.7	–4.6	–6.9	–8.0	5.7	5.5	–3.6	–3.5
Drought tolerant II	7.9†	9.2†	6.9	5.9	–1.8	–2.9	7.8	8.8	7.5	6.4	–1.9	–2.5
Heat tolerant I	3.3	3.8	4.7	4.9	7.1	8.3	3.8	9.3†	4.5	7.8	8.6	13.3†
Heat tolerant II	4.2	4.7	6.3	6.4	9.5	11.2	4.8	12.2†	6.0	10.5	11.3	18.7†
High yielding	0.7	–0.3	5.8	4.2	7.1	6.2	0.3	2.0	4.7	4.9	7.2	7.8
Long maturity	20.1†	22.3†	18.8†	20.9†	23.2†	26.2†	20.9†	26.4†	19.4†	23.2†	24.6†	28.7†
Irrigation Water Use (ΔI)												
Drought tolerant I	2.3	2.1	4.4†	3.0	6.8†	7.6†	2.4	2.0	4.5†	3.0	7.0†	7.9†
Drought tolerant II	–0.3	–0.3	1.7	0.3	7.0†	7.1†	–0.4	–0.6	1.8	0.3	6.9†	6.6†
Heat tolerant I	–0.1	–0.2	–0.7	–0.6	–1.3	–6.0	–0.2	–0.3	–0.8	–0.9	–1.5	–10.5†
Heat tolerant II	–0.1	–0.3	–1.2	–1.0	–1.9	–1.9	–0.3	–0.4	–1.1	–1.2	–2.1	–1.9
High yielding	1.8	1.6	0.7	0.8	0.0	0.3	1.8	1.4	1.0	1.1	0.3	0.8
Long maturity	9.1†	9.1†	7.9†	7.6†	7.0†	6.6†	9.1†	7.9†	8.2†	7.1†	7.1†	7.1†

† indicates that the change is significant at 0.05 significance level

The irrigation water use of cotton increased significantly for the longer maturity cultivar across all sites. Irrigation water use also increased marginally with high yield trait. An increase in water use was simulated with drought tolerant I cultivar at all three sites. At Lamesa, the increase in irrigation water use with drought tolerant I and II cultivars was significant. This was attributed to coarser soil and lower water holding capacity at Lamesa. Combined the effects on irrigated yield and irrigation water use, high yield potential trait was found to be the most desirable trait for the THP region. Although longer maturity trait resulted in yield gains, it is not advisable due to significant increase in irrigation water use. The increased crop water demand would further intensify groundwater mining and will likely exceed the allowable pumping limits, currently at 460 mm $acre^{-1}$ $year^{-1}$ (HPWD, 2015).

Dryland cotton production was benefitted the most from longer maturity cultivar under all scenarios. The drought tolerant I trait was found to be the least efficient cultivar. While most virtual cultivars resulted in yield increase, yield loss was simulated in few cases. At Bushland, drought tolerant I trait resulted in lower yield than the baseline cultivar. The reduction in dryland yield with altered root properties was likely due to higher root water uptake and faster exhaustion of stored soil water. The resultant reduced availability of water later in the season especially during reproductive stages likely led to reduced seed cotton yield. In contrast, reducing the maximum water uptake per unit root length (drought tolerant II) resulted in yield gain at Bushland, which further supports the aforementioned hypothesis. At Lamesa, however, both drought tolerant I and II traits resulted in lower yield than the no-adaptation scenario.

These results suggest that care should be taken while designing ideotypes for dryland production based on root hydraulic properties. On the other hand, heat tolerant traits I and II always resulted in greater yield than no-adaptation scenario. Yield gain due to heat tolerance were more under RCP 8.5 than RCP 4.5, and greater in the late-century than in the mid-century. Overall, for dryland cotton production, heat tolerance and longer maturity traits were found to be optimum among the traits tested in this study.

5.5. Conclusions

Irrigated seed cotton yield at Bushland and Halfway is expected to increase by 21% and 13%, respectively, by mid-century (2036–2065) compared to the historic period (1976–2005). In contrast, irrigated seed cotton yield at Lamesa (with warmer weather and coarser soil) is expected to reduce by 2% by mid-century compared to the historic period, primarily due to higher than optimal temperature during cotton growing season. Irrigation water use is expected to increase at all three sites by an average of 8% in the mid-century compared to the historic period.

Among the virtual cultivars tested, maximum gains in irrigated seed cotton yield were obtained with the long maturity trait (8%) followed by high yield potential trait (7%) and drought tolerance (7%) compared to no adaptation. However, irrigation water use of cotton with long maturity trait was significantly higher (9% more) than that for the no-adaptation scenario. These results show that cotton production could benefit from CO_2 enrichment if the mean temperature during the cotton growing season remains below the optimal limit (~25°C). Shifting to a longer maturity cultivar under CC could minimize

yield loss, if any, due to temperature rise. However, associated increase in irrigation water requirement makes it a less desirable trait for irrigated cotton production in the THP. Increasing area of full leaf, enhancing partitioning of assimilates to reproductive growth (high yield potential), and increasing root length per unit root weight (drought tolerance) were identified as desirable climate-change-adaptive traits for irrigated cotton production in the THP region.

6. POTENTIAL BENEFITS OF GENOTYPE-BASED ADAPTATION STRATEGIES FOR WINTER WHEAT PRODUCTION IN THE TEXAS HIGH PLAINS UNDER CLIMATE CHANGE

6.1. Synopsis

The goals of this study were to assess the impacts of CC on wheat yield and irrigation water use, and evaluate potential adaptation strategies using the DSSAT-CSM-CERES-Wheat model. The model was evaluated against data from field experiments conducted at Bushland. A thorough calibration resulted in adequate simulation of onset of growth stages, leaf area index, grain yield (percent error, $|PE| < 4.7\%$), biomass ($|PE| < 7.1\%$), and seasonal evapotranspiration ($|PE| < 11.9\%$). The evaluated model was then used for: (i) predicting crop yield and seasonal irrigation under future climate scenarios, and (ii) evaluating six potential wheat genetic traits under CC at three sites in the THP.

Mixed trends in irrigated yield were found at the three sites. Irrigated grain yield at Bushland and Halfway increased in the future due to increased biomass under elevated CO_2 levels. In contrast, irrigated yield at Lamesa decreased in the future compared to the historic period, likely due to greater temperature stress and nutrient leaching due to coarser soils than other two sites. Seasonal irrigation is expected to decrease in the future at all sites due to improved water use efficiency of wheat under elevated CO_2 levels and reduced growing season length due to temperature rise. Dryland wheat yield are expected to increase under all scenarios due to improved crop water use efficiency and increased rainfall in some cases.

Among the genetic traits tested for CC adaptation, increased potential number of grains and denser root system were found to be the most desirable traits. Increasing grain number increased grain yield significantly without increasing seasonal irrigation, compared to the baseline cultivar. Dense root system also resulted in yield gains and reduced seasonal irrigation compared to the baseline cultivar. Early-flowering trait was found to be suitable for irrigated production at Lamesa due to heat avoidance. Other genetic traits were less desirable due to either lower yield or higher seasonal irrigation compared to the baseline cultivar. Significant increase in irrigation water use were simulated with longer-grain-filling period and stay-green trait.

These results showed that wheat production in the THP could benefit from CC under milder climatic conditions (mean growing season temperature <13°C). For a reduced seasonal irrigation demand, similar yield levels could be maintained at the THP, given that beneficial effects of CO_2 offset temperature stress. Enhancing yield potential traits and root architecture should be used for screening wheat cultivars for CC adaptation.

6.2. Introduction

Climate change (CC) could potentially affect crop productivity and food supply (Wheeler and von Braun, 2013) and hence there is an urgent need to adapt agriculture to future CC (Howden et al., 2007). Wheat (*Triticum aestivum* L.) is a widely grown cereal crop, covering 22% of the total agricultural land in the world (Leff et al., 2004). Developing adaptation strategies on global and regional scales to enhance CC resilience of wheat production could ameliorate food insecurity. The response of crops to CC is

primarily governed by the atmospheric carbon dioxide (CO_2) levels, air temperature, and precipitation (Hatfield et al., 2011). Wheat response to changes in these climatic variables has been documented in several controlled-environment experiments and simulation studies (Asseng et al., 2014; Kimball et al., 1999; Wall et al., 2000).

Free-air CO_2 enrichment (FACE) systems allow exposure of growing plants to elevated CO_2 levels under open-air conditions (Ainsworth and Long, 2004). Wheat growth and development in FACE systems has been monitored in various parts of the world including Australia (O'Leary et al., 2014), Germany (Högy et al., 2009), and the United States (US) (Kimball et al., 1999; Wall et al., 2000). These FACE studies have shown that under elevated CO_2 levels—wheat grain yield, leaf area index, biomass, water use efficiency, and accumulation of carbon increases; whereas, stomatal conductance, seasonal crop water use, and daily evapotranspiration decreases. In majority of the FACE studies, the effects of changes in temperature were not considered, however. Only a handful of researchers (Dias de Oliveira et al., 2015; Tan et al., 2018) have studied the effects of changes in CO_2 and temperature simultaneously using field experiments. Using natural light-controlled temperature, CO_2 and irrigation (N-CTCI) field facilities in Australia, Dias de Oliveira et al. (2015) showed that at higher temperature (ambient temperature + 3°C), grain-filling rate increased and time to physiological maturity reduced. The enhanced understanding of crop-climate relation as a result of physical experiments can be extrapolated to a wider range of climatic conditions using crop simulation models (Asseng et al., 2015). Studying wheat production under a wide range

of CO_2 levels, temperature, and rainfall patterns, as projected under CC scenarios (IPCC, 2014), will be instrumental in selecting strategies to adapt wheat production to CC.

Results from different simulation studies have shown mixed trends in wheat grain yield under CC. Results from recent studies (Ahmed et al., 2017; Dixit et al., 2018; Kapur et al., 2019; Tang et al., 2018; Xiao et al., 2018) indicated that grain yield is expected to increase due to increase in CO_2 levels. However, negative effects of CC on wheat yield have also been simulated in some studies due to the combined effect of CO_2, temperature, and rainfall. Dryland grain yield decreased in the US Plains (Tubiello et al., 2002) and in South Australia (Luo et al., 2005) due to projected reduction in precipitation in the future. Irrigated grain yield decreased at some sites in a global study due to temperature stress (Balkovič et al., 2014). Similarly, wheat yield responses to CC varied at different locations in Australia, with increasing trends in colder regions and decreasing trends in warmer regions (Wang et al., 2017). In a multi-model global study, considering the effects of temperature alone, researchers (Asseng et al., 2014) estimated a 6% reduction in wheat yield for each degree rise in temperature. In summary, these simulation studies demonstrated that projected increase in CO_2 levels and temperature in the future would likely have positive and negative effects on wheat production, respectively. Overall, CC may benefit colder regions while temperature stress would offset beneficial effects from elevated CO_2 in warmer regions. Wheat response to CC depends on local climatic conditions; therefore, CC impact and potential adaptation analysis in major wheat producing regions that have not been studied in the past, could contribute to the ongoing efforts to enhance climate resilience of wheat production.

The US High Plains region, which is termed as the “grain basket” of the US (Scanlon et al., 2012), accounted for about 47% of US wheat production between 1965 to 2010 (Grassini et al., 2013). The Texas High Plains (THP) region is a key part of the US High Plains, with 1.1 million ha of winter wheat grown annually (2007–2017), out of which 34% area was irrigated (USDA-NASS, 2018). Irrigation water in the THP region comes from the southern portion of the exhaustible Ogallala Aquifer (Colaizzi et al., 2009). Therefore, crop production in the THP region not only faces challenges from CC, but also from unsustainable irrigation water supplies. It is imperative to consider water constraints while studying the implications of CC and analyzing potential adaptation for wheat production in the THP.

Potential strategies to adapt wheat production to CC have included alternate management practices (Nouri et al., 2017) and identifying critical genetic traits better suited under CC (Semenov and Stratonovitch, 2015; Wang et al., 2019). Using the Sirius model, researchers (Semenov and Stratonovitch, 2015; Semenov et al., 2014; Senapati et al., 2018; Stratonovitch and Semenov, 2015) identified longer grain-filling period, maintaining green leaf area (stay-green), and heat tolerance around flowering as desirable traits for adapting wheat to CC in Europe. Using the APSIM model, Wang et al. (2019) identified longer grain-filling period, shorter vegetative period, greater radiation use efficiency, and bigger grain size (compared to historic cultivar) as desirable traits for adapting wheat to CC in Australia. A similar model-aided evaluation of genetic traits for the THP region could assist producers in this region in better preparing for the anticipated future climatic conditions.

Although the CERES-Wheat model (Jones et al., 2003; Ritchie et al., 1998) has been widely used in the CC impact analysis (Eitzinger et al., 2003; Tubiello et al., 2002; Yang et al., 2017), it has been rarely used for testing genetic traits of wheat for CC adaptation. In this study, genetic traits were not only evaluated based on wheat grain yield, but also on seasonal irrigation, which is important for the THP region. The overarching goal of this study was to assess the impacts of CC on wheat growth in the THP region and evaluate potential CC adaptive genetic traits. The specific goals of this study were to (a) evaluate the CERES-Wheat model for the THP region, (b) assess the impacts of CC on winter wheat production (i.e., irrigated and dryland yield and seasonal irrigation), and (c) test potential climate-change-adaptive virtual cultivars.

6.3. Materials and Methods

6.3.1. Study Locations

Three sites within the THP region were selected for this study. The selected sites, Bushland, Halfway, and Lamesa, are located in the northern, middle, and southern parts of the THP region, respectively. For the calibration and evaluation of the CERES-Wheat model, data from field experiments conducted at Bushland (Xue et al., 2006) were used. The evaluated model parameters were used for developing CC scenarios for all three sites. The daily historic weather data used during model evaluation came from the Texas High Plains ET Network weather station (Porter et al., 2005). The missing values were filled with AgMERRA climate data (Ruane et al., 2015b). The daily climate variables used include solar radiation, maximum and minimum air temperature, precipitation, wind

speed, and relative humidity. During the 1980–2010 period, mean annual rainfall at Bushland (494 mm) and Halfway (515 mm) was comparable and slightly lower at Lamesa (478 mm). For the same period, mean annual air temperature at Bushland (14.2°C) was lower than that at Halfway (15.1°C) and Lamesa (16.1°C) (NOAA, 2017).

Soil data file was created using the SBuild tool (Uryasev et al., 2004) within the DSSAT model, which was populated based on field measurements and published studies (Adhikari et al., 2016). Average clay content in the top 180 cm soil profile at Bushland, Halfway, and Lamesa is 36%, 29%, and 10%, respectively. More information about soil properties and climate at the three sites is given in Chapters IV and V.

6.3.2. DSSAT-CSM-CERES-Wheat model

The CERES-Wheat (Ritchie et al., 1998) module within the DSSAT v4.6 (Hoogenboom et al., 2015) cropping system model was used in this study. It is one the most widely used models for wheat modeling studies (Tubiello and Ewert, 2002) and the detailed information about the model is available in other published studies (Ritchie and Otter, 1984; Ritchie et al., 1998; White et al., 2008). The CERES-Wheat model uses radiation-use-efficiency-based approach to calculate biomass. The biomass is partitioned into different components of plant according to growth stage. The biomass is adjusted in case of nutrient/water stress. Plant development rate increases linearly as temperature increases up to 26°C, above which the growth rate is plateaued (White et al., 2008). To compensate for the elevated CO_2 on stomatal conductance, plant transpiration is reduced by a multiplier as CO_2 is increased (Tubiello and Ewert, 2002). Grain yield is increased

by 27% when CO_2 is doubled (Boote et al., 2010). A greater grain yield response (40–45% increase) to doubling CO_2 is simulated under drought conditions (Boote et al., 2010). The CO_2 response functions in CERES-Wheat were based on field experiments, which are summarized in Kimball et al. (1999). The capability of CERES-Wheat to simulate changes in climatic variables and its widespread use makes it an ideal choice for this study. The minimum input data required for simulating crop growth and development using DSSAT includes daily weather data, soil properties, and crop management (e.g., planting date, seeding rate, fertilizer) (Jones et al., 2003).

6.3.3. Model Calibration and Evaluation

6.3.3.1. Field Experiments

For the CERES-Wheat model calibration, field experimental data collected from winter wheat field studies conducted at Bushland during 1992–1993 (Xue et al., 2006; Xue et al., 2003) was used. Winter wheat was planted on October 1 at 70 kg ha^{-1} seeding density and 0.25 m row spacing. In these experiments, irrigation water was applied at eight levels based on different growth stages, i.e., jointing, booting, anthesis, and grain filling. In addition, a rainfed treatment was also studied. All the nine treatments received a starter irrigation of about 25 mm before planting. A 140 kg N ha^{-1} fertilizer was applied to all the plots one week prior to planting. The observed data used for calibration included dates of onset of growth stages, leaf area index (LAI), grain yield, biomass yield, and seasonal evapotranspiration (ET_c). Detailed information about these experiments has been documented in previous studies (Xue et al., 2006; Xue et al., 2003).

For model evaluation, data from the field experiments conducted at Bushland during 1980–1981 (Eck, 1988) and 1997–1999 (Schneider and Howell, 2001) were used. In the first set of experiments (Eck, 1988), winter wheat was planted on October 15, 1980 at 50 kg ha^{-1} seeding rate. Irrigation was applied at four levels; fall irrigation only, and fall irrigation plus one/two/three spring irrigations. Fertilizer treatments were 0 kg N ha^{-1}, 70 kg N ha^{-1}, 140 kg N ha^{-1}, and 210 kg N ha^{-1}. In the second set of experiments (Schneider and Howell, 2001), winter wheat was planted on October 2, 1997 and September 29, 1998 at a seeding rate of 67 kg ha^{-1} with 0.1 m row width. Irrigation was applied at five levels to meet 100%, 75%, 50%, 25%, and 0% ET_c. Fertilizer was applied before planting at 123 kg N ha^{-1} and 140 kg N ha^{-1} in 1997 and 1998, respectively. The observed data used for evaluation from these experiments included grain yield, biomass yield, and seasonal ET_c.

6.3.3.2. Calibration Methodology

CERES-Wheat model was calibrated systematically based on the approach described in Thorp et al. (2010). Firstly, the parameters related to crop development or phenology were adjusted to get a good match between observed and simulated dates of onset of growth stages. In this process, the observed (Xue et al., 2003) and simulated dates of onset of growth stages, expressed as Zadoks number (Zadoks et al., 1974) and day of year (DOY), were compared. After simulating phenology adequately, parameters related to crop growth were adjusted to improve the simulation of in-season leaf area index (LAI). Finally, the parameters were adjusted to get a good match between measured and

simulated end-of-season biomass and grain yield. After fine-tuning genotype parameters during calibration, using the measured data from Xue et al. (2006) experiments, model was evaluated against the remaining experimental data (Eck, 1988; Schneider and Howell, 2001) without further adjusting the genotype parameters. Lastly, model performance in simulating seasonal ET_c was evaluated using data from all three field experiments. The indicators used to test the model performance included graphical comparison and commonly used performance statistics (Adhikari et al., 2016): co-efficient of determination (R^2) (Legates and McCabe, 1999), percent error (*PE*), and percent root mean squared error (*%RMSE*). Model calibration was continued until a 'good' calibration, *%RMSE* <20% (Bannayan and Hoogenboom, 2009), was achieved.

6.3.4. Crop Management Data for Future scenarios

Winter wheat was planted on October 1st at a seeding rate of 200 seeds m^{-2}, which is the widely recommended seeding rate for central U.S. Great Plains (Paulsen, 1987). Initial conditions set up in the top 210 cm soil profile were—soil water at field capacity (Attia et al., 2016) and soil nitrogen at 50 kg N ha^{-1}, which is within the range of values reported at Bushland, TX (Eck, 1988). For irrigated and dryland winter wheat production, 140 kg N ha^{-1} nitrate-nitrogen fertilizer was applied one week prior to planting in accordance with the irrigated experiments at Bushland, TX (Schneider and Howell, 2001; Xue et al., 2006). Irrigation was simulated using "auto-irrigation" feature of DSSAT. Irrigation was applied to replenish plant available water content in the top 30 cm profile to 100% whenever it dropped to 50%.

6.3.5. Climate Change Scenarios

Simulated CC scenarios were based on two trajectories of greenhouse gas emissions, Representative Concentration Pathways (RCPs) 4.5 and 8.5 (Van Vuuren et al., 2011). The numeral in the pathway represents the projected radiative forcing (W m^{-2}), which is defined as the difference between total incoming and outgoing atmospheric solar radiation (Procopio et al., 2004). RCP 8.5 is a high emission scenario with rapid increase in projected CO_2 concentration, whereas, CO_2 levels stabilize around 2100 under RCP 4.5. In this study, CO_2 was varied annually (Figure 6.1) based on the projections from (IPCC, 2014), using "environment modification" functionality. Other climate variables, solar radiation, maximum and minimum air temperature, precipitation, wind speed, and relative humidity, were varied daily according to the projected climate data. Climate forcing from nine Global Climate Models (GCMs) of the Coupled Model Intercomparison Project 5 (Taylor et al., 2012) were drawn from the MACAv2-METDATA dataset (Abatzoglou and Brown, 2012) and used in this study. The MACA dataset contains daily climate projections at 4–6 km resolution, which were statistically downscaled and bias corrected using the Multivariate Adapted Constructed Analogs (MACA) method (Abatzoglou and Brown, 2012), with observed training data from Abatzoglou (2013). The MACA dataset includes daily data for the historic (1950–2005) and future (until 2099) period. In this study, simulations were run for the entire duration (1950–2099). Results from three 30-year periods, representing historic (1976–2005), mid-century (2036–2065), and late-century (2066–2095) were used for CC impact and adaptation analysis. The combination of two RCPs and nine GCMs resulted in 18 CC scenarios.

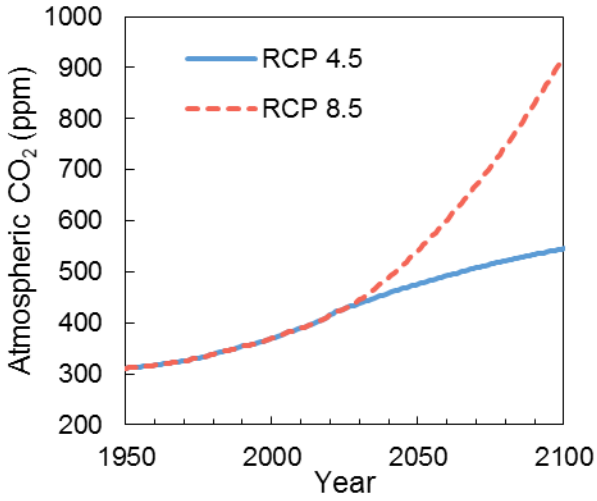

Figure 6.1 Projected atmospheric CO_2 concentration under the two future scenarios: Representative Concentration Pathways (RCPs) 4.5 and 8.5 used in this study, adapted with permission from IPCC (2014).

6.3.6. Climate Change Adaptation / Virtual Cultivar

The set of genotype parameters obtained after model calibration is referred to as the baseline cultivar. A total of six alternate cultivars were tested for CC adaptation. They were created by changing one (or more) parameter(s) from the baseline cultivar.

6.3.6.1. Denser Roots

Differences in root architecture could lead to winter wheat yield benefits especially under water-deficit conditions (Manschadi et al., 2006). In this study, a potential cultivar with denser roots than the baseline cultivar was created by increasing root density at different soil depths. This was done by changing soil root growth factor (SRGF) in the soil file from $e^{-0.02\times Z}$ to $(1–Z/500)^6$; where Z is the soil depth in cm. This methodology is similar to the approach used for sorghum (Singh et al., 2014c), chickpea (Singh et al., 2014a), groundnut (Singh et al., 2014b), and maize (Tesfaye et al., 2018), in which SRGF

was increased and soil water lower limit were decreased. However, in this study only SRGF was increased and soil water lower limit was kept the same for baseline and virtual cultivars.

6.3.6.2. Stay-Green (Delayed Senescence)

Stay-green or delayed leaf senescence has been identified as one of the important drought tolerant traits of wheat (Cossani and Reynolds, 2012; Senapati et al., 2018; Stratonovitch and Semenov, 2015). In this study, stay green trait was incorporated by modifying the parameters related to leaf senescence in the ecotype file. Parameter LSPHS (final leaf senescence starts, growth stage) was increased from 4.2 to 4.7, and LSPHE (final leaf senescence ends, growth stage) was increased from 5.5 to 6. These parameter values were within the range of values tested by Li et al. (2018).

6.3.6.3. Higher Root Water Uptake

Positive effects of increased root water uptake on wheat yield have been demonstrated in many field studies (Manschadi et al., 2006; Xue et al., 2003). Using the Sirius wheat model, Senapati et al. (2018) have shown that increasing root water uptake could increase yield potential under CC. In this study, a drought tolerant cultivar was created by increasing the RWUMX (maximum water uptake rate (cm3/cm root-day) in the species file from its default value of 0.03 to 0.04. Root hydraulic properties have not been studied using the CERES-Wheat model before and hence the range of RWUMX parameter values was not found in the literature.

6.3.6.4. Heat Tolerant (I and II) | Longer Grain Filling Period

Heat stress due to rising temperature under CC could affect winter wheat yield by shortening grain filling duration and hastening crop maturity; therefore, extended grain filling duration has been identified as one of the important heat tolerant traits (Lopes et al., 2018; Stratonovitch and Semenov, 2015). In this study, two virtual cultivars with longer grain filling duration than the baseline cultivar were created. These cultivars are referred to as heat tolerant cultivars. Heat tolerant (I) winter wheat cultivar was created by increasing the parameter P5 (Grain filling phase duration (°C d)) from 500 to 550 (or by 10%) in the cultivar file. Changing P5 from 500 to 550 resulted in about 2 days longer grain filling period. Therefore, another heat tolerant cultivar (II) was created by increasing P5 from 500 to 700, based on literature value for the THP region (Attia et al., 2016). Changing P5 from 500 to 700 resulted in 8 days longer grain filling period.

6.3.6.5. High Yield Potential | More Number of Kernels Per Head

A high yield potential wheat cultivar was created by increasing the potential number of kernel (G1) by 10%, from 16 to 18. This was in accordance with a controlled-environment study (Dias de Oliveira et al., 2015), in which researchers emphasized on the need for developing wheat varieties with greater number of potential grains. They found that number of grains were not affected by climate variables and therefore increasing potential number of grains could increase grain yield under CC.

6.3.6.6. Short Vegetative Phase | Early Flowering

Early flowering has been shown to ameliorate yield loss due to CC. In a FACE study, early-sown wheat had higher biomass, leaf area and yield because earliness prevented from exposure to hotter temperature late in the season (O'Leary et al., 2014). Exposure to higher temperature in the late season could also reduce the duration of grain filling period, which could reduce grain yield (Lopes et al., 2018). In this study, one virtual cultivar was created by reducing the vegetative phase or time to flowering. Parameters P1, P2, and P3, which affect earliness per se (Herndl et al., 2008), were reduced to reduce the pre-anthesis period. These values were reduced by 10% from their calibrated values: P1 from 350 to 315, P2 from 250 to 225, and P3 from 180 to 162. These changes in parameters reduced the number of days to anthesis by about 7 days.

6.4. Results and Discussion

6.4.1. Model Calibration and Evaluation

The genotype parameters adjusted during the CERES-Wheat model calibration are presented in Table 6.1. The parameter P1V (days required to complete vernalization under optimum vernalizing temperature) was adjusted to 21, which is within the range of typically observed values (5–45 days) for winter wheat in Texas (Neely et al., 2014). The parameters representing the duration between different growth stages (P1, P2, P3, P4, and P5) were adjusted sequentially to improve the simulation of phenological stages. Adjustment of parameters related to crop development resulted in a close match between observed and simulated dates of onset of growth stages (Figure 6.2a). The observed and

simulated days to physiological maturity were very close at 263 and 265 days after planting (DAP), respectively. Simulated onset of anthesis (225 DAP) was also within the range of observed days to anthesis (222–225 DAP). Adjustment of crop growth related parameters resulted in a good match between the measured and simulated in-season LAI values (Figure 6.2b).

In the final phase of calibration, the measured and simulated end-of-season grain yield, and biomass yield were compared. Model performance was satisfactory during calibration (Figure 6.3a–b) as indicated by the performance statistics (*%RMSE* <18.8%, |*PE*| <7.1%, and R^2 >0.66). There was a reasonable match between observed and simulated grain yield and biomass during the model evaluation (Figure 6.3c–d), as indicated by the performance statistics (*%RMSE* <26.2%, |*PE*| <4.8%, and R^2 >0.57). During the evaluation of seasonal ET_c, *%RMSE* of 26.9% and *PE* of −11.9% was obtained (Figure 6.4). Based on *%RMSE* model performance in prediction of grain yield and biomass was considered good during calibration (<18.8%) and fair during evaluation (<26.2%) (Bannayan and Hoogenboom, 2009).

Summarizing, the CERES-Wheat model was evaluated against data from three separate field experiments. The field dataset included four winter wheat growing seasons (1980–81, 1992–93, 1997–98, and 1998–99); five fertilizer levels (between 0 kg N ha^{-1} to 210 kg N ha^{-1}); and 18 different irrigation levels from three different irrigation scheduling methods—based on growth stage, combination of fall and spring irrigation, and wheat ET_c based. An adequate model performance under a wide range of water, fertilizer, and

environment conditions suggests that model could be used for testing environment and management scenarios with reasonable confidence.

Table 6.1 Genotype parameters of CERES-Wheat model adjusted during calibration.

Parameter	Description	Calibrated value
	Crop Development	
P1V	Days, optimum vernalizing temperature, required for vernalization	21
P1D	Photoperiod response (% reduction in rate/10 h drop in pp)	70
P1	Duration of phase end juvenile to terminal spikelet (°C d)	350
P2	Duration of phase terminal spikelet to end leaf growth (°C d)	250
P3	Duration of phase end leaf growth to end spike growth (°C d)	180
P4	Duration of phase end spike growth to end grain fill lag (°C d)	450
P5	Grain filling phase duration (°C d)	500
PHINT	Interval between successive leaf tip appearance.	100
	Crop Growth	
PARUE	PAR conversion to dm ratio, before last leaf stage (g/MJ).	2.4
PARU2	PAR conversion to dm ratio, after last leaf (g/MJ).	2.0
LA1S	Area of standard first leaf (cm).	2.6
LAFV	Increase in potential area of leaves, vegetative phase (fr/leaf).	0.15
LAFR	Increase in potential area of leaves, reproductive phase.	0.30
SLAS	Specific leaf area, standard first leaf (cm^2/g)	400
LSPHS	Final leaf senescence starts (Growth Stage)	4.2
LSPHE	Final leaf senescence ends (Growth Stage)	5.5
	Crop Yield	
G1	Kernel number per unit canopy weight at anthesis (g).	16
G2	Standard kernel size under optimum conditions (mg).	30
G3	Standard non-stressed mature tiller wt (incl grain) (g dwt).	2.8

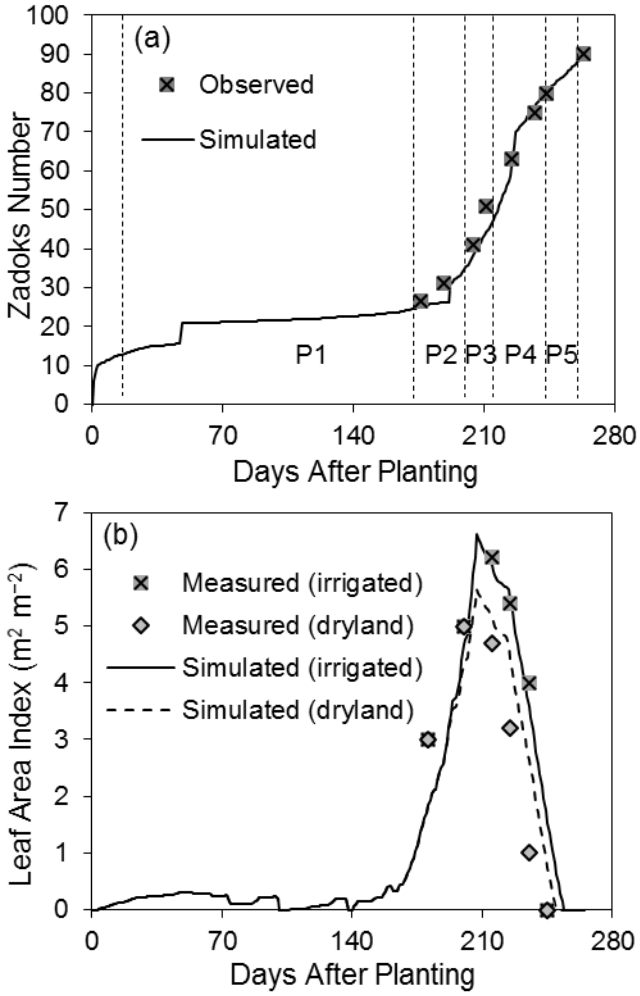

Figure 6.2 Comparison of measured and simulated (a) crop development stages expressed as Zadoks number, (b) and leaf area index (LAI) of dryland and irrigated conditions.

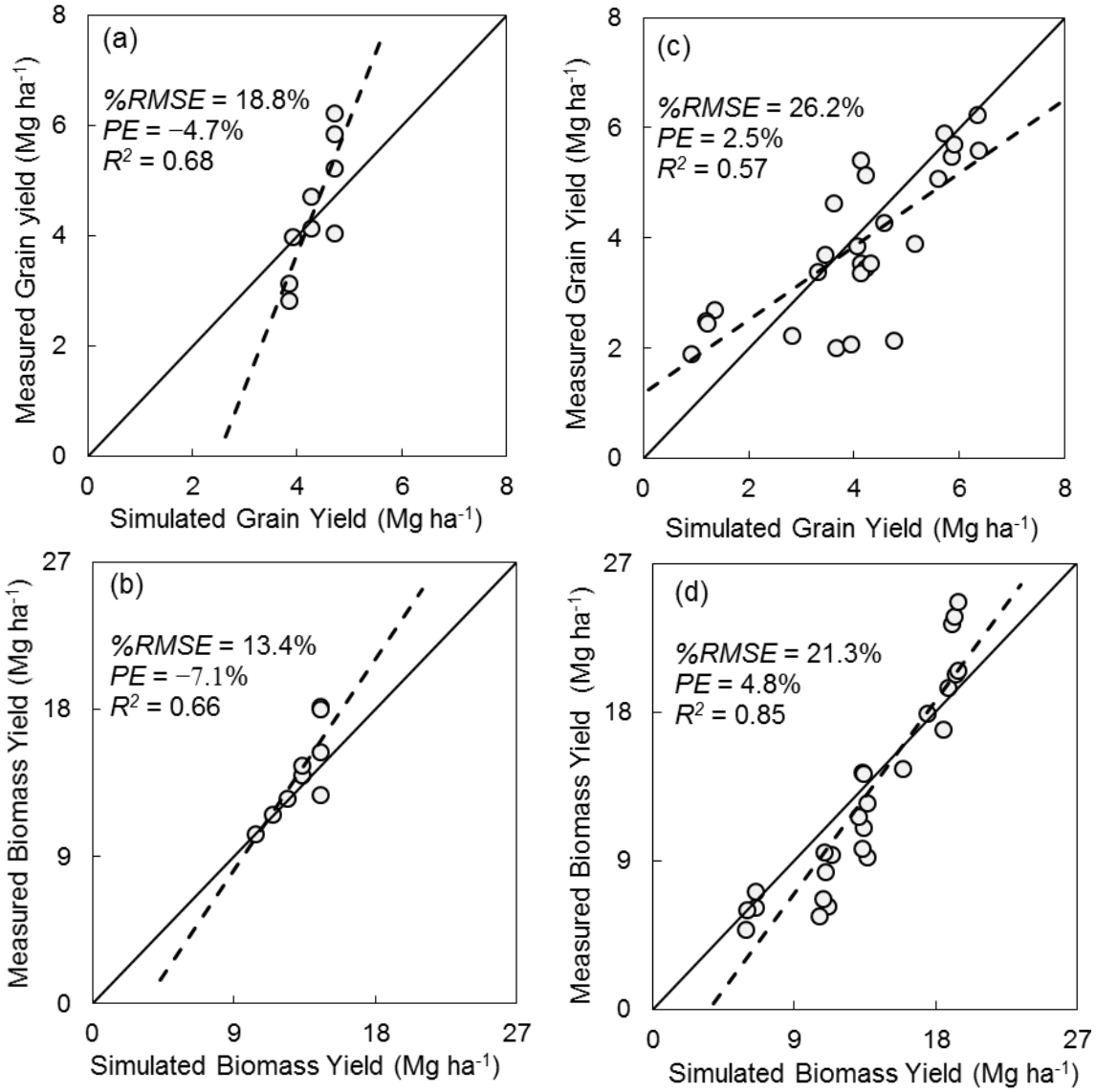

Figure 6.3 Comparison of measured and simulated (a) grain yield; and (b) biomass yield at maturity; during model calibration, (c) grain yield; and (d) biomass yield at maturity during model evaluation.

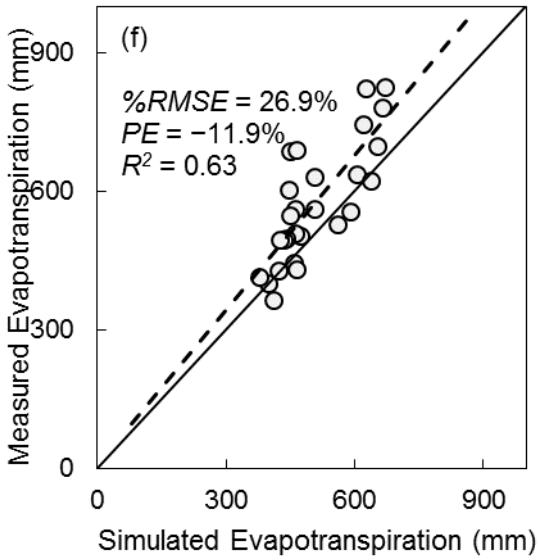

Figure 6.4 Comparison of measured and simulated seasonal evapotranspiration during model evaluation.

6.4.2. Climate Change Impacts on Winter Wheat Production

6.4.2.1. Climate change Impacts on Irrigated Winter Wheat Yield

The change in irrigated grain yield under CC as ensemble average based on nine GCM projections is presented in Table 6.2. The irrigated grain yield increased at Bushland and Halfway, in the future compared to the historic period, whereas it decreased at Lamesa. This change was statistically significant for both RCPs and future periods for all three sites except for RCP 8.5 in the late-century at Bushland. The percent change in irrigated grain yield in the future compared to the historic period, considering individual GCM projections, varied between –20% (RCP 8.5 2080s at Lamesa under CNRM-CM5.1) and 10% (RCP 8.5 2080s at Halfway under BCC-CSM1.1) (Figure 6.5). Temperature rise was the main driver of irrigated yield decline in the future, whereas, increased biomass accumulation due to CO_2 fertilization was the primary reason for yield increase in the

future. Unlike at Bushland and Halfway, the positive effects of CO_2 fertilization were suppressed by temperature rise at Lamesa and therefore grain yield decreased. The CV was about the same in the historic and future time periods at all three sites.

The magnitude of irrigated grain yield was the lowest at Lamesa when compared to Bushland and Halfway (Table 6.2). The possible reasons for the lowest irrigated grain yield at Lamesa could be the differences in growing season length, soil types, and temperature regimes. The historic average growing season length at Bushland, Halfway, and Lamesa was 250, 244, and 231 days, respectively. The shorter growing season at Lamesa implied lesser time for biomass accumulation and grain filling, hence the lower grain yields as compared to other sites. Another reason for lower grain yield at Lamesa could be the coarser soil at Lamesa, which allowed greater nitrogen leaching than the other two locations (data not shown). This is consistent with a simulation study conducted at three soil types and six locations in Australia (Milroy et al., 2008), in which the risk of drainage and leaching was higher at coarser soils with low water and nutrient holding capacity than it was at finer soils. In addition, the lower nitrogen uptake at Lamesa as a result of higher leaching than other two sites could be another reason for the contrasting trend in irrigated yield under CC, i.e. reduction in yield at Lamesa and increase in yield at Bushland and Halfway. The lower nitrogen uptake at Lamesa due to higher leaching has further added to the negative effects of temperature stress. This is consistent with a glasshouse chamber study in the United Kingdom (Mitchell et al., 1993), in which elevated CO_2 did not increase grain yield at low nitrogen supply/level. This trend is also similar to the trend observed in a FACE and simulation study at Maricopa in Arizona, where the

yield gains associated with elevated CO_2 were smaller at low nitrogen supply than at higher nitrogen supply (Jamieson et al., 2000).

The difference in temperature regimes at the three sites was another reason for the difference in projected yield under CC. The historic period growing season mean temperature for Bushland, Halfway, and Lamesa was 9°C, 10°C, and 12°C, respectively. A comparison of irrigated grain yield and growing season (planting–harvest) mean temperature for individual simulations (149 years × 9 RCPs × 3 locations) is presented in Figure 6, which shows that grain yield tended to decline when the growing season mean temperature increased beyond 11–13°C. Future growing season temperature projected by most GCMs at Lamesa fell outside the threshold of 11–13°C, which explains the decline in grain yield at Lamesa under CC, whereas, the other two locations benefitted from increased vegetative biomass due to CO_2 fertilization.

6.4.2.2. Climate Change Impacts on Dryland Winter Wheat Yield

The dryland grain yield, as ensemble average based on nine GCM projections, increased at all three sites, in the future compared to the historic period (Table 6.2). This change was statistically significant for most RCPs and future periods for all three sites, except for both future periods under RCP 4.5 at Bushland and for late-century under both RCPs at Lamesa. The percent change in dryland grain yield in the future compared to the historic period, considering individual GCM projections, varied between –34% (RCP 8.5 2080s at Lamesa under IPSL-CM5A-LR) and 71% (RCP 8.5 2080s at Halfway under GFDL-ESM2M) (Figure 6.5).

The greatest reduction in yield (of 34%) was the result of 26% lower Oct–May rainfall, 4.6°C warmer growing season (planting–harvest), 35% lower biomass at the end of vegetative phase, and 20 days shorter crop cycle, compared to the historic period. On the other hand, the maximum increase in yield (71%) was simulated under 2% higher Oct–May rainfall, 2.2°C warmer growing season (planting–harvest), 98% higher biomass at the end of vegetative phase, and 17 days shorter crop cycle than the historic period. Changes in dryland yield were highly correlated with changes in biomass at the end of vegetative phase (Figure 6.7a). The reasons behind increased dryland yield and vegetative biomass under CC were—improved water use efficiency of the plant and increased rainfall in case of some GCMs, especially in December and February (Figure 6.7b). Winter wheat was planted on October and the months of December and February corresponded with the growth stages between end of dormancy and terminal spikelet. The correlation between water stress during early growth stages (until booting) and dryland yield was greater than the correlation between water stress during reproductive stages and dryland yield. There was a negative correlation between water stress at different growth stages and dryland yield, except for the grain filling phase. These results are consistent with the findings from field experiments conducted at Bushland, TX (Xue et al., 2006), in which water stress during grain filling led to an increase in grain yield. They also reported that deficit irrigation during early growth stages (jointing and booting) increased grain yield by a greater amount than applying irrigation at later stages (anthesis and grain filling).

Such a large window of expected change in dryland yield under CC was also reported in previous studies. Using the DSSAT model, Tubiello et al. (2002) simulated

yield increase between 6 to 20% under one GCM and yield decrease under another GCM between −50% to −10% in the 2030s. Using the EPIC crop model, Izaurralde et al. (2003) simulated a 7 to 80% increase in dryland yield in the late-century compared to historic period (1961–1990). Stöckle et al. (2018) simulated up to 85% increase in dryland yield in the late-century compared to the historic period (1980–2010) using the CropSyst model and MACA climate projections. Xiao et al. (2018) simulated a change in dryland yield between −45 to 50% under RCP 8.5 in 2080s with the APSIM model.

The range of change in dryland yield projected under different GCMs was much larger than the future projections of change in irrigated yield. Larger uncertainty in dryland yield projections is expected due to the uncertainty in water availability, which is compensated for, in case of irrigated production. Consequently, the CV for dryland yield was much greater compared to the CV for irrigated yield. (Tubiello et al., 2002) also reported a higher CV for dryland winter wheat yield (30–50%) compared to irrigated yield (10–15%) for different locations in the US.

Another interesting finding is that the magnitude of percent yield increase under dryland conditions was greater than the percent increase under irrigated conditions. This was especially prominent in case of Lamesa, where irrigated yield was projected to decrease whereas dryland yield was projected to increase under CC. This is likely due to the differential effect of CO_2 fertilization under well-watered and limited-water conditions. Using the APSIM-N Wheat model, Ludwig and Asseng (2006) showed that increase in grain yield due to CO_2 fertilization was more under water limited conditions than under well-watered conditions. Similar results were reported by Ahmed et al. (2017)

in a multi-model simulation study for the US Pacific Northwest. Their results are also consistent with the findings of a FACE study in Maricopa, AZ (Pinter et al., 2000) and a closed-top field chamber study in Manhattan, KS (Chaudhuri et al., 1990), in which yield gain under elevated CO_2 was higher under water stress.

In general, dryland grain yield increased at all locations under most GCMs. The magnitude of increase was the highest at Halfway and lowest at Lamesa (Table 6.2). One reason behind greater increase in dryland yield at Halfway could be the change in grain yield-transpiration productivity (kg ha^{-1} mm^{-1}) under CC (Figure 6.7c). The grain yield-transpiration productivity at Halfway increased under most cases and by a larger margin than other two sites. The primary reason for increased yield-water productivity in the future was CO_2 fertilization, which increased plant growth and reduced transpiration per unit area, especially under soils with low water holding capacity (Thaler et al., 2012). The differences in growing season length and temperature regimes among the three sites as explained in section 3.3 also contributed to the differences in CC impacts on dryland yield. Differences in rainfall projections among the sites and resultant water stress at different growth stages also likely contributed to differences in dryland yield projections among the three sites. In summary, changes in dryland grain yield under CC were due to the interactive effects of growing season length, rainfall, temperature, and soil type.

6.4.2.3. Climate Change Impacts on Irrigation Water Use

The irrigation water use, as ensemble average based on nine GCMs, decreased at all three sites, in the future compared to the historic period for both RCPs and future

periods, except at Bushland under RCP 4.5 in the mid-century (Table 6.2). This change was statistically significant for Lamesa under both RCPs and periods and under RCP 8.5 in the late-century for all sites. The percent change in irrigation water use in the future compared to the historic period, considering individual GCM projections, varied between –16% (RCP 8.5 2080s at Bushland under GFDL-ESM2M)) and 10% (RCP 4.5 2050s at Bushland under IPSL-CM5A-LR) (Figure 6.5). The reduction in seasonal irrigation was more under RCP 8.5 than RCP 4.5, similar to the findings of Xiao et al. (2018). Possible reasons for reduced irrigation water use were—improved water use efficiency under elevated CO_2 levels, reduced growing season or period for which irrigation was required, and increased rainfall in some cases. Seasonal ET_c also decreased under CC (data not shown). Reduction in ET_c despite an increase in irrigated yield under CC on doubling CO_2 has been also reported in a CERES-Wheat study in Austria (Eitzinger et al., 2003).

Out of 36 scenarios (9 GCMs × 2 RCPs × 2 future periods), increase in seasonal irrigation was projected under 12, 13, and 4 scenarios at Bushland, Halfway, and Lamesa, respectively (Figure 6.5g–i). In other words, a reduction in seasonal irrigation under CC at Lamesa was simulated under more number of scenarios than at other two sites. This is because beneficial effects of CO_2 fertilization on grain yield and vegetative biomass were suppressed at Lamesa due to higher temperatures and coarser soils than at other two sites. These results suggest that the irrigated wheat grain yield in the THP can be maintained at historic level even with slightly lower irrigation amounts than the historic levels, due to the beneficial effects of CO_2 fertilization, provided seasonal mean temperatures remain under optimum levels (~13°C).

Table 6.2 Projected irrigated and dryland grain yields, and irrigation water use of winter wheat (ensemble averages based on 9 GCM projections) and temporal/inter-annual coefficient of variation (CV)

	Historic (1976–2005)		2050s (2036–2065)				2080s (2066–2095)			
			RCP 4.5		RCP 8.5		RCP 4.5		RCP 8.5	
	Y (kg ha^{-1}) or I (mm)	CV[a] (%)	ΔY[b] (%)	CV (%)	ΔY (%)	CV (%)	ΔY (%)	CV (%)	ΔY (%)	CV (%)
Irrigated grain yield (Y)										
Bushland	5956	4	1.9†	3	2.8†	3	2.5†	4	–0.1	4
Halfway	6303	4	4.3†	4	5.1†	3	4.7†	4	1.9†	3
Lamesa	4349	3	–5.6†	4	–7.4†	4	–7.5†	4	–12.7†	4
Dryland grain yield										
Bushland	2262	20	4.1	20	13.0†	19	10.6	20	16.8†	26
Halfway	2170	17	11.1†	19	20.3†	17	15.1†	14	25.9†	21
Lamesa	2074	14	6.4†	16	8.4†	12	5.6	10	4.1	16
Winter wheat irrigation water use (I)										
Bushland	366	7	0.9	6	–1.5	7	–0.5	8	–7.0†	8
Halfway	373	6	–0.4	5	–2.4	6	–0.4	7	–5.3†	7
Lamesa	378	5	–2.8†	4	–5.5†	5	–3.1†	5	–8.2†	6

[a] CV is coefficient of variation: CV = (standard deviation)/(30-year average yield).

[b] ΔY is the percent change in yield/irrigation from the historic period: $\Delta Y = (Y_i - Y_{Historic}) \div Y_{Historic} \times 100$.

† indicates that the change is significant at 0.05 significance level.

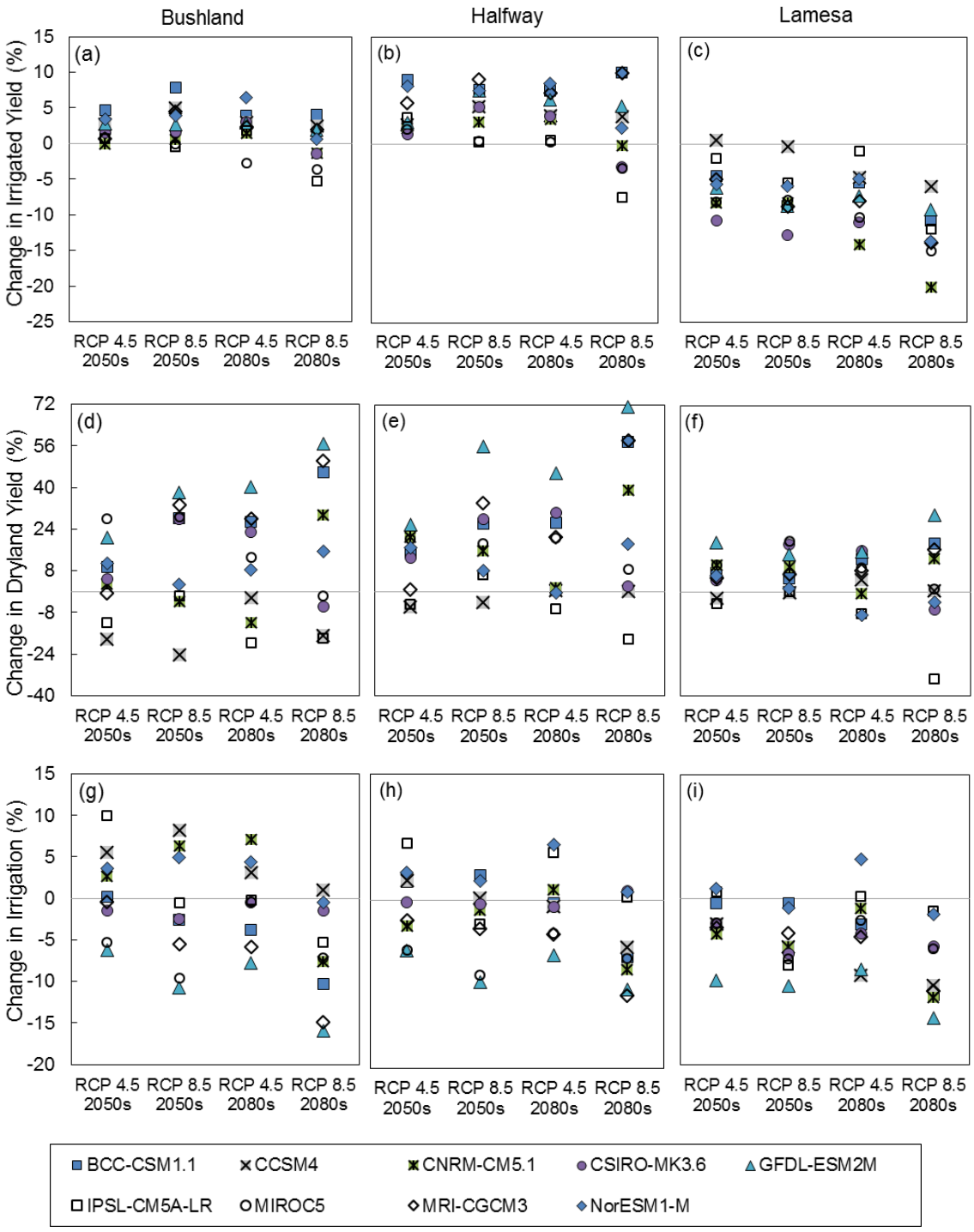

Figure 6.5 Percent change in irrigated and dryland grain yield and irrigation water use of winter wheat in 2050s and 2080s compared to the historic period under nine GCMs.

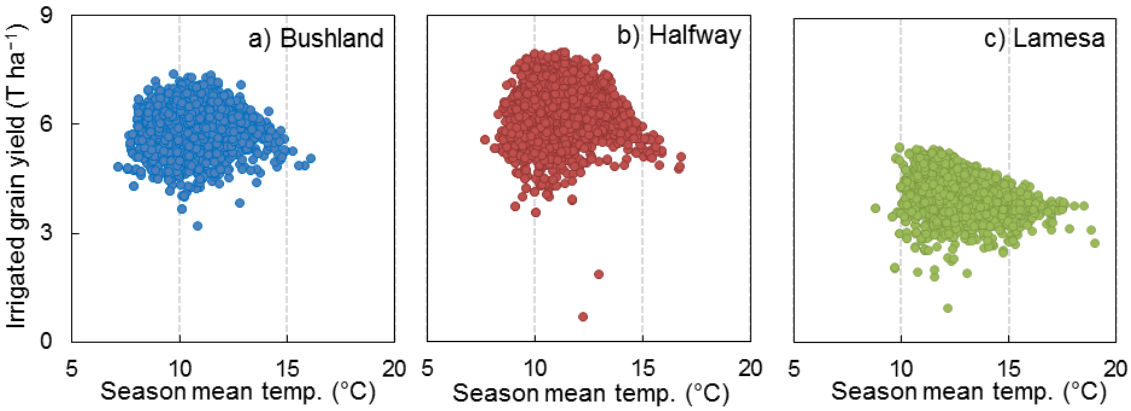

Figure 6.6 Relation between growing season (planting–harvest) mean temperature and irrigated grain yield. Simulated for the three sites (a–c) under 2 RCPs, 9 GCMs, and 149 years (1950–2098).

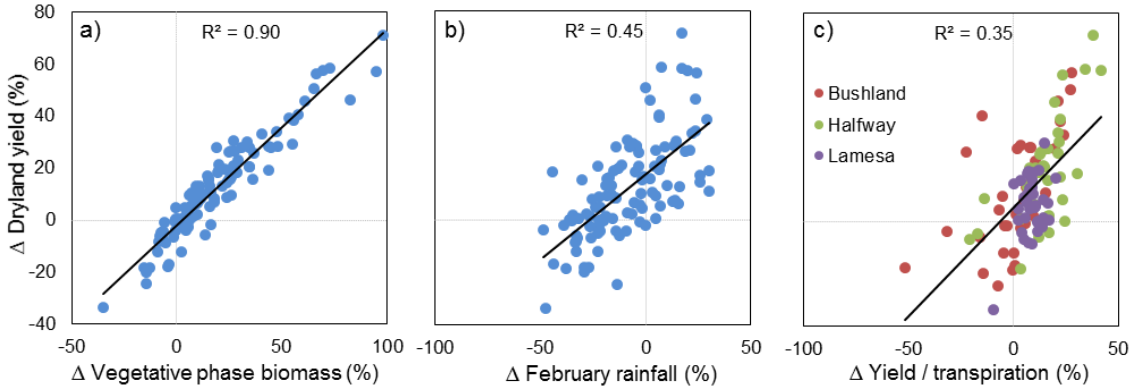

Figure 6.7 Relation between change in dryland yield (y-axis) and change in—a) biomass at the end of vegetative phase; b) rainfall in February; c) grain yield-transpiration productivity, kg ha−1 mm−1. Simulated for 3 sites × 2 RCPs × 9 GCMs × 2 future periods.

6.4.3. Climate Change Adaptation

6.4.3.1. Climate Change Adaptation: Bushland

For irrigated wheat production, all modifications in genetic traits tested in this study resulted in yield gain under CC, except early flowering under RCP 4.5 in 2050s (Table 6.3). Yield gain refers to the percent increase in grain yield under a virtual cultivar compared to the baseline cultivar. Genotype parameters of baseline cultivar were set during model calibration. The yield gain was highest with stay-green trait (up to 6.1%) followed by high yield potential trait (up to 4.2%); both of these yield gains were significant. Yield gain with other genetic traits under different CC scenarios was marginal (<2.6%).

Irrigation water use for virtual cultivar with stay-green trait was significantly higher (up to 10%) than the baseline cultivar. Increasing duration of grain filling period by 8 days resulted in an increase in irrigation water use by 3–4% and yield gain of about 1%. Irrigation water use did not change with high yield potential trait, i.e., increasing potential kernel numbers per unit canopy weight. On the other hand, irrigation water use was significantly lower with short vegetative period (up to 5.1%) and with denser roots (up to 4.3%), compared to the baseline cultivar. Irrigation water use for other virtual cultivars was about the same as the baseline cultivar.

Considering irrigated yield and irrigation water use together, high yield potential (increased potential kernel number per unit canopy weight) trait seems to be the best strategy for Bushland. With high yield potential trait, yield gain was significant and irrigation water use remained the same as the baseline cultivar. Although, stay-green trait

(delayed leaf senescence) resulted in significant yield gain, it also increased seasonal irrigation significantly compared to the baseline cultivar. Making roots denser could be the second desirable trait as it reduced irrigation water use while the irrigated yield was about the same as the baseline cultivar.

Table 6.3 Simulated changes (%) in irrigated and dryland grain yield (Y), and irrigation water use (I) at Bushland under different adaptation scenarios with respect to no-adaptation.

	Irrigated Yield (ΔY)[a]				Dryland Yield (ΔY)				Irrigation Water Use (ΔI)[b]			
	2050s (2036–2065)		2080s (2066–2095)		2050s (2036–2065)		2080s (2066–2095)		2050s (2036–2065)		2080s (2066–2095)	
RCP / Adaptation$_{(i)}$	4.5	8.5	4.5	8.5	4.5	8.5	4.5	8.5	4.5	8.5	4.5	8.5
Dense roots	1.2	1.2	1.2	1.7	8.2	8.3	8.2	9.8	−3.9†	−4.0†	−4.3†	−4.2
Stay-green	3.7†	4.5†	4.2†	6.1†	0.7	0.2	0.1	1.9	8.9†	9.4†	10.0†	9.8†
High water uptake	0.1	0.1	0.1	0.2	0.2	0.2	0.3	0.2	0.5	0.4	0.3	0.1
Heat tolerant I	0.3	0.3	0.2	0.3	0.5	0.8	0.5	0.9	0.8	0.9	0.9	0.8
Heat tolerant II	1.0	1.0	1.0	0.9	1.9	2.6	2.0	2.8	3.7†	3.4	3.4	4.0
High yielding	4.2†	3.3†	3.7†	3.3†	8.5	7.8	8.8	6.6	0.0	0.0	0.0	0.0
Early flowering	−0.1	1.1	0.6	2.6†	−3.0	−2.2	−3.8	0.9	−4.7†	−5.1†	−4.8†	−4.7†

[a] ΔY= percent difference between yield under baseline (no adaptation) and virtual cultivars (adaptation$_{(i)}$)
$\Delta Y = [(Y_{Adaptation(i)} - Y_{No\ Adaptation})/Y_{No\ Adaptation}] \times 100$

[b] ΔI is the percent difference between irrigation water use under baseline and virtual cultivars

† indicates that the change is significant at 0.05 significance level

For dryland production, yield gain was simulated under all virtual cultivars, except the early flowering cultivar. Dryland wheat yield gain was the highest with denser roots (up to 9.8%) followed by high yield potential (up to 8.8%). The third highest yield gain (up to 2.8%) was simulated when grain filling period was increased by about 8 days. Yield gain for other virtual cultivars was marginal (<2%). Early flowering cultivar resulted in yield gain (0.9%) only under RCP 8.5 in 2080s. Thus, early flowering appears to be an

unsuitable trait for CC adaptation in near future. For dryland production, increasing yield potential trait and using denser roots were found to be equally desirable traits for Bushland.

6.4.3.2. Climate Change Adaptation: Halfway

Yield gain in irrigated wheat production was significant and the highest with high yield potential trait (up to 8.4%) followed by stay-green trait (up to 3.7%). Yield gain with other genetic traits was negligible and a yield loss was simulated with early flowering trait (except under RCP 8.5 in 2080s).

Differences in seasonal irrigation under a virtual cultivar compared to the baseline cultivar were similar to that at Bushland. Seasonal irrigation water use was significantly higher (up to 11.5%) with stay-green trait. Seasonal irrigation water use with longer-grain-filling-duration trait was also higher (up to 3.6%) and this increase was significant in the 2050s. In contrast, seasonal irrigation water use was significantly lower (up to 5.6%) with early flowering trait. Irrigation water use also reduced with denser roots (up to 2.9%). Irrigation water use for the remaining virtual cultivars was the same as that under the baseline cultivar.

These results suggest that high yield potential is a desirable trait for irrigated winter wheat at Halfway, due to largest yield gain without any additional irrigation compared to the baseline cultivar. Denser roots could be another desirable trait due to associated reduction in irrigation water use, even though yield gain was negligible with this trait. Stay-green trait slightly increased yield, but it also significantly increased seasonal irrigation water use. Increasing grain filling duration increased irrigation water use by a

much larger percent than the increase in grain yield. Although early flowering trait reduced irrigation water use, it also reduced grain yield.

Table 6.4 Simulated changes (%) in irrigated and dryland Grain yield (Y), and irrigation water use (I) at Halfway under different adaptation scenarios with respect to no adaptation.

	Irrigated Yield (ΔY)				Dryland Yield (ΔY)				Irrigation Water Use (ΔI)			
	2050s (2036–2065)		2080s (2066–2095)		2050s (2036–2065)		2080s (2066–2095)		2050s (2036–2065)		2080s (2066–2095)	
RCP / Adaptation	4.5	8.5	4.5	8.5	4.5	8.5	4.5	8.5	4.5	8.5	4.5	8.5
Dense roots	0.8	1.0	0.8	0.9	8.1	8.4	8.4†	7.7	−2.7	−2.4	−2.6	−2.9
Stay-green	2.5	2.8†	2.6†	3.7†	1.2	1.1	1.1	1.4	10.8†	11.5†	11.2†	11.4†
High water uptake	0.1	0.1	0.1	0.1	0.2	0.2	0.2	0.1	0.6	0.7	0.6	0.8
Heat tolerant I	0.1	0.1	0.0	0.2	0.3	0.3	0.1	0.2	0.8	0.9	1.1	1.1
Heat tolerant II	0.3	0.3	0.2	0.6	0.9	1.0	0.4	0.8	3.4†	3.6†	3.6	3.5
High yielding	8.4†	7.6†	7.7†	6.8†	10.7	10.2†	10.3†	10.1	0.0	0.0	0.0	0.0
Early flowering	−1.1	0.1	−1.0	1.7	−3.6	−2.9	−3.5	−1.3	−5.4†	−5.6†	−5.3†	−5.5†

[a] ΔY= percent difference between yield under baseline (no adaptation) and virtual cultivars (adaptation$_{(i)}$)
$\Delta Y = [(Y_{Adaptation(i)} - Y_{No\ Adaptation})/Y_{No\ Adaptation}] \times 100$

[b] ΔI is the percent difference between irrigation water use under baseline and virtual cultivars

† indicates that the change is significant at 0.05 significance level

For dryland wheat production, highest yield gain was simulated with high yield potential (up to 10.7%), followed by denser roots (up to 8.4%). Other genetic traits had minor effect on dryland yield. Early flowering cultivar had lower yield than the baseline cultivar. Therefore, the most desirable traits for dryland wheat production at Halfway were found to be high yield potential trait followed by denser root system trait.

6.4.3.3. Climate Change Adaptation: Lamesa

The response of irrigated wheat production to different genetic traits was different at Lamesa than at other two sites. The highest and significant yield gain was simulated

with stay-green (up to 7.8%), early-flowering (up to 5.0%), and denser root (up to 3.1%) traits. High yield potential trait, which resulted in the highest yield gain at other two sites, resulted in a significant yield gain (2.4%) at Lamesa only under RCP 8.5 in 2080s. Yield gain with other genetic traits was marginal (<1.6%). Minor yield reduction was simulated with high-root-water-uptake trait. Although genetic traits had a different effect on irrigated yield at different sites, their effect on seasonal irrigation water use was similar at the three sites. Irrigation water use at Lamesa increased significantly with stay-green (up to 12.7%) and longer-grain-filling-duration (up to 3.6%) traits. In contrast, irrigation water use reduced significantly with early-flowering (up to 5.6%) and denser-root-system (up to 3%) traits. The irrigation water use for the remaining virtual cultivars was comparable to that with the baseline cultivar. The most desirable trait for irrigated wheat production at Lamesa was found to be early-flowering, followed by dense roots. Both of these traits resulted in significant yield gain and significant reduction in irrigation water use compared to the baseline cultivar.

Dryland grain yield gains were maximum with high yield potential trait (up to 9.3%) followed by the dense roots trait (up to 6.8%). Stay-green trait also resulted in a marginal yield gain (up to 2.5%). Minor yield loss was simulated with early-flowering trait under RCP 4.5 and with high root water uptake trait. Similar to Bushland and Halfway, dryland wheat production at Lamesa could benefit from incorporating high-yield-potential and dense-root-system traits.

Table 6.5 Simulated changes (%) in irrigated and dryland Grain yield (Y), and irrigation water use (I) at Lamesa under different adaptation scenarios with respect to no adaptation.

	Irrigated Yield (ΔY)				Dryland Yield (ΔY)				Irrigation Water Use (ΔI)			
	2050s (2036–2065)		2080s (2066–2095)		2050s (2036–2065)		2080s (2066–2095)		2050s (2036–2065)		2080s (2066–2095)	
RCP / Adaptation	4.5	8.5	4.5	8.5	4.5	8.5	4.5	8.5	4.5	8.5	4.5	8.5
Dense roots	2.8†	2.9†	3.1†	2.5†	6.8	5.7	6.2†	4.8	−2.7†	−3.0†	−2.7†	−3.0
Stay-green	7.6†	7.5†	7.8†	6.7†	1.3	1.9	1.6	2.5	12.0†	12.6†	12.3†	12.7†
High water uptake	0.0	−0.1	0.0	−0.2	0.0	−0.2	−0.2	−0.2	0.3	0.4	0.5	0.1
Heat tolerant I	0.3	0.3	0.5	0.5	0.3	0.3	0.4	0.1	0.9	0.7	0.8	0.8
Heat tolerant II	1.3	1.4	1.5	1.6	0.8	1.0	1.3	0.7	3.5†	3.6†	3.6†	3.0
High yielding	1.6	1.5	1.6	2.4†	9.3†	9.3†	9.3†	9.2†	0.0	0.0	0.0	0.0
Early flowering	4.7†	4.6†	5.0†	4.5†	−1.3	0.6	−0.6	2.0	−5.5†	−5.6†	−5.6†	−5.6†

[a] ΔY= percent difference between yield under baseline (no adaptation) and virtual cultivars (adaptation$_{(i)}$)
$\Delta Y = [(Y_{Adaptation(i)} - Y_{No\ Adaptation})/Y_{No\ Adaptation}] \times 100$

[b] ΔI is the percent difference between irrigation water use under baseline and virtual cultivars

† indicates that the change is significant at 0.05 significance level

6.4.4. Discussion: Climate Change-Adaptive Genetic Traits

It is not surprising that increasing soil root growth factor (SRGF) increased grain yield and reduced seasonal irrigation water use. Increasing SRGF has likely led to greater soil water extraction at different depths, compared to the baseline cultivar. Similar beneficial effects of increasing SRGF have been reported on yield of other crops such as sorghum in India and Africa (Singh et al., 2014c) and soybean in Brazil (Battisti and Sentelhas, 2017). Yield gain due to dense-root-system was higher at Lamesa (coarser soil) than other two sites (clay loam soil) (Tables 6.3–6.5). The yield gain with dense roots was more for dryland production than for irrigated production. This could be explained by a better utilization of stored soil water, which is more important for dryland production.

Stay-green trait increased water use and irrigated yield at all three sites in all CC scenarios (Table 6.3–6.5). A possible explanation could be that stay-green trait and CO_2

fertilization effects (due to elevated CO_2 levels in the future) had a beneficial effect on leaf area and vegetative biomass. The increased vegetative biomass and green leaf area likely increased crop consumptive use. Water was not limited for irrigated production in this study, due to the use of auto-irrigation tool, which led to increased seasonal irrigation as well as increased grain yield. However, dryland wheat yield did not increase substantially with stay-green trait, due to the limitation of water supply. For the THP region, stay-green trait may not be a suitable CC adaptation strategy for both dryland and irrigation wheat production. In general, possible benefits of CO_2 fertilization should be accounted for while considering stay-green trait for CC adaption. Another interesting finding is that yield gain with stay-green trait was greater at Lamesa than at other two sites. This is likely because maintaining green area compensated for reduced biomass accumulation due to temperature stress, which was more sever at Lamesa than the other two sites.

Increasing maximum water uptake rate (by 0.01 cm^3 cm-$root^{-1}$ day^{-1}) did not have substantial effect on either yield or seasonal irrigation. Interestingly, increasing root water uptake had slight positive yield gain at Bushland and Halfway, and some yield loss at Lamesa. The minor yield loss at Lamesa could be attributed to the soil properties; low-water holding capacity. In addition, high water uptake rate might have led to a faster depletion of soil water at Lamesa. Using root chamber experiments in Australia, Manschadi et al. (2006) showed that modifying root traits may penalize wheat yield due to early exhaustion of stored soil water and lack of water during grain filling season.

Although increasing grain-fill duration (by about 8 days) increased irrigated and dryland grain yield, the increase in yield was not significant (<3%). On the other hand, seasonal irrigation increased by a greater percent than irrigated yield, with longer-grain-filling-duration compared to the baseline cultivar. The marginal increase in grain yield and associated greater increase in seasonal irrigation demand makes longer-grain-fill-duration a less desirable CC adaptive trait for the THP region. However, researchers have proposed longer grain filling duration as a potential strategy to combat CC at other locations. Using Sirius model in Europe (Semenov and Stratonovitch, 2015) and APSIM model in Australia (Wang et al., 2019), researchers showed that when they allowed variation of certain model parameters with the aim of maximizing grain yield, grain-fill-duration parameter always reached its maximum value.

High yield potential (increasing potential kernel number per unit canopy weight) increased grain yield in all cases, while irrigation water use was the same as the baseline cultivar. Therefore, high yield potential appears to be the most suitable CC adaptive trait for the THP and other locations.

Early flowering trait showed great potential for irrigated production at Lamesa, with significant yield gain and reduced irrigation water use. For other sites and water treatments, there was a mixed trend. It should be noted that early flowering meant shorter length of vegetative phase since the planting date was the same for all scenarios. Shorter vegetative phase could potentially reduce grain yield by limiting the time for biomass accumulation (He et al., 2015); however, early anthesis could mean advancing crop cycle and shifting reproductive phase into cooler parts of the season (Ludwig and Asseng, 2010).

The mixed effect of early flowering on grain yield makes it a risky trait for the THP region. However, a positive aspect of early flowering and shorter vegetative phase is the significant reduction in irrigation water use. Perhaps, in the hotter southern regions of the THP, early flowering could help in wheat production by avoiding heat stress later in the season.

6.5. Conclusions

The CERES-Wheat model was evaluated using in-season (phenology and LAI) and end-of-season (grain yield, biomass, and evapotranspiration) data from field experiments at Bushland, TX. After obtaining a satisfactory model performance, the calibrated model parameters were used to simulate CC scenarios and adaptation strategies. The CC scenarios were based on daily weather projections from nine GCMs and two RCPs for three sites in the THP: Bushland, Halfway, and Lamesa. Simulated irrigated grain yield increased (up to 10%) at Bushland and Halfway due to beneficial effects of CO_2 fertilization on biomass and yield. However, irrigated grain yield decreased (up to 20%) at Lamesa, where temperature rise suppressed the positive effects of elevated CO_2 levels. Unlike the projections of irrigated grain yield, projections for seasonal irrigation were in the same direction for all three sites, i.e. reduced in the future compared to the historic period. This was attributed to improved water use efficiency, reduced length of growing season, and increased projected rainfall under some scenarios. This suggests that the historic irrigation levels at the THP could maintain historic irrigated grain yield levels in the future or even produce more yield in the milder temperature (northern) regions. The

projected changes in dryland grain yield in the late-century compared to the historic period fell between −34% and +71%. Average projection of nine GCMs indicated an increase in dryland grain yields at all three sites. Dryland grain yield increased by a greater extent than irrigated yield. This was likely because the beneficial effects of CO_2 fertilization on yield and water use efficiency were greater under limited-water conditions than under ample water conditions. Based on water use and yield, high yield potential and denser roots were identified as the most suitable CC adaptive traits, for both irrigated and dryland production. Longer-grain-filling-duration trait increased seasonal irrigation by a greater extent than it increased yield, therefore it was not recommended for the THP region. Similarly, due to significant increase in seasonal irrigation, stay-green trait (delayed senescence) was not suggested. Early flowering trait benefitted irrigated production at Lamesa likely due to heat stress avoidance, while mixed trends were simulated across sites and CC scenarios. Nonetheless, seasonal irrigation was lower with early flowering trait compared to the baseline cultivar. Therefore, early flowering could be recommended for warmer regions within the THP. Irrigated yield responses to changes in different traits were different across sites, whereas, seasonal irrigation water use responses to these traits were similar across the three sites.

7. ASSESSING THE IMPACTS OF CLIMATE CHANGE ON CROP PRODUCTION IN THE EDWARDS AQUIFER REGION OF TEXAS USING THE SWAT MODEL

7.1. Synopsis

Edwards Aquifer is a valuable water resource in central Texas, which is shared by different stakeholders. Projected shifts in water allocation and potential impacts of climate change (CC) on water resources and agricultural production could lead to water shortage for agriculture. In this study, SWAT model was used to analyze the CC impacts on crop production in the Lower Medina River Watershed in the Edwards Aquifer region. The SWAT model was calibrated and validated against streamflow and crop yield data for the 2003–2017 period. Model performance was reasonable during the calibration and evaluations periods with Nash Sutcliffe Efficiency of 0.69 and 0.58, respectively. Simulated and county-level observed crop yield, of cotton, corn, grain sorghum, and winter wheat, generally matched well as indicated by a percent bias of < 25% during model calibration. The evaluated model was then used to simulate crop yield and irrigation demand, using auto-irrigation tool, under six global climate model projections and two representative concentration pathways (RCPs 4.5 and 8.5) scenarios. The atmospheric carbon di-oxide (CO_2) for the baseline period (1976–2005) was kept at 380 ppm and for mid-century (2036–2065), it was changed to 499 ppm (RCP 4.5) and 571 ppm (RCP 8.5). Results suggested an increase in crop yields in the future indicating that beneficial effects of CO_2 and resultant increase in radiation use efficiency (RUE) were far greater than any negative effects of temperature stress or rainfall variability. Increase in yield in the mid-

century compared to the baseline were greater under dryland conditions than irrigation condition, greater under RCP 8.5 than RCP 4.5; this could be attributed to reduced stomatal conductance and increase RUE at higher CO_2, respectively. Two types of virtual cultivars were tested for CC adaptation: i) heat tolerant cultivar with a 2 °C increase in optimal temperature threshold; and ii) drought tolerant cultivar with 9-20% deeper roots. Results showed minor and slightly negative effects of increasing temperature thresholds on crop yields and irrigation water use. The only positive effect, substantial increase in yield and reduction in water demand, was simulated for winter wheat with 20% deeper roots.

7.2. Introduction

The Edwards Aquifer is an important water resource in the south-central Texas. Water from the aquifer is used for agricultural, industrial, military, municipal, and recreational purposes (Chen et al., 2001). Nearly two million people, including in the city of San Antonio, depend on the aquifer for their water needs (Tremallo et al., 2015). The springs fed by the aquifer support endangered species, e.g., Barton Springs salamander and Comal Springs fountain darter (Stamm et al., 2014). Reliance of multiple users on the Edwards Aquifer presents unique challenges for water management in this region (Adams et al., 2015). In addition, the aquifer is highly porous due to the presence of fractures, faults, sinkholes and other dissolution cavities (Sims et al., 2004). Aquifer recharge is highly sensitive to precipitation (Musgrove and Banner, 2004) due to the karst nature of the aquifer. Chen et al. (2001), using a hydrologic and economic simulation model, indicated

that water availability in the region is expected to reduce while water demand is expected to increase under climatic change. They suggested that in order to maintain spring flows at levels required to protect the endangered species, reduction in municipal and agricultural water usage would be necessary.

Majority of water withdrawals from the aquifer for agriculture take place in the Uvalde, Medina, and Bexar counties (Schaible et al., 1999). The irrigated crops grown in this region include corn, grain sorghum, cotton, wheat and vegetables (Piccinni et al., 2009). In 2012, corn, winter wheat, upland cotton, and grain sorghum were planted on 15%, 12%, 9%, and 6%, respectively, of the total cropland area (~1500 km^2) in these three counties (USDA-NASS, 2018). Due to competitive demand for water (Adams et al., 2015) and expected reduction in water availability in the future (Chen et al., 2001), it becomes imperative that agricultural water users in the region utilize water judiciously. In addition, the sensitivity of agricultural production to CC (Adams et al., 1990) must be taken into consideration in long-term planning efforts to conserve groundwater and sustain crop yield.

The greenhouse gas emission scenarios developed by the Intergovernmental Panel on CC (IPCC, 2014) play a pivotal role in assessing potential CC impacts on crop production. The IPCC-Assessment Report 5 (IPCC AR5) established four greenhouse gas emission scenarios (IPCC, 2014), termed as representative concentration pathways (RCPs 2.6, 4.5, 6.0 and 8.5). The numeral represent radiative forcing in W m^{-2}, difference between incoming and outgoing solar radiation (Procopio et al., 2004). These scenarios were based on the assumptions about future land use, technology, population, and policies. Projections

of crop yield and water requirement under CC scenarios in the Edwards Aquifer region would provide new insight into future prospects of agricultural productivity and water demand. Previously, projections of crop yield and water demand in the region were derived from Blaney-Criddle method (Chen et al., 2001) and Erosion Productivity Impact Calculator (EPIC) model (Wang, 2012). In these studies, climate projections from earlier versions of IPCC scenarios (IPCC, 1992; Meehl et al., 2007) were used. The present study aims at assessing CC impacts on crop production in the region based on the recent IPCC scenarios, using a process-based simulation model.

Simulation models, when meticulously calibrated against observed field data, could be used for simulating hydrologic and crop growth processes under a wide range of climate scenarios. The Soil and Water Assessment Tool (SWAT) (Arnold et al., 1998) is one such simulation model that has been extensively used in CC impact studies (Ashraf Vaghefi et al., 2014; Ficklin et al., 2009; Palazzoli et al., 2015; Wang et al., 2016). In this study, the SWAT model was used to simulate production of four major field crops (corn, winter wheat, cotton, and grain sorghum) in the Edwards Aquifer region, based on the recent IPCC (IPCC, 2014) CC scenarios. The specific objectives of this study were to: i) evaluate the SWAT model for hydrologic and crop yield predictions in an agricultural watershed, Lower Medina Watershed in the Edwards Aquifer region; ii) assess the impacts of CC on yield and irrigation water use of major crops grown in the study region; and iii) evaluate the CC adaptation strategies for major irrigated crops in the region, corn, winter wheat, cotton, and sorghum.

7.3. Material and Methods

7.3.1. SWAT Model Description

The Soil and Water Assessment Tool (SWAT) model is a semi-distributed hydrologic model developed by the United States Department of Agriculture (Arnold et al., 1998). SWAT simulates various hydrologic and crop growth processes at the watershed scale, typically on daily-basis. Major model inputs consist of climate data, soil, land use/land cover and crop management data. The model setup begins with defining topography of the watershed, which is generally input in the form of a digital elevation model (DEM). Topographic information is used for creating stream network and delineating watershed boundary. In the next step, the watershed is discretized into smaller homogenous units called the Hydrologic Response Units (HRUs). An HRU is a unique combination of land cover, soil and slope classes, which allows preservation of spatial variability while simulating hydrologic processes. After defining stream network, watershed boundary, and HRUs, weather data is entered into the model database. The minimum required weather variables include daily precipitation, and minimum and maximum temperature. Optional weather inputs include solar radiation, wind speed, dew point temperature, and relative humidity. Model database contains numerous empirical and physically-based parameters (Neitsch et al., 2011), which allow modelers to incorporate watershed-specific characteristics. Over-parameterization, however, could lead to equifinality (Beven, 2006); therefore, care should be taken while selecting model parameters. In this study, Geographic Information System (GIS) interface for the SWAT model, ArcGIS-SWAT

(Olivera et al., 2006), was used. The GIS and SWAT versions used in this study were: ArcGIS 10.5.1 and SWAT 2012.

7.3.2. Study Area

The drainage, recharge and artesian zones of the Edwards Aquifer cover 15 counties in central Texas (Schaible et al., 1999). The average annual rainfall and temperature in the Edwards Plateau for the 1981–2010 period were 621 mm and 18.7°C, respectively (NOAA, 2018). A representative watershed, Lower Medina River watershed (HUC 1210030205), which lies below the recharge zone of the aquifer was selected for this study (Figure 7.1). The watershed is a part of the drainage area of the Texas Gulf Region (HUC 12). The watershed falls within the Medina and Bexar counties, and it contains substantial agricultural acreage.

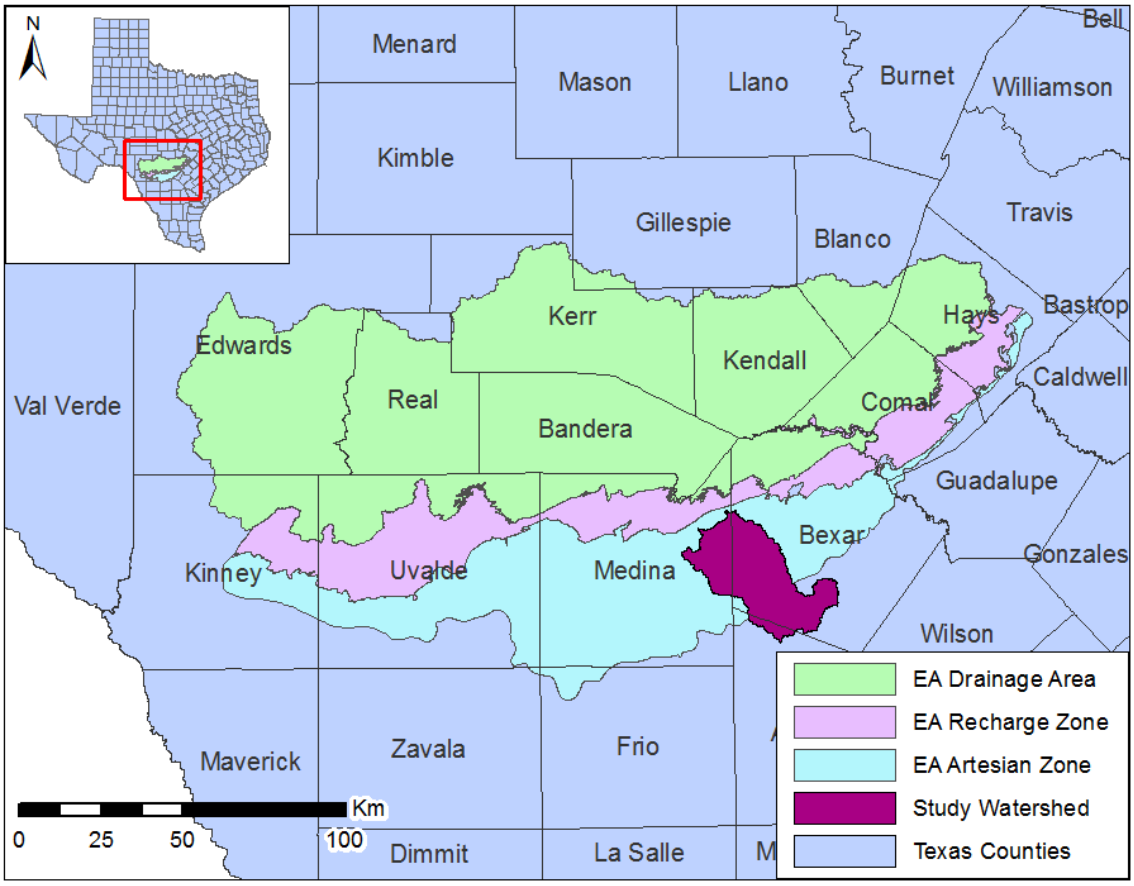

Figure 7.1 Location of the Edwards Aquifer (EA) region in Texas, inset box. Different zones of the aquifer and location of the study watershed (EA map retrieved from https://www.edwardsaquifer.org/).

7.3.3. Model Setup and Data Sources

7.3.3.1. Topography, soil, land cover, and weather

To define the topography of the watershed, Digital Elevation Model (DEM) raster grid of 30 m × 30 m resolution was used. Stream network was generated based on a minimum area threshold, to form streams of 2000 ha. The DEM was obtained from the National Hydrography Dataset website (http://www.horizon-systems.com/NHDPlus/NHDPlusV2_data.php). The DEM was used for creating stream

network and defining slope classes. To define soils, the State Soil Geographic dataset (STATSGO) soil data (USDA, 1993) available within the ArcSWAT database was used. The National Agricultural Statistics Service (NASS) Cropland data layer for the year 2008 was retrieved from Geospatial Data Gateway (NRCS, 2019) and used in this study to define/map different land uses in the watershed. Meteorological data, which included daily precipitation, and maximum and minimum temperature, was obtained from five weather stations (NOAA, 2017). The selected weather stations include—Riomedina (USC00417628), San Antonio Seaworld (USC00418169), Lackland AFB 3.5 SSE (US1TXBXR015), Lytle 3 W (USC00415454), and San Antonio Stinson Municipal Airport (USW00012970). The first two stations are within the watershed and the remaining three stations are outside, but adjacent to the watershed boundary.

7.3.3.2. Hydrologic Response Unit (HRU) definition

HRUs are defined based on a combination of slope, soil, and land cover. Slope of the watershed was categorized into four classes, viz. 0%–2%, 2%–4%, 4%–6%, and >6%. Dominant land cover classes in the watershed were—shrubland (RNGB), grassland/pasture (PAST), and deciduous forest (FRSD), which covered 23.7%, 18.9%, and 9.3% of the total watershed area, respectively (Figure 7.2). The crops of interest, corn, grain sorghum, cotton, and winter wheat covered 7.4%, 2.6%, 1.4%, and 1.2% of the total watershed area, respectively. The HRUs were created by using thresholds of 10% for slope, 10% for soil, and 0% for land cover classes. A lower threshold for land cover definition was necessary to obtain HRUs with individual crops of interest. There were a

total of 2731 HRUs and 28 sub-basins in the watershed. The HRUs of the four crops of interest were sub-divided into two parts, irrigated and dryland conditions. This division was based on historic planted acres in the Bexar or Medina counties (1990–2017 annual average), depending on the data availability (USDA-NASS, 2018 216). The irrigated area under cotton, corn, grain sorghum, and winter wheat as per the above division criteria was 62%, 31%, 12%, and 8%, respectively.

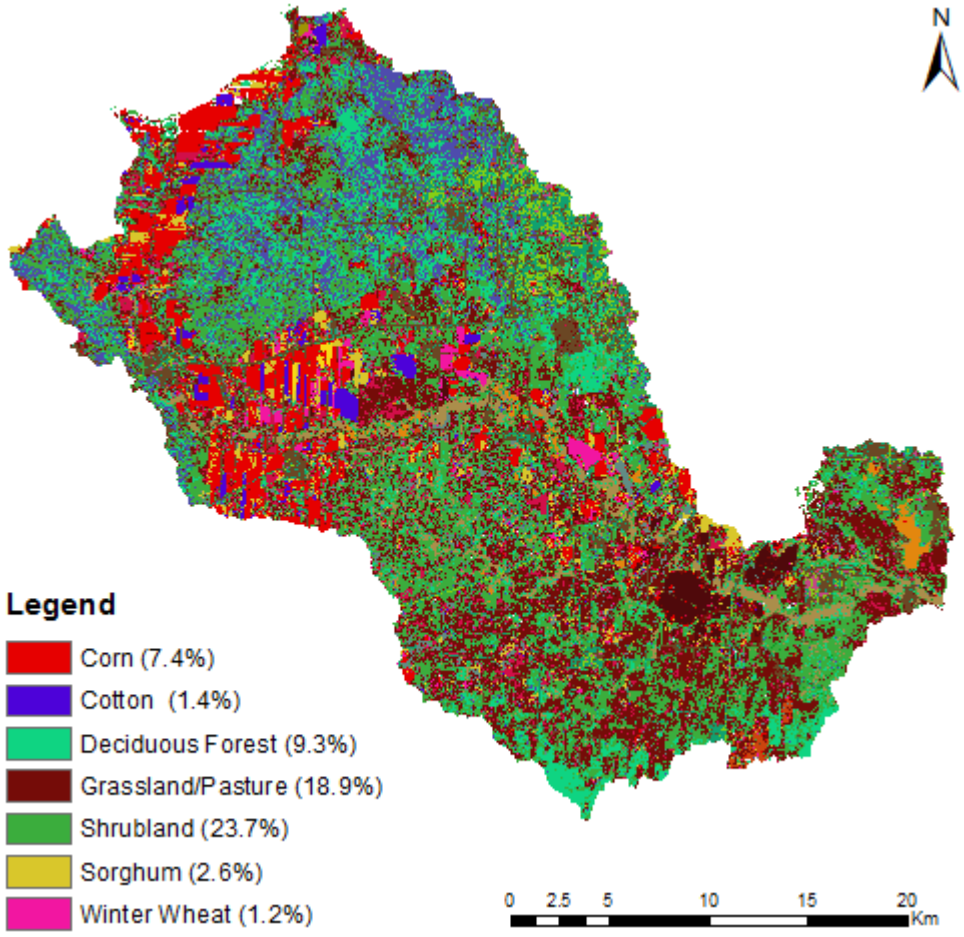

Figure 7.2 Major land cover/land use types in the study watershed.

7.3.3.3. Streamflow

The outlet of the watershed is located on the Medina River at San Antonio stream gage (USGS 08181500). There is a stream gage upstream of the watershed, which carries outflow from a large reservoir, Lake Medina. Daily streamflow from this stream gage, Medina River near Riomedina (USGS 08180500), was entered as inflow to the watershed. Streamflow data for the inlet and outlet gages were downloaded from the National Water Information System's web interface (https://waterdata.usgs.gov). At the watershed outlet, long-term streamflow data (1939–2019) were available. At the watershed inlet, however, streamflow data were available for a shorter period (2001–2007 and 2017–2018). Daily average (2001–2007) inflow into and outflow from the watershed were 3.5 m^3/s and 15.8 m^3/s, respectively. Despite the absence of inflow data from 2007–2017, model was run from 2000 to 2017 to get more data points for crop yield calibration.

7.3.3.4. Reservoir

A reservoir, Mitchell Lake Dam, exists within the watershed, and it is managed and operated by the San Antonio Water System (SAWS). Data required for parameterization of the reservoir were taken from the technical documents available at the SAWS website (https://www.saws.org/environment/MitchellLake/treatment.cfm). The surface area of the reservoir when filled up to emergency spillway and principal spillway was taken as 364 ha and 271 ha, respectively. Volume of water needed to fill the reservoir to the emergency and principal spillways was estimated as 617×10^4 m^3 and 326×10^4 m^3, respectively. Average value of initial reservoir volume was therefore assumed at 326×10^4 m^3 (SWAS-

Arcadis, 2014). Daily average principal spillway discharge rate of 1.4 m3/s was used, which was based on the reported discharge values for 2015 (SWAS-Merrick, 2015). Due to the absence of measured daily or monthly water release rates from the reservoir, "average annual release rate" method was used for simulating reservoir flow. For the remaining reservoir parameters, default values within the model database were used.

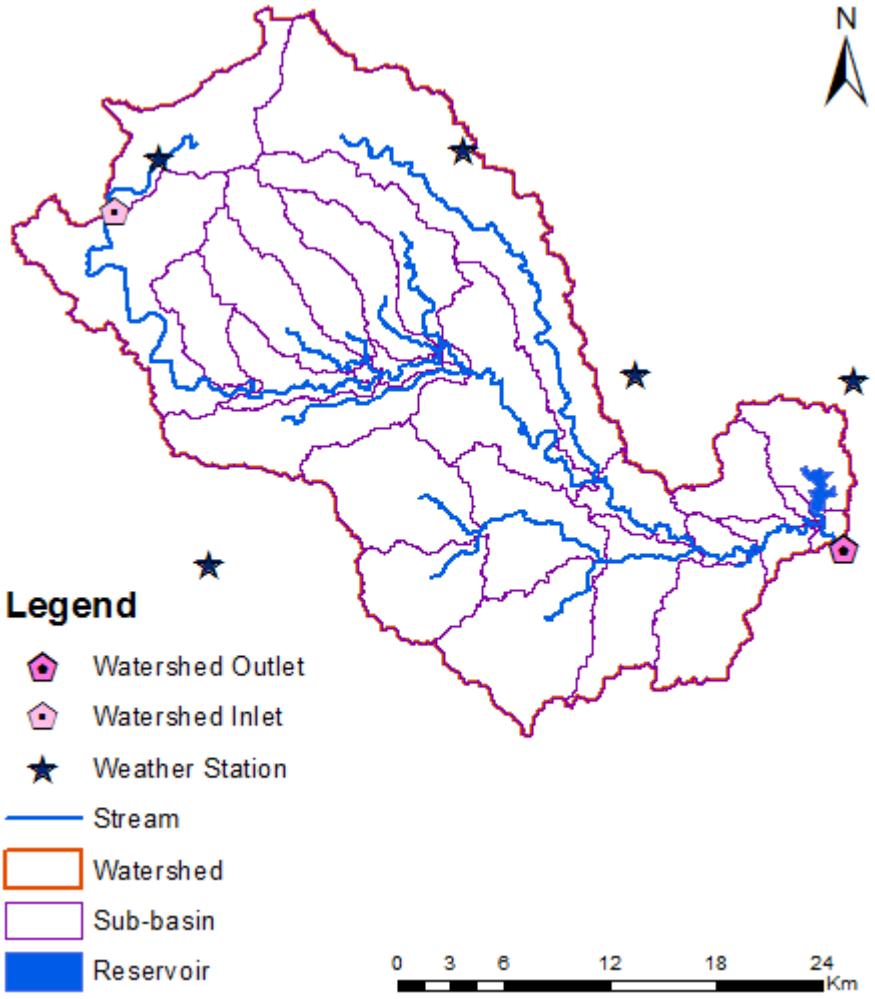

Figure 7.3 Lower Medina Watershed as delineated in the SWAT model, and the location of critical model features.

7.3.3.5. Crop management inputs

Dates for planting and harvesting, and heat units required from planting to maturity were based on typical values for the region (Table 7.1). Auto-fertilization option was used for both dryland and irrigated conditions. Parameter for triggering fertilizer application based on nitrogen stress (AUTO_NSTRS) was adjusted during calibration. Auto-irrigation option was used only for irrigated condition. Both, auto-fertilization and auto-irrigation were initiated on the day of planting. Auto-irrigation was scheduled based on "Plant Water Demand" option. Irrigation efficiency was set at 75% based on the historic conditions. In the Edwards Aquifer Groundwater Conservation district, according to Gayley (2013), 43% of irrigated area is under Center pivot (95% efficiency) and 56.6% is under flood irrigation (60% efficiency), which gives a weighted average of 75%. Water source for irrigation was indicated as the "Shallow Aquifer". Parameter for triggering irrigation based on water stress (AUTO_WSTRS) was adjusted during calibration. Other crop related parameters that were adjusted during model evaluation are given in Table 7.2. Remainder of the parameters for crop growth and management were set at their default values.

7.3.3.6. Crop yield

For the period of model evaluation (2003–2017), simulated crop yields were compared with observed yields, which were obtained from the National Agricultural Statistics Survey (USDA-NASS, 2018). Data on observed yield of upland cotton, corn, grain sorghum, and winter wheat were taken from county-level data for the Medina County. NASS reported cotton yields are in lb lint $acre^{-1}$ at standard moisture of 5%

(USDA-NASS, 2012) whereas the SWAT simulated cotton yield is in tons/ha lint+seed weight (Chen et al., 2016) at 20% moisture (Srinivasan et al., 2010). Eqn. 1 was used for converting NASS cotton yield into equivalent SWAT yield.

$$\mathrm{Yld_{SWAT,}} = \mathrm{Yld_{NASS,}} \times \left(1.12085\ \frac{\mathrm{kg}}{\mathrm{ha}}\right) \times (1 - \mathrm{MC_{std}}) \times (1 + \mathrm{MC_{swat}}) \times \frac{1}{1000\ \frac{\mathrm{kg}}{\mathrm{ton}}} \times \frac{1}{\mathrm{TO}} \qquad (7.1)$$

Where, $\mathrm{Yld_{SWAT,}}$ is seed cotton (lint + seed) weight in tons /ha at 20% moisture content. $\mathrm{Yld_{NASS,}}$ is cotton lint weight in lb/acre at 5% moisture content. $\mathrm{MC_{std}}$ is standard moisture content at which NASS cotton yields are reported (0.05). $\mathrm{MC_{swat}}$ is moisture content at which SWAT yields are simulated (0.2). TO is turnout ratio or ratio of lint yield over lint+seed yield, TO was taken as 0.43 in this study, which was four-year average (2014–2017) for the state of Texas reported by NASS.

Eqn. 2 was used for converting NASS cereal grain yield into equivalent SWAT yield.

$$\mathrm{Yld_{SWAT}} = \mathrm{Yld_{NASS}} \times (\mathrm{Wt_{std}}) \times \left(1.12085\ \frac{\mathrm{kg}}{\mathrm{ha}}\right) \times (1 - \mathrm{MC_{std}}) \times (1 + \mathrm{MC_{swat}}) \times \frac{1}{1000\ \frac{\mathrm{kg}}{\mathrm{ton}}} \qquad (7.2)$$

Where, $\mathrm{Yld_{SWAT}}$ is grain weight in tons/ha at 20% moisture content, equivalent to SWAT simulated yield. $\mathrm{Yld_{NASS}}$ is grain weight in bushels/acre at standard grain moisture content, $\mathrm{MC_{std,}}$ in fraction. $\mathrm{Wt_{std}}$ is standard weight of 1 bushel in lbs. $\mathrm{MC_{std}}$ and $\mathrm{Wt_{std}}$ for corn, wheat, and sorghum are given in Table 7.1. MCswat, grain moisture content of SWAT simulated yield, is 0.2.

Table 7.1 Crop management inputs used for model setup. Data used for converting NASS crop yield (bushel/acre or lb/acre) into model simulated yield (t/ha).

Crop	Management inputs[a]		Reported NASS yield[b]	
	Plant–harvest, MM/DD	Heat units	Standard (grain/lint) moisture, percent	Standard bushel weight, lb
Cotton	04/15–10/01	1810	5	NA[c]
Winter Wheat	11/15–05/25	1980	12	60
Corn	03/15–08/15	2500	15.5	56
Grain sorghum	03/25–08/05	1980	12.5	56

[a] Ko et al. (2009a), and Ko et al. (2009b) Ko et al. (2009a), and Piccinni et al. (2009)
[b] KASS (2002), Lamm et al. (2010), and USDA-NASS (2012)
[c] not applicable, NASS cotton yield are reported as lbs/acre

7.3.3.7. Model parameterization

After setting up the model for the study watershed using data related to topography, soil, land cover, crop management, watershed inlet, and reservoir; the remaining parameters were either fixed or adjusted during calibration (or) input based on the literature values. Specific yield of the shallow aquifer (GW_SPYLD) was assumed as 0.017 m/m, based on a USGS survey (Slade Jr et al., 1986), in which spring flow recession curves and numerical modeling was applied on the Barton Spring segment of the aquifer. For other hydrologic parameters, previous SWAT modeling studies conducted in the nearby regions were reviewed. The watersheds/basins simulated in these studies include—Upper Guadalupe River Basin (Afinowicz et al., 2005); Nueces River Headwater Basin (Jain et al., 2015); Dry Comal Creek Basin (Sullivan and Gao, 2016); and San Antonio River Basin (Elhassan et al., 2016). More information about the calibrated parameters is given in Table 7.2.

7.3.4. Calibration Methodology

A stepwise manual calibration scheme was followed for model evaluation, which was adopted from Chen et al. (2016). Firstly, hydrologic parameters were adjusted to get a good match between simulated and USGS measured streamflow, on a monthly-scale. Secondly, crop growth related parameters were fine-tuned to get a good match between simulated and NASS reported crop yield, on an annual-scale. Finally, streamflow calibration was re-evaluated and minor adjustments in parameters were made, if necessary. SWAT simulations were performed for 18 years, from 2000 to 2017. First three years (2000–2002) were considered warm-up years and were not used for model evaluation. During calibration, model parameters were adjusted based on seven years (2003–2009) of monthly streamflow data. Results from the remaining eight years (2010–2017), were used for model validation.

After getting a satisfactory model performance for streamflow, crop growth related parameters were adjusted. For crop yield calibration, simulations were performed on annual basis, and a calibration period of 2003–2012 was used. After obtaining a satisfactory calibration, model was validated for the 2013–2017 period. The selection of calibration/validation period for crop yield was based on the availability of observed NASS yield data. Crop yield was not reported for all years, which led to different number of data points for the selected four crops.

7.3.5. Model Performance Evaluation

Model performance in streamflow prediction was assessed using three quantitative statistical indicators and graphical techniques as suggested by Moriasi et al. (2007). Time-series of monthly simulated and observed hydrographs were plotted. The statistical performance indicators used included: Nash Sutcliffe Efficiency (NSE), Root Mean Square Error-standard deviation ratio (RSR), and percent bias (PBIAS). Model parameters were fine-tuned until model performance was satisfactory. Model performance was considered satisfactory if NSE > 0.5, |PBIAS| <25%, and RSR ≤ 0.7 (Moriasi et al., 2007). Model performance in crop yield prediction was assessed using one statistical indicator (PBIAS).

7.3.5.1. Nash Sutcliffe Efficiency (NSE)

The NSE (Nash and Sutcliffe, 1970) is defined as one minus the sum of absolute squared differences between observed and predicted values normalized by the variance of observed values (Equation 7.1). It varies from one to $-\infty$, one being the perfect fit. It was chosen because of its extensive use in the field of hydrologic modeling studies, which facilitates comparison. However, it is highly sensitive to peak flows resulting in negligence of low flows.

$$\mathrm{NSE} = 1 - \frac{\sum_{i=1}^{N}(Q_o - Q_{sim})^2}{\sum_{i=1}^{N}(Q_o - \bar{Q}_o)^2} \tag{7.3}$$

Where, Q_o represents the observed streamflow; Q_{sim} is the simulated streamflow; $\bar{Q}_o$is the average of observed streamflow; and N is the number of values in the time-series.

7.3.5.2. ***Root Mean Square Error-Standard Deviation Ratio (RSR)***

The RSR is the ratio of root mean square error and the standard deviation of the observed data. Low values of RSR indicate better model performance.

$$\mathrm{RSR} = \frac{\left[\sum_{i=1}^{N}(Q_o - Q_{sim})^2\right]^{0.5}}{[\sum_{i=1}^{N}(Q_o - \overline{Q_o})^2]^{0.5}} \tag{7.4}$$

7.3.5.3. Percent bias (PBIAS)

The PBIAS is a measure of determining over prediction (negative values of PBIAS) or under prediction (positive values) by the model. The optimal value of PBIAS is zero.

$$\mathrm{PBIAS} = \frac{\sum_{i=1}^{N}(Q_o - Q_{sim})\,100}{\sum_{i=1}^{N}(Q_o)} \tag{7.5}$$

7.3.6. Climate Change Scenarios

Future climate forcings from six Global Climate Models (GCMs) of the Coupled Model Intercomparison Project Phase 5 (CMIP5) were obtained from the Multivariate Adaptive Constructed Analogs (MACA) dataset (Abatzoglou, 2013). The latest version of MACAv2-METADATA provides daily data for temperature, precipitation, solar radiation, wind speed, and relative humidity, downscaled at 4–6 km resolution. Daily time series for the future period up to 2099 and historic period (1950-2005) were available.

In this study, precipitation, minimum and maximum temperature data were downloaded for point locations, corresponding to the NCDC weather stations used during model evaluation. The six GCMs considered in this study were BCC-CSM-1-1, CCSM4, CNRM-CM5, GFDL-ESM2M, IPSL-CM5A-LR, and MIROC5. Projections of

greenhouse gas emission included one intermediate (RCP 4.5) and one worst case (RCP 8.5) scenario. SWAT model was run with the baseline crop management and future weather data for the mid-century period (2036–2065). The atmospheric CO_2 concentration for the baseline period was kept at 380 ppm. Two sets of simulations were conducted 1) with the same CO_2 concentration (380 ppm) in the future, and 2) with elevated CO_2 concentration for the future period. For mid-century, CO_2 concentration was set at 499 ppm and 571 ppm for RCP 4.5 and RCP 8.5, according to (Rosenzweig et al., 2013), and similar to previous studies (Rahman et al., 2018; Ullah et al., 2019). Crop yield and water use were averaged over two 30-year periods for comparison, baseline (1976–2005) and mid-century (2036–2065) periods.

7.3.7. Climate Change Adaptation

Two adaptation strategies were tested in this study: i) increasing optimal temperature for plant growth (T_OPT) by 2°C for all four crops; and ii) increasing maximum root depth (RDMX) (Table 7.2). In SWAT, T_OPT is used for calculating temperature stress. As the daily average temperature diverges from the optimal temperature, plant undergoes temperature stress. The temperature stress in turn reduces plant growth achieved in a given day, through reductions in biomass and leaf area (Neitsch et al., 2011). Therefore, by increasing T_OPT, heat tolerance of the plant at higher temperatures can be enhanced. Similar methodology was adopted for incorporating heat tolerance in previous studies (Singh et al., 2014b; Singh et al., 2014c; Tesfaye et al., 2018) using the DSSAT cropping system model (Jones et al., 2003).

Research shows that deeper roots could increase crop yield by allowing extraction of water from deeper soil layers, especially under water-limited conditions (Jordan et al., 1983; Sinclair and Muchow, 2001). The RDMX parameter affects potential water uptake from the soil surface. Increasing RDMX would allow extraction of water from deeper soil surface, which has been identified as a drought tolerant trait (Blum, 1998; Hund et al., 2009; Pierret et al., 2016). The modified root depth was within the range of published values for corn (2.4 m; (Fan et al., 2016), sorghum (2.5 m; (Assefa et al., 2010), and winter wheat (2.2 m; (Thorup-Kristensen et al., 2009). This adaptation was not possible for cotton because the default maximum root depth of cotton (2.5 m) was already greater than the maximum rooting depth for soils (SOL_ZMX) in the study watershed. In SWAT, plant roots are allowed to grow as deep as the shallower of the two parameters, RDMX and SOL_ZMX (Neitsch et al., 2011).

Table 7.2 Adaptation strategies tested in this study and associated adjustments in parameters.

Parameter	Adaptation-I		Adaptation-II	
	T_OPT, °C (optimal temperature for plant growth)		RDMX, m (maximum root depth)	
	Default	Modified	Default	Modified
Corn	25	27	2.0	2.18[a]
Cotton	30	32	2.5	NA[b]
Grain Sorghum	30	32	2.0	2.18
Winter Wheat	18	20	1.3	1.60

[a] value corresponds to the maximum soil rooting depth SOL_ZMX

[b] could not be replicated for cotton because default roots already reached the maximum possible soil depth available for root development, i.e., RDMX > SOL_ZMX

7.4. Results and Discussion

7.4.1. Streamflow Calibration and Validation

The calibrated values of model parameters are listed in Table 7.3. The NSE values during model calibration and validation were 0.69 and 0.58, respectively (Table 7.4), which were comparable to the values obtained in previous studies in the region. For example, (Elhassan et al., 2016) obtained NSE of 0.7 for the San Antonio River Basin and (Afinowicz et al., 2005) reported NSE between 0.29 and 0.5 for the Upper Guadalupe River Basin. Overall, model performance statistics indicated that streamflow simulation was satisfactory according to criteria specified by (Moriasi et al., 2007). Average annual evapotranspiration (2000–2017) was 73% of the total precipitation, which was comparable to reported values for the Edwards Aquifer region (68% (Hauwert and Sharp, 2014) and 61% (Afinowicz et al., 2005)).

Table 7.3 Default and calibrated values of the hydrologic parameters adjusted during model calibration.

Parameter	Definition[a]	Testing range	Calibrated value
CN2	SCS curve number (-)	±20%	+10%
ESCO (.hru)	Soil evaporation compensation coefficient (-)	0.01–1.0	0.7
ALPHA_BF	Baseflow recession constant (days)	0.01–1	0.015
RCHRG_DP	Aquifer percolation coefficient (-)	0–0.40	0.30
GWQMN	Threshold water level in shallow aquifer for baseflow (mm H_2O)	0–5000	200
GW_DELAY	Delay time for aquifer recharge (days)	0–31	0
GW_REVAP	Revap coefficient	0.02–0.2	0.2
REVAPMN	Threshold water level in shallow aquifer for revap (mm H_2O)	0–750	200
FFCB	Initial soil water storage (-)	0–1	1
CH_K2	Effective channel hydraulic conductivity (mm/hr)	0–50	10

[a] (Neitsch et al., 2011)

Comparison of observed and simulated streamflow (Figure 7.3) indicated that the model was able to capture monthly variability well; however, peak flows were underestimated. This was likely due to the influence from karst formations and absence of reservoir release data from the Mitchell Lake dam for the entire model evaluation period. Although the watershed is in the artesian zone of the Edwards Aquifer; the highly karstic recharge zone and underground fractures likely affected flow peaks in the watershed, which were not explained by precipitation alone. In addition, flow regulation from the reservoir influences streamflow especially during high flow period (Sullivan and Gao, 2016). Under-prediction of peak flows has also been reported in previous studies in this region (Afinowicz et al., 2005; Elhassan et al., 2016; Sullivan and Gao, 2016). Future efforts will take into account flow regulation and groundwater fluxes. Based on this analysis, streamflow calibration was considered satisfactory and further calibration focused on crop yield.

Table 7.4 Model performance statistics for streamflow calibration and validation.

	NSE	RSR	PBIAS
Calibration	0.69*	0.56	21.54
Validation	0.58	0.65	−21.35

*Performance is satisfactory if NSE > 0.5, |PBIAS| <25%, and RSR ≤ 0.7 (Moriasi et al., 2007)

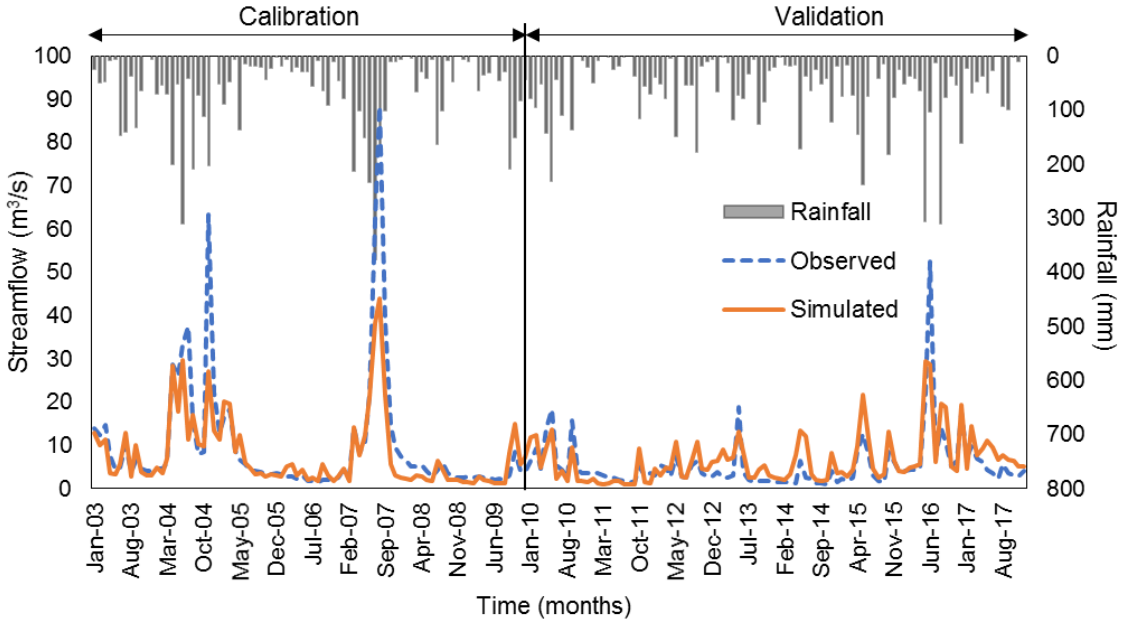

Figure 7.4 Simulated and observed monthly streamflow during SWAT model evaluation.

7.4.2. Crop Yield Calibration and Validation

The calibrated crop related parameters are summarized in Table 7.5. A comparison between annual SWAT-simulated yield and NASS-reported yield is shown in Figure 7.5. NASS yield data was not available throughout the model evaluation period, resulting in different number of data points across crop and water treatment. During calibration, model performance was satisfactory for all crops as indicated by PBIAS < 25% (Table 7.6). Model performance was good for irrigated corn, irrigated and dryland grain sorghum, and irrigated winter wheat (PBIAS <10%). During validation, PBIAS was within the acceptable range for most crops, except for dryland corn. This could be attributed to the high annual variability in observed data (Figure 7.5), which was not captured by the model. Like many crop/hydrologic models, SWAT does not account for crop damage due to pest

and disease. In addition, crop growth during extreme weather events is not simulated well by the SWAT model (Srinivasan et al., 2010).

Another reason for the differences between observed and simulated yield was the lack of crop management input data. Management inputs such as irrigation and fertilizer were simulated automatically based on stress factors and other inputs were kept the same in different years. Under field conditions, however, management practices may vary across years and farms. Despite the annual variability, on average, the simulated and observed yield were comparable for most cases. As for the irrigation water use, the simulated average annual irrigation for corn (405 mm), cotton (755 mm), grain sorghum (245 mm), and winter wheat (268 mm), were within the range of published data (Ko et al., 2009a; Piccinni et al., 2009). The calibrated model parameters and baseline crop management inputs were therefore used for further scenario analysis. For scenario analysis, multi-year average yield was considered.

Table 7.5 Default and calibrated values of crop related parameters adjusted in SWAT.

	Corn		Cotton		Grain sorghum		Winter wheat	
Parameter	Default	Final	Default	Final	Default	Final	Default	Final
BLAI	6	4	4	3	3	2	4	3 (2)[†]
BIO_E	39	27.3 (20)	15	11	33.5	23.5	30	21
HVSTI	0.5	0.45 (0.3)	0.5	0.5	.45	.45 (0.35)	0.4	0.4 (0.3)
DLAI	0.7	0.4	0.95	0.75 (0.65)	0.64	0.44 (0.34)	0.5	0.3 (0.2)
EPCO	1	0.4	1	0.5	1	0.5	1	0.7 (0.5)
EXT_COEF	0.65	0.3	0.65	0.65 (0.50)	0.65	0.50	0.65	0.65 (0.48)
AUTO_NSTRS	0.75	0.75 (0.3)	0.75	0.75	0.75	0.75	0.75	0.75 (0.3)

[†]Values reported in parenthesis are for dryland conditions. Values without a parenthesis are common for both irrigated and dryland conditions.
BLAI: Maximum potential leaf area (m^2/m^2)
BIO_E: Radiation use efficiency ((kg/ha)/(MJ/m^2))
HVSTI: Harvest index for optimal growing conditions ((kg/ha)/(kg/ha))
DLAI: Fraction of growing season when leaf area begins to decline (heat units/heat units)
EPCO: Plant uptake compensation factor (-)
EXT_COEF: Light extinction coefficient (-)
AUTO_NSTRS: Nitrogen stress factor to trigger fertilization (-)

Table 7.6 Model performance statistic, PBIAS, for crop yield calibration and validation.

	Corn		Cotton		Grain sorghum		Winter wheat	
	Irrigated	Dryland	Irrigated	Dryland	Irrigated	Dryland	Irrigated	Dryland
Calibration	−8	−22	−23	−17	−4	−7	−4	−22
Validation	−10	33	15	−21	−25	−1	−16	21

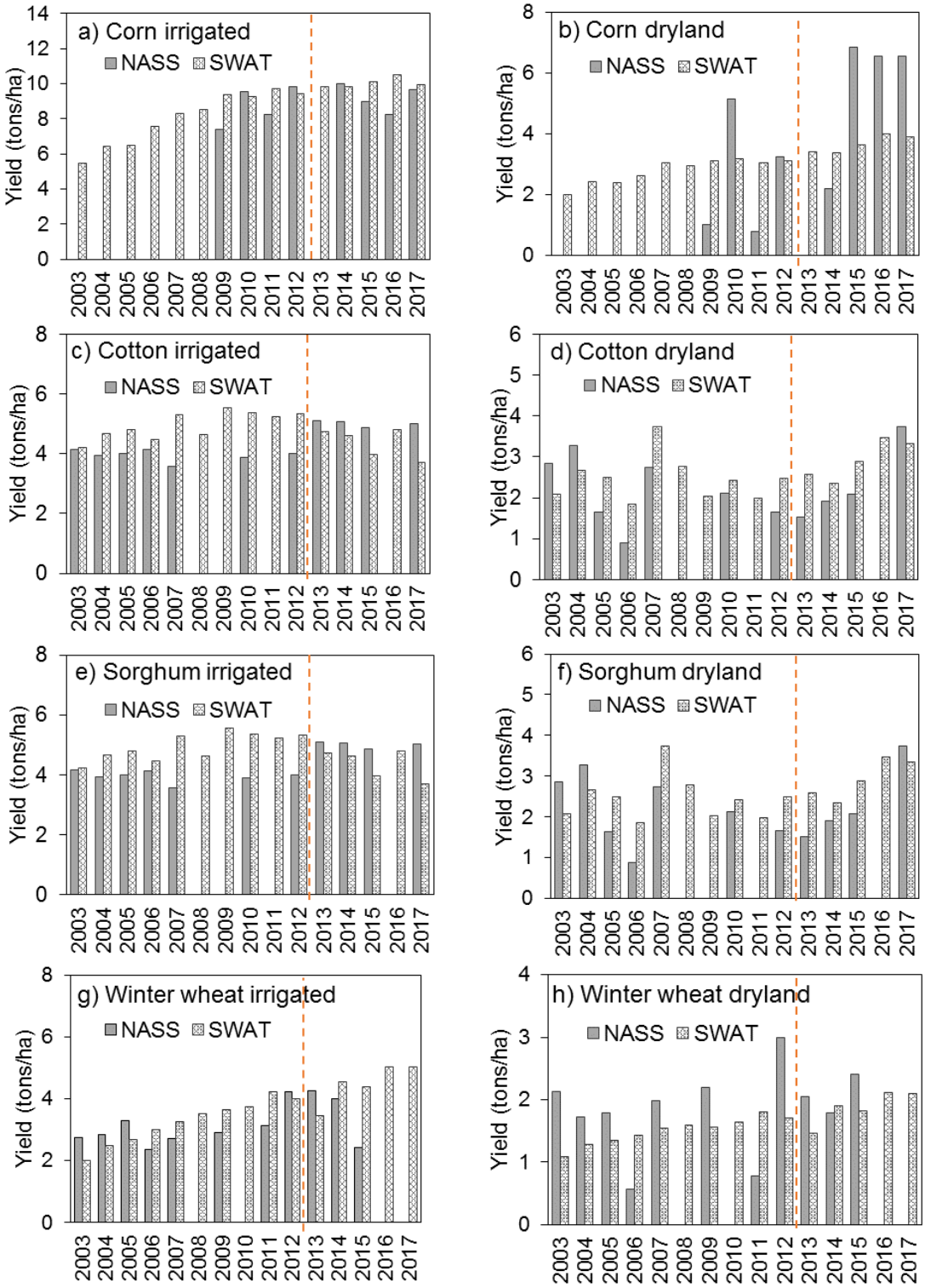

Figure 7.5 Comparison of simulated and observed crop yield. A dotted red line separates the calibration (left) and validation (right) periods.

7.4.3. Future Climate

A total of 12 future climate scenarios (6 GCMs × 2 RCPs) were considered in this study. The changes in monthly rainfall and average temperature in the mid-century period in comparison to the baseline period are presented in Figure 7.6. Average annual temperature is expected to increase between 1.4°C (GFDL-ESM2M) and 2.4°C (MIROC5). Annual precipitation in the future is expected to vary between −13% (IPSL-CM5A-LR) and 4% (CCSM4). Monthly precipitation varied across GCMs, months, and RCPs. In general, rainfall is projected to be higher in the future than the baseline period in September under RCP 8.5 scenario. Temperature under RCP 8.5 was greater than that under RCP 4.5. The deviation in future rainfall from the historic values was greater under RCP 8.5 than under RCP 4.5 (Figure 7.6).

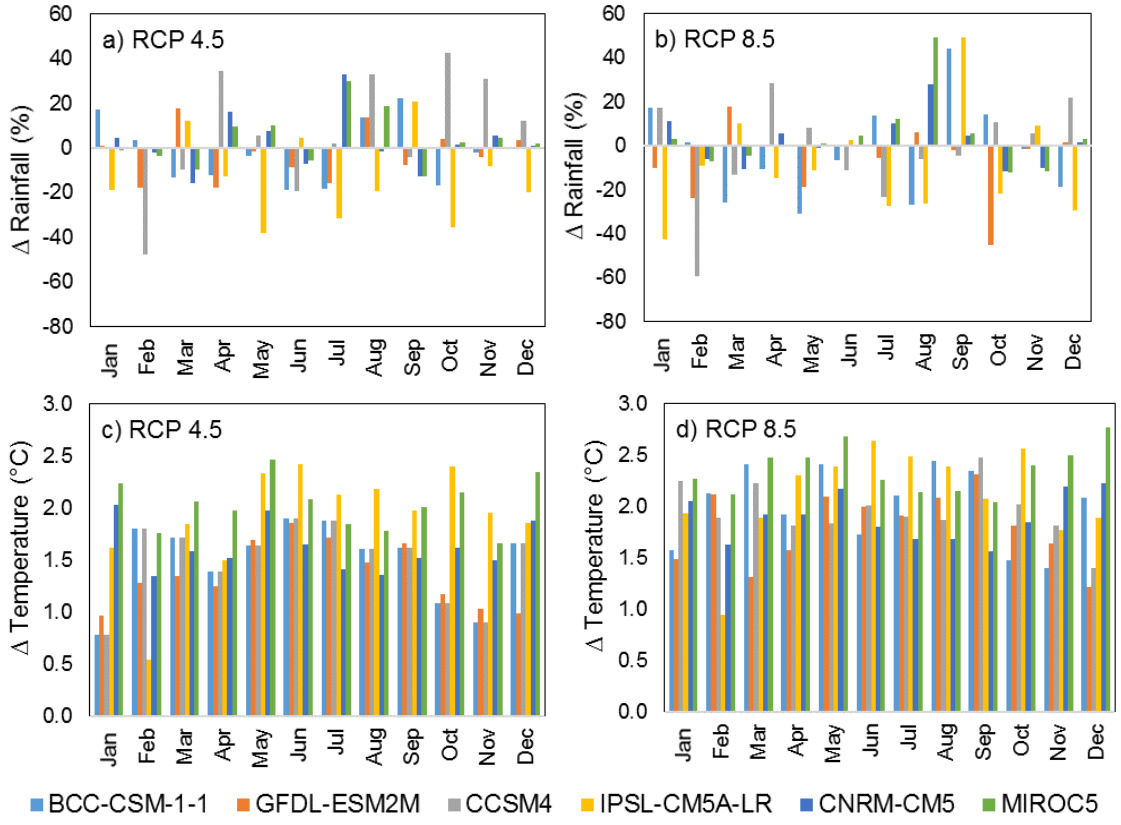

Figure 7.6 Difference between monthly rainfall and average temperature in the mid-century (2036–2065) compared to the baseline (1976–2005) projected by six GCMs.

7.4.4. Climate Change Impact Assessment

Projected changes in crop yield in the mid-century period compared to the baseline period are presented in Figure 7.7. Yield of all crops increased when higher CO_2 levels were considered in the future. The increase in yield was greater for dryland conditions than irrigation conditions, and higher under RCP 8.5 than under RCP 4.5. This could be attributed to increased radiation use efficiency, biomass production per unit solar radiation intercepted, at elevated CO_2 levels (Neitsch et al., 2011; Yang et al., 2018). Greater yield

increase under dryland conditions was likely due to reduced stomatal conductance at elevated CO_2 levels (Ficklin et al., 2009).

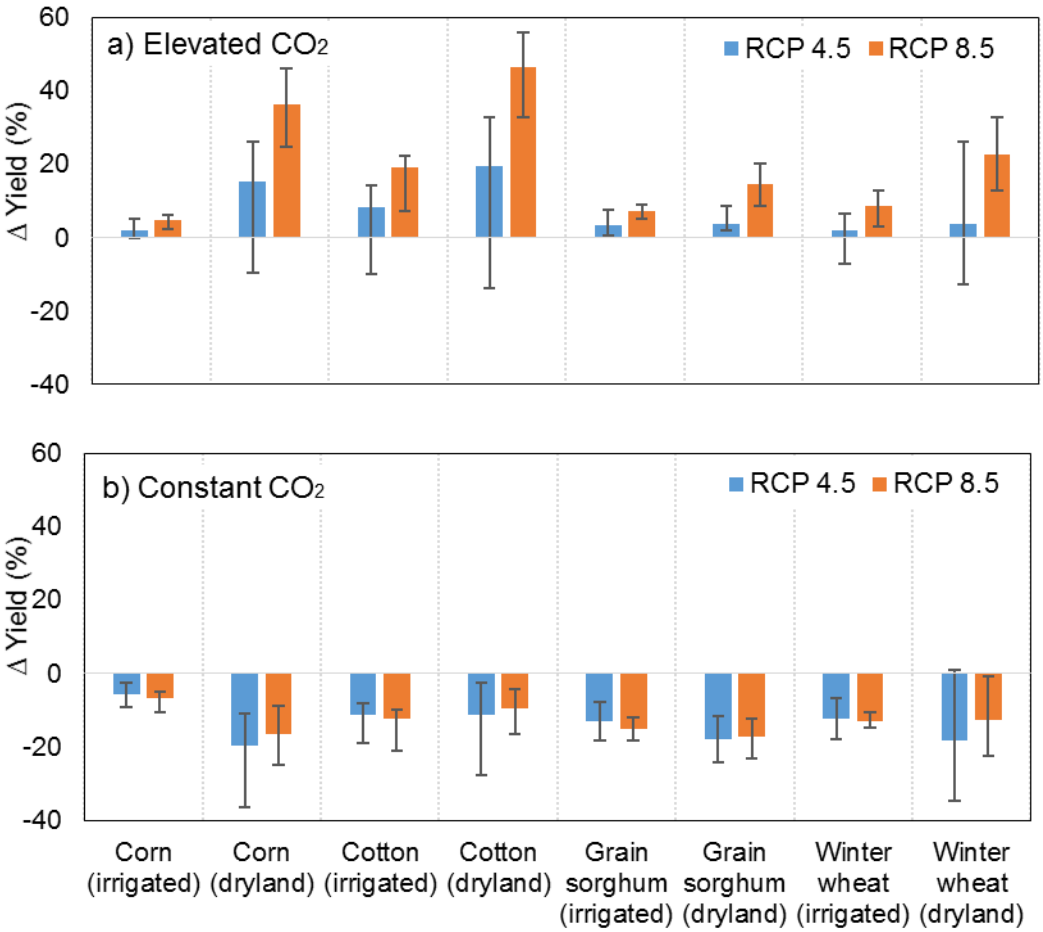

Figure 7.7 Difference between the baseline and future crop yield assuming increased CO_2 concentration in the future at, a) elevated levels of 499 ppm, RCP 4.5 and 571 ppm, RCP 8.5, and b) same as the baseline level at 380 ppm. Error bars represent range of change.

Under irrigated conditions, on average (ensemble of six GCMs), increase in yield was maximum for cotton (19%), followed by winter wheat (9%), sorghum (7%), and corn (5%). Under dryland conditions, increase in yield was maximum for cotton (47%),

followed by corn (36%), winter wheat (23%), and sorghum (15%) (Figure 7.7a). When the effect of elevated CO_2 was not considered, yield of all crops decreased in the future compared to the baseline (Figure 7.7b). This indicated that the positive effects of CO_2 on crop yield were much greater than the negative effects of increased temperature (in case of all GCMs) and reduced rainfall (some GCMs).

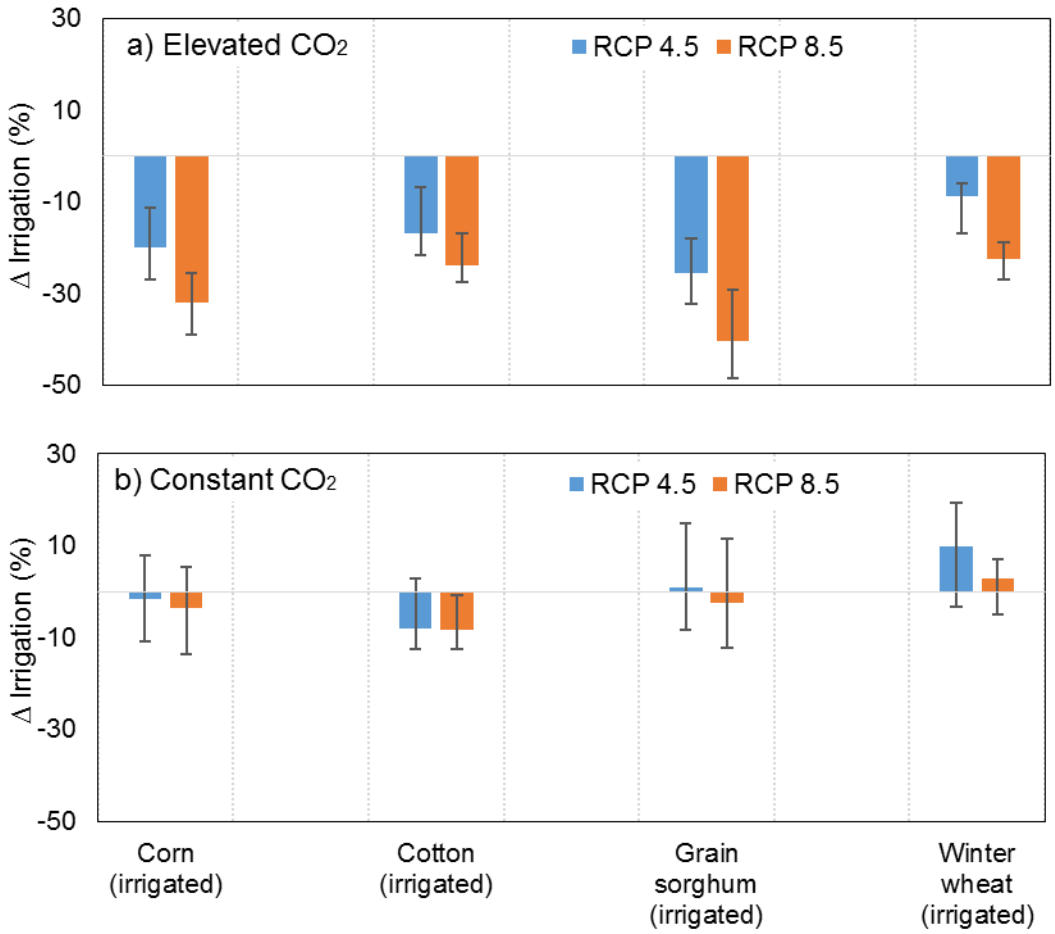

Figure 7.8 Difference between baseline and future irrigation water use assuming future CO_2 concentration at, a) elevated levels of 499 ppm, RCP 4.5 and 571 ppm, RCP 8.5, and b) constant level of 380 ppm. Error bars represent range of change among the six GCMs.

Most GCMs in the elevated CO_2 scenarios resulted in an increase in crop yield, except for IPSL-CM5A-LR GCM under RCP 4.5. In this scenario, annual mean temperature was about 2°C higher and the rainfall was 13% lower than the baseline period. Key growing months (May–Oct) were the warmest compared to other GCMs in RCP 4.5 and driest compared to all GCMs and RCPs (Figure 7.6). Although, temperatures under RCP 8.5 scenario were higher than those under RCP 4.5, higher CO_2 levels in the former compensated for the adverse effects of temperature rise.

Irrigation water use decreased in the future compared to the baseline when elevated CO_2, and associate reduction in stomatal conductance, were considered (Figure 7.8). Under elevated CO_2, maximum irrigation demand reduced for grain sorghum by 41%, followed by corn (32%), cotton (24%), and winter wheat (23%). Reduction in irrigation water demand could be due to reduced biomass due to temperature stress. On the other hand, irrigation water use showed mixed trends when the effects of CO_2 were neglected. In the absence of CO_2 fertilization effect, irrigation demand reduced for cotton, (8%), corn (4%), and sorghum (3%). In contrast, irrigation water demand of winter wheat increased by 3%. Irrigation water use of cotton decreased by a greater magnitude than other crops, likely due to increased rainfall during August and September. The increase in winter wheat water demand was likely due to reduced winter rainfall especially in February (Figure 7.6). This is consistent with Ficklin et al. (2009), who reported that with increasing temperature, irrigation water use increased in winter months. They also reported that increase in temperature could shift plant growth pattern and re-distribute water over months.

In this study, the effects of temperature, CO_2 and rainfall were studied only on four crops, and the CC effect on other crops was not studied. Shifts in plant growth pattern and water use of other plants could have also affected water availability for the four crops considered in this study. In addition, SWAT routines for stomatal conductance with respect to CO_2 levels follow an inverse linear relationship (Ficklin et al., 2009), which tends to overestimate reductions in evapotranspiration at elevated CO_2 levels (Butcher et al., 2014). Therefore, care should be taken while extrapolating results from this study. It is advisable to compare results from projections by larger number of GCMs to minimize uncertainty due to model structure.

7.4.5. Climate Change Adaptation

Simulated yield and irrigation water use under an adaptation scenario compared to the baseline cultivar in the mid-century are presented in Tables 7.7–7.8. Increasing optimal temperature by 2°C, had mostly negative effects on irrigated and dryland crop yield, except for minor yield increase in irrigated winter wheat and dryland corn under RCP 4.5. Irrigation water use slightly decreased under RCP 4.5 for cotton, sorghum, and wheat and slightly increased for cotton, sorghum, and corn. These negative effects indicate that increasing optimal temperature resulted in a greater number of days when growing season temperatures fell outside, mainly below, the optimal growth range. These results are opposite to the trends in the Texas High Plains region presented in previous chapters and also in other studies in which similar method was implemented using the DSSAT model (Singh et al., 2014c). This could be likely because while DSSAT model uses two

temperature thresholds, minimum and maximum thresholds, and temperature stress is simulated outside these thresholds. In contrary, the SWAT model uses single optimal temperature, and temperature stress is simulated when air temperature deviates from the optimal threshold on either side of the temperature response function (Figure 7.9). Research shows that improving temperature functions in fifteen crop models reduced uncertainty in crop response to CC (Maiorano et al., 2017). Further calibration and perhaps improvement in SWAT algorithms to accurately simulate heat stress on biomass growth, leaf senescence, grain number, and phenology would enhance confidence in adopting SWAT model for CC impact and heat tolerance simulations.

Table 7.7 Percent changes in yield and irrigation water use with CC adaptation I, increased optimal temperature, compared to baseline cultivar in the mid-century.

	ΔYield Irrigated		ΔIrrigation		ΔYield Dryland	
	RCP 4.5	RCP 8.5	RCP 4.5	RCP 8.5	RCP 4.5	RCP 8.5
Corn	−0.85	−0.73	1.36	3.47	2.72	−0.16
Cotton	−1.59	−1.41	−0.21	0.65	−0.71	−1.84
Grain Sorghum	−1.60	−1.41	−0.84	0.87	−1.17	−2.41
Winter Wheat	0.59	0.36	−0.43	−0.31	−0.20	−0.28

Table 7.8 Percent changes in yield and irrigation water use with CC adaptation II, increased root depth, compared to baseline cultivar in the mid-century.

	ΔYield Irrigated		ΔIrrigation		ΔYield Dryland	
	RCP 4.5	RCP 8.5	RCP 4.5	RCP 8.5	RCP 4.5	RCP 8.5
Corn	−0.01	0.07	0.00	−0.69	0.22	−0.47
Grain Sorghum	0.14	0.05	−0.24	−0.54	0.07	0.18
Winter Wheat	10.07	10.63	−20.89	−20.14	18.38	14.04

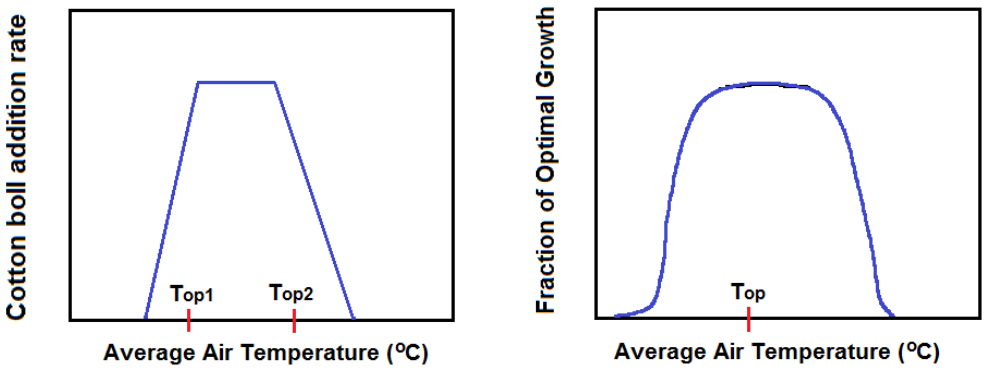

Figure 7.9 Schematic of plant growth response to temperature changes in the DSSAT model (left) and SWAT model (right); adapted with permission from Singh et al. (2014a) and Neitsch et al., (2011), respectively.

The second CC adaptation scenario, increasing rooting depth by about 20% for wheat and 9% for corn and sorghum, showed mixed results among crops. The default rooting depth of wheat was smaller than the other three crops, which allowed testing of a greater increase in rooting depth. However, only 9% increase in root depth was possible for corn and sorghum due to the limitation of SOL_ZMX (Table 7.2). Substantial benefits, yield increase and irrigation demand reduction, were simulated for winter wheat. Minor benefits were simulated for grain sorghum. The effects on corn were negligible. This could be because root depth was increased by a greater percent in wheat (20%) than the other two crops. A smaller (9%) increase in root depth was not sufficient to influence crop yield and irrigation.

7.5. Conclusions

In this study, potential impact of CC on crop yield and irrigation water use in the Edwards Aquifer area was assessed using the SWAT model. Four major crops in the

region, corn, upland cotton, grain sorghum and winter wheat were considered in this study. The simulated results indicate that yield of the four crops would increase under CC while the irrigation water use would decrease. The primary reason for these changes was higher CO_2 concentration in the future. This was indicated by a greater yield increase under RCP 8.5 than RCP 4.5, and by a comparison with constant CO_2 scenarios. At higher atmospheric CO_2 levels, biomass production per unit intercepted solar radiation increased and stomatal conductance reduced. In the absence of beneficial effects of CO_2, crop yield decreased while irrigation water demand showed a mixed trend; on average, irrigation water use of cotton declined and that of winter wheat increased. On average, positive effects of CO_2 compensated for adverse effects of temperature rise or rainfall variability for all crops. These results are highly dependent on the ability of SWAT model to incorporate CO_2 fertilization effects. Impact of pest and disease were not considered, and the crops were automatically fertilized based on nutrient stress. Care should be taken while interpreting these results. It is recommended to carry out similar experiment with different crop models to gain more confidence in the results. Out of the two adaptation scenarios tested, only increasing root depth by 20% resulted in substantial yield benefits for winter wheat. Existing temperature response functions of SWAT model may have affected crop response to CC, further research into heat stress functions and comparison with other crop models would improve confidence in using SWAT model for CC impact and heat tolerance assessment.

8. SUMMARY AND CONCLUSIONS

8.1. Summary

Research efforts are needed on global and regional scales to improve climate change (CC) resilience of agriculture. The adverse effects of CC coupled with dwindling irrigation water supplies pose a threat to sustainability of Texas agriculture. The overarching goal of this study was to provide recommendations on water-use-efficient and climate-change-adaptive strategies to sustain agricultural productivity in two important agricultural regions in Texas: Texas High Plains (THP) and the Edwards Aquifer (EA) region. The study focused on four major crops: grain sorghum, cotton, winter wheat, and corn (EA region only). Special emphasis was placed on grain sorghum in the THP because it was not studied very well in this region despite its lower water requirement and reliable performance under harsh weather conditions.

Future climate projections used in this study came from nine CMIP5 Global Climate Models (GCMs) and two representative concentration pathways (RCPs 4.5 and 8.5). Two simulation models, Decision Support System for Agrotechnology Transfer (DSSAT) model and the Soil and Water Assessment Tool (SWAT) were used in this study. Capabilities of the DSSAT model in simulating irrigation practices were thoroughly utilized to evaluate multiple irrigation strategies for grain sorghum production in the THP. The cultivar database of the DSSAT model was examined carefully to identity potential climate-change-adaptive genetic traits for the THP region. Attempts were made to evaluate similar adaptations in the EA region using the SWAT model.

The DSSAT-CSM-CERES-Sorghum and DSSAT-CSM-CROPGRO-Cotton models were initially evaluated against field data from irrigation experiments conducted at Halfway in the THP. The evaluated CERES-Sorghum model was then used for identifying optimal soil water threshold at planting and thresholds to start and stop irrigation for grain sorghum at Halfway under cold, warm, wet, dry, and normal climate variability classes. In addition, the impacts of climate change on grain sorghum yield and irrigation water use at Halfway under full and deficit irrigation strategies (both crop-growth-stage based and percent evapotranspiration-replacement strategies) was studied. Furthermore, the impacts of climate change on crop yield and irrigation water use of grain sorghum at two other sites in the THP, Bushland and Lamesa were assessed and eight different climate change adaptation strategies (increasing soil root density at different soil depths, increasing root length to weight ratio, increasing and decreasing maximum root water uptake per unit length, increasing upper optimum and failure temperature thresholds by 2°C and 3°C, increasing yield potential, lengthening crop growing period) were evaluated for all three sites in the THP based on the simulated crop yield and irrigation water use. Similarly, the evaluated CROPGRO-Cotton model was used to assess the climate change impacts on cotton production at Halfway, Bushland and Lamesa and six adaptation strategies (drought tolerance incorporated by altering root hydraulic and physical properties and maximum photosynthesis rate, heat tolerance by increasing temperature thresholds by 2°C and 3°C for process related to boll development, increased yield potential, and longer maturity) were evaluated for these three sites.

The DSSAT-CSM-CERES-Wheat model was evaluated for the Bushland site in the THP. The evaluated model was used to assess the climate change impacts on winter wheat production at Bushland, Halfway and Lamesa and test seven genetic-adaptations—denser roots, stay-green, high root water uptake, heat tolerance, high yield potential, and early flowering.

Finally, the SWAT model was evaluated for the Lower Medina Watershed in the EA region. The model was calibrated and validated against monthly streamflow and annual crop yield data. The evaluated model was then used to assess the impacts of climate change on crop yield and irrigation water use of grain sorghum, cotton, corn and winter wheat using future climate data projected by six CMIP5 GCMs under two RCPs. Two adaptation strategies were tested for this study watershed—increasing optimal temperature threshold by 2°C and increasing maximum rooting depth.

8.2. Conclusions

The following conclusions were drawn from this study:

1. Efficient irrigation strategies identified for grain sorghum production in the THP:
    a. Maintaining soil water at planting at 75% of available water content (AWC) optimized irrigation water use efficiency.
    b. Initiating irrigation at 50% AWC and stopping it at 85% AWC was found to be adequate under normal, colder and wet conditions.
    c. Under warm-dry weather, initiating irrigation at 60% AWC and stopping it at 100% AWC was found to be a better strategy to optimize irrigation water use.

d. Climate variability was found to affect sorghum yield more than the differences in simulated irrigation strategies.
e. Best use of limited irrigation for grain sorghum could be achieved by applying irrigation during early reproductive stages (panicle initiation through early grain filling).

2. Climate change impacts on crop production and irrigation water use in the THP
   a. Irrigated grain sorghum yield was simulated to decrease, on an average by 13% and 21% by mid-century (2036–2065) and late-century (2066–2095), respectively under RCP 8.5 compared to the baseline (1976–2005). The irrigation water use was simulated to decrease by 8% and 15% by the mid-century and late-century, respectively under RCP 8.5, mainly due to shortening of growing season and lowering of transpiration per unit leaf area.
   b. The percent yield loss under deficit irrigation versus full irrigation was higher in the future under climate change than under baseline conditions. An irrigation deficit of 30% resulted in a yield loss of up to 20%, 25%, and 27%, under the baseline, mid-century, and late-century periods, respectively.
   c. Irrigated cotton yield was simulated to increase at Bushland and Halfway, on an average by 17% and 16%, respectively, whereas yield at Lamesa (that has a coarser soil and warmer weather) was simulated to decrease by 2% and 10%, by the mid-century and late-century, respectively under RCP 8.5. Irrigation water use was simulated to increase at all three sites by about 8% and 14%, by mid-

century and late-century, respectively, most likely due to increased leaf area as a result of CO_2 fertilization.

d. Irrigated winter wheat yield was simulated to increase at Bushland and Halfway, on an average by 4 and 1%, whereas yield at Lamesa was simulated to decrease by 7% and 13%, by mid-century and late-century, respectively under RCP 8.5. An opposite trend at Lamesa was most likely because adverse effects of temperature stress surpassed beneficial effects of CO_2 fertilization, and coarser soils at Lamesa might have led to greater nutrient leaching and lower fertility than the other two sites. Winter wheat irrigation water use was simulated to decrease at all three sites by about 3% and 7%, by mid-century and late-century, respectively, primarily due to improved plant-transpiration-use-efficiency.

3. Ideal CC adaptation strategies for the THP
    a. For grain sorghum, the ideal CC-adaptive traits were identified as higher yield potential followed by denser roots under both irrigated and dryland conditions.
    b. For cotton, the ideal CC-adaptive trait was found to be high yield potential for irrigated production, and longer maturity and heat tolerance for dryland production.
    c. The ideal CC-adaptive traits for winter wheat were identified as higher yield potential and denser roots for both irrigated and dryland production. Early-flowering trait was also found suitable for Lamesa due to heat avoidance, and thus it could be recommended for the southern THP region.

Overall, an increase in yield was simulated with high yield potential traits with minor changes in irrigation water use, making it an ideal adaptation strategy for most cases. These cultivars have higher—radiation use efficiency, partitioning to reproductive growth, relative leaf size, and number of grains; than the no-adaptation case. An increase in yield was also simulated with increasing root density. However, changing other root hydraulic and physical properties had minor and mixed effects on yield and irrigation water use. Use of longer maturity cultivar increased irrigation water use significantly and was thus found to be not advisable.

4. Climate change impacts on crop production in the EA region
    a. Grain sorghum yield was simulated to increase by 7% and 15% under irrigated and dryland conditions, respectively. Simulated irrigation water use reduced by 41%.
    b. Cotton yield was simulated to increase by 19% and 47% under irrigated and dryland conditions, respectively. Simulated irrigation water use reduced by 24%.
    c. Winter wheat yield was simulated to increase by 9% and 23% under irrigated and dryland conditions, respectively. Simulated irrigation water use reduced by 23%.
    d. Corn yield was simulated to increase by 5% and 36% under irrigated and dryland conditions, respectively. Simulated irrigation water use reduced by 32%.

An increase in yield and reduction in irrigation water use were simulated for all crops in the EA region due to increased radiation use efficiency and reduced stomatal

conductance due to CO_2 fertilization. These positive effects were far greater than any adverse effects of temperature rise or reduction in rainfall.

5. Climate change adaptation strategies for the EA region
    a. Grain sorghum yield was simulated to decrease with increasing optimal temperature threshold, and increase slightly with increased rooting depth.
    b. Similarly, cotton yield was simulated to reduce marginally with increasing optimal temperature threshold.
    c. Winter wheat yield and water use were also simulated to change slightly with increasing optimal temperature threshold. However, yield was simulated to increase substantially (~10% under irrigated and ~16% under dryland conditions), and irrigation water use was simulated to reduce substantially (~20%) by increasing rooting depth by 20%.
    d. Corn yield was simulated to stay about the same with increasing optimal temperature threshold and increasing rooting depth.

In summary, increasing optimal temperature threshold in the SWAT model in view of higher temperatures in the future, did not improve yield or irrigation water use, and instead minor reductions in yield were simulated. Increasing rooting depth for corn and sorghum by 9% (from 2 to 2.18 m) had minor effect on crop production. In contrast, increasing rooting depth of winter wheat by 20% (from 1.3 to 1.6 m) showed substantial benefits.

8.3. Future work

Some suggestions for future work are: i) evaluation of genetic traits for CC adaptation by automatically varying selected genetic parameters within a certain range. This would allow exploration of full potential of the effect of changes in parameters on crop yield; ii) development of virtual cultivars by combining multiple traits together; iii) testing of virtual cultivars under different climatic conditions by classifying future climate data into different climate variability classes such as wet, dry, cold, hot, and normal years iv) collaboration with crop breeders to design cultivars based on recommendations from simulation models and test them under field conditions; and v) comparison of SWAT temperature response and CO_2 compensation functions with those in other crop models.

REFERENCES

Abatzoglou, J. T. 2013. Development of gridded surface meteorological data for ecological applications and modelling. *International Journal of Climatology* 33(1):121–131.

Abatzoglou, J. T., and T. J. Brown. 2012. A comparison of statistical downscaling methods suited for wildfire applications. *International Journal of Climatology* 32(5):772–780.

Adam, M., K. A. Dzotsi, G. Hoogenboom, P. C. S. Traoré, C. H. Porter, H. F. W. Rattunde, B. Nebie, W. L. Leiser, E. Weltzien, and J. W. Jones. 2018. Modelling varietal differences in response to phosphorus in West African sorghum. *European Journal of Agronomy* 100:35–43.

Adams, R. M., B. H. Hurd, S. Lenhart, and N. Leary. 1998. Effects of global climate change on agriculture: an interpretative review. *Climate Research* 11(1):19–30.

Adams, R. M., C. Rosenzweig, R. M. Peart, J. T. Ritchie, B. A. McCarl, J. D. Glyer, R. B. Curry, J. W. Jones, K. J. Boote, and L. H. Allen. 1990. Global climate change and US agriculture. *Nature* 345(6272):219–224.

Adams, W. G., R. D. Blanchard, and R. A. Earl. 2015. Edwards Aquifer Region Stakeholder Frame Analysis. *Papers in Applied Geography* 1(3):235–242.

Adhikari, P., S. Ale, J. P. Bordovsky, K. R. Thorp, N. R. Modala, N. Rajan, and E. M. Barnes. 2016. Simulating future climate change impacts on seed cotton yield in the Texas High Plains using the CSM-CROPGRO-Cotton model. *Agricultural Water Management* 164:317–330.

Adhikari, P., P. H. Gowda, G. W. Marek, D. K. Brauer, I. Kisekka, B. Northup, and A. Rocateli. 2017. Calibration and validation of CSM-CROPGRO-Cotton model using lysimeter data in the Texas High Plains. *Journal of Contemporary Water Research & Education* 162(1):61–78.

Afinowicz, J. D., C. L. Munster, and B. P. Wilcox. 2005. Modeling effects of brush management on the rangeland water budget. Edwards Plateau, Texas. *Journal of the American Water Resources Association* 41(1):181–193.

Ahmed, M., C. O. Stöckle, R. Nelson, and S. Higgins. 2017. Assessment of climate change and atmospheric CO_2 impact on winter wheat in the Pacific Northwest using a multimodel ensemble. *Frontiers in Ecology and Evolution* 5:51.

Ainsworth, E. A., and S. P. Long. 2004. What have we learned from 15 years of free-air CO_2 enrichment (FACE)? A meta-analytic review of the responses of photosynthesis, canopy properties and plant production to rising CO_2. *New Phytologist* 165(2):351–372.

Alagarswamy, G., K. Boote, L. Allen, and J. Jones. 2006. Evaluating the CROPGRO–Soybean model ability to simulate photosynthesis response to carbon dioxide levels. *Agronomy Journal* 98(1):34–42.

Alagarswamy, G., and J. Ritchie. 1991. Phasic development in CERES-Sorghum model. In *Predicting Crop Phenology*, 143–152. T. Hodges, ed. Boca Raton: CRC Press.

Allen, R. G., L. S. Pereira, D. Raes, and M. Smith. 1998. Crop evapotranspiration: guidelines for computing crop water requirements. *Irrigation and Drainage Paper No. 56*. FAO, Rome, Italy.

Amosson, S. H., L. K. Almas, F. Bretz, D. Gaskins, B. Guerrero, D. Jones, T. H. Marek, L. New, and N. Simpson. 2005. Water Management Strategies for Reducing Irrigation Demands in Region A. Report to the Panhandle Water Planning Group, Amarillo, TX, January. http://www.panhandlewater.org/2006_reg_plan/Plan/Appendix%20Q%20WMS%20for%20reducing%20Irrigation%20Demands.pdf (accessed March 2, 2018).

Amthor, J. S. 2001. Effects of atmospheric CO_2 concentration on wheat yield: review of results from experiments using various approaches to control CO_2 concentration. *Field Crops Research* 73(1):1–34.

Anapalli, S. S., K. D. Fisher, N. K. Reddy, T. W. Pettigrew, R. Sui, and R. L. Ahuja. 2016. Vulnerabilities and adapting irrigated and rainfed cotton to climate change in the Lower Mississippi Delta Region. *Climate* 4(4):1–20.

Antle, J. M., S. Cho, S. M. H. Tabatabaie, and R. O. Valdivia. 2018. Economic and environmental performance of dryland wheat-based farming systems in a 1.5 °C world. *Mitigation and Adaptation Strategies for Global Change* 24(2):165–180.

Araya, A., I. Kisekka, P. H. Gowda, and P. V. Prasad. 2017. Evaluation of water-limited cropping systems in a semi-arid climate using DSSAT-CSM. *Agricultural Systems* 150:86–98.

Arnold, J. G., D. N. Moriasi, P. W. Gassman, K. C. Abbaspour, M. J. White, R. Srinivasan, C. Santhi, R. Harmel, A. Van Griensven, and M. W. Van Liew. 2012. SWAT: Model use, calibration, and validation. *Transactions of the ASABE* 55(4):1491–1508.

Arnold, J. G., R. Srinivasan, R. S. Muttiah, and J. R. Williams. 1998. Large area hydrologic modeling and assessment part I: model development. *Journal of the American Water Resources Association* 34(1):73–89.

Ashraf Vaghefi, S., S. J. Mousavi, K. C. Abbaspour, R. Srinivasan, and H. Yang. 2014. Analyses of the impact of climate change on water resources components, drought and wheat yield in semiarid regions: Karkheh River Basin in Iran. *Hydrological Processes* 28(4):2018–2032.

Assefa, Y., S. A. Staggenborg, and V. P. Prasad. 2010. Grain sorghum water requirement and responses to drought stress: a review. *Crop Management* 9(1).

Asseng, S., F. Ewert, P. Martre, R. P. Rötter, D. B. Lobell, D. Cammarano, B. A. Kimball, M. J. Ottman, G. W. Wall, J. W. White, M. P. Reynolds, P. D. Alderman, P. V. V. Prasad, P. K. Aggarwal, J. Anothai, B. Basso, C. Biernath, A. J. Challinor, G. De Sanctis, J. Doltra, E. Fereres, M. Garcia-Vila, S. Gayler, G. Hoogenboom, L. A. Hunt, R. C. Izaurralde, M. Jabloun, C. D. Jones, K. C. Kersebaum, A. K. Koehler, C. Müller, S. Naresh Kumar, C. Nendel, G. O'Leary, J. E. Olesen, T. Palosuo, E. Priesack, E. Eyshi Rezaei, A. C. Ruane, M. A. Semenov, I. Shcherbak, C. Stöckle, P. Stratonovitch, T. Streck, I. Supit, F. Tao, P. J. Thorburn, K. Waha, E. Wang, D. Wallach, J. Wolf, Z. Zhao, and Y. Zhu. 2014. Rising temperatures reduce global wheat production. *Nature Climate Change* 5:143.

Asseng, S., Y. Zhu, E. Wang, and W. Zhang. 2015. Chapter 20 - Crop modeling for climate change impact and adaptation. In *Crop Physiology (Second Edition)*, 505–546. V. O. Sadras, and D. F. Calderini, eds. San Diego: Academic Press.

Attia, A., N. Rajan, Q. Xue, S. Nair, A. Ibrahim, and D. Hays. 2016. Application of DSSAT-CERES-Wheat model to simulate winter wheat response to irrigation management in the Texas High Plains. *Agricultural Water Management* 165:50–60.

Auer, I., and R. Böhm. 1994. Combined temperature-precipitation variations in Austria during the instrumental period. *Theoretical and Applied Climatology* 49(3):161–174.

Awika, J. M., and L. W. Rooney. 2004. Sorghum phytochemicals and their potential impact on human health. *Phytochemistry* 65(9):1199–1221.

Balkovič, J., M. van der Velde, R. Skalský, W. Xiong, C. Folberth, N. Khabarov, A. Smirnov, N. D. Mueller, and M. Obersteiner. 2014. Global wheat production potentials and management flexibility under the representative concentration pathways. *Global and Planetary Change* 122:107–121.

Balota, M., D. A. Herbert, D. L. Holshouser, and J. Dahlberg. 2013. 2009–2011 Performance of Sorghum Hybrids in the Virginia-Carolina Region. Virginia Cooperative Extension, Blacksburg. http://hdl.handle.net/10919/55677 (accessed March 10, 2018).

Bannayan, M., and G. Hoogenboom. 2009. Using pattern recognition for estimating cultivar coefficients of a crop simulation model. *Field Crops Research* 111(3):290–302.

Battisti, R., and P. C. Sentelhas. 2017. Improvement of soybean resilience to drought through deep root system in Brazil. *Agronomy Journal* 109(4):1612–1622.

Baumhardt, R., and O. Jones. 2002. Residue management and tillage effects on soil-water storage and grain yield of dryland wheat and sorghum for a clay loam in Texas. *Soil and Tillage Research* 68(2):71–82.

Bean, B. W., O. Jones, P. Unger, and L. Baumhardt. 2003. Sorghum Tillage in the Texas High Plains. Texas FARMER Collection. http://publication.tamu.edu/CORN_SORGHUM/PUB_Sorghum%20Tillage%20in%20the%20Texas%20High%20Plains.pdf (accessed February 11, 2018).

Beven, K. 2006. A manifesto for the equifinality thesis. *Journal of Hydrology* 320(1):18–36.

Bloom, A. J., J. S. R. Asensio, L. Randall, S. Rachmilevitch, A. B. Cousins, and E. A. Carlisle. 2012. CO_2 enrichment inhibits shoot nitrate assimilation in C3 but not C4 plants and slows growth under nitrate in C3 plants. *Ecology* 93(2):355–367.

Blum, A. 1998. *Plant Breeding for Stress Environments*. CRC press, Boca Raton, FL.

Booker, J., K. Bronson, C. Trostle, J. Keeling, and A. Malapati. 2007. Nitrogen and phosphorus fertilizer and residual response in cotton–sorghum and cotton–cotton sequences. *Agronomy Journal* 99(3):607–613.

Boote, K., and N. Pickering. 1994. Modeling photosynthesis of row crop canopies. *HortScience* 29(12):1423–1434.

Boote, K. J. 1999. Concepts for calibrating crop growth models. In *DSSAT v3, vol. 4*, 179–200. G. Hoogenboom, P. W. Wilkens, and G. Y. Tsuji, eds. Hawaii, Honolulu: Univ. of Hawaii.

Boote, K. J., L. H. Allen, P. V. V. Prasad, and J. W. Jones. 2010. Testing effects of climate change in crop models. In *Handbook of Climate Change and Agroecosystems*, 109–129. D. Hillel, and C. Rosenzweig, eds. London: Imperial College Press.

Boote, K. J., J. W. Jones, and G. Hoogenboom. 1998. Simulation of crop growth: CROPGRO model. In *Agricultural Systems Modeling and Simulation*, 651–692. R. M. Peart, and R. B. Curry, eds. New York: Marcel Dekker.

Bordovsky, J., and W. Lyle. 1996. LEPA irrigation of grain sorghum with varying water supplies. *Transactions of the ASAE* 39(6):2033–2038.

Bordovsky, J. P., J. Mustian, A. Cranmer, and C. Emerson. 2011. Cotton-grain sorghum rotation under extreme deficit irrigation conditions. *Applied Engineering in Agriculture* 27(3):359–371.

Bordovsky, J. P., J. T. Mustian, G. L. Ritchie, and K. L. Lewis. 2015. Cotton irrigation timing with variable seasonal irrigation capacities in the Texas south plains. *Applied Engineering in Agriculture* 31(6):883–897.

Bowen, W. T., P. K. Thornton, and G. Hoogenboom. 1998. The simulation of cropping sequences using DSSAT. In *Understanding Options for Agricultural Production*, 313–327. G. Y. Tsuji, G. Hoogenboom, and P. K. Thornton, eds. Dordrecht, the Netherlands: Kluwer Academic Publishers.

Bronson, K., and R. Bowman. 2009. Nutrient management for Texas High Plains cotton production. Texas AgriLife Research and Extension, College Station, TX. http://lubbock.tamu.edu/files/2011/10/nutrmgmtforcot.pdf (accessed December 5, 2017)

Bronson, K., A. Malapati, J. Booker, B. Scanlon, W. Hudnall, and A. Schubert. 2009. Residual soil nitrate in irrigated Southern High Plains cotton fields and Ogallala groundwater nitrate. *Journal of Soil and Water Conservation* 64(2):98–104.

Bronson, K., A. Onken, J. Keeling, J. Booker, and H. Torbert. 2001. Nitrogen response in cotton as affected by tillage system and irrigation level. *Soil Science Society of America Journal* 65(4):1153–1163.

Broughton, K. J., R. A. Smith, R. A. Duursma, D. K. Tan, P. Payton, M. P. Bange, and D. T. Tissue. 2017. Warming alters the positive impact of elevated CO_2 concentration on cotton growth and physiology during soil water deficit. *Functional Plant Biology* 44(2):267–278.

Butcher, J. B., T. E. Johnson, D. Nover, and S. Sarkar. 2014. Incorporating the effects of increased atmospheric CO_2 in watershed model projections of climate change impacts. *Journal of Hydrology* 513:322–334.

Cammarano, D., and D. Tian. 2018. The effects of projected climate and climate extremes on a winter and summer crop in the southeast USA. *Agricultural and Forest Meteorology* 248:109–118.

Carbone, G. J., W. Kiechle, C. Locke, L. O. Mearns, L. McDaniel, and M. W. Downton. 2003. Response of soybean and sorghum to varying spatial scales of climate change scenarios in the southeastern United States. In *Issues in the Impacts of Climate Variability and Change on Agriculture: Applications to the southeastern United States*, 73–98. L. O. Mearns, ed. Dordrecht, the Netherlands: Springer Netherlands.

Challinor, A. J., J. Watson, D. Lobell, S. Howden, D. Smith, and N. Chhetri. 2014. A meta-analysis of crop yield under climate change and adaptation. *Nature Climate Change* 4(4):287–291.

Chaudhuri, S., and S. Ale. 2014. Long-term (1930–2010) trends in groundwater levels in Texas: influences of soils, landcover and water use. *Science of the Total Environment* 490:379–390.

Chaudhuri, U. N., M. B. Kirkham, and E. T. Kanemasu. 1990. Carbon dioxide and water level effects on yield and water use of winter wheat. *Agronomy Journal* 82:637–641.

Chen, C.C., D. Gillig, and B. A. McCarl. 2001. Effects of climatic change on a water dependent regional economy: a study of the Texas Edwards Aquifer. *Climatic Change* 49(4):397–409.

Chen, Y., S. Ale, N. Rajan, C. L. S. Morgan, and J. Park. 2016. Hydrological responses of land use change from cotton (Gossypium hirsutum L.) to cellulosic bioenergy crops in the Southern High Plains of Texas, USA. *GCB Bioenergy* 8(5):981–999.

Chipanshi, A., R. Chanda, and O. Totolo. 2003. Vulnerability assessment of the maize and sorghum crops to climate change in Botswana. *Climatic Change* 61(3):339–360.

Chmielewski, F. M., and J. M. Potts. 1995. The relationship between crop yields from an experiment in southern England and long-term climate variations. *Agricultural and Forest Meteorology* 73(1):43–66.

Clouse, R. W. 2006. Spatial application of a cotton growth model for analysis of site-specific irrigation in the Texas High Plains. Doctoral Dissertation. Texas A&M University, College Station, TX. http://hdl.handle.net/1969.1/5887 (accessed May 1, 2017).

Colaizzi, P., P. Gowda, T. Marek, and D. Porter. 2009. Irrigation in the Texas High Plains: A brief history and potential reductions in demand. *Irrigation and Drainage* 58(3):257–274.

Conley, M. M., B. Kimball, T. Brooks, P. Pinter, D. Hunsaker, G. Wall, N. Adam, R. LaMorte, A. Matthias, and T. Thompson. 2001. CO_2 enrichment increases water-use efficiency in sorghum. *New Phytologist* 151(2):407–412.

Cossani, C. M., and M. P. Reynolds. 2012. Physiological Traits for Improving Heat Tolerance in Wheat. *Plant Physiology* 160(4):1710.

Coumou, D., and S. Rahmstorf. 2012. A decade of weather extremes. *Nature Climate Change* 2:491.

Craufurd, P. Q., and J. M. Peacock. 2008. Effect of heat and drought stress on sorghum (Sorghum Bicolor). II. grain yield. *Experimental Agriculture* 29(1):77–86.

DeJonge, K., J. Ascough II, A. Andales, N. Hansen, L. Garcia, and M. Arabi. 2012. Improving evapotranspiration simulations in the CERES-Maize model under limited irrigation. *Agricultural Water Management* 115:92–103.

Dias de Oliveira, E., J. A. Palta, H. Bramley, K. Stefanova, and K. H. M. Siddique. 2015. Elevated CO_2 reduced floret death in wheat under warmer average temperatures and terminal drought. *Frontiers in Plant Science* 6:1010–1010.

Dicko, M. H., H. Gruppen, A. S. Traoré, A. G. Voragen, and W. J. Van Berkel. 2006. Sorghum grain as human food in Africa: relevance of content of starch and amylase activities. *African Journal of Biotechnology* 5(5):384–395.

Dixit, P. N., R. Telleria, A. N. Al Khatib, and S. F. Allouzi. 2018. Decadal analysis of impact of future climate on wheat production in dry Mediterranean environment: A case of Jordan. *Science of the Total Environment* 610–611:219–233.

Doherty, R. M., L. O. Mearns, K. R. Reddy, M. W. Downton, and L. McDaniel. 2003. Spatial scale effects of climate scenarios on simulated cotton production in the southeastern U.S.A. *Climatic Change* 60(1–2):99–129.

Dufresne, J. L., M. A. Foujols, S. Denvil, A. Caubel, O. Marti, O. Aumont, Y. Balkanski, S. Bekki, H. Bellenger, R. Benshila, S. Bony, L. Bopp, P. Braconnot, P. Brockmann, P. Cadule, F. Cheruy, F. Codron, A. Cozic, D. Cugnet, N. de Noblet, J. P. Duvel, C. Ethé, L. Fairhead, T. Fichefet, S. Flavoni, P. Friedlingstein, J. Y. Grandpeix, L. Guez, E. Guilyardi, D. Hauglustaine, F. Hourdin, A. Idelkadi, J. Ghattas, S. Joussaume, M. Kageyama, G. Krinner, S. Labetoulle, A. Lahellec, M. P. Lefebvre, F. Lefevre, C. Levy, Z. X. Li, J. Lloyd, F. Lott, G. Madec, M. Mancip, M. Marchand, S. Masson, Y. Meurdesoif, J. Mignot, I. Musat, S. Parouty, J. Polcher, C. Rio, M. Schulz, D. Swingedouw, S. Szopa, C. Talandier, P. Terray, N. Viovy, and N. Vuichard. 2013. Climate change projections using the IPSL-CM5 Earth System Model: from CMIP3 to CMIP5. *Climate Dynamics* 40(9):2123–2165.

Dunne, J. P., J. G. John, A. J. Adcroft, S. M. Griffies, R. W. Hallberg, E. Shevliakova, R. J. Stouffer, W. Cooke, K. A. Dunne, and M. J. Harrison. 2012. GFDL's ESM2 global coupled climate–carbon earth system models. Part I: Physical formulation and baseline simulation characteristics. *Journal of Climate* 25(19):6646–6665.

Eck, H., and O. Jones. 1992. Soil nitrogen status as affected by tillage, crops, amd crop sequences. *Agronomy Journal* 84(4):660–668.

Eck, H. V. 1988. Winter Wheat Response to Nitrogen and Irrigation. *Agronomy Journal* 80(6):902–908.

Eck, H. V., and J. T. Musick. 1979. Plant Water Stress Effects on Irrigated Grain Sorghum. I. Effects on Yield1. *Crop Science* 19(5):589–592.

Eitzinger, J., M. Štastná, Z. Žalud, and M. Dubrovský. 2003. A simulation study of the effect of soil water balance and water stress on winter wheat production under different climate change scenarios. *Agricultural Water Management* 61(3):195–217.

Elhassan, A., H. Xie, A. A. Al-othman, J. McClelland, and H. O. Sharif. 2016. Water quality modelling in the San Antonio River Basin driven by radar rainfall data. *Geomatics, Natural Hazards and Risk* 7(3):953–970.

Elias, E., A. Marklein, J. T. Abatzoglou, J. Dialesandro, J. Brown, C. Steele, A. Rango, and K. Steenwerth. 2018. Vulnerability of field crops to midcentury temperature changes and yield effects in the Southwestern USA. *Climatic Change* 148(3):403–417.

Elliott, J., D. Deryng, C. Müller, K. Frieler, M. Konzmann, D. Gerten, M. Glotter, M. Flörke, Y. Wada, N. Best, S. Eisner, B. M. Fekete, C. Folberth, I. Foster, S. N. Gosling, I. Haddeland, N. Khabarov, F. Ludwig, Y. Masaki, S. Olin, C. Rosenzweig, A. C. Ruane, Y. Satoh, E. Schmid, T. Stacke, Q. Tang, and D. Wisser. 2014. Constraints and potentials of future irrigation water availability on agricultural production under climate change. *Proceedings of the National Academy of Sciences* 111(9):3239.

Errebhi, M., C. J. Rosen, S. C. Gupta, and D. E. Birong. 1998. Potato yield response and nitrate leaching as influenced by nitrogen management. *Agronomy Journal* 90(1):10–15.

Fan, J., B. McConkey, H. Wang, and H. Janzen. 2016. Root distribution by depth for temperate agricultural crops. *Field Crops Research* 189:68–74.

Ficklin, D. L., Y. Luo, E. Luedeling, and M. Zhang. 2009. Climate change sensitivity assessment of a highly agricultural watershed using SWAT. *Journal of Hydrology* 374(1):16–29.

Fu, T., J. Ko, G. W. Wall, P. J. Pinter, B. A. Kimball, M. J. Ottman, and H. Y. Kim. 2016. Simulation of climate change impacts on grain sorghum production grown under free air CO_2 enrichment. *International Agrophysics* 30(3):311–322.

Gayley, A. 2013. SWAT-based evapotranspirative water conservation analysis performed onirrigated croplands to determine potential regional water savings. *Journal of Irrigation and Drainage Engineering* 139(6):456–462.

Gent, P. R., G. Danabasoglu, L. J. Donner, M. M. Holland, E. C. Hunke, S. R. Jayne, D. M. Lawrence, R. B. Neale, P. J. Rasch, and M. Vertenstein. 2011. The community climate system model version 4. *Journal of Climate* 24(19):4973–4991.

Gérardeaux, E., R. Loison, O. Palaï, and B. Sultan. 2018. Adaptation strategies to climate change using cotton (Gossypium hirsutum L.) ideotypes in rainfed tropical cropping systems in Sub-Saharan Africa. A modeling approach. *Field Crops Research* 226:38–47.

Gérardeaux, E., B. Sultan, O. Palaï, C. Guiziou, P. Oettli, and K. Naudin. 2013. Positive effect of climate change on cotton in 2050 by CO_2 enrichment and conservation agriculture in Cameroon. *Agronomy for Sustainable Development* 33(3):485–495.

Gerik, T., B. W. Bean, and R. Vanderlip. 2003. Sorghum growth and development. In *Texas FARMER Collection*. Amarillo, TX: Texas AgriLife Extension Service.

Gleaton, C., and J. Robinson. 2016. *Facts about Texas and US agriculture* Texas AgriLife Extension, Department of Agricultural Economics, Texas A&M University, College Station, TX.

Grassini, P., K. M. Eskridge, and K. G. Cassman. 2013. Distinguishing between yield advances and yield plateaus in historical crop production trends. *Nature Communications* 4:2918.

Guerrero, B., and S. Amosson. 2013. The importance of irrigated crop production to the Texas High Plains economy. In *Proceedings of the Southern Agricultural Economics Association Annual Meeting*. Orlando, Florida, USA, February 2–5, 2013.

Guo, R., Z. Lin, X. Mo, and C. Yang. 2010. Responses of crop yield and water use efficiency to climate change in the North China Plain. *Agricultural Water Management* 97(8):1185–1194.

Hao, B., Q. Xue, B. W. Bean, W. L. Rooney, and J. D. Becker. 2014. Biomass production, water and nitrogen use efficiency in photoperiod-sensitive sorghum in the Texas High Plains. *Biomass and Bioenergy* 62:108–116.

Hao, B., Q. Xue, T. H. Marek, K. E. Jessup, X. Hou, W. Xu, E. D. Bynum, and B. W. Bean. 2015. Soil water extraction, water use, and grain yield by drought-tolerant maize on the Texas High Plains. *Agricultural Water Management* 155:11–21.

Harrison, P. A., and R. Butterfield. 1996. Effects of climate change on Europe-wide winter wheat and sunflower productivity. *Climate Research* 7(3):225–241.

Hatfield, J. L., K. J. Boote, B. Kimball, L. Ziska, R. C. Izaurralde, D. Ort, A. M. Thomson, and D. Wolfe. 2011. Climate impacts on agriculture: implications for crop production. *Agronomy Journal* 103(2):351–370.

Hauwert, N. M., and J. M. Sharp. 2014. Measuring autogenic recharge over a karst aquifer utilizing eddy covariance evapotranspiration. *Journal of Water Resource and Protection* 6(9):11.

Havlin, J., D. Kissel, L. Maddux, M. Claassen, and J. Long. 1990. Crop rotation and tillage effects on soil organic carbon and nitrogen. *Soil Science Society of America Journal* 54(2):448–452.

He, D., E. Wang, J. Wang, and M. J. Robertson. 2017. Data requirement for effective calibration of process-based crop models. *Agricultural and Forest Meteorology* 234–235:136–148.

He, L., S. Asseng, G. Zhao, D. Wu, X. Yang, W. Zhuang, N. Jin, and Q. Yu. 2015. Impacts of recent climate warming, cultivar changes, and crop management on winter wheat phenology across the Loess Plateau of China. *Agricultural and Forest Meteorology* 200:135–143.

Herndl, M., J. W. White, S. Graeff, and W. Claupein. 2008. The impact of vernalization requirement, photoperiod sensitivity and earliness per se on grain protein content of bread wheat (Triticum aestivum L.). *Euphytica* 163(2):309–320.

Högy, P., H. Wieser, P. Köhler, K. Schwadorf, J. Breuer, J. Franzaring, R. Muntifering, and A. Fangmeier. 2009. Effects of elevated CO_2 on grain yield and quality of wheat: results from a 3-year free-air CO_2 enrichment experiment. *Plant Biology* 11(s1):60–69.

Hoogenboom, G., J. W. Jones, P. C. S. Traore, and K. J. Boote. 2012. Experiments and data for model evaluation and application. In *Improving Soil Fertility Recommendations in Africa using the Decision Support System for Agrotechnology Transfer (DSSAT)*, 9–18. J. Kihara, D. Fatondji, J. W. Jones, G. Hoogenboom, R. Tabo, and A. Bationo, eds. Dordrecht, the Netherlands: Springer.

Hoogenboom, G., J. W. Jones, P. W. Wilkens, C. H. Porter, K. J. Boote, L. A. Hunt, U. Singh, J. L. Lizaso, J. W. White, and O. Uryasev. 2015. *Decision Support System for Agrotechnology Transfer (DSSAT) Version 4.6. 1.0 (www. DSSAT. net)* DSSAT Foundation, Prosser, Washington, USA.

Hornbeck, R., and P. Keskin. 2014. The Historically Evolving Impact of the Ogallala Aquifer: Agricultural Adaptation to Groundwater and Drought. *American Economic Journal: Applied Economics* 6(1):190–219.

Howden, S. M., J.-F. Soussana, F. N. Tubiello, N. Chhetri, M. Dunlop, and H. Meinke. 2007. Adapting agriculture to climate change. *Proceedings of the National Academy of Sciences* 104(50):19691–19696.

Howell, T. A., S. R. Evett, J. A. Tolk, K. S. Copeland, P. D. Colaizzi, and P. H. Gowda. 2008. Evapotranspiration of corn and forage sorghum for silage. In *Environmental and Water Resources Institute World Congress*. Honolulu, Hawaii.

HPWD. 2015. Rules of the High Plains Underground Water Conservation District No. 1. http://www.hpwd.org/rules/ (accessed May 11, 2017).

Huang, B., and J. D. Fry. 1998. Root anatomical, physiological, and morphological responses to drought stress for tall fescue cultivars. *Crop Science* 38(4):1017–1022.

Hund, A., N. Ruta, and M. Liedgens. 2009. Rooting depth and water use efficiency of tropical maize inbred lines, differing in drought tolerance. *Plant and Soil* 318(1):311–325.

Hunt, L. A., J. W. White, and G. Hoogenboom. 2001. Agronomic data: advances in documentation and protocols for exchange and use. *Agricultural Systems* 70(2):477–492.

IPCC. 1992. The supplementary report to the IPCC scientific assessment. *Intergovernmental Panel on Cllmate Change, Cambrldge Univ Press, Cambridge*.

IPCC. 2014. Climate Change 2014: Synthesis Report. Contribution of Working Groups I, II and III to the Fifth Assessment Report of the Intergovernmental Panel on Climate Change [Core Writing Team, R.K. Pachauri and L.A. Meyer (eds.)]. IPCC, Geneva, Switzerland, 151 pp.

Iqbal, M., M. A. Khan, M. Naeem, U. Aziz, J. Afzal, and M. Latif. 2013. Inducing drought tolerance in upland cotton (Gossypium hirsutum L.), accomplishments and future prospects. *World Applied Sciences Journal* 21(7):1062–1069.

Izaurralde, R. C., N. J. Rosenberg, R. A. Brown, and A. M. Thomson. 2003. Integrated assessment of Hadley Center (HadCM2) climate-change impacts on agricultural productivity and irrigation water supply in the conterminous United States: Part II. Regional agricultural production in 2030 and 2095. *Agricultural and Forest Meteorology* 117(1):97–122.

Jain, S., S. Ale, C. L. Munster, R. J. Ansley, and J. R. Kiniry. 2015. Simulating the hydrologic impact of Arundo donax invasion on the headwaters of the Nueces river in Texas. *Hydrology* 2(3):134–147.

Jamieson, P. D., J. Berntsen, F. Ewert, B. A. Kimball, J. E. Olesen, P. J. Pinter, J. R. Porter, and M. A. Semenov. 2000. Modelling CO_2 effects on wheat with varying nitrogen supplies. *Agriculture, Ecosystems & Environment* 82(1):27–37.

Jamieson, P. D., J. R. Porter, and D. R. Wilson. 1991. A test of the computer simulation model ARCWHEAT1 on wheat crops grown in New Zealand. *Field Crops Research* 27(4):337–350.

Jiang, X., and Z. L. Yang. 2012. Projected changes of temperature and precipitation in Texas from downscaled global climate models. *Climate Research* 53(3):229–244.

Jones, J. W., G. Hoogenboom, C. H. Porter, K. J. Boote, W. D. Batchelor, L. A. Hunt, P. W. Wilkens, U. Singh, A. J. Gijsman, and J. T. Ritchie. 2003. The DSSAT cropping system model. *European Journal of Agronomy* 18(3–4):235–265.

Jordan, W., W. Dugas, and P. Shouse. 1983. Strategies for crop improvement for drought-prone regions. *Agricultural Water Management* 7(1–3):281–299.

Kapur, B., M. Aydın, T. Yano, M. Koç, and C. Barutçular. 2019. Interactive Effects of Elevated CO_2 and Climate Change on Wheat Production in the Mediterranean Region. In *Climate Change Impacts on Basin Agro-ecosystems*, 245–268. T. Watanabe, S. Kapur, M. Aydın, R. Kanber, and E. Akça, eds. Cham: Springer International Publishing.

Karimi, T., C. O. Stöckle, S. Higgins, and R. Nelson. 2018. Climate change and dryland wheat systems in the US Pacific Northwest. *Agricultural Systems* 159:144–156.

Keeling, C. D., R. B. Bacastow, A. E. Bainbridge, C. A. Ekdahl Jr, P. R. Guenther, L. S. Waterman, and J. F. Chin. 1976. Atmospheric carbon dioxide variations at Mauna Loa observatory, Hawaii. *Tellus* 28(6):538–551.

Kerns, D. L., C. G. Sansone, K. T. Siders, and B. A. Baugh. 2009. *Managing Cotton Insects in the High Plains, Rolling Plains and Trans Pecos Areas of Texas*. Texas AgriLife Extension Bull. E-6.

Kerr, A., J. Dialesandro, K. Steenwerth, N. Lopez-Brody, and E. Elias. 2018. Vulnerability of California specialty crops to projected mid-century temperature changes. *Climatic Change* 148(3):419–436.

Kimball, B., K. Kobayashi, and M. Bindi. 2002. Responses of agricultural crops to free-air CO_2 enrichment. *Advances in Agronomy* 77(2002):293–368.

Kimball, B. A., R. L. LaMorte, P. J. Pinter Jr., G. W. Wall, D. J. Hunsaker, F. J. Adamsen, S. W. Leavitt, T. L. Thompson, A. D. Matthias, and T. J. Brooks. 1999. Free-air CO_2 enrichment and soil nitrogen effects on energy balance and evapotranspiration of wheat. *Water Resources Research* 35(4):1179–1190.

Kiniry, J. R., and A. J. Bockholt. 1998. Maize and sorghum simulation in diverse Texas environments. *Agronomy Journal* 90(5):682–687.

Kirkevag, A., T. Iversen, O. Seland, J. B. Debernard, T. Storelvmo, and J. E. Kristjansson. 2008. Aerosol-cloud-climate interactions in the climate model CAM-Oslo. *Tellus A: Dynamic Meteorology and Oceanography* 60(3):492–512.

Kisekka, I., J. P. Aguilar, D. H. Rogers, J. Holman, D. M. O'Brien, and N. Klocke. 2016. Assessing deficit irrigation strategies for corn using simulation. *Transactions of the ASABE* 59(1):303–317.

Ko, J., G. Piccinni, T. Marek, and T. Howell. 2009a. Determination of growth-stage-specific crop coefficients (Kc) of cotton and wheat. *Agricultural Water Management* 96(12):1691–1697.

Ko, J., G. Piccinni, and E. Steglich. 2009b. Using EPIC model to manage irrigated cotton and maize. *Agricultural Water Management* 96(9):1323–1331.

Konzmann, M., D. Gerten, and J. Heinke. 2013. Climate impacts on global irrigation requirements under 19 GCMs, simulated with a vegetation and hydrology model. *Hydrological Sciences Journal* 58(1):88–105.

Kothari, K., S. Ale, J. P. Bordovsky, K. R. Thorp, D. O. Porter, and C. L. Munster. 2019. Simulation of efficient irrigation management strategies for grain sorghum production over different climate variability classes. *Agricultural Systems* 170:49–62.

Krupa, K., N. Dalawai, H. Shashidhar, and K. Harinikumar. 2017. Mechanisms of drought tolerance in sorghum: a review. *International Journal of Pure and Applied Bioscience* 5(4):221–237.

Leakey, A. D., M. Uribelarrea, E. A. Ainsworth, S. L. Naidu, A. Rogers, D. R. Ort, and S. P. Long. 2006. Photosynthesis, productivity, and yield of maize are not affected by open-air elevation of CO_2 concentration in the absence of drought. *Plant Physiology* 140(2):779–790.

Leff, B., N. Ramankutty, and J. A. Foley. 2004. Geographic distribution of major crops across the world. *Global Biogeochemical Cycles* 18(1).

Legates, D. R., and G. J. McCabe. 1999. Evaluating the use of "goodness-of-fit" measures in hydrologic and hydroclimatic model validation. *Water Resources Research* 35(1):233–241.

Levi, A., A. H. Paterson, V. Barak, D. Yakir, B. Wang, P. W. Chee, and Y. Saranga. 2009. Field evaluation of cotton near-isogenic lines introgressed with QTLs for productivity and drought related traits. *Molecular Breeding* 23(2):179–195.

Lewis, R. B., E. A. Hiler, and W. R. Jordan. 1974. Susceptibility of grain sorghum to water deficit at three growth stages. *Agronomy Journal* 66(4):589–591.

Li, Z., J. He, X. Xu, X. Jin, W. Huang, B. Clark, G. Yang, and Z. Li. 2018. Estimating genetic parameters of DSSAT-CERES model with the GLUE method for winter wheat (Triticum aestivum L.) production. *Computers and Electronics in Agriculture* 154:213–221.

Lilley, J. M., and J. A. Kirkegaard. 2016. Farming system context drives the value of deep wheat roots in semi-arid environments. *Journal of Experimental Botany* 67(12):3665–3681.

Liu, Z., Y.-L. Yuan, S.-Q. Liu, X.-N. Yu, and L.-Q. Rao. 2006. Screening for high-temperature tolerant cotton cultivars by testing in vitro pollen germination, pollen tube growth and boll retention. *Journal of Integrative Plant Biology* 48(6):706–714.

Lobell, D. B., and M. B. Burke. 2008. Why are agricultural impacts of climate change so uncertain? The importance of temperature relative to precipitation. *Environmental Research Letters* 3(3):034007.

Loison, R., A. Audebert, P. Debaeke, G. Hoogenboom, L. Leroux, P. Oumarou, and E. Gérardeaux. 2017. Designing cotton ideotypes for the future: Reducing risk of crop failure for low input rainfed conditions in Northern Cameroon. *European Journal of Agronomy* 90:162–173.

Lokhande, S., and K. R. Reddy. 2014. Quantifying temperature effects on cotton reproductive efficiency and fiber quality. *Agronomy Journal* 106(4):1275–1282.

Long, D., B. R. Scanlon, L. Longuevergne, A. Y. Sun, D. N. Fernando, and H. Save. 2013. GRACE satellite monitoring of large depletion in water storage in response to the 2011 drought in Texas. *Geophysical Research Letters* 40(13):3395–3401.

Lopes, M. S., C. Royo, F. Alvaro, M. Sanchez-Garcia, E. Ozer, F. Ozdemir, M. Karaman, M. Roustaii, M. R. Jalal-Kamali, and D. Pequeno. 2018. Optimizing winter wheat resilience to climate change in rainfed crop systems of Turkey and Iran. *Frontiers in Plant Science* 9(563).

Lopez, J. R., J. E. Erickson, S. Asseng, and E. L. Bobeda. 2017. Modification of the CERES grain sorghum model to simulate optimum sweet sorghum rooting depth for rainfed production on coarse textured soils in a sub-tropical environment. *Agricultural Water Management* 181:47–55.

Ludwig, F., and S. Asseng. 2006. Climate change impacts on wheat production in a Mediterranean environment in Western Australia. *Agricultural Systems* 90(1):159–179.

Ludwig, F., and S. Asseng. 2010. Potential benefits of early vigor and changes in phenology in wheat to adapt to warmer and drier climates. *Agricultural Systems* 103(3):127–136.

Luo, Q., W. Bellotti, M. Williams, and B. Bryan. 2005. Potential impact of climate change on wheat yield in South Australia. *Agricultural and Forest Meteorology* 132(3):273–285.

Mace, R. E., R. Petrossian, R. Bradley, W. Mullican, and L. Christian. 2008. *A Streetcar Named Desired Future Conditions: The New Groundwater Availability for Texas (Revised)*. Texas Water Development Board, Austin, TX.

Magalhães, P. C., T. C. de Souza, A. O. Lavinsky, P. E. P. de Albuquerque, L. L. de Oliveira, and E. M. de Castro. 2016. Phenotypic plasticity of root system and shoots of'Sorghum bicolor'under different soil water levels during pre-flowering stage. *Australian Journal of Crop Science* 10(1):81–87.

Maiorano, A., P. Martre, S. Asseng, F. Ewert, C. Müller, R. P. Rötter, A. C. Ruane, M. A. Semenov, D. Wallach, E. Wang, P. D. Alderman, B. T. Kassie, C. Biernath, B. Basso, D. Cammarano, A. J. Challinor, J. Doltra, B. Dumont, E. E. Rezaei, S. Gayler, K. C. Kersebaum, B. A. Kimball, A.-K. Koehler, B. Liu, G. J. O'Leary, J. E. Olesen, M. J. Ottman, E. Priesack, M. Reynolds, P. Stratonovitch, T. Streck, P. J. Thorburn, K. Waha, G. W. Wall, J. W. White, Z. Zhao, and Y. Zhu. 2017. Crop model improvement reduces the uncertainty of the response to temperature of multi-model ensembles. *Field Crops Research* 202:5–20.

Maiti, R. 1996. *Sorghum Science*. Science Publishers Inc., Lebanon, New Hampshire, USA.

Malla, G. 2008. Climate change and its impact on Nepalese agriculture. *Journal of Agriculture and Environment* 9:62–71.

Manschadi, A. M., J. Christopher, P. deVoil, and G. L. Hammer. 2006. The role of root architectural traits in adaptation of wheat to water-limited environments. *Functional Plant Biology* 33(9):823–837.

Marek, G. W., T. H. Marek, Q. Xue, P. H. Gowda, S. R. Evett, and D. K. Brauer. 2017. Simulating evapotranspiration and yield response of selected corn varieties under full and limited irrigation in the Texas High Plains using DSSAT-CERES-Maize. *Transactions of the ASABE* 60(3):837–846.

Marin, F. R., J. W. Jones, A. Singels, F. Royce, E. D. Assad, G. Q. Pellegrino, and F. Justino. 2013. Climate change impacts on sugarcane attainable yield in southern Brazil. *Climatic Change* 117(1):227–239.

Marsalis, M. A., R. P. Flynn, L. M. Lauriault, A. Mesbah, and M. K. O'Neill. 2015. *New Mexico 2015 Corn and Sorghum Performance Tests.* Agricultural Experiment Station, Cooperative Extension Service, College of Agricultural, Consumer and Environmental Sciences, New Mexico State University.

Mauney, J. R., B. A. Kimball, P. J. Pinter, R. L. LaMorte, K. F. Lewin, J. Nagy, and G. R. Hendrey. 1994. Growth and yield of cotton in response to a free-air carbon dioxide enrichment (FACE) environment. *Agricultural and Forest Meteorology* 70(1):49–67.

McClure, A., S. Ebelhar, C. Lee, E. Nafziger, and T. Wyciskalla. 2010. *High Plains Production Handbook*. United Sorghum Checkoff Program, Lubbock, Texas, USA.

Meehl, G. A., T. F. Stocker, W. D. Collins, P. Friedlingstein, T. Gaye, J. M. Gregory, A. Kitoh, R. Knutti, J. M. Murphy, and A. Noda. 2007. Global climate projections. In *Climate Change 2007: The Physical Science Basis. Contribution of Working Group I to the Fourth Assessment Report of the Intergovernmental Panel on Climate Change*, 505–546. D. Qin, Solomon S., M. Manning, M. Marquis, K. Averyt, M.M.B. Tignor, H.L. Miller Jr, and Z. Chen, eds. Cambridge: Cambridge University Press.

Messina, C., P.B. Ramkrishnan, J.W. Jones, K.J. Boote, G. Hoogenboom, and J.T. Ritchie. 2004. A simulation model of cotton growth and development for CSM. In *Proc. Biological Systems Simulation Group (BSSG) Conference* 54–55 pp.

Milroy, S. P., S. Asseng, and M. L. Poole. 2008. Systems analysis of wheat production on low water-holding soils in a Mediterranean-type environment: II. Drainage and nitrate leaching. *Field Crops Research* 107(3):211–220.

Mitchell, C. C., and J. A. Entry. 1998. Soil C, N and crop yields in Alabama's long-term 'Old Rotation' cotton experiment. *Soil and Tillage Research* 47(3–4):331–338.

Mitchell, R. A. C., V. J. Mitchell, S. P. Driscoll, J. Franklin, and D. W. Lawlor. 1993. Effects of increased CO_2 concentration and temperature on growth and yield of winter wheat at two levels of nitrogen application. *Plant, Cell & Environment* 16(5):521–529.

Modala, N. R., S. Ale, D. W. Goldberg, M. Olivares, C. L. Munster, N. Rajan, and R. A. Feagin. 2017. Climate change projections for the Texas High Plains and Rolling Plains. *Theoretical and Applied Climatology* 129(1):263–280.

Modala, N. R., S. Ale, N. Rajan, C. L. Munster, P. B. DeLaune, K. R. Thorp, S. S. Nair, and E. M. Barnes. 2015. Evaluation of the CSM-CROPGRO-Cotton model for the Texas rolling plains region and simulation of deficit irrigation strategies for increasing water use efficiency. *Transactions of the ASABE* 58(3):685–696.

Moriasi, D. N., J. G. Arnold, M. W. Van Liew, R. L. Bingner, R. D. Harmel, and T. L. Veith. 2007. Model evaluation guidelines for systematic quantification of accuracy in watershed simulations. *Transactions of the ASABE* 50(3):885–900.

Msongaleli, B., F. Rwehumbiza, S. D. Tumbo, and N. Kihupi. 2014. Sorghum yield response to changing climatic conditions in semi-arid central Tanzania: evaluating crop simulation model applicability. *Agricultural Sciences* 5(10):822–833.

Müller, C., and R. D. Robertson. 2013. Projecting future crop productivity for global economic modeling. *Agricultural Economics* 45(1):37–50.

Musgrove, M., and J. L. Banner. 2004. Controls on the spatial and temporal variability of vadose dripwater geochemistry: Edwards aquifer, central Texas11Associate editor: L. M. Walter. *Geochimica et Cosmochimica Acta* 68(5):1007–1020.

Musick, J., and D. Dusek. 1971. Grain sorghum response to number, timing, and size of irrigations in the Southern High Plains. *Transactions of the ASAE* 14(3):401–404.

Naab, J. B., K. J. Boote, J. W. Jones, and C. H. Porter. 2015. Adapting and evaluating the CROPGRO-peanut model for response to phosphorus on a sandy-loam soil under semi-arid tropical conditions. *Field Crops Research* 176:71–86.

Nash, J. E., and J. V. Sutcliffe. 1970. River flow forecasting through conceptual models part I — A discussion of principles. *Journal of Hydrology* 10(3):282–290.

NASS. 2012. Census of Agriculture, Ag Census Web Maps. www.agcensus.usda.gov/Publications/2012/Online_Resources/Ag_Census_Web_Maps/Overview/ (accessed April 18, 2017).

Neely, C., C. Trostle, and M. Welch. 2014. Wheat Freeze Injury in Texas. Texas A&M AgriLife Extension. https://agrilifecdn.tamu.edu/lubbock/files/2017/04/Wheat-Freeze-Injury-in-Texas-ESC-026-2014.pdf (accessed January 15, 2018).

Neitsch, S. L., J. G. Arnold, J. R. Kiniry, and J. R. Williams. 2011. *Soil and water assessment tool theoretical documentation version 2009*. College Station, Texas: Texas Water Resources Institute, 647 pp.

Nelson, J. R., R. J. Lascano, J. D. Booker, R. E. Zartman, and T. S. Goebel. 2013. Evaluation of the precision agricultural landscape modeling system (PALMS) in the semiarid Texas Southern High Plains. *Open Journal of Soil Science* 3(4):13.

Nielsen-Gammon, J. W. 2011. The changing climate of Texas. In *Impact of Global Warming on Texas*, 39–68. Austin, Texas: University of Texas Press.

NOAA. 2017. Daily Meteorological Data. National Oceanic and Atmospheric Administration. National Climatic Data Center. https://www.ncdc.noaa.gov (accessed March 11, 2017).

NOAA. 2018. National Centers for Environmental information, Climate at a Glance: Divisional Time Series. https://www.ncdc.noaa.gov/cag/ (accessed June 18, 2018)

Nouna, B. B., N. Katerji, and M. Mastrorilli. 2000. Using the CERES-Maize model in a semi-arid Mediterranean environment. Evaluation of model performance. *European Journal of Agronomy* 13(4):309–322.

Nouri, M., M. Homaee, M. Bannayan, and G. Hoogenboom. 2017. Towards shifting planting date as an adaptation practice for rainfed wheat response to climate change. *Agricultural Water Management* 186:108–119.

NRCS. 2019. Geospatial Data Gateway. United States Department of Agriculture, Natural Resources Conservation Service. https://datagateway.nrcs.usda.gov/GDGHome_DirectDownLoad.aspx (accessed January 15, 2019).

O'Leary, G. J., B. Christy, J. Nuttall, N. Huth, D. Cammarano, C. Stöckle, B. Basso, I. Shcherbak, G. Fitzgerald, Q. Luo, I. Farre-Codina, J. Palta, and S. Asseng. 2014. Response of wheat growth, grain yield and water use to elevated CO_2 under a Free-Air CO_2 Enrichment (FACE) experiment and modelling in a semi-arid environment. *Global Change Biology* 21(7):2670–2686.

O'Shaughnessy, S. A., S. R. Evett, P. D. Colaizzi, J. A. Tolk, and T. A. Howell. 2014. Early and late maturing grain sorghum under variable climatic conditions in the Texas High Plains. *Transactions of the ASABE* 57(6):1583–1594.

Olivera, F., M. Valenzuela, R. Srinivasan, J. Choi, H. Cho, S. Koka, and A. Agrawal. 2006. ARCGIS-SWAT: A geodata model and GIS interface for SWAT. *JAWRA Journal of the American Water Resources Association* 42(2):295–309.

Ortiz, B., G. Hoogenboom, G. Vellidis, K. Boote, R. Davis, and C. Perry. 2009. Adapting the CROPGRO-Cotton model to simulate cotton biomass and yield under southern root-knot nematode parasitism. *Transactions of the ASABE* 52(6):2129–2140.

Ottman, M. J., B. A. Kimball, P. J. Pinter, G. W. Wall, R. L. Vanderlip, S. W. Leavitt, R. L. LaMorte, A. D. Matthias, and T. J. Brooks. 2001. Elevated CO_2 increases sorghum biomass under drought conditions. *New Phytologist* 150(2):261–273.

Palazzoli, I., S. Maskey, S. Uhlenbrook, E. Nana, and D. Bocchiola. 2015. Impact of prospective climate change on water resources and crop yields in the Indrawati basin, Nepal. *Agricultural Systems* 133:143–157.

Palosuo, T., K. C. Kersebaum, C. Angulo, P. Hlavinka, M. Moriondo, J. E. Olesen, R. H. Patil, F. Ruget, C. Rumbaur, and J. Takáč. 2011. Simulation of winter wheat yield and its variability in different climates of Europe: a comparison of eight crop growth models. *European Journal of Agronomy* 35(3):103–114.

Parry, M. L., C. Rosenzweig, A. Iglesias, M. Livermore, and G. Fischer. 2004. Effects of climate change on global food production under SRES emissions and socio-economic scenarios. *Global Environmental Change* 14(1):53–67.

Pathak, T., C. Fraisse, J. Jones, C. Messina, and G. Hoogenboom. 2007. Use of global sensitivity analysis for CROPGRO cotton model development. *Transactions of the ASABE* 50(6):2295–2302.

Paulsen, G. M. 1987. Wheat stand establishment. In *Wheat and Wheat Improvement* (second edition), 384–389. E.G. Heyne, ed. Madison, USA: American Society of Agronomy.

Piccinni, G., J. Ko, T. Marek, and T. Howell. 2009. Determination of growth-stage-specific crop coefficients (KC) of maize and sorghum. *Agricultural Water Management* 96(12):1698–1704.

Pierret, A., J.-L. Maeght, C. Clément, J.-P. Montoroi, C. Hartmann, and S. Gonkhamdee. 2016. Understanding deep roots and their functions in ecosystems: an advocacy for more unconventional research. *Annals of Botany* 118(4):621–635.

Pinter, P. J., B. A. Kimball, G. W. Wall, R. L. LaMorte, D. J. Hunsaker, F. J. Adamsen, K. F. A. Frumau, H. F. Vugts, G. R. Hendrey, K. F. Lewin, J. Nagy, H. B. Johnson, F. Wechsung, S. W. Leavitt, T. L. Thompson, A. D. Matthias, and T. J. Brooks. 2000. Free-air CO_2 enrichment (FACE): blower effects on wheat canopy microclimate and plant development. *Agricultural and Forest Meteorology* 103(4):319–333.

Polania, J., C. Poschenrieder, I. Rao, and S. Beebe. 2017. Root traits and their potential links to plant ideotypes to improve drought resistance in common bean. *Theoretical and Experimental Plant Physiology* 29(3):143–154.

Porter, D., T. Marek, T. Howell, and L. New. 2005. *The Texas High Plains Evapotranspiration Network (TXHPET) User Manual. Publ. AREC 05–37*. Amarillo, TX: Texas Agricultural Experiment Station.

Porter, K., M. Jensen, and W. Sletten. 1960. The effect of row spacing, fertilizer and planting rate on the yield and water use of irrigated grain sorghum. *Agronomy Journal* 52(8):431–434.

Prasad, P. V., K. J. Boote, and L. H. Allen Jr. 2006. Adverse high temperature effects on pollen viability, seed-set, seed yield and harvest index of grain-sorghum [Sorghum bicolor (L.) Moench] are more severe at elevated carbon dioxide due to higher tissue temperatures. *Agricultural and Forest Meteorology* 139(3–4):237–251.

Prasad, P. V. V., S. R. Pisipati, R. N. Mutava, and M. R. Tuinstra. 2008. Sensitivity of grain sorghum to high temperature stress during reproductive development. *Crop Science* 48(5):1911–1917.

Prior, S. A., H. A. Torbert, G. B. Runion, and H. H. Rogers. 2003. Implications of elevated CO_2-induced changes in agroecosystem productivity. *Journal of Crop Production* 8(1/2):217–244.

Procopio, A. S., P. Artaxo, Y. J. Kaufman, L. A. Remer, J. S. Schafer, and B. N. Holben. 2004. Multiyear analysis of amazonian biomass burning smoke radiative forcing of climate. *Geophysical Research Letters* 31(3).

Rahman, M. H. u., A. Ahmad, X. Wang, A. Wajid, W. Nasim, M. Hussain, B. Ahmad, I. Ahmad, Z. Ali, W. Ishaque, M. Awais, V. Shelia, S. Ahmad, S. Fahd, M. Alam, H. Ullah, and G. Hoogenboom. 2018. Multi-model projections of future climate and climate change impacts uncertainty assessment for cotton production in Pakistan. *Agricultural and Forest Meteorology* 253–254:94–113.

Reddy, K. R., G. H. Davidonis, A. S. Johnson, and B. T. Vinyard. 1999. Temperature regime and carbon dioxide enrichment alter cotton boll development and fiber properties. *Agronomy Journal* 91(5):851–858.

Reddy, K. R., H. F. Hodges, and J. M. McKinion. 1995. Carbon dioxide and temperature effects on pima cotton growth. *Agriculture, Ecosystems & Environment* 54(1):17–29.

Riahi, K., S. Rao, V. Krey, C. Cho, V. Chirkov, G. Fischer, G. Kindermann, N. Nakicenovic, and P. Rafaj. 2011. RCP 8.5—A scenario of comparatively high greenhouse gas emissions. *Climatic Change* 109(1):33.

Riaz, M., J. Farooq, G. Sakhawat, A. Mahmood, M. Sadiq, and M. Yaseen. 2013. Genotypic variability for root/shoot parameters under water stress in some advanced lines of cotton (Gossypium hirsutum L.). *Genetics and Molecular Research* 12(1):552–561.

Ritchie, J., and S. Otter. 1984. CERES-Wheat: A user oriented wheat yield model. Preliminary documentation. United States Department of Agriculture. *Agricultural Research Service, ARS* 38:159–175.

Ritchie, J. T., U. Singh, D. C. Godwin, and W. T. Bowen. 1998. Cereal growth, development and yield. In *Understanding Options for Agricultural Production*, 79–98. G. Y. Tsuji, G. Hoogenboom, and P. K. Thornton, eds. Dordrecht, the Netherlands: Springer.

Rooney, W. L., J. Blumenthal, B. Bean, and J. E. Mullet. 2007. Designing sorghum as a dedicated bioenergy feedstock. *Biofuels, Bioproducts and Biorefining* 1(2):147–157.

Rosenzweig, C., A. Iglesias, X. B. Yang, P. R. Epstein, and E. Chivian. 2001. Climate change and extreme weather events; implications for food production, plant diseases, and pests. *Global Change and Human Health* 2(2):90–104.

Rosenzweig, C., J. W. Jones, J. L. Hatfield, A. C. Ruane, K. J. Boote, P. Thorburn, J. M. Antle, G. C. Nelson, C. Porter, S. Janssen, S. Asseng, B. Basso, F. Ewert, D. Wallach, G. Baigorria, and J. M. Winter. 2013. The Agricultural Model Intercomparison and Improvement Project (AgMIP): Protocols and pilot studies. *Agricultural and Forest Meteorology* 170:166–182.

Rosenzweig, C., and M. L. Parry. 1994. Potential impact of climate change on world food supply. *Nature* 367:133–138.

Rotstayn, L. D., S. J. Jeffrey, M. A. Collier, S. M. Dravitzki, A. C. Hirst, J. I. Syktus, and K. K. Wong. 2012. Aerosol- and greenhouse gas-induced changes in summer rainfall and circulation in the Australasian region: a study using single-forcing climate simulations. *Atmospheric Chemistry and Physics* 12(14):6377–6404.

Ruane, A. C., R. Goldberg, and J. Chryssanthacopoulos. 2015a. Climate forcing datasets for agricultural modeling: Merged products for gap-filling and historical climate series estimation. *Agricultural and Forest Meteorology* 200:233–248.

Ruane, A. C., J. M. Winter, S. P. McDermid, and N. I. Hudson. 2015b. AgMIP climate data and scenarios for integrated assessment. *Journal of Climate Change and Agroecosystems* 3(1):45–78.

Sau, F., K. J. Boote, W. M. Bostick, J. W. Jones, and M. I. Mínguez. 2004. Testing and improving evapotranspiration and soil water balance of the DSSAT crop models. *Agronomy Journal* 96(5):1243–1257.

Scanlon, B. R., C. C. Faunt, L. Longuevergne, R. C. Reedy, W. M. Alley, V. L. McGuire, and P. B. McMahon. 2012. Groundwater depletion and sustainability of irrigation in the US High Plains and Central Valley. *Proceedings of the National Academy of Sciences* 109(24):9320–9325.

Schaible, G. D., B. A. McCarl, and R. D. Lacewell. 1999. The Edwards Aquifer water resource conflict: USDA farm program resource-use incentives? *Water Resources Research* 35(10):3171–3183.

Schneider, A., and T. Howell. 2000. Surface runoff due to LEPA and spray irrigation of a slowly permeable soil. *Transactions of the ASAE* 43(5):1089.

Schneider, A., and T. Howell. 2001. Scheduling deficit wheat irrigation with data from an evapotranspiration network. *Transactions of the ASAE* 44(6):1617.

Schnell, R., D. Pietsch, K. Horn, J. Moreno, W. L. Rooney, and G. Peterson. 2015. *Grain Sorghum Performance Tests in Texas, SCS-2016-05.* Lubbock, TX: Texas A&M AgriLife Research.

Schober, T. J., M. Messerschmidt, S. R. Bean, S. H. Park, and E. K. Arendt. 2005. Gluten-free bread from sorghum: quality differences among hybrids. *Cereal Chemistry* 82(4):394–404.

Segarra, E., J. W. Keeling, and J. R. Abernathy. 1991. Tillage and cropping system effects on cotton yield and profitability on the Texas southern high plains. *Journal of Production Agriculture* 4(4):566–571.

Semenov, M. A., and P. Stratonovitch. 2015. Adapting wheat ideotypes for climate change: accounting for uncertainties in CMIP5 climate projections. *Climate Research* 65:123–139.

Semenov, M. A., P. Stratonovitch, F. Alghabari, and M. J. Gooding. 2014. Adapting wheat in Europe for climate change. *Journal of Cereal Science* 59(3):245–256.

Senapati, N., P. Stratonovitch, M. J. Paul, and M. A. Semenov. 2018. Drought tolerance during reproductive development is important for increasing wheat yield potential under climate change in Europe. *Journal of Experimental Botany*:226–226.

Sharma, B., C. I. Mills, C. Snowden, and G. L. Ritchie. 2015. Contribution of boll mass and boll number to irrigated cotton yield. *Agronomy Journal* 107(5):1845–1853.

Sims, D. W., D. A. Ferrill, D. J. Waiting, A. P. Morris, N. M. Franklin, and A. L. Schultz. 2004. Structural framework of the Edwards Aquifer recharge zone in south-central Texas. *GSA Bulletin* 116(3–4):407–418.

Sinclair, T. R., and R. C. Muchow. 2001. System analysis of plant traits to increase grain uield on limited water supplies. *Agronomy Journal* 93(2):263–270.

Singh, P., S. Nedumaran, K. J. Boote, P. M. Gaur, K. Srinivas, and M. C. S. Bantilan. 2014a. Climate change impacts and potential benefits of drought and heat tolerance in chickpea in South Asia and East Africa. *European Journal of Agronomy* 52:123–137.

Singh, P., S. Nedumaran, B. R. Ntare, K. J. Boote, N. P. Singh, K. Srinivas, and M. C. S. Bantilan. 2014b. Potential benefits of drought and heat tolerance in groundnut for adaptation to climate change in India and West Africa. *Mitigation and Adaptation Strategies for Global Change* 19(5):509–529.

Singh, P., S. Nedumaran, P. Traore, K. Boote, H. Rattunde, P. V. Prasad, N. Singh, K. Srinivas, and M. Bantilan. 2014c. Quantifying potential benefits of drought and heat

tolerance in rainy season sorghum for adapting to climate change. *Agricultural and Forest Meteorology* 185:37–48.

Singh, R. P., P. V. V. Prasad, K. Sunita, S. N. Giri, and K. R. Reddy. 2007. Influence of high temperature and breeding for heat tolerance in cotton: a review. In *Advances in Agronomy* 93:313–385.

Singh, V., C. T. Nguyen, G. McLean, S. C. Chapman, B. Zheng, E. J. van Oosterom, and G. L. Hammer. 2017. Quantifying high temperature risks and their potential effects on sorghum production in Australia. *Field Crops Research* 211:77–88.

Singh, V., C. T. Nguyen, E. J. van Oosterom, S. C. Chapman, D. R. Jordan, and G. L. Hammer. 2015. Sorghum genotypes differ in high temperature responses for seed set. *Field Crops Research* 171:32–40.

Slade Jr, R. M., M. E. Dorsey, and S. L. Stewart. 1986. *Hydrology and water quality of the Edwards Aquifer associated with Barton Springs in the Austin area, Texas (No. 86-4036)*. Austin, TX: US Geological Survey. https://doi.org/10.3133/wri864036

Snowden, M. C., G. L. Ritchie, F. R. Simao, and J. P. Bordovsky. 2014. Timing of episodic drought can be critical in cotton. *Agronomy Journal* 106(2):452–458.

Soler, C. T., V. Bado, K. Traore, W. M. Bostick, J. Jones, and G. Hoogenboom. 2011. Soil organic carbon dynamics and crop yield for different crop rotations in a degraded ferruginous tropical soil in a semi-arid region: a simulation approach. *The Journal of Agricultural Science* 149(5):579–593.

Speed, T. R., R. Sheetz, and D. Shoemaker. 2008. DP 104 B2RF - A new early maturity variety for the Texas High Plains. In *Proceedings of Beltwide Cotton Conferences*. Nashville, Tennesse, USA, January 8–11, 2008.

Srinivasan, R., X. Zhang, and J. Arnold. 2010. SWAT ungauged: hydrological budget and crop yield predictions in the upper mississippi river basin. *Transactions of the ASABE* 53(5):1533–46.

Srivastava, A., S. Naresh Kumar, and P. K. Aggarwal. 2010. Assessment on vulnerability of sorghum to climate change in India. *Agriculture, Ecosystems & Environment* 138(3–4):160–169.

Stackhouse, P. 2006. Prediction of worldwide energy resources. Hampton, Virginia: NASA Langley Research Center. http://power.larc.nasa.gov (accessed January 15, 2017).

Stamm, J. F., M. F. Poteet, A. J. Symstad, M. Musgrove, A. J. Long, B. J. Mahler, and P. A. Norton. 2014. Historical and projected climate (1901–2050) and hydrologic response

of karst aquifers, and species vulnerability in south-central Texas and western South Dakota. Reston, Virginia: US Geological Survey. https://doi.org/10.3133/sir20145089

Stöckle, C. O., S. Higgins, R. Nelson, J. Abatzoglou, D. Huggins, W. Pan, T. Karimi, J. Antle, S. D. Eigenbrode, and E. Brooks. 2018. Evaluating opportunities for an increased role of winter crops as adaptation to climate change in dryland cropping systems of the U.S. Inland Pacific Northwest. *Climatic Change* 146(1):247–261.

Stratonovitch, P., and M. A. Semenov. 2015. Heat tolerance around flowering in wheat identified as a key trait for increased yield potential in Europe under climate change. *Journal of Experimental Botany* 66(12):3599–3609.

Sullivan, T. P., and Y. Gao. 2016. Assessment of nitrogen inputs and yields in the Cibolo and Dry Comal Creek watersheds using the SWAT model, Texas, USA 1996–2010. *Environmental Earth Sciences* 75(9):725.

Sultan, B., P. Roudier, P. Quirion, A. Alhassane, B. Muller, M. Dingkuhn, P. Ciais, M. Guimberteau, S. Traore, and C. Baron. 2013. Assessing climate change impacts on sorghum and millet yields in the Sudanian and Sahelian savannas of West Africa. *Environmental Research Letters* 8(1):014040.

Sun, C., and L. Ren. 2014. Assessing crop yield and crop water productivity and optimizing irrigation scheduling of winter wheat and summer maize in the Haihe plain using SWAT model. *Hydrological Processes* 28(4):2478–2498.

Susan, A. O. S., R. E. Steven, D. C. Paul, A. T. Judy, and A. H. Terry. 2014. Early and late maturing grain sorghum under variable climatic conditions in the Texas High Plains. 57(6):1583–1594.

SWAS-Arcadis. 2014. Mitchell Lake Hydologic and Hydraulic Analysis. https://www.saws.org/environment/MitchellLake/treatment.cfm (accessed February 10, 2019).

SWAS-Merrick. 2015. Mitchell Lake Dam Conceptual Design. https://www.saws.org/environment/MitchellLake/treatment.cfm (accessed February 10, 2019).

Sweeten, J. M., and W. R. Jordan. 1987. Irrigation water management for the Texas High Plains: A research summary. Texas Water Resources Institue, TR-139. http://hdl.handle.net/1969.1/6189

TALR. 2014. Three year summary (2012–2014) grain sorghum performance test, Perryton, Texas. Lubbock, TX: Texas A&M AgriLife Research.

TALR. 2016. Texas A&M AgriLife Research, Helms Farm Research Reports. Available at: https://lubbock.tamu.edu/programs/disciplines/irrigation-water/helms-farm-research-reports/ (accessed September 15, 2016).

Tan, K., G. Zhou, X. Lv, J. Guo, and S. Ren. 2018. Combined effects of elevated temperature and CO_2 enhance threat from low temperature hazard to winter wheat growth in North China. *Scientific Reports* 8(1):4336–4336.

Tang, X., N. Song, Z. Chen, J. Wang, and J. He. 2018. Estimating the potential yield and ETc of winter wheat across Huang-Huai-Hai Plain in the future with the modified DSSAT model. *Scientific Reports* 8(1):15370.

Tardieu, F., X. Draye, and M. Javaux. 2017. Root water uptake and ideotypes of the root system: whole-plant controls matter. *Vadose Zone Journal* 16(9).

Taylor, K. E., R. J. Stouffer, and G. A. Meehl. 2012. An overview of CMIP5 and the experiment design. *Bulletin of the American Meteorological Society* 93(4):485–498.

Tesfaye, K., G. Kruseman, J. E. Cairns, M. Zaman-Allah, D. Wegary, P. H. Zaidi, K. J. Boote, D. Rahut, and O. Erenstein. 2018. Potential benefits of drought and heat tolerance for adapting maize to climate change in tropical environments. *Climate Risk Management* 19:106–119.

Thaler, S., J. Eitzinger, M. Trnka, and M. Dubrovsky. 2012. Impacts of climate change and alternative adaptation options on winter wheat yield and water productivity in a dry climate in Central Europe. *The Journal of Agricultural Science* 150(5):537–555.

Thomson, A. M., K. V. Calvin, S. J. Smith, G. P. Kyle, A. Volke, P. Patel, S. Delgado-Arias, B. Bond-Lamberty, M. A. Wise, L. E. Clarke, and J. A. Edmonds. 2011. RCP4.5: a pathway for stabilization of radiative forcing by 2100. *Climatic Change* 109(1):77.

Thoning, K. W., P. P. Tans, and W. D. Komhyr. 1989. Atmospheric carbon dioxide at Mauna Loa Observatory: 2. Analysis of the NOAA GMCC data, 1974–1985. *Journal of Geophysical Research: Atmospheres* 94(D6):8549–8565.

Thornton, P. K., and G. Hoogenboom. 1994. A computer program to analyze single-season crop model outputs. *Agronomy Journal* 86(5):860–868.

Thornton, P. K., G. Hoogenboom, P. W. Wilkens, and W. T. Bowen. 1995. A computer program to analyze multiple-season crop model outputs. *Agronomy Journal* 87(1):131–136.

Thorp, K. R., E. M. Barnes, D. J. Hunsaker, B. A. Kimball, J. W. White, V. J. Nazareth, and G. Hoogenboom. 2014. Evaluation of CSM-CROPGRO-Cotton for simulating

effects of management and climate change on cotton growth and evapotranspiration in an arid environment. *Transactions of the ASABE* 57(6):1627–1642.

Thorp, K. R., D. J. Hunsaker, A. N. French, J. W. White, T. R. Clarke, and P. J. Pinter Jr. 2010. Evaluation of the CSM-CROPSIM-CERES-Wheat model as a tool for crop water management. *Transactions of the ASABE* 53(1):87–102.

Thorup-Kristensen, K., M. Salmerón Cortasa, and R. Loges. 2009. Winter wheat roots grow twice as deep as spring wheat roots, is this important for N uptake and N leaching losses? *Plant and Soil* 322(1):101–114.

Timsina, J., D. Godwin, E. Humphreys, S. Kukal, and D. Smith. 2008. Evaluation of options for increasing yield and water productivity of wheat in Punjab, India using the DSSAT-CSM-CERES-Wheat model. *Agricultural Water Management* 95(9):1099–1110.

Timsina, J., and E. Humphreys. 2006. Performance of CERES-Rice and CERES-Wheat models in rice–wheat systems: A review. *Agricultural Systems* 90(1):5–31.

Tolk, J. A., and T. A. Howell. 2003. Water use efficiencies of grain sorghum grown in three USA southern Great Plains soils. *Agricultural Water Management* 59(2):97–111.

Tolk, J. A., T. A. Howell, J. L. Steiner, and S. R. Evett. 1997. Grain sorghum growth, water use, and yield in contrasting soils. *Agricultural Water Management* 35(1):29–42.

Tremallo, R., S. Johnson, J. Hamilton, J. Winterle, S. Eason, and J. Hernandez. 2015. *Edwards Aquifer Authority Hydrogeologic Data Report for 2014. Report 15-01*. San Antonio, Texas: Edwards Aquifer Authority, 86 pp.

Triggs, J. M., B. A. Kimball, P. J. Pinter, G. W. Wall, M. M. Conley, T. J. Brooks, R. L. LaMorte, N. R. Adam, M. J. Ottman, A. D. Matthias, S. W. Leavitt, and R. S. Cerveny. 2004. Free-air CO_2 enrichment effects on the energy balance and evapotranspiration of sorghum. *Agricultural and Forest Meteorology* 124(1):63–79.

Tsuji, W., S. Inanaga, H. Araki, S. Morita, P. An, and K. Sonobe. 2005. Development and distribution of root system in two grain sorghum cultivars originated from Sudan under drought stress. *Plant Production Science* 8(5):553–562.

Tsvetsinskaya, E., L. Mearns, T. Mavromatis, W. Gao, L. McDaniel, and M. Downton. 2003. The effect of spatial scale of climatic change scenarios on simulated maize, winter wheat, and rice production in the southeastern United States. *Climatic Change* 60:37–72.

Tubiello, F., C. Rosenzweig, R. Goldberg, S. Jagtap, and J. Jones. 2002. Effects of climate change on US crop production: simulation results using two different GCM scenarios. Part I: Wheat, potato, maize, and citrus. *Climate Research* 20(3):259–270.

Tubiello, F. N., M. Donatelli, C. Rosenzweig, and C. O. Stockle. 2000. Effects of climate change and elevated CO_2 on cropping systems: model predictions at two Italian locations. *European Journal of Agronomy* 13(2):179–189.

Tubiello, F. N., and F. Ewert. 2002. Simulating the effects of elevated CO_2 on crops: approaches and applications for climate change. *European Journal of Agronomy* 18(1):57–74.

TWDB. 2012. Water for Texas—2012 State Water Plan. http://www.twdb.texas.gov/publications/state_water_plan/2012/2012_SWP.pdf (accessed March 22, 2019).

Ullah, A., I. Ahmad, A. Ahmad, T. Khaliq, U. Saeed, M. Habib-ur-Rahman, J. Hussain, S. Ullah, and G. Hoogenboom. 2019. Assessing climate change impacts on pearl millet under arid and semi-arid environments using CSM-CERES-Millet model. *Environmental Science and Pollution Research* 26(7):6745–6757.

Ullah, A., H. Sun, X. Yang, and X. Zhang. 2017. Drought coping strategies in cotton: increased crop per drop. *Plant Biotechnology Journal* 15(3):271–284.

Unger, P. W. 1978. Straw-mulch rate effect on soil water storage and sorghum yield I. *Soil Science Society of America Journal* 42(3):486–491.

Unger, P. W. 1991. Organic matter, nutrient, and pH distribution in no- and conventional-tillage semiarid soils. *Agronomy Journal* 83(1):186–189.

Unger, P. W., and R. L. Baumhardt. 1999. Factors related to dryland grain sorghum yield increases: 1939 through 1997. *Agronomy Journal* 91(5):870–875.

Uryasev, O., A. J. Gijsman, J. W. Jones, and G. Hoogenboom. 2004. DSSAT v4 soil data editing program (SBuild). In *Decision Support System for Agrotechnology Transfer Version 4.0*, 1–14. Honolulu, Hawaii, USA: University of Hawaii.

USDA-NASS. 2012. The yield forecastiing program of NASS. Staff Report Number SMB 12-01 https://www.nass.usda.gov/Education_and_Outreach/Understanding_Statistics/Yield_Forecasting_Program.pdf (accessed January 22, 2019).

USDA-NASS. 2018. Quick Stats-Crops https://quickstats.nass.usda.gov/ (accessed October 28, 2018).

USDA. 1993. State Soil Geographic Data Base (STATSGO)-Data Users Guide. 100.

Vadez, V. 2014. Root hydraulics: the forgotten side of roots in drought adaptation. *Field Crops Research* 165:15–24.

Vadez, V., L. Krishnamurthy, C. T. Hash, H. D. Upadhyaya, and A. K. Borrell. 2011. Yield, transpiration efficiency, and water-use variations and their interrelationships in the sorghum reference collection. *Crop and Pasture Science* 62(8):645–655.

Van Vuuren, D. P., J. Edmonds, M. Kainuma, K. Riahi, A. Thomson, K. Hibbard, G. C. Hurtt, T. Kram, V. Krey, and J.-F. Lamarque. 2011. The representative concentration pathways: an overview. *Climatic Change* 109(1–2):5.

Venkataraman, K., S. Tummuri, A. Medina, and J. Perry. 2016. 21st century drought outlook for major climate divisions of Texas based on CMIP5 multimodel ensemble: Implications for water resource management. *Journal of Hydrology* 534:300–316.

Voldoire, A., E. Sanchez-Gomez, D. Salas y Mélia, B. Decharme, C. Cassou, S. Sénési, S. Valcke, I. Beau, A. Alias, M. Chevallier, M. Déqué, J. Deshayes, H. Douville, E. Fernandez, G. Madec, E. Maisonnave, M. P. Moine, S. Planton, D. Saint-Martin, S. Szopa, S. Tyteca, R. Alkama, S. Belamari, A. Braun, L. Coquart, and F. Chauvin. 2013. The CNRM-CM5.1 global climate model: description and basic evaluation. *Climate Dynamics* 40(9):2091–2121.

W. Marek, G., P. H. Gowda, S. R. Evett, R. Louis Baumhardt, D. K. Brauer, T. A. Howell, T. H. Marek, and R. Srinivasan. 2016. Calibration and validation of the SWAT Model for predicting daily ET over irrigated crops in the Texas High Plains using lysimetric data. *Transactions of the ASABE* 59(2):611–622.

Wall, G. W., N. R. Adam, T. J. Brooks, B. A. Kimball, P. J. Pinter, R. L. LaMorte, F. J. Adamsen, D. J. Hunsaker, G. Wechsung, F. Wechsung, S. Grossman-Clarke, S. W. Leavitt, A. D. Matthias, and A. N. Webber. 2000. Acclimation response of spring wheat in a free-air CO_2 enrichment (FACE) atmosphere with variable soil nitrogen regimes. 2. Net assimilation and stomatal conductance of leaves. *Photosynthesis Research* 66(1):79–95.

Wall, G. W., T. J. Brooks, N. R. Adam, A. B. Cousins, B. A. Kimball, P. J. Pinter, R. L. LaMorte, J. Triggs, M. J. Ottman, S. W. Leavitt, A. D. Matthias, D. G. Williams, and A. N. Webber. 2001. Elevated atmospheric CO_2 improved Sorghum plant water status by ameliorating the adverse effects of drought. *New Phytologist* 152(2):231–248.

Wang, B., P. Feng, C. Chen, D. L. Liu, C. Waters, and Q. Yu. 2019. Designing wheat ideotypes to cope with future changing climate in South-Eastern Australia. *Agricultural Systems* 170:9–18.

Wang, B., D. L. Liu, G. J. O'Leary, S. Asseng, I. Macadam, R. Lines-Kelly, X. Yang, A. Clark, J. Crean, T. Sides, H. Xing, C. Mi, and Q. Yu. 2017. Australian wheat production expected to decrease by the late 21st century. *Global Change Biology* 24(6):2403–2415.

Wang, R., L. C. Bowling, and K. A. Cherkauer. 2016. Estimation of the effects of climate variability on crop yield in the Midwest USA. *Agricultural and Forest Meteorology* 216:141–156.

Wang, W. W. 2012. Three essays on climate change impacts, adaptation and mitigation in agriculture. Doctoral Dissertation. Texas A&M University, College Station, TX. http://hdl.handle.net/1969.1/ETD-TAMU-2012-08-11485 (accessed May 1, 2018)

Watanabe, M., T. Suzuki, R. O'ishi, Y. Komuro, S. Watanabe, S. Emori, T. Takemura, M. Chikira, T. Ogura, and M. Sekiguchi. 2010. Improved climate simulation by MIROC5: mean states, variability, and climate sensitivity. *Journal of Climate* 23(23):6312–6335.

Weinheimer, J., P. Johnson, D. Mitchell, J. Johnson, and R. Kellison. 2013. Texas High Plains initiative for strategic and innovative irrigation management and conservation. *Journal of Contemporary Water Research & Education* 151(1):43–49.

Welch, B. L. 1938. The significance of the difference between two means when the population variances are unequal. *Biometrika* 29(3/4):350–362.

Wheeler, T., and J. von Braun. 2013. Climate change impacts on global food security. *Science* 341(6145):508.

White, J., G. Alagarswamy, M. J. Ottman, C. Porter, U. Singh, and G. Hoogenboom. 2015. An overview of CERES–sorghum as implemented in the cropping system model version 4.5. *Agronomy Journal* 107(6):1987–2002.

White, J. W., M. Herndl, L. A. Hunt, T. S. Payne, and G. Hoogenboom. 2008. Simulation-based analysis of effects of vrn and ppd loci on flowering in wheat. *Crop Science* 48:678–687.

Willmott, C. J. 1981. On the validation of models. *Physical Geography* 2(2):184–194.

Woznicki, S. A., A. P. Nejadhashemi, and M. Parsinejad. 2015. Climate change and irrigation demand: Uncertainty and adaptation. *Journal of Hydrology: Regional Studies* 3:247–264.

Wu, T. 2012. A mass-flux cumulus parameterization scheme for large-scale models: Description and test with observations. *Climate Dynamics* 38(3–4):725–744.

Xiao, D., H. Bai, and L. D. Liu. 2018. Impact of future climate change on wheat production: a simulated case for China's wheat system. *Sustainability* 10(4):1277.

Xue, Q., Z. Zhu, J. T. Musick, B. Stewart, and D. A. Dusek. 2006. Physiological mechanisms contributing to the increased water-use efficiency in winter wheat under deficit irrigation. *Journal of Plant Physiology* 163(2):154–164.

Xue, Q., Z. Zhu, J. T. Musick, B. A. Stewart, and D. A. Dusek. 2003. Root growth and water uptake in winter wheat under deficit irrigation. *Plant and Soil* 257(1):151–161.

Yadav, S., N. J. Lakshmi, M. Maheswari, M. Vanaja, and B. Venkateswarlu. 2005. Influence of water deficit at vegetative, anthesis and grain filling stages on water relation and grain yield in sorghum. *Indian Journal of Plant Physiology* 10(1):20.

Yang, M., W. Xiao, Y. Zhao, X. Li, Y. Huang, F. Lu, B. Hou, and B. Li. 2018. Assessment of potential climate change effects on the rice yield and water footprint in the Nanliujiang Catchment, China. *Sustainability* 10(2):242.

Yang, X., Z. Tian, L. Sun, B. Chen, F. N. Tubiello, and Y. Xu. 2017. The impacts of increased heat stress events on wheat yield under climate change in China. *Climatic Change* 140(3):605–620.

Yukimoto, S., Y. Adachi, M. Hosaka, T. Sakami, H. Yoshimura, M. Hirabara, T. Y. Tanaka, E. Shindo, H. Tsujino, M. Deushi, R. Mizuta, S. Yabu, A. Obata, H. Nakano, T. Koshiro, T. Ose, and A. Kitoh. 2012. A new global climate model of the Meteorological Research Institute: MRI-CGCM3—model description and basic performance—. *Journal of the Meteorological Society of Japan. Ser. II* 90A:23–64.

Zadoks, J. C., T. T. Chang, and C. F. Konzak. 1974. A decimal code for the growth stages of cereals. *Weed Research* 14(6):415–421.

Zhang, H., E. J. Mu, and A. B. McCarl. 2017. Adaption to climate change through fallow rotation in the U.S. Pacific Northwest. *Climate* 5(3):64.

APPENDIX A

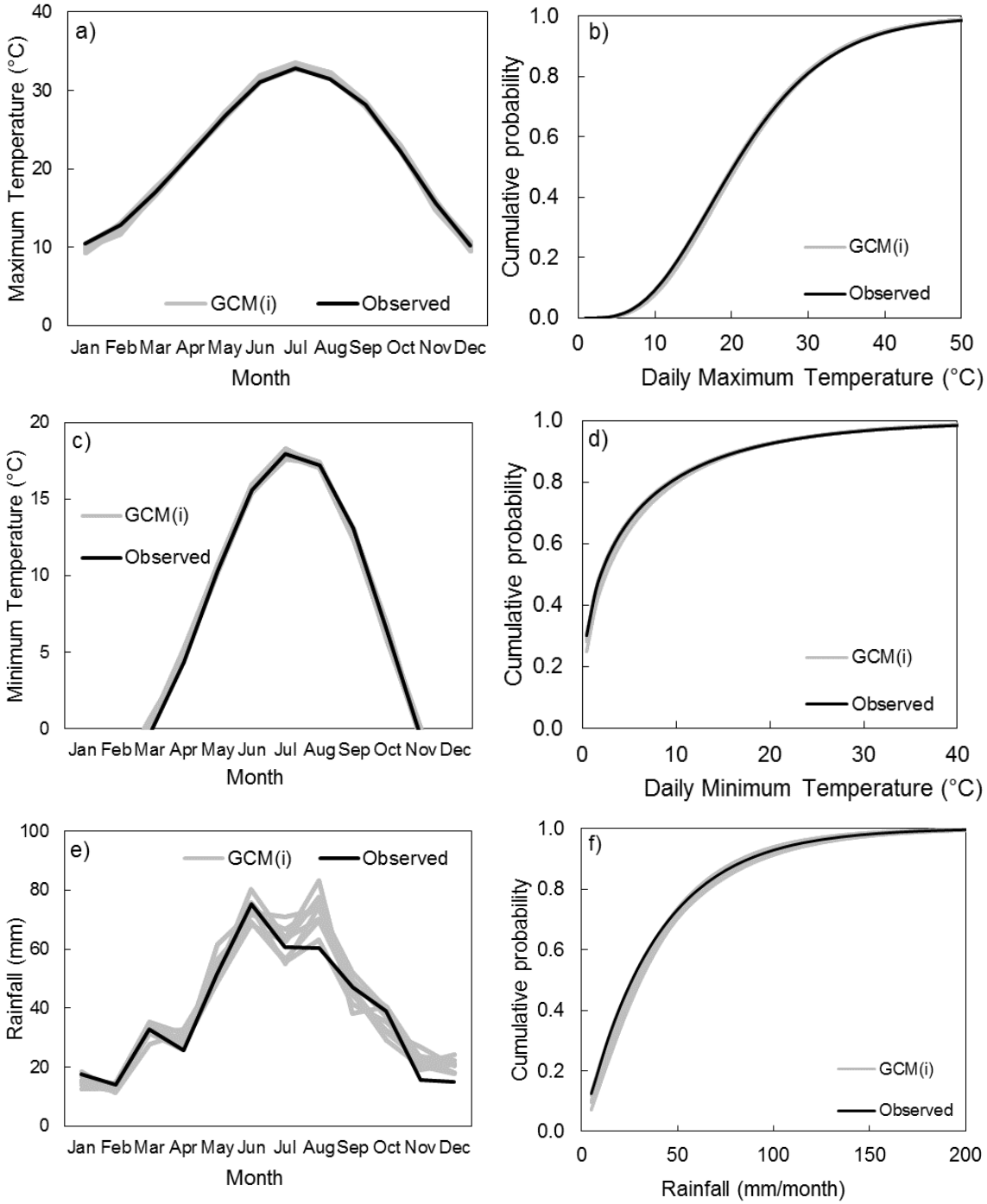

A.1 Comparison of observed weather data (Porter et al., 2005) and GCM projected data (Abatzoglou, 2013) for Bushland for 1980–2005 period.

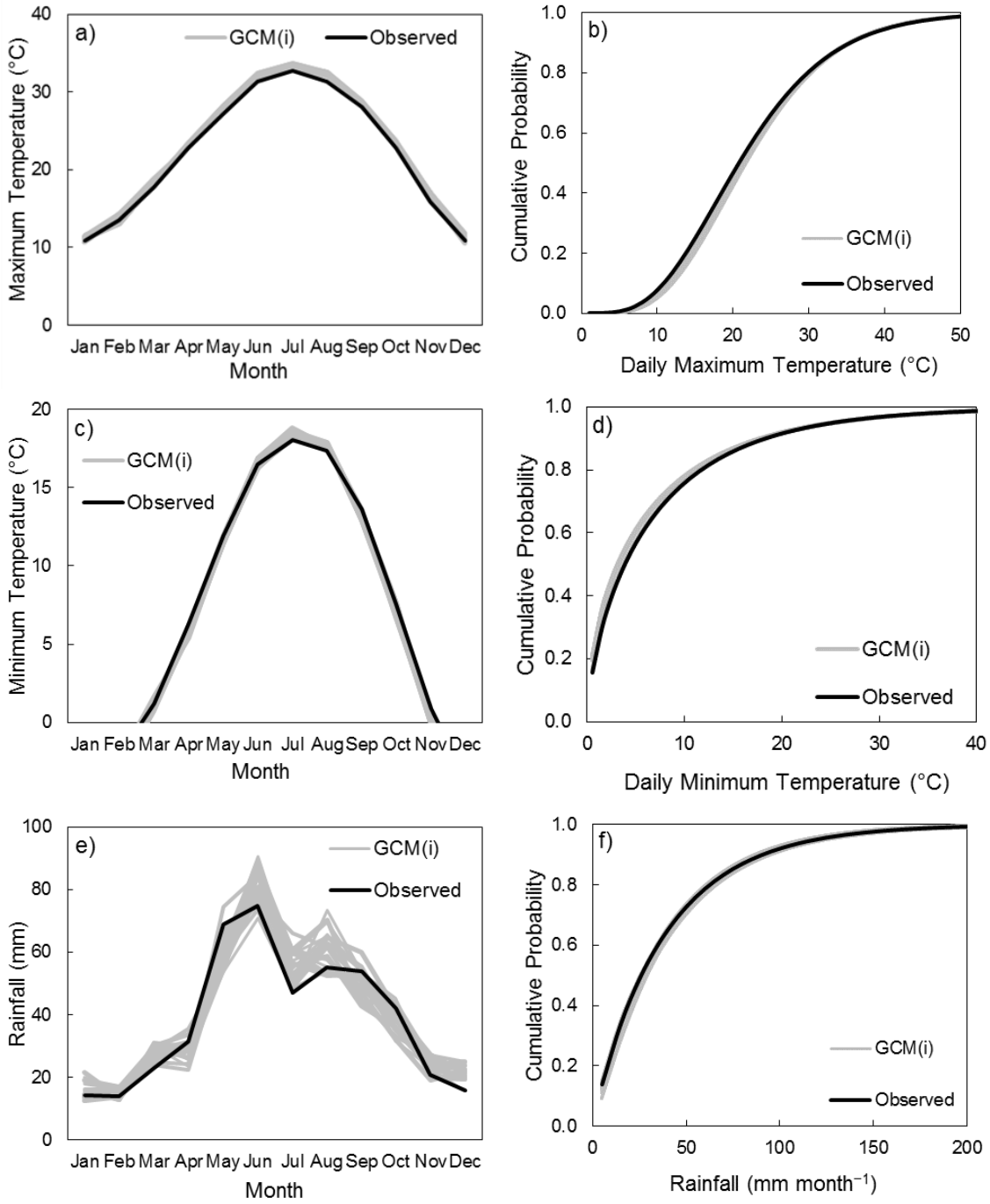

A.2 Comparison of observed weather data (Porter et al., 2005) and GCM projected data (Abatzoglou, 2013) for Halfway for 1977–2005 period.

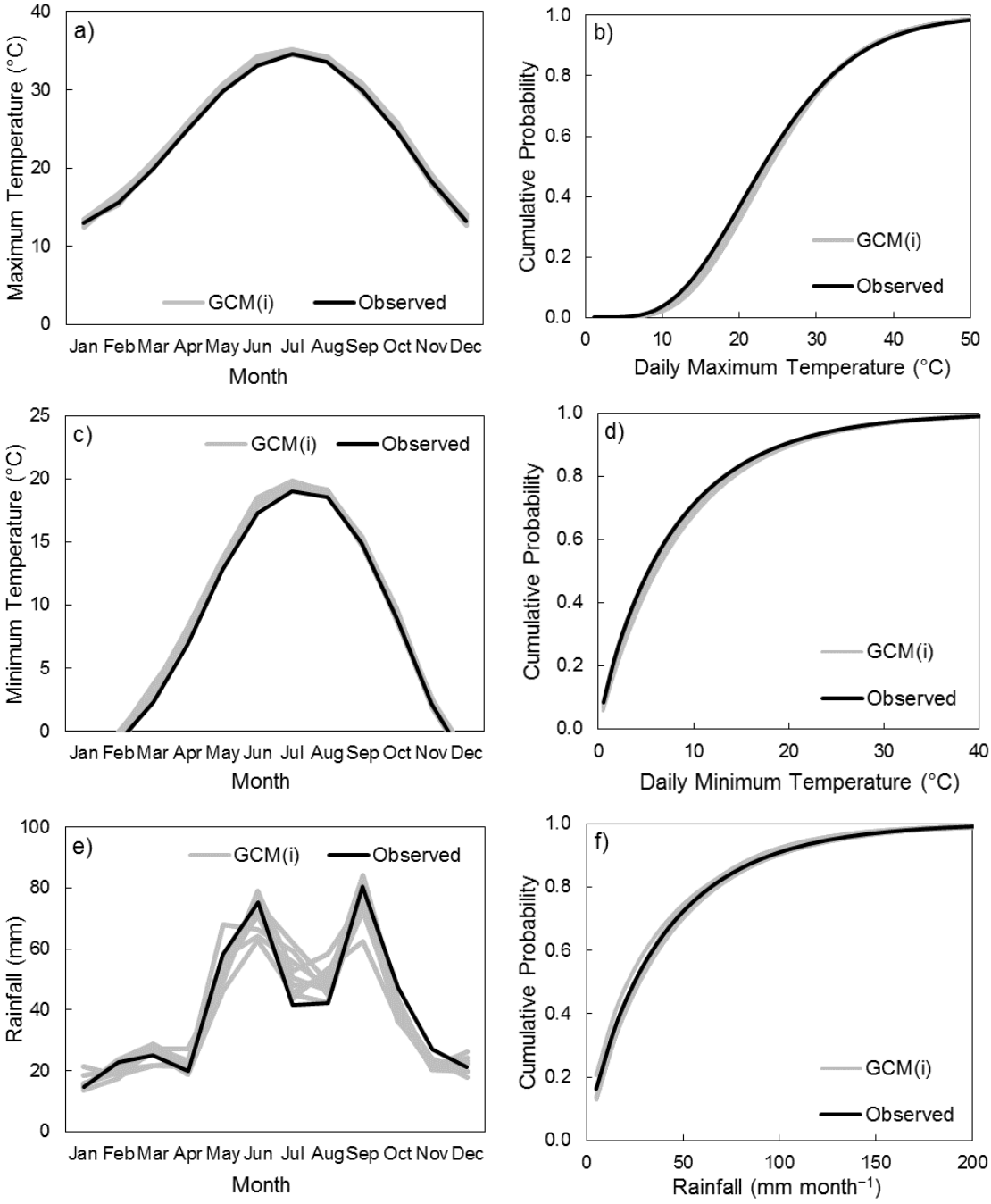

A.3 Comparison of observed weather data (NOAA, 2018) and GCM projected data (Abatzoglou, 2013) for Lamesa for 1980–2005 period.